FACULTY OF SCIENCES
Department of Chemistry
Professor A.-S. Duwez

Elaboration of green bioactive surfaces by combining functionalized plasma layer deposited at atmospheric pressure using a Dielectric Barrier Discharge and covalent immobilization of biomolecules

Academic year 2015-2016

Dissertation presented by

Rodolphe Mauchauffé

to obtain the grade of
Doctor of Sciences

Jury members

Prof. **Bénédicte Vertruyen**, *Université de Liège* (President)

Dr. **Lydie Ploux**, *Institut de Science des Matériaux de Mulhouse, Université de Haute-Alsace*

Dr. **Maryline Moreno**, *Luxembourg Institute of Science and Technology*

Prof. **Jean-Jacques Pireaux**, *Université de Namur*

Dr. **Christophe Detrembleur**, *Université de Liège*

Prof. **Anne-Sophie Duwez,** *Université de Liège* (Supervisor)

Dr. **Patrick Choquet**, *Luxembourg Institute of Science and Technology* (Co-supervisor)

Elaboration of green bioactive surfaces by combining functionalized plasma layer deposited at atmospheric pressure using a Dielectric Barrier Discharge and covalent immobilization of biomolecules

The functionalization of non-reactive surfaces, allowing the immobilization of active compounds for the impartment of new properties, attracted a strong interest from scientific community and industrial R&D. To date, surface modification methods are mainly based on wet chemical processes, involving numerous steps and leading to a high amount of produced wastes. The emergence of dry processes and notably, the deposition of organic coating through plasma methods is offering a new perspective for surface treatments thanks to their environmental aspect, such as the production of few/no wastes and their ability to ensure a fine control of the morphology and chemistry of the produced surfaces. Among the available active molecules, peptides and proteins, renewable resources, show a plethora of potential applications, ranging from antibacterial abilities to catalytic degradation properties of molecules such as antibiotics. Atmospheric pressure plasma techniques allow thin films deposition, adequate for the immobilization of biomolecules. With high deposition rate and operating at low temperature, those processes are easily implementable in production lines for the treatment of different types of materials, showing a real interest for industrial applications. However, such methods still remain poorly studied and reported in literature. This thesis aims at developing and characterizing different layers obtained by Atmospheric Pressure Dielectric Barrier Discharge (AP-DBD) plasma deposition for the immobilization of active biomolecules. Hence, efficient antibacterial coatings were obtained thanks to the immobilization of nisin, an antimicrobial peptide, onto carboxylic-functionalized plasma copolymerized layers deposited onto stainless steel, through a three steps protocol. Despite extremely promising results, in order to reduce the number of the protocol steps, highly reactive epoxy-functionalized layers were developed using pulsed plasma polymerization with Duty Cycles (D.C. = $t_{plasma\ on}/(t_{plasma\ on}+t_{plasma\ off})$) down to 11%. This strategy allowed achieving two different green bioactive layers through the immobilization of microorganisms antiadhesive enzymes and antibiotics degrading enzymes. Further investigations were led for the elaboration of epoxy functionalized layers, using a new approach, involving the use of ultra short plasma pulses, with extremely low D.C. (0.003%), drastically limiting the influence of plasma during layer growth and initiating the free radical polymerization of the precursor, allowing obtaining oligomer chains containing coatings. Multifunctional surfaces properties were additionally obtained combining antibiotics degrading enzymes immobilized on the latter layer and surface saturation with surfactant to lead to protection against microorganisms' adhesion possibly occurring in real use conditions. As plasma techniques are considered as eco-friendly processes, in the last part of the thesis, an effort has been made to reinforce the green dimension of the method. The development of sustainable innovative and robust plasma polymer coatings functionalized with catechol and reactive quinone groups, inspired by the outstanding adhesion properties of mussel feet due to those groups, was achieved for antibiotics degradation purpose through the immobilization of a newly discovered effective enzyme. The formation and growth mechanism understanding of these bio-based coatings show the capacity to immobilize biomolecules thanks to reactive quinone groups and to exploit red-ox properties of present catechol groups, *e.g.* for metal nanoparticles formation. Atmospheric pressure plasma deposition appears as a promising sustainable strategy combined with the immobilization of biomolecules for the development of bioactive surfaces able to face real current industrial, environmental and health issues.

Elaboration de surfaces bioactives durables en combinant le dépôt de couches fonctionnalisées par plasma à la pression atmosphérique utilisant une Décharge à Barrière Diélectrique et l'immobilisation covalente de biomolécules

La fonctionnalisation de surfaces non-réactives, permettant l'immobilisation de composés actifs menant à de nouvelles propriétés de surfaces, n'a eu de cesse ces dernières années d'attirer l'attention de la communauté scientifique et des industriels. Les méthodes, à l'heure actuelle, restent essentiellement basées sur des traitements en plusieurs étapes par voie liquide et générant des déchets à retraiter. L'émergence de traitements par voies sèches et notamment de dépôt de couches polymères par plasma a offert une nouvelle perspective au monde du traitement de surface de par leur aspect environnemental, *i.e.* produisant très peu voire aucun déchets et de par leur contrôle précis des propriétés de surface. Parmi les nombreuses molécules actives disponibles, les peptides et protéines, une ressource renouvelable, présentent tout un éventail d'applications potentielles, allant de propriétés antibactériennes jusqu'à des propriétés catalytiques de dégradation de molécules tels que les antibiotiques. Les traitements par plasma à pression atmosphérique permettent le dépôt de couches minces fonctionnalisées adéquates pour l'immobilisation de ces biomolécules. Ayant des vitesses de dépôt élevées et pouvant opérer à basse température, ces procédés sont implantables dans des lignes de production pour le traitement de différents types de matériaux, présentant un réel intérêt industriel mais restant encore très peu étudiées. Cette thèse a pour but le développement et la caractérisation de couches plasma obtenues à pression atmosphérique avec une décharge à barrière diélectrique (AP-DBD) pour l'immobilisation de biomolécules. Des revêtements antibactériens efficaces sont obtenus sur acier, en immobilisant de la nisine, un peptide antibactérien, par un procédé en 3 étapes, sur des couches plasma co-polymérisées fonctionnalisées par des groupements carboxyliques activés par un linker. En dépit de leur efficacité, afin de réduire le nombre d'étapes pour une implémentation industrielle viable, des couches fonctionnalisées avec des groupements epoxy sont obtenues par polymérisation plasma en mode pulsé, utilisant des duty cycles (D.C. = $t_{plasma\ on}/(t_{plasma\ on}+t_{plasma\ off})$) allant jusqu'à 11% minimum. Cette stratégie permet ainsi le greffage direct d'enzymes pour former d'une part des couches antiadhésives vis-à-vis de microorganismes et d'autre part des couches dégradant des antibiotiques. Par la suite, une nouvelle approche est abordée afin d'élaborer des couches contenant des groupes epoxy, impliquant l'utilisation de pulses de plasma très courts, menant à des D.C. de 0.003%, limitant ainsi grandement l'effet du plasma lors de la croissance de la couche et initiant la polymérisation radicalaire du précurseur, formant des couches composées de courtes chaines de polymères. Des propriétés multifonctionnelles ont été obtenues en combinant sur ces couches le greffage d'enzymes dégradant les antibiotiques et la saturation de la surface avec un surfactant pour protéger la couche de l'adhésion de microorganismes pouvant intervenir dans des conditions réelles d'application. Les techniques plasmas s'inscrivant dans une démarche de développement durable, la dernière partie de la thèse a pour but de renforcer cet aspect par l'utilisation d'un précurseur bio-inspiré par les formidables propriétés d'adhésion des moules. Une méthode robuste, innovante et « verte » a été élaborée, combinant le développement de couches fonctionalisées avec des groupements catéchols et quinones ainsi que l'immobilisation d'une enzyme récemment découverte pour la dégradation d'antibiotiques. Ces couches, au travers de l'étude de la formation et de la compréhension des mécanismes de croissance, montrent leur capacité à pouvoir immobiliser des biomolécules grâce aux groupements quinones et à pouvoir exploiter les propriétés d'oxydo-réduction des groupements catechols présents pour par exemple former des nanoparticules à partir de sels métalliques. Les procédés de dépôt plasma à la pression atmosphérique combinés à l'immobilisation de biomolécules pour le développement de surfaces bioactives semblent fournir des solutions durables à des problématiques environnementales, sanitaires et industrielles et présentent un réel potentiel applicatif.

Remerciements

Je voudrais remercier le Fonds National de la Recherche Luxembourg (FNR) ainsi que la région wallone-DG06, sans qui, le projet européen M-ERA.NET « BioADBD » (INTER/MAT/11-01), rédigé par les docteurs Patrick Choquet et David Duday, impliquant la collaboration entre le Luxembourg Institute of Science and Technology (LIST) à Esch/Alzette et le Groupe Interdisciplinaire de Génoprotéomique Appliquée (GIGA) de Liège, véritable point de départ de ma thèse, n'aurait pu voir le jour.

Je souhaite remercier le Professeur Bénédicte Vertruyen, du Laboratoire de Chimie Inorganique Structurale (LCIS) de l'Université de Liège, pour m'avoir fait l'honneur d'être la présidente du jury de doctorat.

Je remercie aussi le Docteur Lydie Ploux, de l'Institut de Science des Matériaux de Mulhouse (IS2M) ainsi que le Professeur Jean-Jacques Pireaux, de l'Université de Namur, pour leur participation au jury de thèse en tant que rapporteurs. Je souhaite exprimer mes profonds remerciements pour l'intérêt porté à mes travaux.

Je tiens à remercier ma directrice de thèse, le professeur Anne-Sophie Duwez, directrice et fondatrice du laboratoire de NanoChimie et Systèmes Moléculaires à l'Université de Liège, qui m'a permis de réaliser cette thèse. Bien que faisant mes travaux de recherche dans un contexte tout particulier, car passant la plupart de mon temps dans un laboratoire éloigné, au Luxembourg, elle a su prendre son temps pour me suivre tout au long de mon évolution au cours de ces 4 années.

Mes prochains remerciements vont tout droit au co-encadrant de cette thèse au LIST, le Dr. Patrick Choquet, qui m'a accueilli dans son équipe de recherche, pour réaliser ma thèse dans le cadre du projet qu'il a rédigé. Son expertise dans le domaine des dépôts de couches minces par dépôt chimique en phase vapeur assisté par plasma (PE-CVD) a permis, au travers de nos nombreux échanges enrichissants tout au long de ces années, la mise en place et le développement des différentes stratégies présentées dans ce manuscrit ainsi que la rédaction de différentes publications scientifiques. Son expérience lui a permis de toujours manager son équipe pour en tirer le meilleur tout en mettant en place une atmosphère propice pour mener à bien mes travaux de thèse.

Bien évidemment, je ne pourrais jamais assez remercier le Dr. Maryline Moreno-Couranjou, qui m'a encadré et suivi au jour le jour pendant toutes ces années et qui a su me former au travail de chercheur. Sa passion, son dévouement dans son travail, ses connaissances de la littérature scientifique, son esprit de synthèse et sa rigueur scientifique resteront pour moi un exemple. Son aide et son soutien, dans les bons moments comme dans les moins bons qui ont rythmé le déroulement de cette thèse, sont inestimables.

Un remerciement particulier au Dr. Nicolas Boscher, pour qui, science rhyme aussi avec endurance et performance. Il m'aura appris à me dépasser et que la persévérance finit toujours par payer, pas seulement sur une paillasse mais aussi dehors, sur la route, dans la boue ou dans l'eau.

Un grand merci au Dr Sébastien Bonot, avec qui j'ai pris grand plaisir à travailler et à échanger sur nos deux domaines bien distincts mais tellement complémentaires, me permettant ainsi d'élargir le spectre de mes compétences en partageant avec moi son savoir sans faille sur la protéomique et surtout sur la microbiologie.

Je souhaite aussi remercier le professeur Christophe Detrembleur, dont l'expertise dans le domaine de la chimie des quinones et catechols a été d'une grande aide tout au long de ma thèse. Merci aussi pour l'ensemble des discussions enrichissantes et les bons conseils toujours donnés dans la bonne humeur, avec enthousiasme.

Je remercie toute l'équipe du GIGA de Liège, dirigée par le Dr. Cécile Van de Weerdt, pour leurs conseils, discussions et les nombreuses campagnes de tests antibactériens et antibiofilms menées ensemble.

Je voudrais aussi remercier tous les autres membres de notre équipe de traitement de surface, anciennement l'équipe UTS, et tous les membres du laboratoire d'analyse pour tous les bons moments passés au labo ou en dehors.

Je tiens à remercier le Dr. Giuseppe Camporeale, avec qui il fut bon travailler pour mener à bien l'élaboration de couches fonctionnelles mais aussi avec qui il fut plaisant de partager quelques moments lors de son séjour au laboratoire.

Je ne peux pas ne pas remercier tous mes collègues du bureau F1.14, ce lieu rempli d'histoire, qui ont partagé la même aventure que moi, partis depuis bien longtemps ou que je laisse derrière moi. Sans eux toutes ces années auraient eu un goût bien différent.

Encore un grand merci à vous tous et aussi aux personnes que je n'ai pas mentionnées, dont le soutient, pour certains, aura su traverser les frontières et parfois même les continents et aura eu une importance toute particulière tout au long de ces années.

Pour finir, un immense merci à mes parents et à ma sœur pour leur soutien de tous les instants qui m'a permis de me concentrer sur mon travail.

“A journey of a thousand miles begins with a single step.”

Laozi

Table of contents

List of abbreviations

AB	Antibacterial
AGE	Allyl glycidyl ether
AFM	Atomic Force Microscopy
AP	Atmospheric Pressure
APTES	(3-Aminopropyl)triethoxysilane
APTMS	(3-Aminopropyl)trimethoxysilane
BSA	Bovine Serum Albumine
COP	Cyclo olefin polymer
CPA	Cyclopropylamine
CW	Continuous Wave
DBD	Dielectric Barrier Discharge
D.C.	Duty Cycle
DOA	Dopamine Acrylamide
DspB	Dispersin B
EDC	1-Ethyl-3-(3-dimethylaminopropyl)carbodiimide
EGDMA	Ethyleneglycoldimethacrylate
FTIR	Fourier Transform InfraRed Spectroscopy
GMA	Glycidyl Methacrylate
HDPE	High Density Polyethylene
HEPES	4-(2-hydroxyethyl)-1-piperazineethanesulfonic acid
LDPE	Low Density Polyethylene
LP	Low Pressure
MA	Maleic Anhydride
MAA	methacrylic acid
NDM-1	New Delhi metallo-β-lactamase 1
NHS	N-hydroxysuccinimide
PBS	Phosphate Buffered Saline
PCL	Polycaprolactone
PE	Polyethylene
PET	Polyethylene Terephthalate
PFM	Pentafluorophenyl methacrylate
PHA	Polyhydroxyalkanoate
PLGA	*poly(lactic-co-glycolic acid*)
PLLA	Polylactic acid
PP	Polypropylene
PW	Pulsed Wave
SEM	Scanning Electron Microscopy
SS	Stainless Steel
TMDSO	Tetramethyldisiloxane
ToF-SIMS	Time of Flight – Secondary Ion Mass Spectrometry
VTMOS	Vinyltrimethoxysilane
WTP	Water Treatment Plant
XPS	X-ray Photoelectron Spectroscopy

Aim of the thesis

Since decades, a strong will to impart new surface properties to widen the field of application of unreactive materials commonly used for their good physical or chemical properties is rising. To this end, several strategies are developed. Among others, the chemical modification of the topmost surface of the materials is widely reported in literature in order to favor interactions allowing an efficient immobilization of active compounds.

Different ways of modifying surfaces to allow biomolecule immobilization were investigated. In literature, wet chemical methods are extensively reported. However, these techniques, characterized by time-consuming multi-steps procedures and wastes production, present poor industrial up-scaling perspectives. Therefore, dry processes, in particular plasma-based techniques, are investigated for their environmentally friendly aspects (*i.e.* low consumption of chemical compounds and generation of few wastes), their easy up-scaling to industrial-size surfaces and their ability to operate various surface modifications on any type of materials at low temperature. The surface properties of materials such as surface energy, roughness as well as the introduction of a wide range of functional groups can be finely tuned through plasma treatment or fast thin films deposition, providing a versatile way for active compound immobilization.

Recently, research groups and industry have become growingly concerned with the substitution of toxic, non-renewable or pollutant active compounds with more environmentally friendly alternatives. The use of biomolecules appears to be an efficient bio-inspired sustainable solution to impart new functionalities to the surface. Indeed, living organisms like bacteria or plants, offer a large renewable feedstock of biomolecules. The complexity of these organisms, constantly evolving, involves numerous reactions with enzymes and proteins/peptides, each presenting very specific functions. Thus, the production and use of those biomolecules allow a wide range of possible applications, such as antibacterial, antibiofouling or xenobiotic degradation properties.

In addition to lead to biofunctional surfaces, the immobilization of proteins substantially increases their lifetime and activity compared to their free form in solution and facilitates their use by avoiding filtration steps required for medium and biomolecules separation. Thanks to this synergy, the combination of biomolecules immobilization and surface modification by plasma techniques, notably the deposition of plasma polymerized thin films, shows a real interest for the sustainable development of viable new applications. However, still a large part of the reported work in literature are performing plasma surface

modification at low pressure, hence, involving the use of pumps and making its implementation more difficult in view of a potential upscaling in a roll-to-roll process for example. Despite an increased amount of articles these last years, relatively few works remain published on atmospheric pressure plasma functionalized surfaces.

The aim of the thesis is to elaborate green bioactive surfaces through the covalent immobilization of active biomolecules over substrates previously coated with highly chemically reactive functional plasma deposited thin films at atmospheric pressure (**Scheme 1**).

The main challenges here are both the control and optimization of the synthesis at atmospheric pressure of plasma polymerized layers using an atmospheric pressure dielectric barrier discharge (AP-DBD) setup and the determination of the optimal parameters for the right immobilization of biomolecules to conserve their bioactivity. Indeed, the deposited layers should provide suitable surface properties for the covalent immobilization of biomolecules, *i.e.* available and sufficient functional groups, favorable surface morphology and good resistance to provide high stability in the targeted applications. Several parameters such as plasma power, continuous/pulsed signal, precursor injection method and flow rate can be controlled in order to finely tune both morphology and chemistry of the layers. The choice of the chemical precursor also allows obtaining a wide range of functional groups with different reactivity. The parameters of the biomolecule immobilization step, such as biomolecule solution buffer type, pH, temperature and reaction duration can influence the structure of the biomolecules, their orientation on the surface and the reactivity of the functional groups, hence having an effect on the efficiency of the resulting bioactive layer.

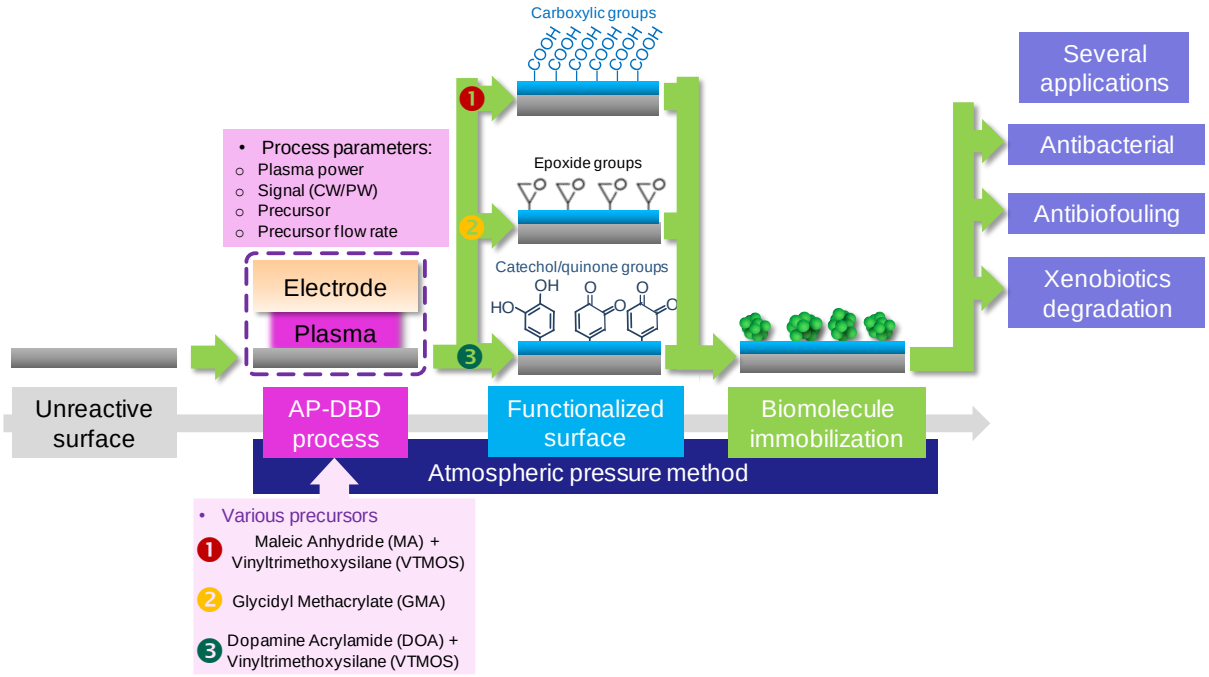

Scheme 1: Summary of the different developed atmospheric pressure methods comprising an atmospheric pressure plasma deposition step to form functionalized coatings subsequently exploited for biomolecule immobilization in a second step, imparting various properties to the initially non-reactive surface.

In this work, we report on different methods to produce bioactive surfaces through the immobilization of various biomolecules on carboxylic, epoxide and quinone functionalized plasma deposited interlayers. To avoid their denaturation the covalent immobilization has to be performed in mild conditions either in a single step (on epoxide and quinone groups) or two steps (carboxylic groups) for surfaces needing an activation step. For example, Nisine and Dispersin B were respectively used to provide antibacterial and antibiofouling properties to a stainless steel surface. Laccase, β-lactamase from *Pseudomonas aeruginosa* and New Dehli Metallo β-lactamase 1 (NDM-1) were grafted on polymeric grid for the degradation of antibiotics in solution.

This manuscript is divided into six chapters. The first one is a state-of-the-art of the recent advances in plasma surface modifications for the immobilization of biomolecules while the five following chapters focus on the elaboration and study of three different types of functionalized layers. All chapters are written as articles already published or to be published in peer-reviewed journals.

In the first chapter, the last advances in the field of surface modification by plasma techniques for the immobilization of biomolecules are reviewed. This chapter shows the

versatility of the plasma methods thanks to the tuning of process parameters. Numerous plasma based immobilization strategies are reported, ranging from reversible/irreversible surface immobilization over materials via surface plasma treatment or plasma-polymerized functionalized thin film deposition, to the formation of plasma deposited biocomposites for the entrapment of biomolecules into a layer.

The second chapter reports the synthesis of carboxylic functionalized plasma thin films deposited by an atmospheric pressure dielectric barrier discharge process for the covalent grafting of Nisin, a natural antimicrobial peptide, to confer antibacterial properties to stainless steel. The three different steps of the developed procedure, namely the deposition of a carboxyl rich thin layer, its surface activation by using a zero-length crosslinking agent and the nisin immobilization, are reported and thoroughly characterized. The influence of the resulting plasma polymer properties on the antibacterial properties of the layers after immobilization is also assessed.

The third chapter aims at improving the biomolecule immobilization procedure by exploiting a highly chemically reactive surface allowing a one-step biomolecule grafting in mild conditions. To this end, an atmospheric-pressure dielectric barrier discharge process is exploited for the fast deposition of adherent epoxy-rich layers from glycidyl methacrylate (GMA), a vinyl based monomer. The influence of the plasma discharge pulse duration, leading to duty cycles (D.C. = $t_{plasma\ on}/(t_{plasma\ on}+t_{plasma\ off})$) ranging from 11% to 100%, on the chemical and morphological properties of the deposited layers and on their subsequent possible exploitation for chemical interfacial reactions, is investigated. In order to prove the versatility of the developed surfaces, two enzymes with drastically different biological properties, namely dispersin B, an antibiofilm protein, and a laccase, able to degrade antibiotics, were immobilized onto the functionalized surfaces leading to bioactive materials.

In the fourth chapter, an innovative layer deposition approach is described based on the formation of epoxy functionalized surfaces using Plasma initiated Chemical Vapor Deposition (PiCVD), a newly developed process at atmospheric pressure. Indeed, nanosecond square plasma pulses coupled with long plasma off times (several ms), hence leading to small duty cycles (D.C.~0.003%), allow limiting the effect of the plasma discharge on the growing layer and initiating the free radical polymerization of GMA, forming coatings composed of poly(GMA) oligomers. These layers are used as a platform for the immobilization of enzymes degrading antibiotics (laccase and β-lactamase). In view to

upscale the method to waste water treatment plant containing many microorganisms likely to adhere and reduce the efficiency of the layers, multifunctional coatings are developed, imparting self-defensive properties to the surface through surface saturation with Tween 20.

Feeling concerned about green approaches, the aim of the 5th chapter is to synthesize a bio-inspired functionalized coating. A catechol-bearing monomer, *i.e.* Dopamine Acrylamide (DOA), is plasma copolymerized with Vinyltrimethoxysilane (VTMOS) to form reactive layers containing both catechol groups and their oxidized form quinone groups; known as responsibles of the remarkable mussel feet adhesion and cohesion properties. This new type of surface offers an universal platform able to enable both metal nanoparticles or biomolecule immobilizations. These surfaces are then used to develop an environmentally friendly robust and sustainable alternative method to degrade antibiotics present in waste water. Indeed, this chapter describes pioneering results, on how it is possible to give to a surface the ability to degrade xenobiotics, mimicking an emerging multidrug-resistant bacteria, *i.e.* the newly discovered New Delhi Metallo-β-lactamase-1 (NDM-1)-producing bacteria and its aptitude to hydrolyze and inactivate almost all β-lactam-based antibiotics. To do so, the NDM-1 enzyme is covalently immobilized via the quinone groups of the novel mussel-inspired plasma deposited layer and the efficiency and robustness in water flow of the developed coatings for antibiotics degradation are studied.

The last chapter deals with the understanding of the growth mechanisms of this plasma deposited DOA-VTMOS copolymerized layer. A parametric study is led in order to highlight the influence of the different operating parameters, such as the injected precursor amount and the plasma power, on the chemistry and morphology of the formed layers.

Chapter 1

Recent advances in plasma surface modification of materials for the immobilization of biomolecules

R. Mauchauffé, M. Moreno-Couranjou, P. Choquet, *in preparation.*

Recent advances in plasma surface modification of materials for the immobilization of biomolecules.

Contents

1. Introduction

Metals, polymers or ceramics are surrounding us in our everyday life. Even though their intrinsic properties make them materials of choice for many applications, their environment of use is sometimes harsh and the natural non-reactive surfaces of the majority of those materials can lead to serious issues such as microorganism spreading, prematurated ageing, loss of properties through corrosion etc... To overcome these issues, external maintenance or the setting up of additional protection technologies have to be performed. It is the case, for example, of the materials used to design industrial water pipes, air conditioning or even catheter, lacking or showing few antibacterial and antibiofilm properties. Antibacterial solutions, detergents or filters are used in these cases to limit the propagation of disease, leading to the production of wastes, sometimes toxic or to costly heavy solution to put in place to simply allow those materials to keep their functions.

In the era of smart technologies, the development of advanced materials with reactive surface properties appears as a possible solution to overcome those problems by confering totally new functionalities to a material. With the emergence of bio-inspired materials and the current position of the industries to adopt a sustainable approach, a strong will of combining bio-inspired methods with new surface treatment is rising. Since decades, wet chemistry treatments allowed modifying surfaces to immobilize biomolecules. However these techniques, often time-consuming multi-steps procedures and producing wastes, present poor industrial up-scaling perspectives. Alternative methods, such as dry processes were largely investigated and more especially plasma surface modification methods for their environmentally friendly aspects, their easy up-scaling to industrial-size surfaces and their ability to operate various surface modification on any type of material.

This chapter provides a state-of-the-art related to the current strategies reported for chemical surface functionalization using plasma techniques in order to immobilize biomolecules. Several interesting reviews are already reported in litterature. However, they only focus on some functional groups obtainable by plasma for the covalent immobilization of biomolecules and mainly on low-pressure surface modification, thus offering a poor overview of all the wonderful possibilities offered by the versatility of the plasma techniques. Indeed, plasma methods allow far more possibilities ranging from simple biomolecule adsorption to the complexe elaboration of biocomposite coatings, including the covalent immobilization.

Taking into account the extensive litterature in this field, the present state-of-the-art is mainly focused on the recent developments in research over the last decade.

The aim of this chapter is to give an overview, through the latest innovative findings, of the suitability of these methods to be combined with nature-inspired approach, through the immobilization of biomolecules.

Firstly, the current use of biomolecules, the importance of their immobilization as well as the current grafting methods will be discussed. Secondly, plasma methods exploited to create plasma modified surfaces presenting adequate properties for bio-immobilization will be studied. Finally, the different latest strategies developed to immobilize biomolecules on the plasma modified surfaces for various applications are reviewed.

2. Biomolecules and immobilization techniques

2.1 Biomolecules applications

Bio-inspired and bio-sourced materials are nowadays of main interest and attract a large attention from the research community. Indeed, the study of the living organism structures and survival mechanisms offers a wide source of inspiration to develop bio-inspired processes or materials having a strong potential to overcome emerging economic, ecologic and health challenges.[1–5]

Biomolecules and their various properties, *e.g.* hydrophobicity/hydrophilicity, electric charge, reactive chemical groups, surface energy, enable them to be bioactive and to accomplish a large range of functions. They are produced by living organisms and are present under several forms, from small biomolecules, *e.g.* lipids, saccharides, antibiotics or single amino acids,… to complex macromolecules such as biopolymers like polynucleotides, polysaccharides, polyamino acids (peptides and proteins) or polyterpenes.[6–9]

Beyond the fact that the biomolecules offer a large renewable feedstock, biomolecules are generally considered as an alternative to existing solutions presenting limitations such as non-renewable compound use, toxic chemicals and at a deeper extent may replace solution with long-term issues. This is the case looking at the field of antibacterial properties for example, a large choice of antibacterial agents is available to kill bacteria or inhibit their growth. Biomolecules could substitute the introduction of metallic nanoparticles and quaternary ammonium, which, in spite of their large antibacterial spectra efficiency, are mainly toxic.[10,11] In medicine, for decades, synthetic antibiotics were used to treat bacterial infections but their overuse led to the emergence of bacterial resistance. [12] Indeed, multiresistant drug bacteria strains are nowadays emerging and resist to a large variety of antibiotics and some bacterial infections, *e.g. Staphylococcus Aureus*, are hardly treated, and threaten human lives. Hence, there is a real need to find alternatives such as antimicrobial peptides and proteins, not toxic and with no or with low rate bacterial resistance induction.[13,14]

Among the numerous biomolecules available and potentially interesting for various applications, some are already widely studied. One can cite heparin a natural anticoagulant polysaccharide enhancing hemocompatibility; bone morphogenetic proteins (*e.g.* rhBMP-2) enhancing osteoblast growth; enzymes such as laccases or beta-lactamases catalyzing the degradation of pollutants such as antibiotics; antimicrobial peptides and proteins able to kill

gram + and – bacteria or RGD containing peptides/proteins for enhanced cell growth and biocompatibility.[15–18] All these different properties which can be achieved, explain why nowadays biomolecules are particularly interesting for industrial and economic sectors. Indeed, for example, heparin is produced and injected in patient to avoid blood coagulation and thrombosis.[15] Nisin, an antimicrobial peptide, produced by *Lactococcus lactis*, is largely introduced as a preservative agent in food processing.[19] Nature is a real source of inspiration, which one can try to mimic to overcome problems in an environmentally friendly way.

The exploitation of these biomolecules at an industrial scale remains a challenging topic. Their production involves many prior steps. Parameters such as toxicity, stability, efficiency, etc have to be assessed according to the targeted application and current regulations; and the production protocols, sometimes requiring several time taking steps (*i.e.* for biomolecule extraction from bacteria involving growth and extraction) have to be optimized to get the best yield for mass production.

Biomolecules, despite their eco-friendly aspect and efficiency, are however not devoid of drawbacks. Though the majority of small biomolecules are stable, proteins such as enzymes can be relatively unstable. Indeed, to keep their functional properties, they are dependent of their conformation. Parameters related to their operating environment such as temperature, pH, chemical agents, proteases, ionic strength and mechanical stress can have a strong impact on them. To overcome this drawback, different strategies are possible:

- the production of stable enzymes regarding the targeted environment through the production of proteins mutants,
- the direct chemical modification of the peptides/proteins amino acids using coupling agents,
- the addition of additives such as cofactors, providing that they are compatible with the reactive media.[20]

However, these stabilization methods need a prior phase of development to lead to applicative results and this is why, another strategy is used and preferred to stabilize biomolecules: their immobilization on a surface.[21]

2.2 Techniques for the surface immobilization of biomolecules

Several advantages are obtained through simple surface immobilization. In addition to enhance the activity and the durability of biomolecules (especially in the case of proteins compared to their free form), immobilization also helps isolating the biomolecules from the reaction mixture after reaction, leading to an easier industrial handling optimization and to a potential re-usability of the biomolecules.[22] New surface properties are obtained from the molecules immobilization; from an inert surface we can obtain a bioactive surface. The key factor is however to immobilize biomolecules in a way that their structure and their function/activity are not or just slightly altered.

Immobilization can be just performed thanks to the intrinsic surface properties of the materials such as hydrophobicity, metal affinities (thiol on gold) or via reaction with specific functional groups. However, the majority of materials are usually inert and non-reactive, hence surface modification has to be performed. Surfaces can be modified through direct physical or chemical surface treatment of the material or through introduction of a reactive interlayer. Once modified, surfaces may lead to new surface interactions and may allow of reversible or irreversible immobilization of biomolecules (**Table 1**).

It is worth noticing that immobilization of biomolecules is known to be driven both by the surface properties of the substrate (charges, morphology, functional groups, …) and by the grafting environment of the biomolecule (pH, T, …). Biomolecules generally present functional groups in their structure able to lead to interactions with the surfaces. For example, in the case of proteins, composed of a combination of 21 amino acids, several functional groups may offer a wide range of possible interactions with surfaces. Indeed, proteins are always composed of one terminal free amino group and one free carboxylic group and additional side chain groups, these groups can be either electrically charged, uncharged or hydrophobic (*e.g.* amine/protonated amine, carboxylic/carboxylate, thiol, imidazole/imidazolium, hydroxyl, phenyl, etc…) illustrating the wonderful reactive potential of biomolecules. It is worth noticing that the functional groups charges, either present on the biomolecules or on the surface, might change according to the surrounding medium properties during immobilization step. The pH of the solution, for example, can lead to more or less charged biomolecule or modified surface due to protonation and deprotonation of functional groups leading to a large range of possible interactions and different reactivities.

Reversible immobilization can be obtained through adsorption of biomolecules thanks

to weak interactions such as ionic, electrostatic, hydrogen bonds or hydrophobic interactions. Weak metals affinities interactions or formation of cleavable disulphide bonds can also be exploited. In the contrary, some surface modifications can lead to an irreversible covalent immobilization of biomolecules, possible in proteins, for example, thanks to terminal COOH and NH_2 groups and several side chain groups such as COOH, NH_2, SH and imidazole, allowing obtaining long lasting properties in a large range of conditions but hardly allowing the regeneration of the biomolecules on the surface. Biomolecules can also be immobilized in a deposited interlayer, through physical entrapment or through its cross-linking.

Table 1: Biomolecules immobilization interactions.

		Advantages	Drawbacks	References
Reversible	Adsorption	Reversible upon conditions changes, conservation biomolecules conformation, regenerable	Short term application: sensible to change of environment (ionic strength, pH, temperature, detergent), random orientation	[23–27]
	Metal ion affinity	Reversible	Need presence of specific groups on the biomolecule (*e.g.* imidazole)	[28,29]
	Disulfide bond	Cleavable, high pH stability range	Weak against reductant	[30]
Irreversible	Surface covalent bond formation	Stabilisation of biomolecules, Durable activity	Loss of activity due to loss of conformation in some case, irreversible (bond cleavage can happen at certain pH)	[20,30–33]
	Cross linking	Durable activity	Part of entrapped/cross linked biomolecules in the bulk material are not available for surface reaction	[34]
	Entrapment	Biomolecule properties conservation, controlled leaching possible		[25,35]

Surface treatment or interlayer formation for enhanced surface interactions or entrapment/cross-linking of biomolecules are currently performed by several ways as summarized in **Table 2**. Wet chemical methods allow both to activate surfaces by hydrolysis of polymeric surfaces or through the deposition of a layer by techniques such as layer by layer, sol-gel or dopamine autopolymerisation, … Even though those methods are easily set

up they are mainly based on batches production processes and involve many steps, they are time taking, and generate chemical wastes, hence making them not the most suitable methods nowadays for up-scaling to industry where the current trend is to favor environmentally friendly processes.

Table 2: Summary of different surface modification methods for biomolecule immobilization.

Modification methods			Modification	Advantages	Drawbacks	References
Wet-chemical methods	Surface hydrolysis		Surface activation	One step activation	Compatible with few materials (such as polymers), waste production	[18]
	Layer by layer		Reactive layer deposition	-Easy to apply Suitable for a large range of materials (metals, polymers or ceramics)	Batch processes, chemical wastes, slow deposition rate, numerous and time taking procedure	[36]
	Dopamine autopolymerization					[37]
	Sol-gel					[35]
Dry physical/chemical methods	Chemical Vapor Deposition (CVD)		Layer formation	No/few chemical wastes, high coating purity	Low pressure process, operating at high temperature	[38]
	Plasma processes	Plasma-Enhanced-CVD (PE-CVD)	Surface activation / Layer deposition	Large availability of precursors, deposition on large range of materials (polymers, metals, ceramics), poor chemical amount required, fast deposition rate on large surfaces, low temperature plasma possible	Low pressure, limited shape of the sample to treat due to the reactor geometry	[39,40]
		Plasma-Immersion Ion Implantation (PIII)		Highly reactive groups formation (radicals), linker free	Mainly used on polymer substrates	[41]
		Plasma treatment		Large range of obtainable functional groups and surface radicals	Mainly used on polymer substrates	[31]

3. Versatility of plasma techniques for surface modification

Due to the numerous drawbacks of wet-chemical methods for industrial up-scaling, research groups developed dry processes for surface modification, considered as environmental-friendly processes and industrially interesting thanks to their potential use as continuous processes and low production of wastes, subscribing to a sustainable development approach. Some works show the successful functionalization of surfaces through chemical vapor deposition (CVD) (**Table 2**) by for example pyrolysis of functionalized paracyclophanes, however presenting limited possibilities due to a two-step nature, involving a high temperature step and allowing only the deposition of layers on a surface.[42–44] Another type of CVD, called Initiated CVD (iCVD) overcome some drawbacks, allowing the deposition of functional coatings at low temperature but is involving the use of highly reactive chemical initiators and is still running at low pressure making it still problematic for a potential industrial upscaling.[38,45]

3.1 Plasma processes

Thanks to the reactive energetic species present in plasma, it is possible to broaden the field of application of dry processes. Plasma assisted surface modification techniques, with their environmentally friendly aspects and advantages (**Table 2**), are of main interest for the immobilization of biomolecules on a material surface. Thanks to the versatility of plasma techniques it is possible with an all-in-one one-step process to clean the substrate and to modify the surface through two main different strategies (**Figure 1**):

- *plasma treatment:* the substrate, typically a polymeric materials, is exposed to a plasma discharge, highly energetic species may allow the formation of reactive radicals which can be further exploited to immobilize either a functional monomer, offering the possibility to have a large choice of surface functional groups, or any other molecules, *i.e.* biomolecules. Some reactive plasma gases may also allow the direct introduction of functional groups on the surface of polymeric surfaces. The morphology, *i.e.* roughness, of the surface can also be tuned. [31,46]

- *plasma layer deposition:* a plasma polymer layer can be formed thanks to plasma species initiating the polymerization of a precursor on a large range of materials.[40] Firstly, coatings containing surface functional groups can be synthesized using coating-forming precursors bearing the desired moiety. Secondly, the exposition to ions and other highly reactive species of the growing layer during plasma deposition leads to the formation of radicals in the layer, which can be directly exploited right after plasma polymerization for further immobilization of molecules.[41] Thirdly, the deposition of a plasma polymerized matrix for the entrapment of molecules can also be developed.[47]

As immobilization of biomolecules is reported to be influenced both by the surface properties of the substrate (charges, morphology, functional groups, …) and by the grafting environment of the biomolecule (pH, T, …), plasma techniques appear as a versatile way to efficiently tune the different parameters of the surface for the successful immobilization of biomolecules.

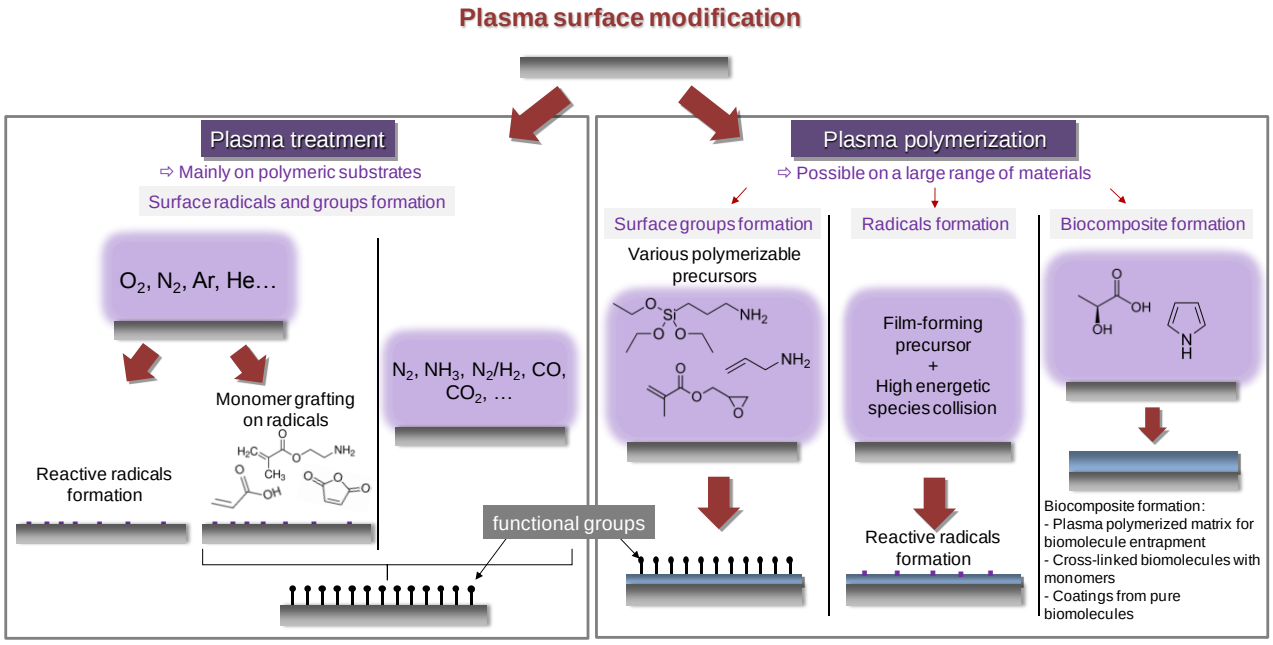

Figure 1: Scheme of the different plasma surface modification pathways. Adapted from [39–41]

Different types of reactor are exploited for the surface modification. Cold plasmas are of main interest thanks to their versatility. They allow the treatment of heat sensitive substrates. Mainly two types of plasma reactor are exploited in the literature for the modification of surfaces for biomolecules immobilization purpose (**Figure 2**):

- Low pressure (LP) reactors, operating at pressure ranging from 0.01 mbar to few mbar and exploiting cold plasma glow discharges generated from DC or AC voltages excitations (most commonly in the Radio Frequency RF range at 13.56 MHz) can be used to treat surfaces with inert gases and deposit coatings from layer-forming precursors. A DC bias voltage can additionally be applied to the substrate to increase the energy of the species entering in contact as in Plasma-immersion ion implantation. These processes are interesting because low vapor pressure precursors can easily be introduced and they offer a confined environment allowing avoiding contamination by the surrounding atmosphere. However due to pumps use to produce vacuum, those low pressure processes are energy costly and time taking hence presenting several drawbacks for an industrial upscaling.

- Atmospheric pressure (AP) reactors are also interesting due to their easy up-scalable properties. Atmospheric pressure plasma processes are already currently used in the industry to clean surfaces of materials or to enhance adhesion. Among these various atmospheric plasma processes, Dielectric Barrier Discharges (DBD) reactors are largely reported in literature to treat/activate surfaces and deposit polymers. Generally, DBD discharge consists in two electrodes which at least one of those electrodes is covered by a dielectric material (quartz, alumina, etc.) and applying an AC excitation to allow the formation of cold discharges at atmospheric pressure between electrodes. Separated of few mm to cms, the dielectric material avoids the formation of plasma arcs even at high voltage. DBD reactors allow either treatment directly in the discharge between the electrodes in presence of all the highly energetic species or in post-discharge afterglow, with a blown discharge, free of the highest energetic species. Atmospheric pressure methods offers several advantages, such as a high deposition rate, higher than at low pressure and has the potential to be implemented in an existing in-line process where the other steps are also performed at atmospheric pressure, hence avoiding investment and substantially saving time.

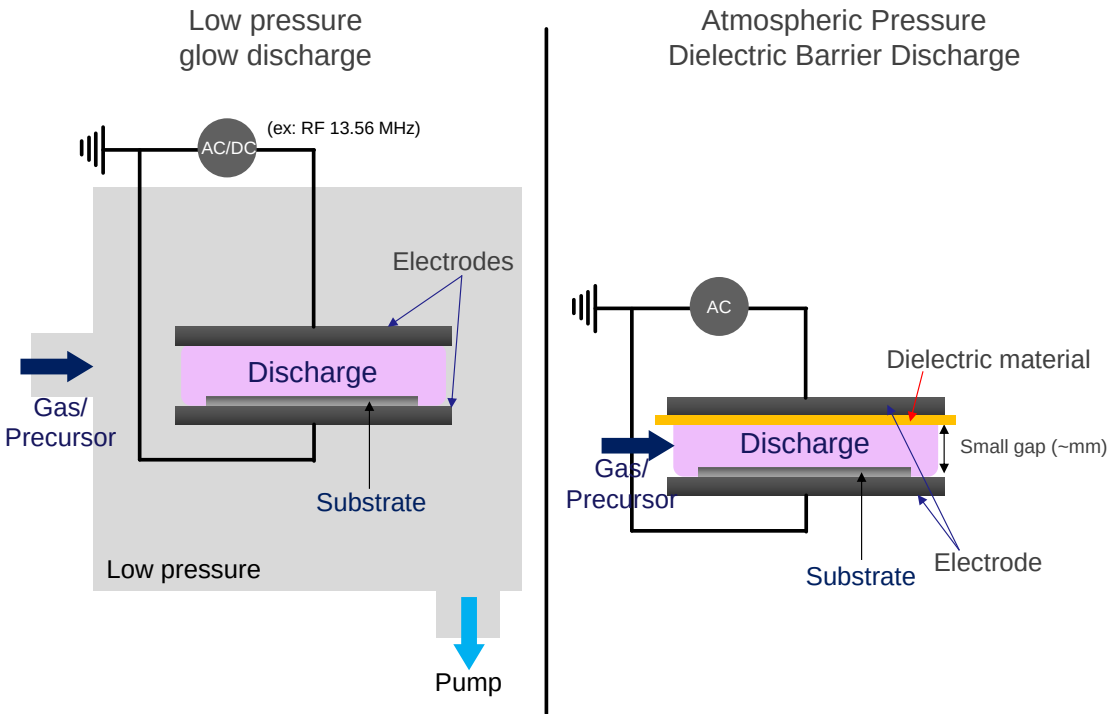

Figure 2: Schematic drawings illustrating the principles of RF/DC glow discharge and DBD direct discharge.

At low pressure, in addition to be able to treat mere planar samples, glow discharge allows the treatment of complex pieces thanks to the high mean free path of species. At higher pressure, species will have lower mean path and tend to recombine before reaching the surface but the reactor geometry can be adapted to treat complex forms, *e.g.* plasma jet for 3D pieces or tube discharge to treat wires.[48] Due to the wide natures of available precursors, several injections systems are developed. At low pressure, low vapor pressure monomers can be easily injected, while at atmospheric pressure the introduction of such precursors become more challenging and imply the use of heated-bubblers or nebulization systems. To enhance the homogeneity of the coatings over the whole surface, either electrodes can be mobile or samples can move under the electrode. Plasma parameters such as power, discharge signal (pulsed or continuous discharge) as well as additional voltage bias can be tuned and may have a strong influence on the coating reactivity and are discussed in the next two sections.

3.2 Plasma gas-based surface treatment

Plasma treatment may lead to the formation of various surface reactive compounds among which radicals and functional groups are of main interest and largely exploited.

3.2.1 Radical formation

The simplest way to use plasma to modify surface is to merely expose material to a plasma discharge. The generation of surface reactive radicals can be, by this mean, easily achieved on surfaces, generally polymers (**Figure 3**). The collision of high energetic species generated in the plasma leads to the breaking of chemical bonds and to the excitation of atoms on the surface and in the bulk material near the interface, part of these generated compounds recombines to further cross link the polymeric surface but some radical groups remain available on the surface or can migrate to the surface from the bulk. The lifetime of the radicals depend on the energy of species in the plasma and is proportional to the depth of implantation of ions.[49] Indeed, the radicals formation can occur by simple exposition to a simple plasma generated using a DBD discharge, RF discharge or DC discharge. However additional energy can be provided to the bombarding ions to increase their energy using a negative DC voltage bias (1-20 keV) applied to the polymer substrate. The latter process involving a plasma and voltage bias is called plasma immersion ion implantation (PIII). PIII treatments were shown to lead to long lasting radicals formation compared to plasma treatment without bias. To avoid the polymer heating during the ion implantation a pulsed bias might be applied. The versatility of this surface modification technique is extensively reviewed in the recent works of Bilek *et al.* [41,49]

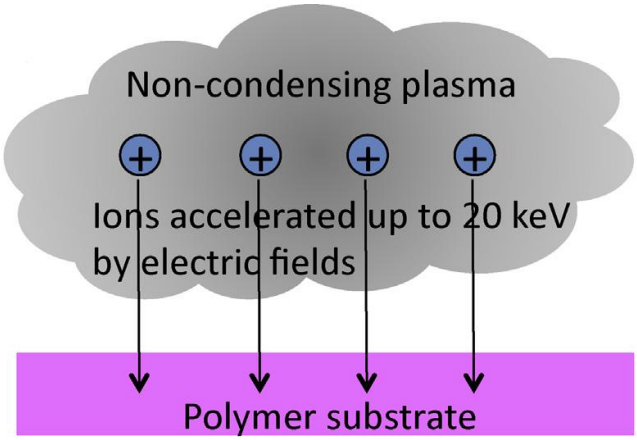

Figure 3: Scheme of the plasma-immersion ion implantation principle on a polymer substrate. Adapted from [49]

3.2.2 Graft polymerization

The production of surface free radicals in polymers by plasma exposure to a discharge is commonly exploited for the grafting of small monomers to introduce various functional groups.[50] Common plasma gases (Ar, O_2, Air, etc.) are used to activate the surface, the remaining free radicals on the surface can be directly exploited after plasma exposure for graft polymerization of monomers and various functional groups can be obtained on the surface (**Table 3**).

To do so, activated radicals containing surfaces are commonly immersed out of the reactor in functional groups-bearing monomer solutions but some works also report the exposition to a monomer vapor in-situ allowed by low pressure systems.

Plasma parameters such as treatment time and power are known to influence the surface reactive species formation.[51] It was shown that under argon plasma treatment, an increase of oxygen-containing species is observed together with the increase of treatment time and the same tendency is observed for the plasma power, more radicals are formed with increasing power however a plateau is reached due to higher recombination of radicals at higher power.[51] Plasma surface modification for graft-polymerization appears in the literature to be mainly performed at low pressure (LP) with radio frequency discharge and only few works are reported on the use of atmospheric pressure plasma processes like Dielectric Barrier Discharges (AP DBD).[52,53]

Graft polymerization is mostly reported to be performed using monomer solutions. The immersion of the treated samples right after treatment for the direct exploitation of radicals is performed in order to form functional groups. Acrylic acid solution is largely used to form carboxylic groups on the surface.[52,54,55] Maleic anhydride is also reported to form carboxylic groups.[56]

Grafting parameters in solution such as monomer concentration, reaction temperature and reaction time are shown to have an influence on the grafting. The monomer concentration is a key parameter because firstly allowing the control of the availability of monomer at the grafting sites and secondly allowing the control of the homopolymerization reaction of the monomer and the solution viscosity change occurring in the medium during grafting. Indeed, at high concentration, high homopolymerization of the monomer is likely to occur, forming long polymer chains that do not attach to the surface, increasing the viscosity of the medium and decreasing the mobility of the monomer and the monomer concentration hence leading to reduced monomer availability and less grafted amount.[51,57,58] To optimize the degree of grafting of monomer on the surface low concentrations of monomers are used (less than 20% in the case of acrylic acid) sometimes combined with the use of salts such as sodium metabisulfite or potassium persulfate as redox agents as observed in the case of acrylic acid grafting to inhibit homopolymerization.[52,59,60] Reaction time study shows that the kinetic of the monomer grafting is slow and reach a plateau after several hours of reaction and explain the observed contact duration from the literature, generally of the order of few hours. The increase of reaction temperature can also be tuned to favor the grafting of monomers.[53]

However the formed radicals during plasma treatment have a short lifetime and if they are not exposed to a monomer directly after formation they will tend to form peroxide groups after few minutes at air. Hopefully a work of Gupta *et al.*[51] shows that those groups are also likely to allow graft polymerization of monomers and several works report the successful immobilization of monomers such as acrylic acid to form carboxylic groups.[53,57,59–62] UV irradiation of samples immersed in grafting solution can also be performed to assist and favor the graft polymerization. Acrylic acid, Glycidyl Methacrylate (GMA) and 2-aminoethyl-methacrylate (AEMA) were grafted to form respectively carboxylic, epoxy and amine functionalized surfaces under UV exposure.[63–66]

To avoid air exposition and to avoid the use of liquid solution showing some drawbacks, vapor phase grafting is employed, introducing monomer vapors directly in the

plasma low pressure reactor after plasma treatment. Vapor of ethylene/propylene diamine, allylamine and pentafluorophenyl methacrylate allowed forming amine and active ester functionalized layers respectively.[58,67,68]

Table 3: Graft polymerization of various monomers for surface functionalization.

Grafted functional group	Substrate	Gas	Grafted monomer	Plasma discharge	References
Active ester	PS	Ar	Pentafluorophenyl methacrylate	LP RF Discharge 13,56 MHz	[68]
COOH	PET	Ar	Acrylic acid	LP DC Glow discharge	[54]
COOH	PE/PP	Ar	Maleic Anhydride	LP RF Discharge 13,56 MHz	[56]
COOH	LDPE	Air	Acrylic acid	AP DBD	[52]
COOH	PP	O_2	Acrylic acid	LP RF Discharge 13,56 MHz	[55]
COOH	PE	O_2	Acrylic acid	LP glow discharge	[63]
COOH	PCL	Ar	Acrylic acid	LP RF discharge 13,56 MHz	[64]
COOH	LDPE	Ar/O_2 (95/5 %)	Acrylic acid	RF Discharge 13,56 MHz	[61,62]
COOH	PLLA	Ar	Acrylic acid	LP RF discharge 13,56 MHz	[59]
COOH	Linen fabric	Air	Acrylic acid	AP DBD	[57]
COOH	PET	Ar	Acrylic acid	LP glow discharge	[53]
COOH	PET/PHA	O_2	Acrylic acid	LP RF discharge 13,56 MHz	[60]
Epoxy	PP	O_2	Glycidyl methacrylate	LP glow discharge	[65]
NH_2	PCL	Ar	2-aminoethyl-methacrylate (AEMA)	LP glow discharge	[66]
NH_2	PP	Ar or O_2	Ethylene/propylene diamine	LP RF discharge 13,56 MHz	[67]
NH_2	LDPE	Air	Allylamine	LP RF discharge	[58]

3.2.3 Plasma gas treatment

While inert gases generate mainly radicals, reactive gases can lead to the introduction of functional groups on the surface upon exposure to generated plasmas. Depending on the used plasma gas, different groups were reported to be formed in the literature (**Table 4**) mainly on polymers (polypropylene (PP), polyethylene (PE), polycaprolactone (PCL), polyethylene terephthalate (PET), etc.) but also on materials like graphite, carbon nanotubes or even ceramics like Gallium Nitride (GaN).

Oxidation of polymer surfaces with oxygen plasma treatment was shown to lead to oxygen-containing groups such as carboxylic, aldehyde and hydroxyl groups.[69–72] The combination of H_2O and O_2 allowed the introduction of hydroxyl groups.[73,74] Thanks to ammonia, ammonia/nitrogen or even air plasma treatment, amine-functionalized surfaces can be formed.[72,75–79] Halogenated surfaces were also obtained using bromine (Br_2), bromoform ($CHBr_3$), krypton (Kr) and tetrafluoromethane (CF_4) plasma treatments.[70,80] Thiol groups were successfully incorporated on carbon nanotubes by H_2S/He plasma exposure.[81] Air plasma treatment, was shown to produce oxygen containing species on polyethylene (PE) surface, the addition of H_2O in the air discharge could lead to amine groups formation on gallium nitride (GaN) surfaces, providing enough hydrogen atoms to form amine groups.[77,82]

Tuning of parameters such as plasma treatment time shows an influence on the functional groups concentration. Via derivatization of amine-functionalized GaN achieved through humidified air plasma the formation of amine groups shows an increase with treatment time until reaching an optimum followed by a decrease of group concentration, likely to be due to surface oxidation after long time plasma exposure.[77] Same behavior was observed during thiol groups formation on carbon nanotubes; a maximum amount of thiol groups is observed after 4 minutes of exposition while a decreased amount is obtained for longer plasma treatment.[81]

However contamination due to residual gases in processes can lead to the incorporation of other groups. Indeed, the presence of residual oxygen might lead, as it is the case for surface modification of ultrananocrystalline diamond, to a competition between the introduction of the desired functional group, *i.e.* here, amine groups formation and non-desired oxygen-containing groups such as OH groups on the surface.[79]

Plasma gas treatment processes are versatile. A simple gas switching, with the same process, allows to change the surface properties of materials, for example, as reported by Recek *et al.* using CF_4 or O_2 to modify PET surfaces, introducing fluorine or oxygen species (COOH, etc.) and making the surface respectively hydrophobic or hydrophilic.[70] Shen *et al.* studied ammonia, carbon dioxide and oxygen plasma using the same process reactor to determine the most suitable gas treatment to optimize the production of functional groups on poly(lactide-co-glycolide) for the best biomolecule immobilization properties showing versatility of the plasma technique.[72]

Although the large majority of the plasma treatments are performed at low pressure, atmospheric pressure processes are also used to form functional groups. Dielectric Barrier Discharge process is exploited to treat PP with oxygen plasma to form oxygen-containing species, *i.e.* COOH and hydroxyl groups.[71] As generated groups either at low pressure and even more during atmospheric pressure treatment may experience hydrolysis and oxidation, the exploitation of those functional groups has to be done promptly after plasma treatment.[69]

Table 4: Summary of plasma treatments, based on various gases, allowing the formation of different functional groups on a wide range of materials.

Functional group	Plasma gas(es)	Substrate	Plasma reactor	References
Br, Kr	Br_2/$CHBr_3$/Kr	Highly-Ordered Pyrolitic Graphite (HOPG)	LP RF	[80]
F	CF_4	Polyethylene Terephthalate (PET)	LP RF 27.12 MHz	[70]
COOH/C=O	O_2	Cyclo Olefin Polymer	LP RF 13.56 MHz	[69]
COOH/C=O/OH	Air	Polyethylene (PE)	LP DBD	[82]
COOH/C=O/OH	O_2	Polyethylene Terephthalate (PET)	LP RF 27.12 MHz	[70]
COOH/C=O/OH	CO_2	Poly(lactide-co-glycolide)	LP RF 13.56 MHz	[72]
COOH/C=O/OH	O_2	Poly(lactide-co-glycolide)	LP RF 13.56 MHz	[72]
COOH/OH	O_2	Polypropylene (PP)	AP DBD	[71]
OH	H_2O/O_2	Polycaprolactone (PCL)	LP 40 KHz glow discharge	[74]
OH	H_2O/O_2	Polyethylene Terephthalate (PET)	LP 40 KHz	[73]
NH_2	NH_3	Polyethylene (PE)	LP 70 kHz glow discharge	[75]
NH_2	NH_3/N_2	Ultrananocrystalline diamond	LP RF 13.56 MHz discharge	[79]
NH_2	Air (75% relative humidity)	Gallium Nitride (GaN)	LP 35 kHz glow discharge	[77]
NH_2	NH_3	Graphite	LP RF 13.56 MHz	[76]
NH_2	NH_3	Poly(lactide-co-glycolide)	LP RF 13.56 MHz	[72]
NH_2	NH_3	Polystyrene (PS)	LP 13.56 MHz	[78]
SH	H_2S/He	Carbon nanotube	AP DBD	[81]

3.3 Plasma polymer deposition

The plasma deposition of coatings is also possible to provide 1) reactive species and functional groups on surfaces for biomolecule immobilization 2) polymerized matrix for the formation of biocomposites.

3.3.1 Plasma polymer for interfacial reactions

3.3.1.1 Radical-containing coatings

The plasma polymerization of a coating-forming precursor, under bombardment of ions and excited species, may lead to the entrapment of reactive radicals in the bulk layer and offer a reactive surface for further biomolecules immobilization. Indeed, Gogoi *et al.* show the possibility to form free radicals containing layers polymerizing aniline under silver sputtering in a magnetron.[83] Plasma-immersion ion implantation processes are also widely used, using a low voltage bias (up to 1 keV) during plasma polymerization.[49] Extensive works on radicals containing layers are reported in the works of Bilek *et al.* highlighting the versatility of this method.[41] This technique is substrate independent compared to ion implantation on a polymeric surface. Plasma polymer coating containing radicals can be deposited over metals, ceramics and polymers and do not alter the underlying material properties. The deposition time and then the layer thickness have an influence on the lifetime of radicals in the layer, as radicals are formed all along the plasma polymer deposition.[49]

3.3.1.2 Functionalized plasma polymer coatings

The deposition of plasma polymerized coatings from precursors bearing functional groups are of main interest, they can be deposited on a large range of materials and the wide choice of available precursors allows forming plasma polymerized coatings with various functional groups. The used precursors generally contains a cross-linking, matrix-forming polymerizable part, such as double carbon bonds, *i.e.* vinyl or allyl, or any easily breakable bonds, i.e. Si-O-CH_3, …, and another other part, bearing specific moieties, offering the introduction of various types of functional groups (**Table 5**).[40]

Table 5: Example of used precursors for functionalized plasma polymer deposition.

Functional	**Precursors**

groups	
Amine	(3-Aminopropyl)triethoxysilane (APTES)[84,85]; (3-Aminopropyl)trimethoxysilane (APTMS)[86]; Allylamine[87–100]; Pyrrole[101]; Cyclopropylamine (CPA)[102,103]; propargylamine[104]
Carboxyl	Acrylic acid (AA)[105–113]; Maleic anhydride/Vinyltrimethoxysilane (MA/VTMOS)[114,115]
Thiol	Allyl mercaptan[116]
Aldehyde	Propionaldehyde[117,118]; Propionaldehyde/Ethanol[119]; 3-Vinylbenzaldehyde[120]
Halogens	2-Bromoethylacrylate[121]; 1-Bromopropane[122,123]
Epoxy	Glycidylmethacrylate (GMA)[124–128]; Allyl glycidyl ether (AGE)[129–132]
Active ester	Pentafluorophenyl methacrylate (PFM)[68,133]
Quinone	Dopamine Acrylamide/Vinyltrimethoxysilane (DOA/VTMOS)

The main used plasma processes are cold plasmas, allowing the deposition on heat sensitive substrates. They are generated either at low pressure commonly using RF (13.56 MHz) discharge or atmospheric pressure (AP), using Dielectric Barrier Discharge, although relatively very few works exploit this latter promising process. While low-pressure plasma reactors allow easy injection of both high vapor pressure precursors and low vapor pressure ones (necessitating in some cases to heat the precursor hence limited to non-heat-sensitive precursors). At atmospheric pressure, the injection is more challenging. Although high vapor pressure precursors can easily be injected through the use of bubblers or heating systems (**Figure 4A**), low vapor pressure ones are more demanding and versatile injection methods were developed, now allowing the introduction of many precursors (**Figure 4B**). The main method referenced in the literature is an aerosol-assisted method consisting in the injection of a spray/mist composed of small liquid droplets (nanometer to micrometer range) in the AP discharge.[47] Other introduction methods report the plasma exposure of previously droplets spray-coated surfaces.[134] As plasma is a highly reactive medium, due to the presence of many energetic species, plasma parameters during plasma deposition such as plasma power or electrical signal (pulsed or continuous) have to be finely tuned to find a compromise between generation of activated species, allowing the cross-linking of the plasma polymer, ensuring the stability of the layer, and the retention of the monomer functional groups, providing surface chemical reactivity.

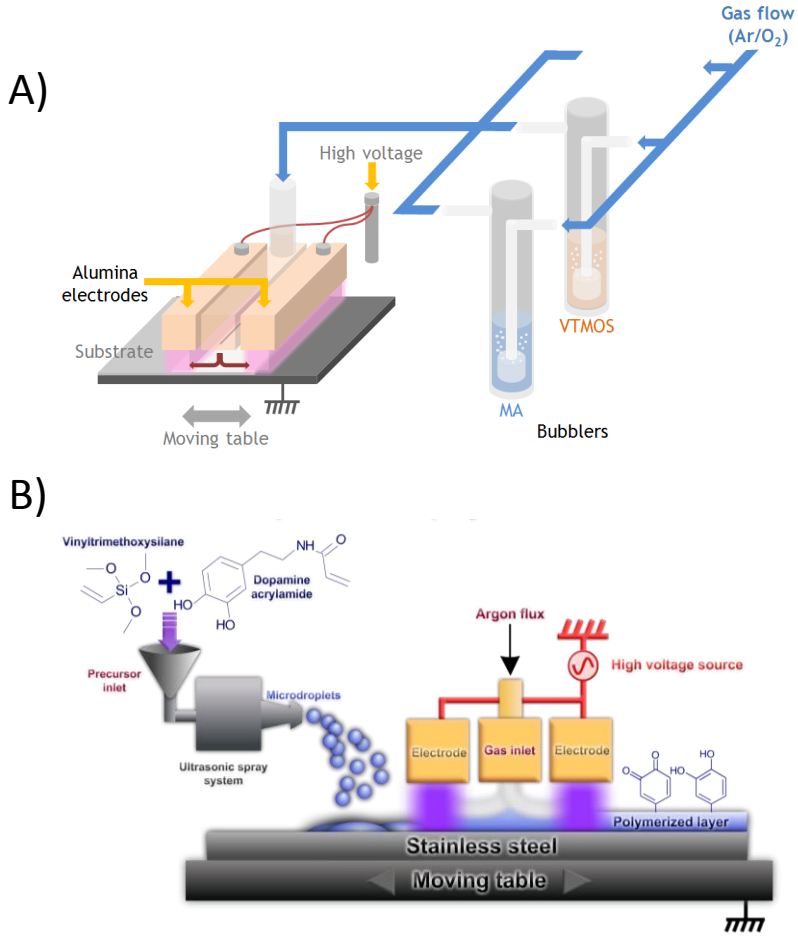

Figure 4: Schematic representation of atmospheric pressure DBD reactors for A) carboxylic functionalized MA-VTMOS plasma co-polymer formation using bubblers system B) aerosol liquid-assisted deposition of quinone/catechol functionalized layer.

Plasma power is shown to have an influence on the amount of functional groups. An increased power will favor the breaking of the monomer bonds, due to a high density of energy. Indeed, the study of aldehyde containing coatings, obtained from propionaldehyde plasma polymerization at low pressure with a RF discharge, show that, at low power (5W), functional groups are retained, while increasing power to 40 W is likely to lead to the destruction of the groups.[118] Low power (10W) was also shown to favor the deposition of primary amine and secondary amine rich coatings using a low pressure reactor.[89] The same behavior is observed at atmospheric pressure for the deposition of a MA-VTMOS copolymer layer using a DBD, where a continuous 5W deposition leads to a 13% COOH content while at 30 W only 5.5% groups are remaining.[114]

However, not only the functional groups concentration is influenced by plasma power, but also the surface morphology. Indeed, the continuous plasma exposure leads at the

same time to the polymerization of the monomer and to the etching of the surface. MA-VTMOS copolymerized layers deposited in continuous mode from 5W to 30W clearly show the influence of the increasing power on the roughness of the layer.[114] Roughness and carboxylic content can then be modified tuning only power parameter.

In comparison to the continuous mode where layer deposition, monomer fragmentation and surface etching are occurring simultaneously, the pulsing of the discharge allows favoring the polymerization of monomers, and more specifically for double bonds bearing monomers, favoring free radical polymerization. Indeed, when the plasma is on (t_{on}), the excited species are generated, among which fragmented monomers, surface radicals and metastables are able, during the time off (t_{off}), to initiate the polymerization of the newly fed monomer.[40] Commonly the percentage of the "time on" duration of the plasma is called the duty cycle: D.C. (D.C. = $t_{on}/(t_{on}+t_{off})$).

Extensive works mainly carried out at low pressure report on the interest of pulsing the discharge to achieve a higher monomer structure retention in the deposited film. The polymerization of 3-vinylbenzaldehyde, using a RF discharge, to form surface aldehyde groups clearly shows that, derivatizing the functional group with fluorescent DNA probe, a short t_{on} coupled with a 4 ms t_{off} (D.C. = 1%)) lead to high fluorescence intensity, hence higher functional groups density.[120] Similarly, highest densities of fluorine containing groups were obtained depositing plasma polymerized pentafluorophenyl methacrylate (PFM) using a pulsed plasma at a duty cycle of about 4%.[133] Plasma polymerization of 2-bromoethylacrylate also shows that pulsed plasma leads to superior structural retention of the monomer compared to continuous mode and interestingly a slight difference of t_{on} from 30 µs to 20 µs with a fixed t_{off} (10 ms) is highlighted to also have an influence on the layer chemistry.[121] Epoxy and amine functionalized layers were also preferably deposited by pulsed plasma polymerization.[87,129] Thierry *et al.* show that allyl glycidyl ether pulsed polymerization leads to good epoxy retention (highlighted by a conservation of the oxygen content compared to the monomer content) using a 25W pulsed discharge (D.C. = 5%) compared to a continuous treatment displaying a significant loss of oxygen of about 44%. However a 50% duty cycle is shown in this work to lead to the same poor functional group retention as continuous wave deposition, highlighting the interest to decrease the duty cycle value and having $t_{on} << t_{off}$.[129]

While a large majority of the plasma coatings are obtained at low pressure, atmospheric pressure deposition, using dielectric barrier discharge reactors (AP-DBD), are also reported for the formation of functional layers. The influence of the discharge pulse

previously exposed is supported by analogous results obtained with these atmospheric pressure plasma processes. Carboxylic groups containing MA-VTMOS copolymer layer deposition, using a time off of 40 ms with a time on discharge of 10 ms (D.C. = 20%) at 20 W allows obtaining 13.5 % COOH while 20W in continuous mode leads to 6.4% of COOH groups.[114] The deposition rate is however slower. Extensive works were performed on the influence of the pulse duration on the epoxy functionalized plasma polymerized Glycidyl methacrylate (GMA). Klages *et al.* first showed that a 1 ms t_{on}/49 ms t_{off} AP DBD treatment (D.C. = 2%) leads to highest retention of the monomer structure, as observed by conventional low-pressure glow-discharge activated plasma deposition.[124] Those results are further supported by Camporeale *et al.* showing that the reduction of the duty cycle leads to high epoxy content and smooth layers.[125] Further investigations were then performed in order to produce layers with ultra short plasma pulses to reach very low duty cycle values to further minimize influence of plasma on the polymer. Boscher *et al.* thanks to a fast voltage rise of about 70V/ns are able to generate nano second range homogeneous discharges with high energy electrons able to produce many free radicals favoring the initiation of a free radical polymerization reaction during a long time off.[126] Glycidyl methacrylate free radical polymerization was performed with duty cycles as low as 0.003% with plasma pulses of 100 ns and time off of 33 ms. This method allows obtaining polyGMA polymer layers with molecular weight up to 30000 g/mol. [127] To summarize, $t_{on} << t_{off}$ appears to be the key parameter to form layers with a high retention of functional groups, generating highly reactive species during a short t_{on}, and allowing the polymerization during a long t_{off}, limiting the influence of plasma during the deposition.

However, Manakhov *et al.* show, polymerizing cyclopropylamine, that, interestingly, pulsing the discharge, in their case, leads to undesirable side functional groups, such as nitriles and imines, while only lowering the power in continuous mode do not show significant amount of those groups.[102] This shows the versatility of plasma and the large possibilities of parameters tuning to reach the desired surface properties.

It was shown at atmospheric pressure that the injected amount of precursor might also have an effect on the final layer chemical properties (*cf.* Chapter 6). Indeed, for a given power, the increase or decrease of precursor amount will vary the ratio energy per monomer. Hence, as presented in chapter 6, in an aerosol-assisted plasma reactor, low injected amount of precursor can lead to a high fragmentation of the monomer. In our case, the silane compounds tend to be fragmented into inorganic silica-like network at low injected precursor whereas at high injected amount of precursor the network is likely to be more organic.

The plasma polymerization in presence of a selected co-monomer is also an alternative solution to tune the layer properties, allowing to increase the layer cross-linking rate, thus its stability in different solvent, and allowing the retention of the co-monomer structure and functional groups. As an example, plasma polymerized acrylic acid-ethylene layers present higher stability during H_2O immersion test than acrylic acid plasma polymerized layer, together with high carboxylic group density.[110]

Compared to low pressure deposition, atmospheric pressure plasma processes are still poorly reported in the literature for the synthesis of plasma polymer coatings for biomolecule immobilization purpose. Although rare, other functional surface moieties introduction is reported using atmospheric pressure processes. Among those works, carboxylic group functionalized surfaces are obtained through acrylic acid polymerization through an atmospheric pressure glow discharge plasma jet [113] and also through deposition of a MA-VTMOS copolymer with a DBD reactor.[114] Amine functionalized coatings were also synthesized at atmospheric pressure comparing influence of two different DBD discharges on the layers properties, showing the formation of stable coating in aqueous media using a post discharge configuration compared to poorly stable coating with direct discharge.[86] Quinone functionalized layers are obtained through an AP aerosol assisted system (*cf.* Chapter 5 & 6).

3.3.2 Plasma polymer for biocomposites formation

Plasma techniques are not only used to form reactive surfaces for the immobilization of biomolecules but are also of main interest to form biomolecules-containing coatings. Indeed, the low temperature of generated plasma, the possibility to perform deposition at atmospheric pressure and the large range of precursors for the formation of polymer coating with different properties is a good source of inspiration for the formation of biocomposites. The formation of biodegradable coatings, such as poly(lactic acid) polymerized layers, interesting for embedded biomolecules control leaching [135] or the synthesis of water stable polymeric networks, obtained from precursors such as ethylene, ethyleneglycoldimethacrylate (EGDMA), methacrylic acid - ethyleneglycoldimethacrylate (MAA-EGDMA), tetramethyldisiloxane (TMDSO) or acetylene, able to durably entrap biomolecules are possible.[47,136–140] Those biomolecules can be entrapped during the formation of a plasma polymeric network under plasma discharge introducing the biomolecule with a spray system.[47] A compromise on the deposition conditions may be

found to allow both polymerization of the matrix and to retain properties of biomolecule and structure.[136,140] The swollen properties of some layers, such as MAA-EGDMA layers, can also be exploited to trap biomolecules through immersion of those layers in biomolecule solutions.[138] Plasma barrier coatings can also be deposited on previously adsorbed or immobilized biomolecules in order to entrap them. For this purpose, plasma versatility allows controlling the deposition time and then the thickness of the layer, a key parameter to control the porosity and permeability of the barrier layer.[137,139] Thanks to the soft conditions possibly reached in plasma reactors, some works show that plasma techniques are promising to directly deposit coatings from the cross-linking of biomolecules themselves or through biomolecules co-polymerization with various other molecules. Amino acids, such as L-tyrosine are exposed to a RF plasma at low pressure to form layers in a custom-built flowing afterglow plasma chamber. In order to show the ability to copolymerize a biomolecule with different co-monomers for a fast, direct and facile biomaterial formation purpose, L-tyrosine is co-polymerized with monomers such as acrylonitrile, 2-hydroxyethyl methacrylate and also titanium tetraisopropoxide.[141] Other types of coatings formed by plasma polymerized peptides were also investigated. Solutions containing small peptides, such as RGDS, KRSR and IKVAV, are injected into a plasma reactor and ionized thanks to a corona plasma discharge under low pressure to successfully form coatings.[142] All these latest developed strategies reported in the literature are presented with further details in the part 4.2 of this chapter.

4. Biomolecule immobilization strategies on plasma modified surfaces

Plasma techniques and their versatility provide a powerful tool to develop original strategies for the immobilization of biomolecules. As referenced in the literature, the immobilization can be performed either through irreversible or reversible interactions with a plasma modified surface (**Table 6**) or through the formation of a biocomposite coating with biomolecules either entrapped or cross-linked in it.

Table 6: Functional groups obtainable by plasma surface modification and possible interactions for biomolecule immobilization.

Surface groups	**Biomolecule surface interactions**		**Biomolecule reactive groups**	**References**
	Reversible	Irreversible		
Carboxyl Amine	Adsorption	Multistep covalent bond formation using linkers (EDC/NHS, Glutaraldehyde, …)	- Non-specific for adsorption - Linker dependent for covalent multistep formation	[23,143]
Thiol	Disulfide bond formation: cleavable in specific solution	-	Thiol	[81]
Aldehyde	Imine formation with amine groups : reversible in acidic conditions	Covalent bond formation: reductive amination of imine bonds	Amine	[31]
Epoxy	-	Direct covalent bond formation	Thiol/Amine	[125]
Halogen	-		Thiol/Amine	[121]
Active ester	-		Amine	[133]
Quinone	-		Thiol/Amine/Imidazole	[144]
Radicals	-		Non-specific	[41]

4.1 Biomolecule surface immobilization techniques

4.1.1 Irreversible immobilization

A large variety of functional groups are obtainable by plasma surface modification of materials to form irreversible covalent bonds with groups present in biomolecules. Among those, some are poorly reactive and necessitate additional steps through a multi-step reaction, using for example linkers, to form a covalent bond with the biomolecules while some other groups have direct affinities with moieties present on biomolecules and can form covalent bonds (**Table 6** and **Figure 5**).

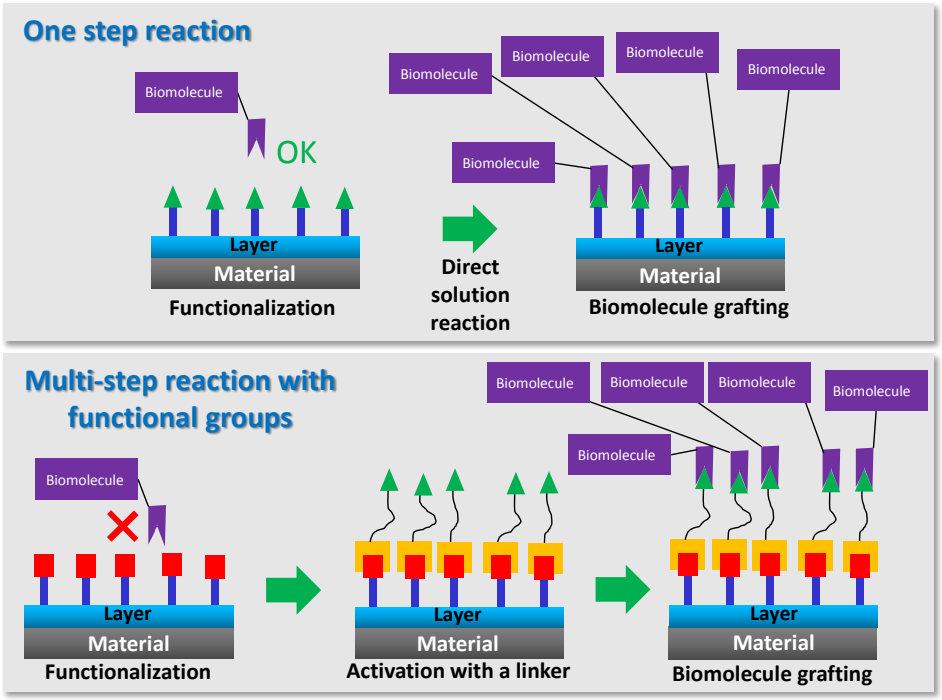

Figure 5: Scheme of one step and multi-step reaction immobilization of biomolecule over a plasma modified surface.

4.1.1.1 Direct covalent binding

The easiest method to immobilize biomolecules on a surface is the direct reaction with groups present on the modified surfaces.

Firstly, the simple ions impacts over surfaces during plasma treatment or coating deposition leads to the entrapment of radicals species in the material surface which can be exploited for the biomolecule direct binding.[145] The radicals diffuse to the surface and unpaired electrons reaching the surface are able to lead to the formation of a covalent bond

with a biomolecule reaching the surface (**Figure 6**).[146] Gogoi *et al.* exploit the plasma generated free radicals present on the surface of a polyaniline layer polymerized under silver sputtering to immobilize Trypsin.[83] Bilek *et al.* successfully immobilized various type of enzymes on PIII treated surfaces.[146–149] The covalent binding properties of PIII treated surfaces are however likely to be affected by the plasma species, while argon and nitrogen plasma lead to good immobilization properties, oxygen and hydrogen addition may lead to a reduction of electron mobility in the material and are suspected to lead to the formation of less reactive radicals toward biomolecules functional groups.[41] Reaction kinetic of radicals with biomolecules is really fast and within the first minute of the reaction grafting is performed. Radical lifetime can be tuned changing the bias modifying the implantation depth of the radicals but their lifetime is relatively short, thus requiring exposing the treated surfaces to the biomolecules solution right after treatment.[150] The surfaces containing radicals exposed to air leads nevertheless to the formation of reactive peroxide groups still exploitable for biomolecules grafting. Enzymes are however grafted non-specifically on surface radicals, no specific functional group present on the biomolecule is targeted to control the orientation, sometimes at the expense of the enzymatic activity.

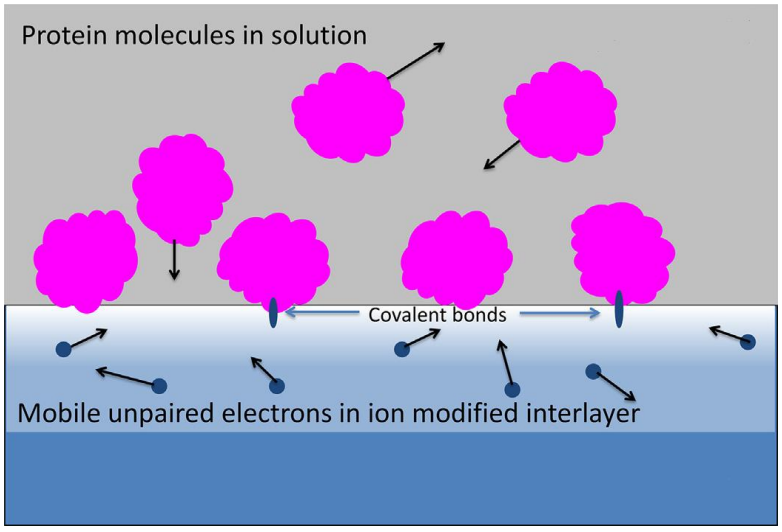

Figure 6: Biomolecules immobilization on plasma treated through covalent bond formation on the surface containing free electrons. Adapted from [49]

Extensive research work has been performed and several types of functional groups are reported to be obtained by plasma techniques. Those groups, with well-known chemical reactions possibilities, allow a better control and understanding on the interactions between functional groups present on biomolecules and on the modified surface. The optimization of

the biomolecules immobilization and a higher probability to conserve the conformation of some sensitive biomolecules such as proteins and peptides and to avoid blocking their active site during immobilization can be achieved.

Among the numerous obtainable groups with plasma techniques, the aldehyde groups allow the formation of Schiff bases, *i.e.* imine bond, with amine groups present on biomolecules.[46] Reductive amination can be performed in an additional step to reduce the imine bond to an amide bond using a reducing agent such as sodium cyanoborohydride to prevent detachment of biomolecule from the surface. However some authors prefer to skip this step, considering that grafting is mainly irreversible even without reduction of imine bonds due to the numerous imine bond formed with certain biomolecules like proteins.[31] Immobilization of biomolecules onto aldehyde plasma polymer is reviewed by Coad *et al.* and shows numerous works assessing the interest for those type of coatings.[31] Among the literature, such coatings were successfully exploited for the immobilization of poly(L-lysine)-g-poly(ethylene glycol) to form protein-repellent surface [117] and of streptavidin, to form bonds with biotin.[118] A method to obtain protein gradient was developed by forming a reactive layer with a gradient of reactive aldehyde groups together with non-reactive hydroxyl groups thank to copolymerisation of propionaldehyde and ethanol.[119] NH_2 terminated DNA was immobilized on both plasma polymerized 3-vinylbenzaldehyde and on an aldehyde-functionalized cyclo-olefin polymer surface activated by an oxygen plasma.[69,120] The use of a reducing agent is mandatory in these two latter cases to form a stable covalent bond to avoid hydrolysis and provide durability to the DNA immobilization as only one imine bond is formed between DNA and the surface.

In order to form strong direct covalent bonds with biomolecules to impart long lasting immobilization and properties to surfaces in a wide range of conditions, some specific groups can be exploited. Numerous works were reported to form epoxy containing plasma polymer by plasma deposition method. Epoxide groups can form covalent bond with nucleophilic groups such as amine or thiol groups according to the biomolecule solution used during immobilization step (T, pH). Some works were led and epoxide functionalized coatings were shown to be a platform for biomolecules immobilization. Sugar-based surfactants are immobilized (70°C during 72h) on a glycidyl methacrylate (GMA) plasma grafted over a PP surface to form surfaces suppressing protein adsorption and platelet adhesion.[65] Pulsed plasma polymer coatings are also widely studied, mainly formed using glycidyl methacrylate and allyl glycidyl ether, allowing the covalent immobilization of biomolecules for several

applications. For biosensing application, an amine-modified DNA probe was successfully immobilized in mild basic conditions (0.1 M $NaHCO_3$). [128] In this work, Chu *et al.* highlight that the surrounding environment parameters are really important for the successful immobilization of biomolecules. Indeed, they show that even though previous works led by other groups suggests immobilization of DNA probes in a stronger basic environment (0.1 M KOH), in their case, immobilization was successfully achieved only in mild conditions. Several other peptides/proteins for different applications were then successfully immobilized on epoxy groups using commonly used phosphate buffered saline or phosphate buffer in mild conditions at pH ranging from 6 to 8.5. Lysozyme as well as several antimicrobial proteins, *i.e.* Nisin, Trp11, 4K-C16 and Dispersin B were immobilized for antibacterial-antibiofilm application.[125,129,131] Herceptin was also immobilized in order to capture cancer cells.[130] Anti-EpCAM monoclonal antibodies were immobilized in order to capture tumor cells.[132] Antibiotics degrading surfaces were developed thanks to immobilizing laccase and β-lactamase on surfaces and showed long lasting properties during weeks and under high speed water flux.[126] The immobilization of laccase on epoxy containing coating, and then the degradation duration, was shown to be higher for an immobilization operated at pH 8.5 than pH 7, while Dispersin B for those two different pH showed the same activity. Those differences are then likely to be due to a rearrangement specific to the structure of the enzyme, once again highlighting the importance in some cases to optimize both surface deposition conditions and grafting conditions.[125]

Despite halogen functionalized surfaces also appear as a promising route for the immobilization of biomolecules, few works are reported. Chlorine and bromine are well-known and are reactive leaving groups for nucleophilic substitution reaction allowing grafting biomolecules containing NH_2 and SH groups.[80] McGettrick *et al.* through pulsed polymerization of 2-bromoethylacrylate were able to functionalize surfaces with Br groups for the immobilization of thiol terminated DNA probes. As nucleophilic substitution mechanism is either acid or base catalyzed, optimal immobilization were obtained at ph 4 and pH 9, with fewer grafting in neutral pH.[121] Such layers were found to be stable in the whole studied range, from 3 to 10, used for biomolecules immobilization. Marchesan *et al.* formed microchannels and microwells presenting reactive and non-reactive areas thanks to UV nanolithography of plasma polymerized 1-bromopropane coating and were able to immobilize different peptides and amino acids.[123]

The formation of plasma functionalized coatings bearing active esters presenting good leaving groups suitable for nucleophilic substitution are poorly reported efficient strategies for the immobilization of biomolecules. Duque *et al.* and Cifuentes *et al.* provided interesting surface active esters bearing pentafluorophenyl groups for covalent immobilization, thanks to plasma polymerization of pentafluorophenyl methacrylate (PFM).[68,133] Such coatings were able to immobilize peptides such as IKVAV and proteins, *e.g.* BSA, fibrinogen in PBS. Cifuentes *et al.* in their work compared the immobilization of BSA on plasma polymerized PFM and on coating formed by PFM grafting on argon plasma treated surface. Higher hydrophobic surfaces were obtained through PFM deposition, although higher number of exposed groups seems available in this case for BSA immobilization, hydrophobic surface leads to high conformal change in the BSA structure.

Recently, a new highly reactive functionalized plasma deposited layer containing quinone groups has just been reported. These groups are originally involved in the remarkable adhesion properties of mussel feet to surfaces, and reported to lead spontaneously in mild conditions to the formation of covalent bonds with biomolecules containing amino, thiols or imidazole groups through Schiff base formation and Michael addition. The work of Mauchauffé *et al.* (*cf.* Chapter 5 and 6) appears as a pioneer work in the deposition, at atmospheric pressure, of plasma polymerized quinone functionalized surfaces for the grafting of biomolecules. The covalent immobilization of a New Delhi metallo-β-lactamase 1 (NDM-1) enzyme were performed on a plasma polymerized coating for antibiotic degradation application (*cf.* chapter 5). The enzyme was engineered adding a Histidine-tag, containing 6 imidazole groups at the extremity of the enzyme to favor the orientation. Unspecific oriented immobilization of a β-lactamase from *Pseudomonas aeruginosa* on these surfaces was also shown to lead to successful amoxicillin degradation (*cf.* chapter 6). The combination of the plasma quinone functionalized surface deposition process, providing a green, fast, versatile method to deposit such coatings and the covalent immobilization of NDM-1 led to robust surfaces conserving both their enzymatic properties and mechanical stability up to 2 weeks under a flux of 30 km/h in presence of BSA proteins (*cf.* chapter 5).

The one step direct binding of biomolecules was also reported in rare papers on carboxylic functionalized surfaces. Indeed, carboxylic, amino or thiol groups do not lead to a one step covalent bond formation in aqueous mild environment (ambient temperature and pH

~7-8) but are known to possibly undergo reaction in presence of catalyst or at elevated temperature. To impart antibacterial properties to polymeric surfaces against gram- and gram+ bacteria such as *E. Coli* and *S. Aureus*, chitosan was covalently immobilized on COOH functionalized polymeric surface generated via air plasma treatment.[71,82] The reaction between COOH from the surface and hydroxyl group from chitosan is catalyzed according to the Fischer method in acidic conditions in acetic acid (2%). The main drawback of this method, explaining why it is not widespread in the literature is the weakness of the majority of biomolecules such as proteins, which may lose their conformation in such acidic conditions. Rivolo *et al.*, however suggest, grafting fluorescent protein on a COOH functionalized surface, that covalent grafting through nucleophilic attack can be performed without catalyst in PBS mild conditions (pH 7.4) thanks to the increase in the polarization of the C=O bond due to hydrogen bonds between adjacent COOH groups, hence improving the nucleophilic character of the carbon atom. However, as reported by the author, the covalent bond formation proof through this method is not unambiguously supported by experimental data.[112]

Carboxylic groups and amine groups (respectively present on the surface and on the biomolecule and *vice versa*) can form amide bonds at elevated temperature (greater than 100°C), in presence of a dehydrating agent or in specific solvents (*e.g.* toluene), in total disagreement with the range of use, *i.e.* stability, of the majority of biomolecules.[20,151] That is why to provide a controlled and easy way to durably immobilize biomolecules on such layers, conserving their properties, multistep strategies are studied, involving intermediate compounds to activate the unreactive surface to allow the reaction in mild condition (ambient temperature and pH 5-8).

4.1.1.2 Multi step binding

A large part of the literature reports on the formation of COOH and NH_2 functionalized surfaces by plasma techniques. Indeed, those surfaces attracted a large interest because of their interesting properties notably to provide biocompatibility to materials.[92,152] The combination of these remarkable properties with the diversified properties of immobilized biomolecules is then an interesting solution to either enhance or give new applications perspectives to the surfaces. The numerous investigations led this last decade allow now to be able to finely tune both layer surface group density and stability in aqueous environment to fulfill the desired criteria for durable biomolecule immobilization.[103]

However as carboxylic groups and amine groups do not react spontaneously with functional groups present in biomolecules an additional step is needed, requiring the use of intermediate reactive compounds called linkers (**Table 7**).

Table 7: Example of used linkers for the immobilization of biomolecules on plasma functionalized surfaces.

Linker	Covalent bond formation between :		Ref.
N,N'-Diisopropylcarbodiimide (DIC)	COOH	NH_2	[143]
1-Ethyl-3-(3-dimethylaminopropyl)carbodiimide (EDC)	COOH	NH_2	[143]
1-Ethyl-3-(3-dimethylaminopropyl)carbodiimide / N-hydroxysuccinimide (EDC/NHS)	COOH	NH_2	[114]
Trifluoroacetic anhydride (TFAA)	COOH	NH_2	[153]
Glutaraldehyde (GA)	NH_2	NH_2	[102,145]
Gallic acid activated with EDC/NHS	NH_2	NH_2/SH/Imidazole	[97]
Glycidyl methacrylate - poly(ethylene glycol) methacrylate copolymer (GMA-PEGMA)	NH_2	NH_2	[94]
Phenyldiisothiocyanate (PDITC)	NH_2	NH_2	[85]
Sulfosuccinimidyl 4-(N-maleimidomethyl)cyclohexane-1-carboxylate (SSMCC)	NH_2	SH	[79]

Carbodiimide compounds, such as N,N'-Diisopropylcarbodiimide (DIC) or the widely used 1-Ethyl-3-(3-dimethylaminopropyl)carbodiimide (EDC), are the main reported linkers for biomolecule immobilization on COOH functionalized plasma modified surfaces.[143] They allow the activation in aqueous or organic solvent of the surface carboxylic group to form amide bond with biomolecules. Reaction of carboxylic acid with the carbodiimide leads to the formation of an O-acyl isourea ester intermediate compound bearing a good leaving group compared to the OH bad leaving group. This linker hence directly allows the primary amino groups present on the biomolecule to perform a nucleophilic attack and form an amide bond with the activated surface without introduction of other compounds in between, it is then called a zero-length linker.

This well-known reaction allowed Gubala *et al.* to efficiently immobilize NH_2 terminated DNA on both plasma treated cyclo olefin polymer (COP) and COOH plasma functionalized coating deposited on COP.[69] Quintieri *et al.* immobilized antibacterial bovine lactoferrin and lactoferricin B on acrylic acid based coating to form an active packaging to

control Mozzarella cheese spoilage by *Pseudomonas*.[110] Titania surface was functionalized and RGD peptides were immobilized for enhanced cell growth.[111] Insulin and heparin were also immobilized on modified PET surface to enhance respectively biocompatibility and hemocompatibility.[60]

As biomolecule accessibility and orientation are key parameters to have available active site of molecule and allow the development of efficient active surfaces. Multi-step processes are interesting to introduce spacer molecules between biomolecules and functionalized surfaces, allowing the right orientation, through specific groups reaction, and better mobility of the biomolecules. Their interest is reported throughout the literature, for example, through silanization of a surface, where the direct grafting of biomolecules on the surface did not allow the formation of active surfaces, while, introducing a spacer in a multi-step process, led to successfully active surfaces.[154] In order to further enhance the antithrombotic properties of insulin/heparin based strategies, poly(ethylene glycol) (PEG) and poly(ethylene oxide) (PEO) spacers was introduced between a carboxylic functionalized surface and the biomolecules through a 2 steps procedure, then allowing a better mobility of the proteins and conferring antifouling properties.[73] Those bis-NH_2 terminated spacers are immobilized on the carboxylic EDC activated surfaces, the NH_2 terminated resulting surface is then immersed in an EDC/biomolecule mixture allowing the activation of the COOH groups from the biomolecules. [54,74] Same procedure was exploited to successfully produce enhanced biocompatible surfaces through immobilization of RGD peptides with a PEG spacer molecule.[155]

However the reaction formation of the amide bond on EDC activated surfaces has a slow kinetic and the really unstable active esters can undergo several other reactions. Even though one of these reactions is the formation of a reactive anhydride groups in presence of another COOH groups, the hydrolysis of the active ester, the regeneration of carboxylic groups as well as the rearrangement of the O-acyl urea forming a stable unreactive N-acyl urea are likely to occur in aqueous solution, reducing the yield of the reaction.[156] To increase the stability of the intermediates reactive compounds and ensure a higher efficiency of the grafting method, N-hydroxysuccinimide (NHS) is added to the reaction to form a NHS ester through reaction of its hydroxyl groups on the EDC activated ester (**Figure 7**), providing a more stable leaving group and increasing the amide formation yield.[143]

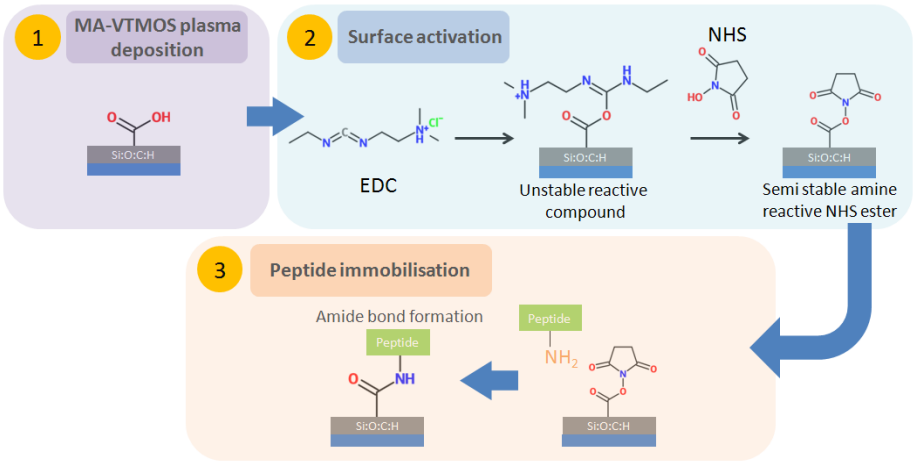

Figure 7: Carboxylic plasma functionalized surface activated with EDC/NHS zero-length linker for amine-bearing biomolecule immobilization.[114]

In the literature, the coupling of NHS with carbodiimide compounds like EDC, commonly noted EDC/NHS, is the main chemical route for surface coupling between amine and carboxylic groups, in mild conditions (pH 6-8), considering its efficiency and is widely used with plasma modified surfaces. Jafari *et al.* highlight that EDC/NHS provides an efficient way for specific immobilization of amino modified DNA.[106] Several other biomolecules were immobilized. Plasma deposited poly (acrylic acid) coatings (ppAA) are largely exploited and allow obtaining various new surface properties: intercellular signaling molecule delta-like-1 (Dll1) capture through mono-clonal antimyc-tag (9E10) antibody tethering[157], enhanced biocompatibility thanks to collagen, bovine serum albumin and fibronectin immobilization[105,153], antimicrobial properties through peptide LL-37 and nisin immobilization [113,114] and bone regeneration improvement thanks to rhBMP-2 immobilization [108]. Acrylic acid graft polymerized surfaces also allow the immobilization of chitosan and gelatin for enhanced endothelialization [59], collagen or silk fibroins for better biocompatibility [53,158] and chitosan-rose Bengal for antibacterial properties.[159]

However, EDC/NHS, being a zero-length linker, leads to the direct bonding of the biomolecule to the surface and this later may lack mobility to react in some applications. Mauchauffé *et al.* show that, for antibacterial purpose, nisin grafted on plasma co-polymerized coatings of maleic anhydride/vinyltrimethoxysilane presenting high roughness, is too closely grafted to the surface through EDC/NHS activation. The nisin immobilized in the valleys of the rough surface and lacking mobility is not able to ensure contact with bacteria to lead to antibacterial properties. Smoother layers, with easy accessibility of the

tethered biomolecules are shown to be totally bactericidal.[114] Introduction of spacer would then be an interesting solution to ensure surface activity. Those spacers are introduced either immobilized first on the surface through EDC/NHS strategies or directly immobilized on the biomolecules.[107,109]

Other types of COOH activation are reported. TFAA (Trifluoroacetic anhydride) activation, forming reactive anhydride reactive groups, was compared to EDC/NHS activation on ppAA coatings. EDC/NHS allowed higher activation of the surface for BSA immobilization and was the only activation allowing coupling with collagen, however the reasons for this behavior remain unknown to the authors.[153]

Amine functionalized surfaces are also widely reported in literature through plasma surface modification to provide a large variety of substrate materials new properties. Nowadays, amine functionalized layer properties can be tuned in a way to be resistant toward hydrolysis and to provide high densities of amine groups for biomolecule immobilization, hence being suitable for aqueous environment applications. As amino groups are not spontaneously reactive, either the surface activation or biomolecule groups activation is needed.

A 3 steps immobilization method developed by Nardulli *et al.* consisted in converting surface amine groups, generated by an ammonia plasma on polystyrene, to carboxylic groups through reaction with succinic anhydride for further activation with EDC/NHS to immobilize galactosamine to study hepatocyte cells response on these surfaces.[78]

Koegler *et al.* covalently grafted a polymerization macroinitiator on plasma polymerized polyallylamine surface through EDC reaction in order to initiate the free radical polymerization of modified polymerizable acrylamide terminated RGD peptides on the surface.[95]

Another 3 steps method is largely used, based on glutaraldehyde, a homobifunctional linker, terminated with two aldehyde terminal groups reactive toward amine groups through nucleophilic attack. This linker may first react with the amino surface and subsequently undergo imine formation with amine-bearing biomolecule (**Figure 8**). An additional reductive amination step is however needed to form a covalent amide bond. This method allowed immobilization of several biomolecules in mild conditions: NeutrAvidin (in de-ionized water) on Gallium nitride treated with air plasma [77], Trypsin was immobilized in PBS pH 6.8 on poly(allylamine) layer on silicon substrate and at pH 7.6 on ammonia plasma

treated PET followed by an imino groups reduction treatment.[75,90] Some works report using glutaraldehyde without reductive amination and without stability problem for certain applications. Indeed, cyclopropylamine plasma polymer was deposited onto quartz crystal microbalance to immobilize anti-HSA antibody in PBS at ph 7 to develop an efficient sensing application (**Figure 8**).[102]

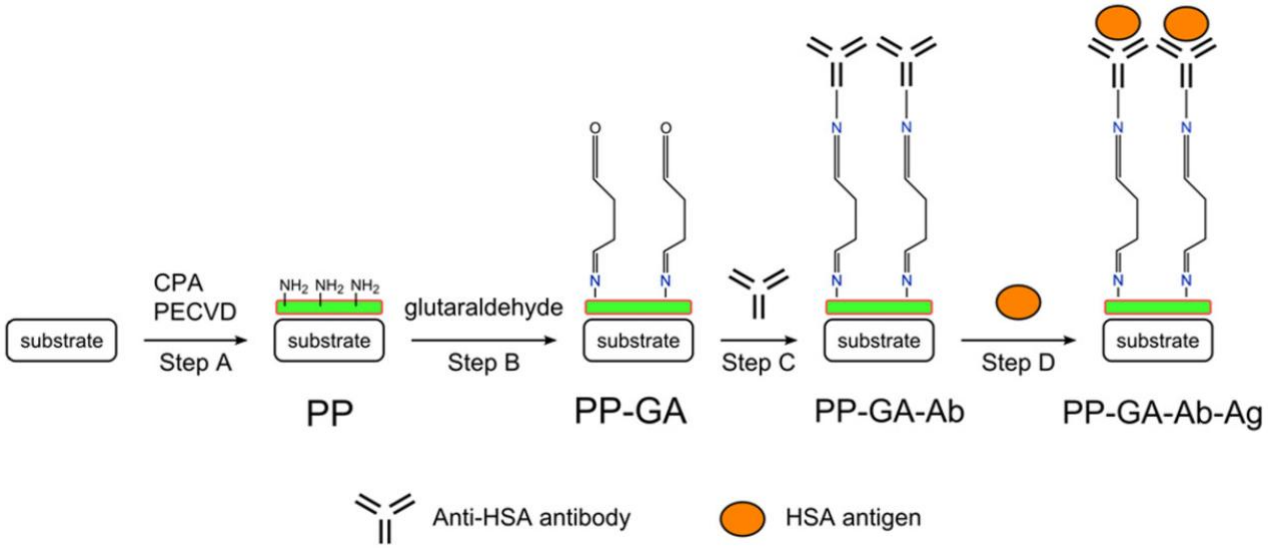

Figure 8: Scheme of antibody immobilization on amine functionalized surface through cyclopropylamine plasma polymerization using a glutaraldehyde linker.[102]

Vartiainen *et al.* also do not perform reduction step to immobilize glucose oxidase. They also go as far as proposing a one pot immobilization in a protein/glutaraldehyde mixture and this method interestingly leads to higher enzymatic activity compared to the 2 steps method but the risk to inhibit the active part of enzymes through this method is really high due to the side reactions and then the lack of control. Immobilization was performed in phosphate buffer at pH 7.2 and in acetate buffer at pH 5.6, showing a slightly higher activity at pH 5.6.[145]

Various other 2 step strategies are developed with the aim of reducing the number of steps. Yang *et al.* (**Figure 9**) activated a plasma polymerized polyallylamine surface through one pot grafting of gallic acid (3,4,5-trihydroxybenzoic acid) assisted by EDC/NHS providing surface quinone groups reactive in phosphate buffered saline for the immobilization of vascular endothelial growth factor (VEGF) for enhanced human umbilical vein endothelial cell growth.[97]

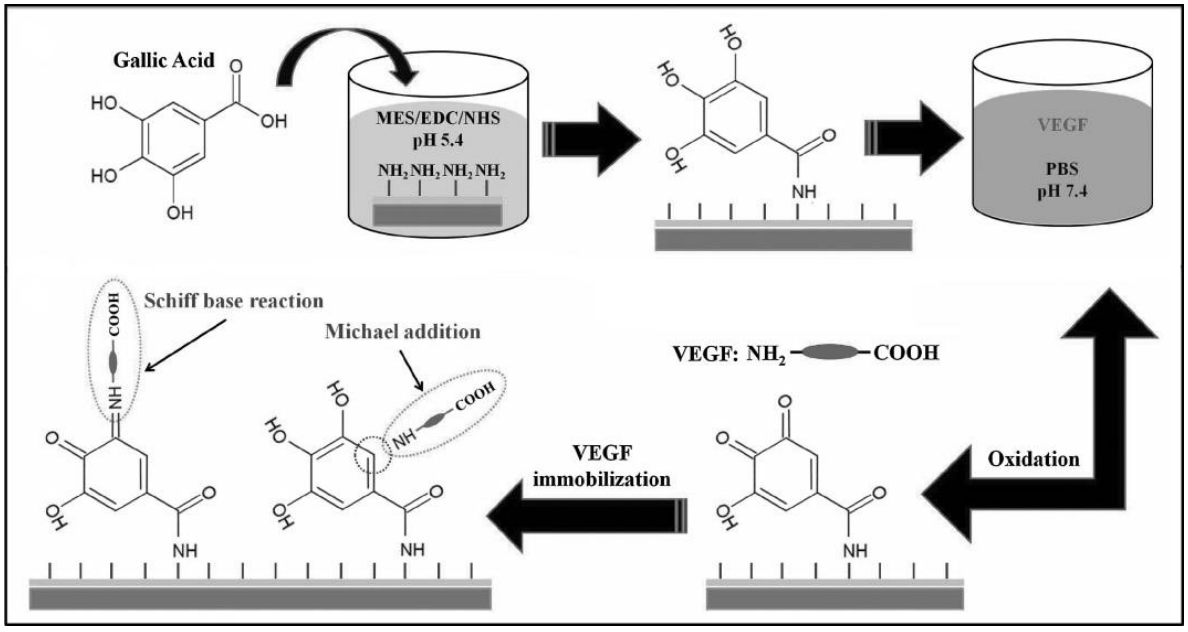

Figure 9: Scheme of vascular endothelial growth factor (VEGF) immobilization on plasma polymerized allylamine through surface activation with gallic acid assisted by EDC/NHS. Adapted from [97].

Kurkuri *et al.*, also working with plasma polymerized allylamine coating, are using a glycidyl methacrylate (GMA) - poly(ethylene glycol) methacrylate (PEGMA) (GMA-PEGMA) copolymer as reactive intermediate linker. This copolymer is either firstly synthesized and then deposited by dip coating or spin coating, or directly synthesized on the plasma layer through radical polymerization of both monomers with AIBN initiator. Indeed, GMA provide reactive epoxy groups toward amines. Hence, those groups allow the copolymer to be covalently immobilized on the amine functionalized surface and subsequently enable covalent anchorage of biomolecules.[94] Another two step in situ process, allowed immobilizing α-chymotrypsin in mild conditions on an ethylene diamine/propylene diamine graft polymerized surface thanks to the formation of a chlorine containing reactive intermediate through oxalyl chloride gaseous exposition.[67] Plasma co-deposited diamine and 3-aminopropyltriethoxysilane (APTES) layers on cycloolefin polymer are activated with phenyldiisothiocyanate, bearing two isothiocyanate groups readily reacting with amine groups, allowing the immobilization of amino terminated DNA.[85] This linker is also used on APTES plasma modified surface to immobilize capture antibody to develop immunoassays.[84]

Heterobifunctional linkers, such as sulfosuccinimidyl 4-(N-maleimidomethyl)cyclohexane-1-carboxylate (SSMCC), bearing on one side an amino reactive succinimide group and on the other side a thiol reactive maleimide group, are

exploited by Koch *et al.*. Amination of diamond surface through ammonia plasma allowed the grafting of a thiol bearing fluorescent compound thanks to SSMCC, hence showing the potential of such method to graft biomolecules.[79]

Instead of activating the surface, the activation of the biomolecule to make it amine-reactive can also be done in a prior step for a 2 steps immobilization. Dextran, a high molecular mass antithrombotic polysaccharide, is oxidized with sodium periodate to form aldehyde groups to allow the amine nucleophilic attack in water to form numerous imine bonds onto ammonia plasma treated graphite-encapsulated magnetic nanoparticles.[76] EDC/NHS activation of biomolecules is however widely used and remains one of the most famous methods for immobilization on NH_2 surface in 2 steps. This method is versatile and allowed obtaining hemocompatible surfaces through heparin activation/immobilization[87], antibacterial surfaces thanks to protein/peptide immobilization such as Nisin on APTMS layer [86], antithrombotic stent surfaces through grafting of hirudin derivative on polyallylamine coating [88] and biosensors application thanks to laccase grafting over a polyallylamine covered carbon-graphite electrode.[89] However using this method the latter work does not exclude the fact that intramolecular crosslinking can occur between biomolecules containing additional free groups during the EDC/NHS activation showing a lack of control.

Multi-step grafting is also a good way to overcome unspecific binding of biomolecules. Indeed, surfaces functionalized with reactive groups such as radicals or epoxy groups for example can interact independently with different functional groups from the biomolecules, whereas EDC/NHS activated COOH will react specifically with an amino group, allowing without biomolecule engineering to avoid grafting on active site.[143] It is also possible through multistep reactions to introduce different type of reactive functional groups on a surface originally composed of a single type of group to co-immobilize two types of biomolecules. Polyfunctional surfaces with carboxylic and benzenetriol groups were obtained by Yang *et al.* thanks to a multistep grafting of gallic acid. Carboxylic surface groups can bind specifically amine groups from the biomolecule through EDC/NHS activation while imidazole, thiol or amine groups of the biomolecule can only react on the oxidized benzenetriol group from gallic acid, involving the grafting of the second biomolecule to be performed in a separate step at a slightly alkaline pH. Co-immobilization of two different biomolecules, namely anti-CD34 antibody and vascular endothelial growth factor (VEGF) is then performed.[96]

4.1.2 Reversible immobilization

Either formed through direct or multistep reaction routes, covalent bonds formation offers stable long lasting immobilization, however the surfaces are hardly regenerable. That is why some research groups investigated reversible immobilization methods through weaker interactions. Despite the fact that some comparison between covalent and weak interactions show lower amount of immobilized biomolecules for adsorbed biomolecules [69], biomolecules are successfully immobilized on the surface and active. Indeed, Ardhaoui *et al.* show that physically adsorbed laccases present only about twice less activity than covalently immobilized ones.[89] However in some cases, such as presented by *Liang et al.*, adsorption can be a better option.[53] Biocompatibility comparison of silk fibroin immobilized on a graft polymerized acrylic acid film on PET through the use of a linker or on a plasma treated PET surface shows that after 5 days higher cell number is present on the adsorbed sample. While the covalent immobilization method appeared to be toxic for cells due to acrylic acid presence, long lasting properties are obtained with simple adsorption. Immobilization is likely due to the tuning of the surface properties occurring under plasma exposure such as roughness or hydrophilicity. Reversible methods are then potentially interesting for biomolecule immobilization and several plasma-based methods are reported in the literature. Depending on the targeted application, *e.g.* antithrombotic application, sensing application, cell endothelialization, etc; direct or multisteps methods, comprising adsorption, disulfide bond formation or metal affinities are reviewed here.

4.1.2.1 Adsorption

Reversible immobilization of biomolecules can be achieved through a mere adsorption on surfaces as a soft way to immobilize them. Biomolecules may have different interactive regions in their structure; indeed for example biomolecules such as proteins present complex structures, able to contain hydrophilic/hydrophobic, charged/neutral, polar/non-polar areas.[70] The material surface properties on which biomolecules have to be immobilized will then play an important role on the nature of the interactions between the surface and the biomolecule and on the biomolecule conformation, orientation or immobilized amount.[23] Indeed, as an example, if a surface is positively charged, then the biomolecule will tend to expose its negatively charged side toward the surface. Oppositely, hydrophilic surface will have affinities to hydrophilic domains of biomolecules. The overall

activity of the immobilized biomolecules can then be affected by the different orientations.[62] The surface functional groups density and roughness are parameters which can also influence the surface activity, modifying the amount of immobilized biomolecules. Structure conformation of these biomolecules is also strongly dependent on the strength of the interactions and on the number of reactive areas or groups present on the surface. It is worth noticing that biomolecules can present several areas with different properties and it is also the case for surfaces which can combine several chemical and physical properties, hence adsorption is more likely to be due to a combination of interactions and may be a complex phenomenon.

Adsorption is a really challenging reaction, as the successful adsorption of biomolecules and conservation of their properties involve finding a compromise between the properties of the biomolecules and the surface to keep the targeted activity. Using non-polar, high surface tension, charged surfaces or hydrophobic are known to lead to strong interactions to retain proteins on the surface, however this may result in a loss of conformation because of those too strong interactions and then to a loss of activities. However, as it is not covalently bonded to the surface, adsorption and desorption phenomenon may occur, either due to temperature, pH, ionic strength change or in presence of biomolecules with higher affinities with the surface, *e.g.* Vroman effect, hence depending on the environment of use the surface properties have to be chosen carefully regarding the targeted application.[160] The biomolecule/surface properties can be tuned to fulfill the desired criteria either modifying the surrounding environment (solution pH, ionic forces and temperature) of the biomolecules to tune their properties or/and modifying directly the surface properties. Plasma treatment and plasma deposition are really interesting methods because they allow obtaining easily a wide range of surfaces properties for reversible immobilization.

- *Plasma treatment*

The effect of roughness modification by direct surface plasma treatment were highlighted by Yeo *et al.*, studying the effect of an oxygen plasma discharge treatment over the properties of a HMDSO polymerized layer for protein adsorption.[161] Some areas of a hydrophobic HMDSO layer were etched by an O_2 discharge and led to enhanced proteins adsorption only on O_2 treated areas while the untreated areas did not lead to immobilization. No significant chemical changes could be observed by FTIR before and after plasma

treatment, however the increase of protein adsorption amount is shown to be due to a 5 times higher surface roughness after oxygen plasma treatment.

Shen *et al.* also used gas plasma treatment in order to modify the surfaces of poly(lactic-co-glycolic acid) (PLGA) surface to enhance the immobilization of recombinant human bone morphogenetic protein (rhBMP-2).[72] Surfaces were treated with ammonia, carbon dioxide and oxygen discharges. It was shown that the larger amount of rhBMP-2 was immobilized on oxygen treated surfaces and a fewer amount but still larger than the untreated PLGA surface was obtained with CO_2. In the case of ammonia treatment, less biomolecules were adsorbed than on the bare PLGA. As carbon dioxide and oxygen treatment lead to the formation of functional groups such as C=O, COOH, CO, increasing the negative surface charge in mild conditions hence leading to higher grafted amount of the positively charged rhBMP-2 protein in PBS solution at pH 7.4. Ammonia leads to the formation of positively charged species hence leading to fewer amount of adsorbed proteins because of electrostatic repulsion. The surface roughness is however increased due to plasma treatment and can have an influence. A difference of oxygen containing functional groups coupled to differences in the morphology of the surface might be an explanation to the observed differences between O_2 and CO_2 treatments. Adsorption of biomolecules is then here suggested to be dependent both of chemical composition and surface morphology.

O_2 and CF_4 plasma treatment were used to modify the surface of polyethylene terephthalate (PET) in order to make respectively the surface hydrophilic or hydrophobic.[70] Both treatment leaded to an enhancement of the amount of immobilized proteins (albumin and cell-culture medium proteins) compared to bare PET however a higher immobilized amount and then a higher efficiency was observed for the surfaces treated with oxygen plasma. In term of adsorption rate, fastest adsorption occurred on O_2 treated surface. Even though hydrophobic surfaces are reported to lead to higher adsorption, this rule cannot be generalized and depend on the biomolecule. The immobilization of chitosan for antimicrobial purpose were also favoured on hydrophilic surfaces, thanks to the formation of oxygen containing functional groups such as COOH and OH on a plasma treated surface. In this work the authors show that the release of the biomolecules are influenced by an increase of both pH and temperature, suggesting that at least a part of the biomolecules are linked to the surface through hydrogen bonds.[71] These works illustrates the complexity of biomolecules/surfaces adsorption interactions occurring and the utility of the versatility of

plasma treatment to finely tune the desired interaction.

- *Plasma deposition*

Polymerized layers are also exploited for the immobilization of biomolecules. Some groups try to introduce amino groups on materials through the formation of plasma polymerized layers to exploit the protonated amino groups NH_3^+ charge properties to immobilize biomolecules. Yang *et al.*, willing to immobilize heparin for anti-thrombotic application show that the pH of incubation (tuned from pH 5 to 7) of a plasma polymerized allylamine layer during the immobilization step strongly influences the amount of bound heparin. The adsorption amount increases with the decrease of pH. At pH 5, due to an increased protonation degree of amino groups on the surface, higher amount of heparin bearing COO^- (pKa ~3.3) and SO_3^- (pKa ~1-1.5) groups at this pH are adsorbed (**Figure 10**).[7,98] Following the same protocol, DNA aptamers were immobilized on plasma polymerized allylamine layers to enhance cell endothelialization.[99] However those studies do not focus on the direct influence of plasma parameters to tune the surface groups density. It was shown by Zhang *et al.* and He *et al.* that amino groups densities can be optimized to reach the desired properties, modifying the applied power during the deposition of respectively allylamine coatings for the elaboration of aptamers immobilized based sensors for thrombin detection and propargylamine based coatings for DNA sensing.[100,104]

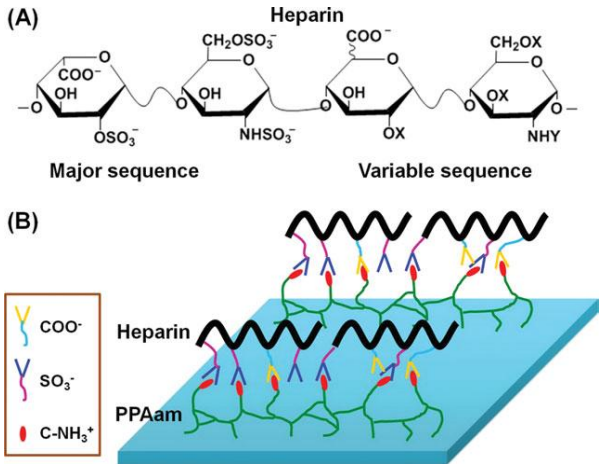

Figure 10: Scheme of heparin (A) and subsequent adsorption on amine functionalized surface through interactions between NH_3^+ and COO^-/SO_3^- charged groups (B).[98]

Alternatively, charge surfaces of polypyrrole conductive coatings deposited by plasma-polymerization at low pressure with a RF discharge were exploited in order to enhance the immobilization of DNA for sensing application.[101] The low plasma power polymerization allows keeping the overall properties of the polymer through the pyrrole structure conservation and was found to allow an optimal amount of immobilized DNA. Indeed, the high amount of positively charged N^+, after immersion in PBS at 7.4 allows high number of electrostatic interactions between DNA and pyrrole matrix.[162] However in another work, Zhang *et al.* show that electrostatic interactions, even if responsible in this case of the DNA adsorption enhancement, might have little influence on the immobilization of other biomolecules.[163] Indeed, a higher amount of bovine serum albumin proteins (BSA) were observed to adsorb on coatings deposited at high power, presenting few N^+ species but showing higher hydrophobicity properties and higher roughnesses, both known to also have an effect on biomolecules immobilization. Even if the immobilization on these coatings is mainly driven by hydrophobic and roughness effect, the optimization of the pH during the immobilization step is also shown to have a slight influence, a higher amount of BSA is adsorbed at lower pH due to increased protonation of nitrogen compounds and negative charge of BSA. [164] Zhang *et al.* then clearly show that charges, surface hydrophobicity and roughness can be altogether involved in the biomolecules immobilization mechanisms. The versatility of plasma allows the fine tuning of plasma parameters to find the right compromise between input power, gas flow rate and polymerization time, together with the tuning of the biomolecule immobilization medium parameters, to control the adsorption mechanisms.[165]

4.1.2.2 Disulfide bonds

A work by Schofield *et al.* exploit the reversibility of the disulfide bond to immobilize a thiol-terminated DNA over a plasma polymerized polyallylmercaptan coating in sodium chloride/sodium citrate (SSC) buffer at pH 4.5. The formation of disulfide bonds is interesting due to its cleavable capacity. Indeed, the S-S bond can be cleaved in solution (using a boiling solution of TrisCl, SSC and sodium dodecyl sulfate (SDS)) to regenerate the SH groups and the coatings were shown to be reutilized up to 5 times for immobilization of DNA without loss of immobilization efficiency.[116]

4.1.2.3 Metal ions affinity binding

Based on the same principle of a technique employed for protein separation: Immobilized metal affinity chromatography (IMAC), exploiting the affinity of phosphoproteins for certain metal ions, Fowler *et al.* developed a plasma based method to reversibly immobilize phosphoproteins, for sensing application in microfluidic devices, to isolate or pre-concentrate proteins.[28] Surfaces were micropatterned by plasma polymerization of acrylic acid and allylamine in order to have functionalized area with carboxylic groups and amine groups respectively, groups present in the commonly used nitrilotriacetic acid (NTA), iminodiacetic acid (IDA) or tris-(carboxymethyl)-ethylenediamine (TED), chelators present in chromatography affinity columns. An additional step of immersion of those layers in a 20 mM gallium nitrate solution in 0.1M sodium acetate/ 1M NaCl at pH 3.8 is performed to immobilize gallium ions on the deprotonated surface carboxylic groups. Those plasma polymerized thin films of acrylic acid (ppAAc) are then able to coordinate gallium to subsequently selectively immobilize phosphoproteins solubilized in solution of 33.3/33.3/33.3/ 0.1 vol% ddH_2O/acetonitrile/methanol/acetic acid (**Figure 11**). Due to the weak interactions between protein and metals, it is possible, using a washing step at high pH (100mM ammonium chloride, pH 10) to remove proteins from the surface and regenerate the plasma polymer surface.

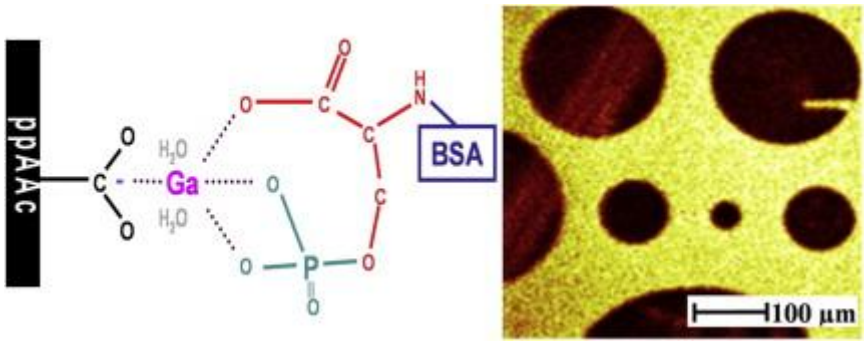

Figure 11: Plasma polymerized poly(acrylic acid) coating coordinates gallium and allows selective immobilization of phosphoproteins. ToF-SIMS allows the visualisation of the chemical selectivity of the developed metal affinity-based method.[28]

Another study, by Salim *et al.*, demonstrates the use of plasma polymerized acrylic acid coating (ppAA) as a simple and direct method to immobilize metal ions to screen phosphometabolites and develop a metabolite array for detecting phosphometabolites coupled

with ToF-SIMS analysis (**Figure 12**).[166] Immobilization of gallium, zirconium, cobalt, copper, zinc, nickel, iron, and chromium were performed on the plasma polymer coatings. Maximal adsorption of gallium, zirconium, copper, chromium, cobalt, nickel and iron was obtained at pH 4 on the negatively charged ppAA surface while zinc optimal adsorption occurred at pH 6. Those coatings are subsequently exposed to metabolites (phospho- and non-phosphometabolites) and compared. High adsorption of phosphometabolites was observed for gallium and zirconium. Some non-specific binding of metabolites to zirconium is observed, however less than in the case of gallium and for both in a lesser extent than for iron, copper, nickel, chromium, cobalt and zinc. This study hence shows the possibility to use a plasma polymerized acrylic acid layer, with a wide range of metals to tune the specific and non-specific interactions for further biomolecules immobilization.

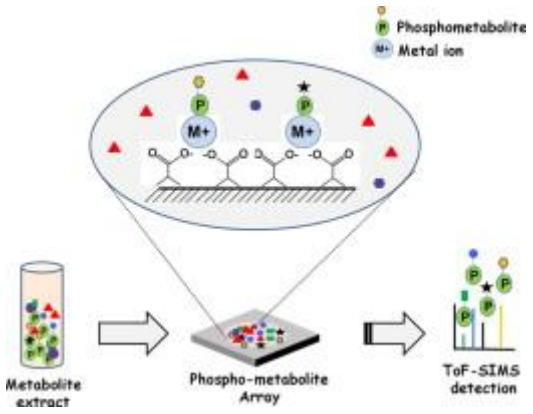

Figure 12: Metal ions affinity binding of different phosphometabolites on various metal coordinated surfaces for sensing purpose coupled with ToF-SIMS analysis.[166]

Those reversible immobilization methods used for protein sensing could then easily be applied to selectively reversibly immobilize enzymes to impart properties to surfaces such is the case in the work of Vesali-Naseh *et al.*. They develop a glucose biosensor through the functionalization of carbon nanotubes with thiol groups thanks to a H_2S/He plasma for the immobilization of gold nanoparticles subsequently exploited to immobilize glucose oxidase, able to form complex with the gold surface thanks to the six cysteine residues in its structure.[81]

4.2 Biocomposite formation

Compared to the richness of literature in the field of biomolecules immobilization on plasma coated or treated surfaces, few works are reported on the formation by plasma techniques of biomolecule-containing layers. Entrapment of biomolecules, formation of coating from the biomolecule itself and cross-linking of the bio-compounds with monomers are developed and reported in the following sections.

4.2.1 Entrapment of biomolecules

The entrapment of biomolecules in plasma formed layers attracted attention. They can be trapped using several strategies leading to reversibly and irreversibly immobilized compounds.

4.2.1.1 Irreversibly entrapped

To reduce the number of steps to immobilize biomolecules on a material, in a pioneering work, Heyse et al.[47] developed an atmospheric pressure one step plasma process aiming at injecting simultaneously an aerosol composed of biomolecule solubilized in PBS with a matrix forming precursor (in the gas phase) into a plasma DBD discharge to entrap the biomolecule into a plasma polymerized matrix. A compromise between power and frequency were found to allow the immobilization and the structural retention of BSA-FITC and allophycocyanin into a matrix formed from polymerized acetylene. Thanks to the fluorescence emission properties of those entrapped proteins, the structure conservation is assessed as well as the homogeneous distribution in the layer, assessing the potentiality of this method for the one step immobilization of a large variety of biomolecules.

In another work, the author shows the possibility to use this strategy to immobilize enzymes.[140] Glucose oxidase and lipase were immobilized in a polyacetylene matrix and alkaline phosphatase was immobilized in a pyrrole matrix. As the elevation of temperature is only few degrees Celsius during the plasma deposition, all type of enzymes can be entrapped without or with little activity loss. The author's hypothesis is the formation of solvent droplets shuttles protecting the proteins from the plasma heat and species. The immobilization method allows increasing the enzyme stability, indeed, the alkaline

phosphatase, already stable at elevated temperature, increases its temperature stability through entrapment in the pyrrole matrix. Only 50% of its original activity is lost after 2h at 150°C in a dry environment compared to the free form enzyme losing half of its activity after only 30 minutes at 90°C.

Among the entrapment methods, some groups developed multi steps methods. Charged polyelectrolyte gels obtained by multilayer wet chemical deposition are a good environment for the immobilization of enzymes.[137] They allow conserving enzymes activities and thermal stabilization through interactions with the gel. Even though enzyme controlled release by pH induced layer decomposition, hydrolysis or charge changes are really interesting properties; the use of such gel for applications as sensing, where time stability is needed, is challenging. To avoid desorption of an alkaline phosphatase (AP) from a polyelectrolyte gel layer of Hyaluronic Acid (HA) and poly-L-lysine (PLL), Amorosi *et al.* produce a plasma polymerized barrier layer from an atmospheric dielectric barrier discharge, made of plasma polymerized ethylene glycol dimethacrylate (ppEGDMA). The tuning of the plasma parameters allows controlling both the enzyme leaching and the diffusion of paranitrophenyl phosphate (PNP), the targeted chemical compound to react with the enzyme. A thin deposited layer (30 nm), do not avoid the leaching of the enzymes (**Figure 13**) while increasing of layer thickness tend to allow the retention of the enzyme and a too thick layer (300 nm) reduces the diffusion rate of PNP into the gel for enzymatic reaction. Layers of intermediate thickness allow then the successful entrapment and diffusion of PNP for enzymatic catalysis.

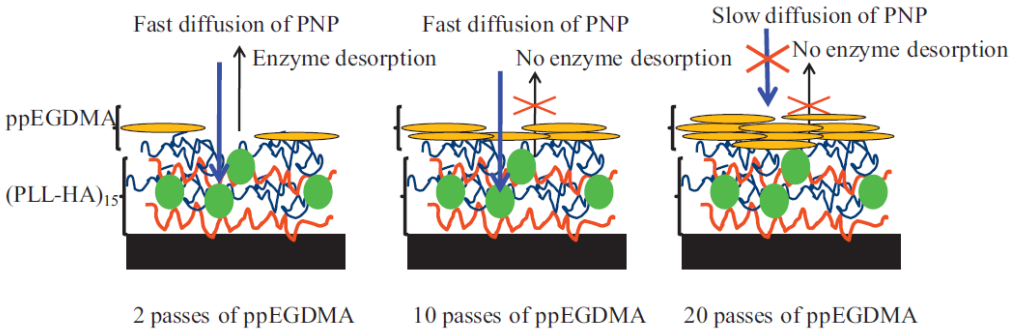

Figure 13: Scheme showing the ppEGDMA barrier coating thickness tuning for control leaching of alkaline phosphatase from polyelectrolyte gel and controlled diffusion rate of paranitrophenyl phosphate (PNP) to be reacted with the enzymes. [137]

In a recent work, Elagli *et al.* [139] compared the activity levels of an entrapped β-galactosidase following three different routes of entrapment using a low pressure plasma reactor operating with a RF plasma remote afterglow discharge (**Figure 14**) : i) tetramethyldisiloxane (TMDSO)/ethanol solution containing the enzymes is vaporized and plasma polymerized in a one-step procedure ii) enzymes are solubilized either in ethanol or in 0.02 M acetate buffer and adsorbed on silicon and subsequently overcoated in a second step by a plasma polymerized TMDSO coating to protect the enzymes from leaching and allowing the migration of the target molecule to degrade iii) enzymes, solubilized either in ethanol or in 0.02 M acetate buffer are adsorbed on a 200 nm precoated TMDSO film on the silicon substrate and overcoated with a second plasma polymerized TMDSO coating, leading to a "sandwich" entrapment of the enzyme. All the employed methods show an activity through the successful hydrolysis of ortho-nitrophenyl- β -D-galactopyranoside (o-NPG) and resorufin- β -D-galactopyranoside (RBG). However the one step process shows a reduced enzymatic activity compared to the others methods due to an uncontrolled amount and loss of injected enzyme with the spray process. The best activity was obtained depositing enzymes on the bare silicon in ethanol with then the deposition of an over coating of TMDSO, clearly showing an influence of the material surface interactions on the enzyme activity. The thickness of the layer once again is the key parameter to limit the amount of leached enzymes: thicker layers leading to fewer enzymes leaching.

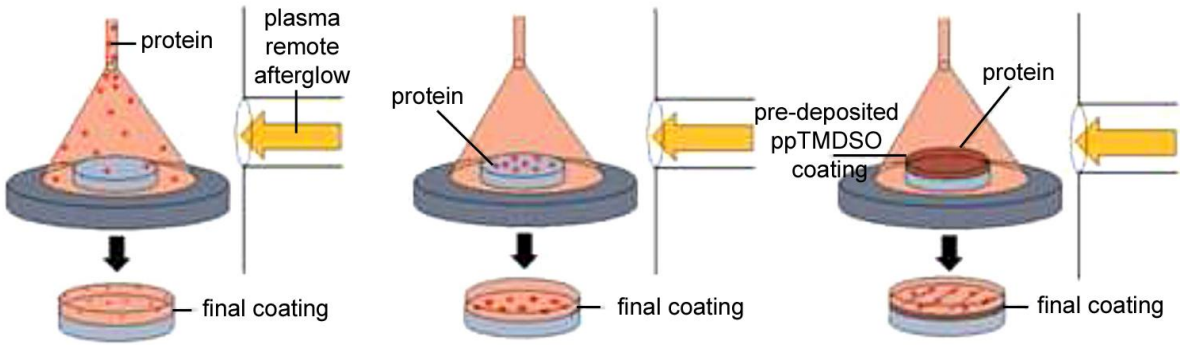

Figure 14: Scheme of the three different ways for the immobilization of biomolecules developed by Elagli et al.[139]

4.2.1.2 Reversibly entrapped

For the development of a biosensor, Amorosi *et al.* exploited the properties of swelling of a plasma deposited polymer to immobilize enzyme by migration in the layer (**Figure 15**).[138] A copolymer of methacrylic acid (MAA) with ethylene glycol dimethacrylate (EGDMA) (ratio 80/20%) was formed by plasma polymerization at atmospheric pressure, this polymer present a porous structure and carboxylic groups able to lead to weak interactions with enzymes and a high water stability. An enzyme, *i.e.* alkaline phosphatase, was immobilized and its enzymatic activity was followed monitoring the production of paranitrophenol due to the enzymatic hydrolysis of paranitrophenyl phosphate (PNP). The enzyme diffusion across the film was confirmed via depth-profile ToF-SIMS analysis and laser scanning confocal microscopy, to diffuse across the layer. The enzyme remains active after immobilization. Due to a higher COOH content on the top surface more enzymes are found to be present on the surface. The mechanism of binding is discussed and supposed to not be only due to electrostatic interactions of enzyme with $COOH/COO^-$ groups and can be also attributed to the mere entrapment of enzymes in a nanoporous network formed in the layer, as suggested by the observed migration of enzyme across the layer. Moreover the desorption of enzymes occurring during and after hydrolysis assay, suggests that the enzymes are encapsulated in the pores or by weak interactions like hydrogen bonds.

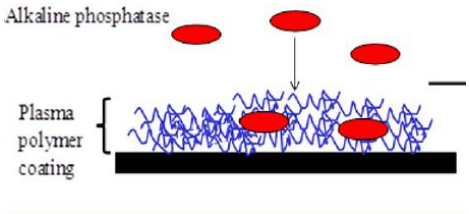

Figure 15: MAA-EGDMA plasma polymer coatings present swelling properties for the entrapment of biomolecules such as Alkaline Phosphatase. [138]

Single step methods were also investigated for the reversible immobilization of biomolecules. Indeed, in order to form surfaces presenting a good response for cell growth, Da Ponte *et al.*, synthesized coatings based on an atmospheric pressure one-step aerosol method (with the same reactor configuration as Heyse *et al.*[47]) through the injection of an aerosol of a mixture of precursor/biomolecule directly in a dielectric barrier discharge to entrap biomolecules in a matrix.[135] In this article a biocompatible and biodegradable plasma polymerized polylactic acid coating entrapping elastin, a protein present in the extracellular

matrix of mammals known to mediate cells interactions, was synthesized. Parameters settings were tuned in a way to retain lactic acid structure as well as elastin structure. The main parameter to retain the structure and more specifically carboxylic and ester groups, involved in the biodegradation of the polymer, was found to be the aerosol amount in the feed. In addition, the performed analyses clearly enlighten the presence of elastin throughout the layer, hence presenting an interesting method to form biodegradable coating with controlled biomolecule leaching for further applications.

One work highlights the possible modifications of the biomolecules due to plasma interaction during the biocomposite formation. Palumbo *et al.* developed lysozyme-embedded polyethylene coatings able to release the immobilized protein and show interest about the protein damages.[136] MALDI-TOF MS analysis on enzymatically digested Lysozyme-embedded samples with trypsin shows that most of the proteins remain unaltered except some amino acid residues such as methionine and tryptophan that are likely to be oxidized by oxidant species generated such as oxygen radicals.

4.2.2 Cross-linked biomolecules coatings

The development of quick and straightforward methods to reduce the number of steps by directly depositing coatings formed mainly by biomolecules attracted some attention and few papers are available in the literature. Plasma assisted deposition of cross-linked biomolecules coatings are mainly developed at low pressure.

Anderson *et al.*, after showing the successful deposition of polymerized amino acids layers, showed the potential of plasma deposition at low pressure for the copolymerization of amino acids with other monomers to form cross-linked layers.[141] PECVD copolymerization of sublimated L-tyrosine amino acids was performed with different co-monomers, *i.e.* acrylonitrile, 2-hydroxyethyl methacrylate and titanium tetraisopropoxide in order to develop a fast, direct and facile way for biomaterial formation. The obtained stable layers demonstrate the feasibility of the copolymerization of amino acids with synthetic material through a one-step and solvent free method.

RGDS (arginine-glycine-aspartic acid-serine), KRSR (lysine-arginine-serine-arginine), and IKVAV (isoleucine-lysine-valine-alanine-valine), peptides cell adhesion promoter for tissue engineering purpose, were separately deposited by Balasundaram *et al.* on anodized nanotubular titanium using molecular plasma deposition (MPD) (**Figure 16**).[142] A corona discharge ionizes a sprayed solution containing the peptide in a low pressure reactor. A voltage bias, between injection needle and surface to coat, induces the deposition of the peptides. Due to the stability of short peptides compared to proteins, the main biomolecules properties was conserved during deposition. After contact with osteoblast cells, the coated layers with RGDS and KRSR show an increased osteoblast densities compared with uncoated titanium substrate and a non-cell adhesive peptide (RGES) coated on anodized nanotubular titanium substrates, hence showing the potential of this method to coat rapidly in a single step any material.

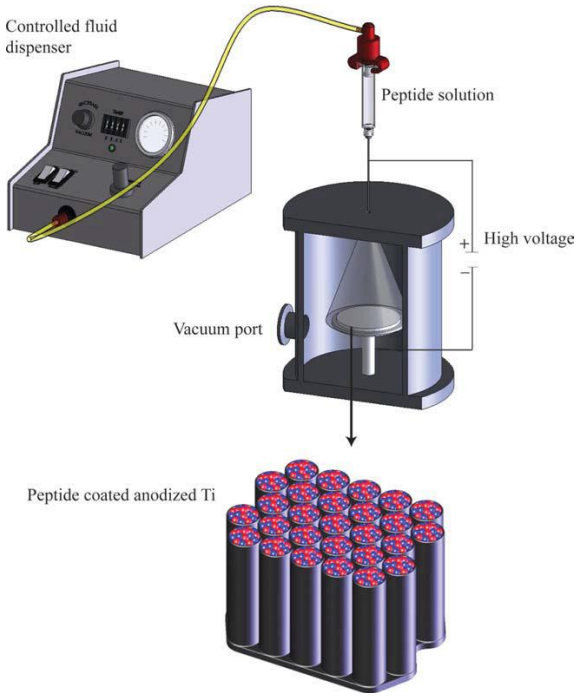

Figure 16: Scheme of the molecular plasma deposition (MPD) reactor used for the deposition of peptide-based coatings.[142]

A sublimation method is also used by Vasudev *et al.* for the deposition of diphenylalanine, to form vertically aligned nanotubes over a surface in a low pressure reactor assisted by a RF discharge.[167] Tunable morphologies and aspect ratio of the nanotubes are obtainable by tailoring the PECVD deposition parameters.

At atmospheric pressure, however, it is worth noticing that Heyse *et al.* do not exclude the possibilities of covalent bond formation between biomolecules and matrix through their developed aerosol assisted one-step method originally employed for simple biomolecules entrapment.[47,140]

5. Conclusion

Since the earliest works on plasma surface modification in the 1960s, marvelous progresses have been achieved in the field of plasma treatment and plasma layer deposition. Extensive works have been done and currently surface chemistry and morphology of numerous types of materials can be finely tuned for interfacial reactions enhancement. Nowadays, the bio inspired technologies attract both scientific community and companies attention. Biomolecules immobilization is of great interest to give new properties to surfaces for a wide range of applications, *e.g.* in medical field, water treatment, food processing… Plasma techniques provide sustainable, versatile and easily up scalable ways to replace non-environmentally friendly processes now employed for surface modification. Numerous plasma methods are reported in the literature and provide a plethora of possibilities for the irreversible or reversible biomolecules surface immobilization. Recent works show strategies ranging from direct immobilization by a single or multi-step method on functionalized surfaces to more elaborated immobilization strategies leading to the formation of biocomposites via entrapment in a plasma formed matrix or through plasma polymerization and cross-linking of biomolecules. However, when it comes to the industrial upscaling of such methods, challenges remain. Indeed, the mass production of numerous different biomolecules is still a limiting point at the moment. At the level of the biomolecule immobilization also, stability and durability in real conditions are still to be assessed. One of the major challenges however is the optimization of the production process of such layers. Indeed, despite all the interesting and original immobilization strategies reviewed in this chapter obtained thanks to the versatility of the deposition processes, it is worth noticing that a large majority are performed at low pressure, hence clearly showing a huge lack in the atmospheric plasma techniques field for biomolecule immobilization. This method, well known to show higher potential for upscaling purpose because easily implemented in continuous processes, needs deeper investigations. The following five chapters of this manuscript will then report on our works performed at atmospheric pressure, using a

Dielectric Barrier Discharge set-up for the modification of surfaces for biomolecules immobilization.

References

[1] K. S. Toohey, N. R. Sottos, J. a Lewis, J. S. Moore, S. R. White, *Nat. Mater.* **2007**, *6*, 581.

[2] E. Munch, M. Launey, D. Alsem, E. Saiz, *Science (80-.).* **2008**, 1516.

[3] B. Ji, H. Gao, *J. Mech. Phys. Solids* **2004**, *52*, 1963.

[4] Z. Guo, W. Liu, B.-L. Su, *J. Colloid Interface Sci.* **2011**, *353*, 335.

[5] H. Lee, B. P. Lee, P. B. Messersmith, *Nature* **2007**, *448*, 338.

[6] P. S. Nigam, *Biomolecules* **2013**, *3*, 597.

[7] S. Murugesan, J. Xie, R. J. Linhardt, **2008**, *000*, 80.

[8] K.-M. Song, S. Lee, C. Ban, *Sensors (Basel).* **2012**, *12*, 612.

[9] M. Rinaudo, *Prog. Polym. Sci.* **2006**, *31*, 603.

[10] S. Prabhu, E. K. Poulose, *Int. Nano Lett.* **2012**, *2*, 32.

[11] A. J. Domb, I. Yudovin-Farber, J. Golenser, N. Beyth, E. I. Weiss, *J. Nanomater.* **2010**, *2010*, DOI 10.1155/2010/826343.

[12] J. Davies, D. Davies, *Microbiol. Mol. Biol. Rev.* **2010**, *74*, 417.

[13] Y. J. Gordon, E. G. Romanowski, A. M. McDermott, *Curr. Eye Res.* **2005**, *30*, 505.

[14] G. Batoni, G. Maisetta, F. Lisa Brancatisano, S. Esin, M. Campa, *Curr. Med. Chem.* **2011**, *18*, 256.

[15] W. H. Geerts, D. Bergqvist, G. F. Pineo, J. a Heit, C. M. Samama, M. R. Lassen, C. W. Colwell, *Chest* **2008**, *133*, 381S.

[16] A. Prieto, M. Möder, R. Rodil, L. Adrian, E. Marco-Urrea, *Bioresour. Technol.* **2011**, *102*, 10987.

[17] K. V. R. Reddy, R. D. Yedery, C. Aranha, *Int. J. Antimicrob. Agents* **2004**, *24*, 536.

[18] X. Punet, R. Mauchauffé, M. I. Giannotti, J. C. Rodríguez-Cabello, F. Sanz, E. Engel, M. A. Mateos-Timoneda, J. A. Planell, *Biomacromolecules* **2013**, *14*, 2690.

[19] P. Taylor, J. N. Hansen, W. E. Sandine, **2009**, 37.

[20] P. V. Iyer, L. Ananthanarayan, *Process Biochem.* **2008**, *43*, 1019.

[21] C. Mateo, J. M. Palomo, G. Fernandez-Lorente, J. M. Guisan, R. Fernandez-Lafuente, *Enzyme Microb. Technol.* **2007**, *40*, 1451.

[22] O. Kirk, T. V. Borchert, C. C. Fuglsang, *Curr. Opin. Biotechnol.* **2002**, *13*, 345.

[23] F. Poncin-Epaillard, T. Vrlinic, D. Debarnot, M. Mozetic, A. Coudreuse, G. Legeay, B. El Moualij, W. Zorzi, *J. Funct. Biomater.* **2012**, *3*, 528.

[24] J. N. Talbert, J. M. Goddard, *Colloids Surf. B. Biointerfaces* **2012**, *93*, 8.

[25] S. Datta, L. R. Christena, Y. R. S. Rajaram, *3 Biotech* **2012**, *3*, 1.

[26] D. Alves, M. Olívia Pereira, *Biofouling* **2014**, *30*, 483.

[27] D. C. Kim, D. J. Kang, *Sensors* **2008**, *8*, 6605.

[28] G. J. S. Fowler, G. Mishra, C. D. Easton, S. L. McArthur, *Polymer (Guildf).* **2009**, *50*, 5076.

[29] B. Brena, P. González-Pombo, F. Batista-Viera, *Methods Mol. Biol.* **2013**, *1051*, 15.

[30] L. Cao, *Curr. Opin. Chem. Biol.* **2005**, *9*, 217.

[31] B. R. Coad, M. Jasieniak, S. S. Griesser, H. J. Griesser, *Surf. Coatings Technol.* **2013**, *233*, 169.

[32] F. Costa, I. F. Carvalho, R. C. Montelaro, P. Gomes, M. C. L. Martins, *Acta Biomater.* **2011**, *7*, 1431.

[33] J. M. Goddard, J. H. Hotchkiss, *Prog. Polym. Sci.* **2007**, *32*, 698.

[34] S. K. Sharma, N. Sehgal, A. Kumar, *Curr. Appl. Phys.* **2003**, *3*, 307.

[35] V. Kandimalla, V. Tripathi, H. Ju, *Crit. Rev. Anal. Chem.* **2006**, *36*, 73.

[36] V. Smuleac, D. Butterfield, D. Bhattacharyya, *Langmuir* **2006**, *40506*, 100.

[37] E. Faure, C. Falentin-Daudré, C. Jérôme, J. Lyskawa, D. Fournier, P. Woisel, C. Detrembleur, *Prog. Polym. Sci.* **2013**, *38*, 236.

[38] W. E. Tenhaeff, K. K. Gleason, *Adv. Funct. Mater.* **2008**, *18*, 979.

[39] K. Vasilev, S. S. Griesser, H. J. Griesser, *Plasma Process. Polym.* **2011**, *8*, 1010.

[40] J. Friedrich, *Plasma Process. Polym.* **2011**, *8*, 783.

[41] M. M. Bilek, D. R. McKenzie, *Biophys. Rev.* **2010**, *2*, 55.

[42] F. Bally, K. Cheng, H. Nandivada, X. Deng, A. M. Ross, A. Panades, J. Lahann, *ACS Appl. Mater. Interfaces* **2013**, *5*, 9262.

[43] Y. Elkasabi, M. Yoshida, H. Nandivada, H.-Y. Chen, J. Lahann, *Macromol. Rapid Commun.* **2008**, *29*, 855.

[44] X. Deng, J. Lahann, *Macromol. Rapid Commun.* **2012**, *33*, 1459.

[45] M.-J. Kim, B. Lee, K. Yang, J. Park, S. Jeon, S. H. Um, D.-I. Kim, S. G. Im, S.-W. Cho, *Biomaterials* **2013**, *34*, 7236.

[46] K. S. Siow, L. Britcher, S. Kumar, H. J. Griesser, *Plasma Process. Polym.* **2006**, *3*, 392.

[47] P. Heyse, M. B. J. Roeffaers, S. Paulussen, J. Hofkens, P. a. Jacobs, B. F. Sels, *Plasma Process. Polym.* **2008**, *5*, 186.

[48] C. Vandenabeele, S. Bulou, R. Maurau, F. Siffer, T. Belmonte, P. Choquet, *ACS Appl. Mater. Interfaces* **2015**, *7*, 14317.

[49] M. M. M. Bilek, *Appl. Surf. Sci.* **2014**, *310*, 3.

[50] S. Ershov, F. Khelifa, P. Dubois, R. Snyders, *ACS Appl. Mater. Interfaces* **2013**, 130508131405002.

[51] B. Gupta, J. G. Hilborn, I. Bisson, P. Frey, *J. Appl. Polym. Sci.* **2001**, *81*, 2993.

[52] A. Popelka, I. Novák, M. Lehocký, I. Junkar, M. Mozetič, A. Kleinová, I. Janigová, M. Slouf, F. Bílek, I. Chodák, *Carbohydr. Polym.* **2012**, *90*, 1501.

[53] M. Liang, J. Yao, X. Chen, L. Huang, Z. Shao, *Mater. Sci. Eng. C. Mater. Biol. Appl.* **2013**, *33*, 1409.

[54] K. N. Pandiyaraj, V. Selvarajan, Y. H. Rhee, H. W. Kim, S. I. Shah, *Mater. Sci. Eng. C* **2009**, *29*, 796.

[55] S. Saxena, A. R. Ray, B. Gupta, *Carbohydr. Polym.* **2010**, *82*, 1315.

[56] H. a. Pearson, M. W. Urban, *J. Mater. Chem. B* **2014**, *2*, 2084.

[57] C. S. Ren, D. Z. Wang, Y. N. Wang, *Surf. Coatings Technol.* **2006**, *201*, 2867.

[58] F. Bílek, T. Křížová, M. Lehocký, *Colloids Surf. B. Biointerfaces* **2011**, *88*, 440.

[59] Y. Xia, F. Boey, S. S. Venkatraman, *Biointerphases* **2010**, *5*, FA32.

[60] K. M. Kamruzzaman Selim, Z. Xing, H. Bae, I. Kang, *Biomater. Res.* **2007**, *11*, 139.

[61] L. Karam, C. Jama, A.-S. Mamede, S. Boukla, P. Dhulster, N.-E. Chihib, *Appl. Microbiol. Biotechnol.* **2013**, *97*, 10321.

[62] L. Karam, C. Jama, N. Nuns, A.-S. Mamede, P. Dhulster, N.-E. Chihib, *J. Pept. Sci.* **2013**, *19*, 377.

[63] Z. Xin, J. Hou, J. Ding, Z. Yang, S. Yan, C. Liu, *Appl. Surf. Sci.* **2013**, *279*, 424.

[64] I. Sousa, A. Mendes, R. F. Pereira, P. J. Bártolo, *Mater. Lett.* **2014**, *134*, 263.

[65] Z. Xin, S. Yan, J. Ding, Z. Yang, B. Du, S. Du, *Appl. Surf. Sci.* **2014**, *300*, 8.

[66] T. Desmet, C. Poleunis, a. Delcorte, P. Dubruel, *J. Mater. Sci. Mater. Med.* **2012**, *23*, 293.

[67] A. de Jesús Martínez-Gómez, S. O. Manolache, R. a. Young, F. S. Denes, *Polym. Bull.* **2010**, *65*, 293.

[68] A. Cifuentes, S. Borro, *Langmuir* **2013**.

[69] V. Gubala, N. C. H. Le, R. P. Gandhiraman, C. Coyle, S. Daniels, D. E. Williams, *Colloids Surfaces B Biointerfaces* **2010**, *81*, 544.

[70] N. Recek, M. Jaganjac, M. Kolar, L. Milkovic, M. Mozetič, K. Stana-Kleinschek, A. Vesel, *Molecules* **2013**, *18*, 12441.

[71] J. Lei, L. Yang, Y. Zhan, Y. Wang, T. Ye, Y. Li, H. Deng, B. Li, *Colloids Surf. B. Biointerfaces* **2014**, *114*, 60.

[72] H. Shen, X. Hu, F. Yang, J. Bei, S. Wang, *Biomaterials* **2009**, *30*, 3150.

[73] H. T. Şaşmazel, S. Manolache, M. Gümüderelioğlu, *Plasma Process. Polym.* **2010**, *7*, 588.

[74] H. T. Saşmazel, S. Manolache, M. Gümüşderelioğlu, *J. Biomater. Sci. Polym. Ed.* **2009**, *20*, 1137.

[75] M. Ghasemi, M. J. G. Minier, M. Tatoulian, M. M. Chehimi, F. Arefi-Khonsari, *J. Phys. Chem. B* **2011**, *115*, 10228.

[76] T. E. Saraswati, A. Ogino, M. Nagatsu, *Carbon N. Y.* **2012**, *50*, 1253.

[77] R. Stine, B. S. Simpkins, S. P. Mulvaney, L. J. Whitman, C. R. Tamanaha, *Appl. Surf. Sci.* **2010**, *256*, 4171.

[78] M. Nardulli, M. Belviso, P. Favia, R. D'Agostino, R. Gristina, *J. Biomed. Mater. Res. - Part B Appl. Biomater.* **2010**, *94*, 97.

[79] H. Koch, W. Kulisch, C. Popov, R. Merz, B. Merz, J. P. Reithmaier, *Diam. Relat. Mater.* **2011**, *20*, 254.

[80] J. F. Friedrich, G. Hidde, A. Lippitz, W. E. S. Unger, *Plasma Chem. Plasma Process.* **2013**, *34*, 621.

[81] M. Vesali-Naseh, Y. Mortazavi, A. A. Khodadadi, P. Parsaeian, A. A. Moosavi-Movahedi, *Sensors Actuators B Chem.* **2013**, *188*, 488.

[82] S. Theapsak, A. Watthanaphanit, R. Rujiravanit, *ACS Appl. Mater. Interfaces* **2012**, *4*, 2474.

[83] D. Gogoi, T. Barman, B. Choudhury, M. Khan, Y. Chaudhari, M. Dehingia, A. R. Pal, H. Bailung, J. Chutia, *Mater. Sci. Eng. C. Mater. Biol. Appl.* **2014**, *43*, 237.

[84] C. Volcke, R. P. Gandhiraman, V. Gubala, J. Raj, T. Cummins, G. Fonder, R. I. Nooney, Z. Mekhalif, G. Herzog, S. Daniels, D. W. M. Arrigan, a a Cafolla, D. E. Williams, *Biosens. Bioelectron.* **2010**, *25*, 1875.

[85] R. P. Gandhiraman, V. Gubala, N. C. H. Le, L. C. H. Nam, C. Volcke, C. Doyle, B. James, S. Daniels, D. E. Williams, *Colloids Surf. B. Biointerfaces* **2010**, *79*, 270.

[86] D. Duday, C. Vreuls, M. Moreno, G. Frache, N. D. Boscher, G. Zocchi, C. Archambeau, C. Van De Weerdt, J. Martial, P. Choquet, *Surf. Coatings Technol.* **2013**, *218*, 152.

[87] Z. Yang, J. Wang, R. Luo, M. F. Maitz, F. Jing, H. Sun, N. Huang, *Biomaterials* **2010**, *31*, 2072.

[88] Z. Yang, Q. Tu, M. F. Maitz, S. Zhou, J. Wang, N. Huang, *Biomaterials* **2012**, *33*, 7959.

[89] M. Ardhaoui, S. Bhatt, M. Zheng, D. Dowling, C. Jolivalt, F. A. Khonsari, *Mater. Sci. Eng. C. Mater. Biol. Appl.* **2013**, *33*, 3197.

[90] A. Abbas, D. Vercaigne-Marko, P. Supiot, B. Bocquet, C. Vivien, D. Guillochon, *Colloids Surf. B. Biointerfaces* **2009**, *73*, 315.

[91] E. Gallino, S. Massey, M. Tatoulian, D. Mantovani, *Surf. Coatings Technol.* **2010**, *205*, 2461.

[92] M. Crespin, N. Moreau, B. Masereel, O. Feron, B. Gallez, T. Vander Borght, C. Michiels, S. Lucas, *J. Mater. Sci. Mater. Med.* **2011**, *22*, 671.

[93] D. Mangindaan, W.-H. Kuo, H. Kurniawan, M.-J. Wang, *J. Polym. Sci. Part B Polym. Phys.* **2013**, *51*, 1361.

[94] M. D. Kurkuri, C. Driever, G. Johnson, G. McFarland, H. Thissen, N. H. Voelcker, *Biomacromolecules* **2009**, *10*, 1163.

[95] P. Koegler, P. Pasic, J. Gardiner, V. Glattauer, P. Kingshott, H. Thissen, *Biomacromolecules* **2014**, *15*, 2265.

[96] Z. Yang, Y. Yang, W. Yan, Q. Tu, J. Wang, N. Huang, *ACS Appl. Mater. Interfaces* **2013**, *5*, 10495.

[97] Z. Yang, J. Wu, X. Wang, J. Wang, N. Huang, *Plasma Process. Polym.* **2012**, *9*, 718.

[98] Z.-L. Yang, S. Zhou, L. Lu, X. Wang, J. Wang, N. Huang, *J. Biomed. Mater. Res. A* **2012**, *100*, 3124.

[99] P. Qi, W. Yan, Y. Yang, Y. Li, Y. Fan, Z. Yang, Q. Tu, N. Huang, *Colloids Surfaces B Biointerfaces* **2014**, *126*, 70.

[100] Z. Zhang, S. Liu, Y. Shi, Y. Zhang, D. Peacock, F. Yan, P. Wang, L. He, X. Feng, S. Fang, *J. Mater. Chem. B* **2014**, *2*, 1530.

[101] Z. Zhang, P. Liang, X. Zheng, D. Peng, F. Yan, R. Zhao, C.-L. Feng, *Biomacromolecules* **2008**, *9*, 1613.

[102] A. Manakhov, P. Skládal, D. Nečas, J. Čechal, J. Polčák, M. Eliáš, L. Zajíčková, *Phys. Status Solidi* **2014**, *211*, 2801.

[103] A. Manakhov, L. Zajíčková, M. Eliáš, J. Čechal, J. Polčák, J. Hnilica, Š. Bittnerová, D. Nečas, *Plasma Process. Polym.* **2014**, *11*, 532.

[104] L. He, Y. Zhang, S. Liu, S. Fang, Z. Zhang, *Microchim. Acta* **2014**, *181*, 1981.

[105] T. He, Z. Yang, R. Chen, J. Wang, Y. Leng, H. Sun, N. Huang, *Mater. Sci. Eng. C* **2012**, *32*, 1025.

[106] R. Jafari, F. Arefi-Khonsari, M. Tatoulian, D. Le Clerre, L. Talini, F. Richard, *Thin Solid Films* **2009**, *517*, 5763.

[107] M. Kastellorizios, G. P. a K. Michanetzis, B. R. Pistillo, S. Mourtas, P. Klepetsanis, P. Favia, E. Sardella, R. d'Agostino, Y. F. Missirlis, S. G. Antimisiaris, *Int. J. Pharm.* **2012**, *432*, 91.

[108] J.-S. Lim, M.-S. Kook, S. Jung, H.-J. Park, S.-H. Ohk, H.-K. Oh, *J. Nanomater.* **2014**, *2014*, 1.

[109] S. Mourtas, M. Kastellorizios, P. Klepetsanis, E. Farsari, E. Amanatides, D. Mataras, B. R. Pistillo, P. Favia, E. Sardella, R. d'Agostino, S. G. Antimisiaris, *Colloids Surf. B. Biointerfaces* **2011**, *84*, 214.

[110] L. Quintieri, B. R. Pistillo, L. Caputo, P. Favia, F. Baruzzi, *Innov. Food Sci. Emerg. Technol.* **2013**, *20*, 215.

[111] H. S. Seo, Y. M. Ko, J. W. Shim, Y. K. Lim, J.-K. Kook, D.-L. Cho, B. H. Kim, *Appl. Surf. Sci.* **2010**, *257*, 596.

[112] P. Rivolo, S. M. Severino, S. Ricciardi, F. Frascella, F. Geobaldo, *J. Colloid Interface Sci.* **2014**, *416*, 73.

[113] G. Chen, M. Zhou, Z. Zhang, G. Lv, S. Massey, W. Smith, M. Tatoulian, *Plasma Process. Polym.* **2011**, *8*, 701.

[114] R. Mauchauffé, M. Moreno-Couranjou, N. D. Boscher, C. Van De Weerdt, A.-S. Duwez, P. Choquet, *J. Mater. Chem. B* **2014**, *2*, 5168.

[115] A. Manakhov, M. Moreno-Couranjou, N. D. Boscher, V. Rogé, P. Choquet, J.-J. Pireaux, *Plasma Process. Polym.* **2012**, *9*, 435.

[116] W. C. E. Schofield, J. McGettrick, T. J. Bradley, J. P. S. Badyal, S. Przyborski, *J. Am. Chem. Soc.* **2006**, *128*, 2280.

[117] T. M. Blättler, S. Pasche, M. Textor, H. J. Griesser, *Langmuir* **2006**, *22*, 5760.

[118] B. R. Coad, T. Scholz, K. Vasilev, J. D. Hayball, R. D. Short, H. J. Griesser, *ACS Appl. Mater. Interfaces* **2012**, *4*, 2455.

[119] B. R. Coad, K. Vasilev, K. R. Diener, J. D. Hayball, R. D. Short, H. J. Griesser, *Langmuir* **2012**, *28*, 2710.

[120] J. D. McGettrick, W. C. E. Schofield, R. P. Garrod, J. P. S. Badyal, *Chem. Vap. Depos.* **2009**, *15*, 122.

[121] J. D. McGettrick, T. Crockford, W. C. E. Schofield, J. P. S. Badyal, *Appl. Surf. Sci.* **2009**, *256*, S30.

[122] C. Wu, G. Zhang, T. Xia, Z. Li, K. Zhao, Z. Deng, D. Guo, B. Peng, *Mater. Sci. Eng. C* **2015**, *55*, 155.

[123] S. Marchesan, C. D. Easton, K. E. Styan, P. Leech, T. R. Gengenbach, J. S. Forsythe, P. G. Hartley, *Colloids Surf. B. Biointerfaces* **2013**, *108*, 313.

[124] C. Klages, K. Höpfner, N. Kläke, R. Thyen, *Plasmas Polym.* **2000**, *5*, 79.

[125] G. Camporeale, M. Moreno-Couranjou, S. Bonot, R. Mauchauffé, N. D. Boscher, C. Bebrone, C. Van de Weerdt, H.-M. Cauchie, P. Favia, P. Choquet, *Plasma Process. Polym.* **2015**, n/a.

[126] S. Bonot, R. Mauchauffé, N. D. Boscher, M. Moreno-Couranjou, H.-M. Cauchie, P. Choquet, *Adv. Mater. Interfaces* **2015**, n/a.

[127] N. D. Boscher, F. Hilt, D. Duday, G. Frache, T. Fouquet, P. Choquet, *Plasma Process. Polym.* **2015**, *12*, 66.

[128] L.-Q. Chu, W. Knoll, R. Förch, *Biosens. Bioelectron.* **2008**, *24*, 118.

[129] B. Thierry, M. Jasieniak, L. C. P. M. de Smet, K. Vasilev, H. J. Griesser, *Langmuir* **2008**, *24*, 10187.

[130] B. Thierry, M. Kurkuri, J. Y. Shi, L. E. M. P. Lwin, D. Palms, *Biomicrofluidics* **2010**, *4*, 32205.

[131] C. Vreuls, G. Zocchi, B. Thierry, G. Garitte, S. S. Griesser, C. Archambeau, C. Van de Weerdt, J. Martial, H. Griesser, *J. Mater. Chem.* **2010**, *20*, 8092.

[132] M. D. Kurkuri, F. Al-Ejeh, J. Y. Shi, D. Palms, C. Prestidge, H. J. Griesser, M. P. Brown, B. Thierry, *J. Mater. Chem.* **2011**, *21*, 8841.

[133] L. Duque, B. Menges, S. Borros, R. Förch, *Biomacromolecules* **2010**, *11*, 2818.

[134] B. Twomey, M. Rahman, G. Byrne, A. Hynes, L.-A. O'Hare, L. O'Neill, D. Dowling, *Plasma Process. Polym.* **2008**, *5*, 737.

[135] G. Da Ponte, E. Sardella, F. Fanelli, S. Paulussen, P. Favia, *Plasma Process. Polym.* **2014**, *11*, 345.

[136] F. Palumbo, G. Camporeale, Y.-W. Yang, J.-S. Wu, E. Sardella, G. Dilecce, C. D. Calvano, L. Quintieri, L. Caputo, F. Baruzzi, P. Favia, *Plasma Process. Polym.* **2015**, n/a.

[137] C. Amorosi, M. Michel, L. Avérous, V. Toniazzo, D. Ruch, V. Ball, *Colloids Surf. B. Biointerfaces* **2012**, *97*, 124.

[138] C. Amorosi, C. Mustin, G. Frache, P. Bertani, A. Fahs, G. Francius, V. Toniazzo, D. Ruch, V. Ball, L. Averous, M. Michel, *J. Phys. Chem. C* **2012**, *116*, 21356.

[139] A. Elagli, K. Belhacene, C. Vivien, P. Dhulster, R. Froidevaux, P. Supiot, *J. Mol. Catal. B Enzym.* **2014**, *110*, 77.

[140] P. Heyse, A. Van Hoeck, M. B. J. Roeffaers, J.-P. Raffin, A. Steinbüchel, T. Stöveken, J. Lammertyn, P. Verboven, P. a. Jacobs, J. Hofkens, S. Paulussen, B. F. Sels, *Plasma Process. Polym.* **2011**, *8*, 965.

[141] K. D. Anderson, S. L. Young, H. Jiang, R. Jakubiak, T. J. Bunning, R. R. Naik, V. V Tsukruk, *Langmuir* **2012**, *28*, 1833.

[142] G. Balasundaram, T. M. Shimpi, W. R. Sanow, D. M. Storey, B. S. Kitchell, T. J. Webster, *J. Biomed. Mater. Res. A* **2011**, *98*, 192.

[143] G. T. Hermanson, *Elsevier* **2008**, *2nd ed.*

[144] H. Lee, S. M. Dellatore, W. M. Miller, P. B. Messersmith, *Science* **2007**, *318*, 426.

[145] J. Vartiainen, M. Rättö, S. Paulussen, *Packag. Technol. Sci.* **2005**, *18*, 243.

[146] S. L. Hirsh, M. M. M. Bilek, D. V. Bax, A. Kondyurin, E. Kosobrodova, K. Tsoutas, C. T. H. Tran, A. Waterhouse, Y. Yin, N. J. Nosworthy, D. R. McKenzie, C. G. dos Remedios, M. K. C. Ng, A. S. Weiss, **2013**, *024126*, 364.

[147] B. K. Gan, a. Kondyurin, M. M. M. Bilek, *Langmuir* **2007**, *23*, 2741.

[148] S. L. Hirsh, N. J. Nosworthy, a. Kondyurin, C. G. dos Remedios, D. R. McKenzie, M. M. M. Bilek, *J. Mater. Chem.* **2011**, *21*, 17832.

[149] C. MacDonald, R. Morrow, A. S. Weiss, M. M. M. Bilek, *J. R. Soc. Interface* **2008**, *5*, 663.

[150] M. M. M. Bilek, D. V Bax, A. Kondyurin, Y. Yin, N. J. Nosworthy, K. Fisher, A. Waterhouse, A. S. Weiss, C. G. dos Remedios, D. R. McKenzie, *Proc. Natl. Acad. Sci. U. S. A.* **2011**, *108*, 14405.

[151] H. S. Stoker, *Cengage Learn.* **2012**.

[152] L. Detomaso, R. Gristina, G. S. Senesi, R. d'Agostino, P. Favia, *Biomaterials* **2005**, *26*, 3831.

[153] S. Strola, G. Ceccone, D. Gilliand, a. Valsesia, P. Lisboa, F. Rossi, *Surf. Interface Anal.* **2010**, *42*, 1311.

[154] M. Gabriel, K. Nazmi, E. C. Veerman, A. V. Nieuw Amerongen, A. Zentner, *Bioconjug. Chem.* **2006**, *17*, 548.

[155] L. De Bartolo, S. Morelli, L. C. Lopez, L. Giorno, C. Campana, S. Salerno, M. Rende, P. Favia, L. Detomaso, R. Gristina, R. d'Agostino, E. Drioli, *Biomaterials* **2005**, *26*, 4432.

[156] J.-J. Young, K.-M. Cheng, T.-L. Tsou, H.-W. Liu, H.-J. Wang, *J. Biomater. Sci. Polym. Ed.* **2004**, *15*, 767.

[157] R. a. Walker, V. T. Cunliffe, J. D. Whittle, D. a. Steele, R. D. Short, *Langmuir* **2009**, *25*, 4243.

[158] R. J. González-Paz, A. M. Ferreira, C. Mattu, F. Boccafoschi, G. Lligadas, J. C. Ronda, M. Galià, V. Cádiz, G. Ciardelli, *React. Funct. Polym.* **2013**, *73*, 690.

[159] A. M. Ferreira, I. Carmagnola, V. Chiono, P. Gentile, L. Fracchia, C. Ceresa, G. Georgiev, G. Ciardelli, *Surf. Coatings Technol.* **2013**, *223*, 92.

[160] B. Lassen, M. Malmsten, *J. Colloid Interface Sci.* **1997**, *186*, 9.

[161] S. Yeo, C. Choi, D. Jung, H. Park, *... KOREAN Phys. Soc.* **2006**, *48*, 1325.

[162] Z. Zhang, S. Liu, Y. Shi, J. Dou, S. Fang, *Biopolymers* **2014**, *101*, 496.

[163] Z. Zhang, J. Dou, F. Yan, X. Zheng, X. Li, S. Fang, *Plasma Process. Polym.* **2011**, *8*, 923.

[164] Z. Zhang, G. Li, F. Yan, X. Zheng, X. Li, *Cent. Eur. J. Chem.* **2012**, *10*, 1157.

[165] Z. Zhang, S. Liu, M. Kang, G. Yang, Y. Li, F. Yan, L. He, X. Feng, P. Wang, S. Fang, *Microchim. Acta* **2014**, *181*, 1059.

[166] M. Salim, G. J. S. Fowler, P. C. Wright, S. Vaidyanathan, *Anal. Chim. Acta* **2012**, *724*, 119.

[167] M. C. Vasudev, H. Koerner, K. M. Singh, B. P. Partlow, D. L. Kaplan, E. Gazit, T. J. Bunning, R. R. Naik, *Biomacromolecules* **2014**, *15*, 533.

[168] E. Faure, C. Falentin-Daudré, T. S. Lanero, C. Vreuls, G. Zocchi, C. Van De Weerdt, J. Martial, C. Jérôme, A.-S. Duwez, C. Detrembleur, *Adv. Funct. Mater.* **2012**, *22*, 5271.

Chapter 2

Robust Bio-Inspired Antibacterial Surfaces Based on the Covalent Binding of Peptides on Functional Atmospheric Plasma Thin Films

Rodolphe Mauchauffé, Maryline Moreno-Couranjou, Nicolas D. Boscher, Cécile Van De Weerdt, Anne-Sophie Duwez and Patrick Choquet, *Journal of Materials Chemistry B*, **2014**, *2*, 5168.

1. Introduction

Iron alloys like stainless steel are currently widely used for a large range of furniture for facilities (kitchen, operating room, cold room, ventilation system …) due to their good properties of forming, welding, corrosion resistance, toughness, and easy cleaning. However, their uses can be limited or associated to very constraining rule of cleaning and disinfecting when hygiene is of main importance because of their lack of antibacterial property. Although detergent cleaning or steaming sterilization are really effective techniques used in the industry to treat and kill bacteria, limitations exist. Indeed,: such techniques might lead to a premature degradation of the stainless-steel[1,2] or to remaining unkilled bacteria.[3] This latter could colonize the surfaces, further leading to important drawbacks such as biologically induced corrosion[4] or proliferation of infections and diseases through the creation of resistant biofilms[5,6,7]. Hence, it is relevant to study other routes to eliminate or substantially reduce bacterial attachment and biofilm formation on surfaces. One promising solution relies on the coating of the surfaces with bactericidal or bacteriostatic substances.

A large variety of antibacterial compounds are available to give these properties. Hence, inorganic biocides such as metal nanoparticles [8,9,10] (like silver, copper, …) have been widely used for their broad antimicrobial activity against both gram- and + bacteria. However, recent studies tend to highlight the potential cytotoxicity of these particles.[11] As an alternative, organic biocides have been exploited. Concerning antibiotics, the observation of antibacterial resistance [12,13,14] tend to limit their exploitation despite their broad spectra activity. In literature, the efficiency as well as the cytotoxicity of quaternary ammonium or other cationic compounds has also been reported.[15] Finally, a new generation of bio-inspired antibacterial surfaces has emerged, based on the exploitation of antimicrobial peptides. Indeed, these molecules, which can be found in animals, plants and bacteria, exhibit excellent antibacterial properties against both gram+ and gram- bacteria.[16] Moreover, low propensity to resistance has been observed and their efficiency is reported even at low concentration.[17,18]

The immobilization of antimicrobial peptides on stainless steel surface is not trivial due to the absence of functional groups. Hence, the deposition of thin films presenting different functionalities (such as carboxylic, primary amino and protonated amino groups) has been exploited for electrostatic, hydrophobic or covalent binding based immobilizations[19]. Only the covalent bonding immobilization route might ensure a long-term activity based on both the high bond strength of the peptide onto the surface and film

stability, this latter being resistant against rinsing with solutions presenting different pH, ionic strength or containing detergents. However, it is worth noting that this strategy remains challenging. Indeed, on the one hand, the peptide is generally immobilized through a random configuration, which might induce a loss of the peptide bioactivity and, in the other hand; the final antibacterial property is related to the functional surface group density. Nevertheless, this approach has already been successfully exploited by using mainly wet chemical techniques[20,21,22] which implies time-consuming multi-step procedure combined with the use of solvent and potential toxic compounds. As a sustainable technique for substrate-independent deposition of adherent thin films carrying highly reactive groups such as amine, epoxy or anhydride groups, the plasma technology has also been exploited by using mainly low pressure processes.[23,24,25] However, it is worth considering the potential of the atmospheric ones as these latters present the advantages to be easily integrated on existing in-line process and allow the fast deposition on large substrates of functional thin films.

Recently, Duday et al. have reported the use of a remote atmospheric pressure Dielectric Barrier Discharge (AP-DBD) plasma process for the elaboration of antibacterial surfaces.[26] However, the peptide immobilization route was based on non-covalent interactions. Here, we report the elaboration and characterization of robust bio-inspired antibacterial metallic surfaces. Our approach relies on the deposition of carboxylic functionalised thin films by using a direct AP-DBD plasma process and the covalent binding of nisin, a natural antibacterial peptide. Nisin was selected as a model peptide because of its high activity against a broad range of Gram-positive bacteria, its wide use as food preservative, its lack of toxicity for humans and its stability when involved in coatings.[20]

In the first part of the chapter, we present the general method for the nisin covalent immobilization on any metallic surfaces. Then, we show how, by adjusting the plasma process parameters, thin interlayers with different morphologies and on top various carboxylic group surface densities, have been deposited. We also report more in details the role of the surface activation and the importance of the peptide immobilization conditions to ensure the nisin covalent binding onto the functionalised thin films, thus leading to robust antibacterial surfaces. Finally, correlations between the chemistry and morphology of the functionalised surfaces with their antibacterial properties, evaluated according to the normalized ISO 22196 tests, are presented and discussed.

2. Experimental details

Supplies

Mirror polished stainless steel disks (304-8ND, 2 cm diameter and 1 mm thickness) were cleaned by successive ultrasonic washings in butanone (5 min.), acetone (1 min.) and absolute ethanol (1min) and further dried under a nitrogen flux. Before plasma deposition, disk surfaces were plasma cleaned and activated through an Ar/O_2 plasma treatment (19 slm/ 1 slm (standard litre per minute)) at 30 W in continuous (CW) discharge mode during 30 sec. Vinyltrimethoxysilane (VTMOS, 98%, Aldrich), Maleic Anhydride (MA, synthesis grade, Merck), *N*-Hydroxysuccinimide (NHS, 98%, Aldrich), 1-(3-dimethylaminopropyl)-N'-ethylcarbodiimide hydrochloride (EDC, commercial grade, Aldrich), Sodium dihydrogen phosphate monohydrate (NaH_2PO_4, Aldrich), Disodium hydrogen phosphate heptahydrate (Na_2HPO_4, Aldrich), 0.01 M phosphate buffered saline (NaCl 0.138 M; KCl - 0.0027 M) pH 7.4 (PBS, Aldrich) were used as received. Before use, nisin (Danisco) was purified up to 95% thanks to a dialysis step and a separation on an ion exchange column.

Reactor design

Atmospheric pressure plasma-enhanced chemical vapour deposition was performed by using an atmospheric pressure dielectric barrier discharge (AP-DBD) process composed of two flat high voltage copper electrodes covered by alumina and a moving table as ground electrode (**Figure 1**). The plasma discharge surface was 19 cm^2. The samples were placed on the moving table and the gap between the substrate and the electrodes was 1 mm. The precursors were introduced in the plasma discharge thanks to two bubbler systems. Argon fluxes of 14.8 L min^{-1} and 0.25 L min^{-1} were introduced through the VTMOS and MA bubblers, respectively. This corresponds to a $6.3\,10^{-6}$ mol L^{-1} concentration for both monomers. The plasma was generated using a Corona generator 7010R (SOFTAL electronic GmbH) delivering a continuous or pulsed sinusoidal voltage signal, whose frequency was fixed at 10 kHz. A 10 mm s^{-1} table speed was used, while the number of runs was adjusted to deposit 100 nm thick layers, according to the deposition rates estimated for each deposition condition. After plasma deposition, the coated substrates were annealed in an oven at 70°C during 1 hour.

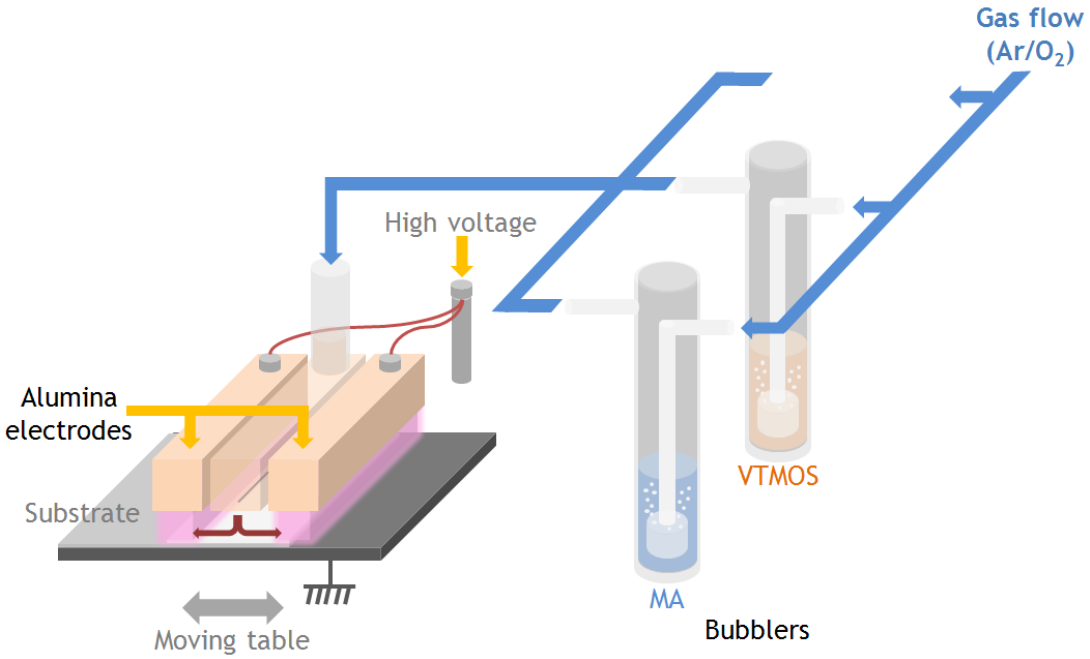

Figure 1: Scheme of the AP-DBD plan-plan plasma process.

Thin films with desired carboxyl group content were prepared by adjusting the peak power values as well as the discharge mode, *i.e.* continuous (CW) or pulsed (PW) discharge. Hence, continuous plasma treatments peak powers were set in range of 5 to 30 W leading to average power density (P_{av}= P_{peak} [t_{on} / (t_{on} + t_{off})] / (Surface discharge), with P_{peak} corresponding to the peak power) varying from 0.27 W cm^{-2} to 1.60 W cm^{-2}. Pulsed mode was performed with fixed 10 ms time on (t_{on}) and 40 ms time off (t_{off}) with peak power ranging from 10 to 60 W, corresponding to average power density varying from 0.11 W cm^{-2} to 0.64 W cm^{-2}.

Surface activation

The COOH functionalised layers were activated using a 10 mM phosphate buffer (Na_2HPO_4, NaH_2PO_4) solution containing a 4mM EDC/10 mM NHS mixture at pH = 5 during 15 min.[27,28] After that, the surfaces were washed once with a pH = 6 phosphate buffer solution during 1 min.

Antibacterial peptide immobilization

The activated layers were immersed in a 1 mL solution containing 5 mg of nisin and left to react under constant agitation during 1 hour at ambient temperature. Nisin immobilization was performed in a 10 mM phosphate buffer at pH= 6. The surfaces were

then rinsed with deionized water 4 times during 5 minutes under 500 rpm stirring to remove unreacted peptides.

Layer characterization

Scanning electron microscopy (SEM) observations were carried out using a field-emission Hitachi SEM-SU-70. Prior to SEM observations, the non-conductive samples were sputter coated with 5 nm of platinum to prevent charging and distortion. Atomic Force Microscopy (AFM) analyses were done in ambient atmosphere using a PicoSPM LE in intermittent-contact mode (Agilent Technologies). The arithmetic mean surface roughness (Ra), the surface roughness depth (Rz) and the mean width of the roughness profile elements (RSm) parameters were calculated from Equation 1, 2 and 3, respectively, thanks to SPIP program and considering 5x5 µm surface areas.

$$R_a = \frac{1}{n}\sum_{i=1}^{n} |Y_i|$$

Equation 1

where n is the number of points in the profile, and Y_i the height of the profile at the point i.

$$R_z = \frac{\sum_{i=1}^{5} |Z_{m_i}| + \sum_{i=1}^{5} |Z_{l_i}|}{5}$$

Equation 2

where Rz is the average distance between the highest local maximum and lowest local minimum obtained on 5 distinct areas of the profile. Zm_i and Zl_i are the local maximum and the local minimum of the area *i*, respectively, *i* varying from 1 to 5.

$$R_{Sm} = \frac{1}{n}\sum_{i=1}^{n} X_i$$

Equation 3

where RSm is the mean distance between two asperities and X_i the distance in µm between two asperities.

FT-IR analyses were performed on a Brüker Hyperion 2000 microscope equipped with a grazing angle objective and a mercury−cadmium−telluride (MCT) detector cooled with liquid nitrogen. Spectra were acquired with 200 scans in the 4000-500 cm^{-1} range. FT-IR cartographies of the carboxylic (COOH) and amide I (C=O) repartition on the treated surfaces were obtained by integration of the 1766-1677 cm^{-1} and 1687-1609 cm^{-1} zones, respectively, using OPUS software. X-ray photon spectroscopy (XPS) analyses were performed on samples after the annealing step by using a Kratos Axis-Ultra DLD instrument using a monochromatic Al Kα X-ray source (hυ=1486.6 eV) at pass energy of 20 eV. CasaXPS program was used to process the XPS spectra. C 1s core level was fitted with 5 main components: hydrocarbon and carbon bonded to Si (~285.0 eV), carbon bonded to anhydride or carboxylic group (~285.7 eV), carbon bonded to oxygen (~286.5 eV), carbon doubly bonded to oxygen (~287.9 eV) and carboxylic or anhydride groups (~289.3 eV). The full width at half maximum (fwhm) was fixed at 1.4 ± 0.1 eV. The Gaussian/Lorentzian ratio was fixed at 30%.

Antibacterial tests

The antibacterial properties of the films against *Bacillus subtilis*, a gram + bacteria, were investigated by using the ISO 22196 antibacterial test. This latter is largely exploited in the industry and derived from the JISZ2801 protocol.[26] Sample surfaces were covered with a 200 µL drop of a known bacteria concentration (about 10^8 cells mL^{-1}). The drop was then covered with a piece of polyethylene film cut from a sterile Stomacher bag (Fisher Scientific) to spread the inoculum onto the substrate and avoid evaporation of the solution. The samples were then placed for incubation at 37°C during 24 hours. The bacteria incubated onto the surface were recollected thanks to the soaking of the disks in a glass jar containing 20 mL of 500 fold diluted Luria-Bertani broth and some 4 mm glass spheres. The jar were agitated for 10 minutes and then sonicated for 2 minutes. 3 drops of 10 µl of the dilution 0 to 10^{-4} from the 20 ml solution were then plated on Luria-Bertani agar and left to grow overnight at 37°C, in order to enumerate the surviving bacteria. A surface is considered as antibacterial if the logarithmic reduction of the survival bacteria is superior than 2. The antibacterial results obtained resulted from at least 2 different series of experiments done in triplicate.

3. Results and Discussion

3.1 Elaboration of bio-inspired antibacterial surfaces

The developed pathway towards the covalent immobilization of nisin peptides on metallic surfaces, depicted in **Figure 2,** is based on a three-step procedure. The first step, aiming at depositing carboxyl-rich thin films (step 1), implies the MA-VTMOS copolymerization from an atmospheric pressure plasma-enhanced chemical vapor deposition (PE-CVD) method. In a second step, the resulting COOH functionalised surfaces are activated by using an EDC/NHS mixture (step 2).[29] Finally, nisin peptides are covalently immobilized onto the surface through the nucleophilic reaction occurring between the terminal NH_2 group of the peptide and the activated carboxylic functions of the surface (step 3). Hereafter, the three steps leading to the elaboration of bio-inspired antibacterial surfaces are fully described and characterised.

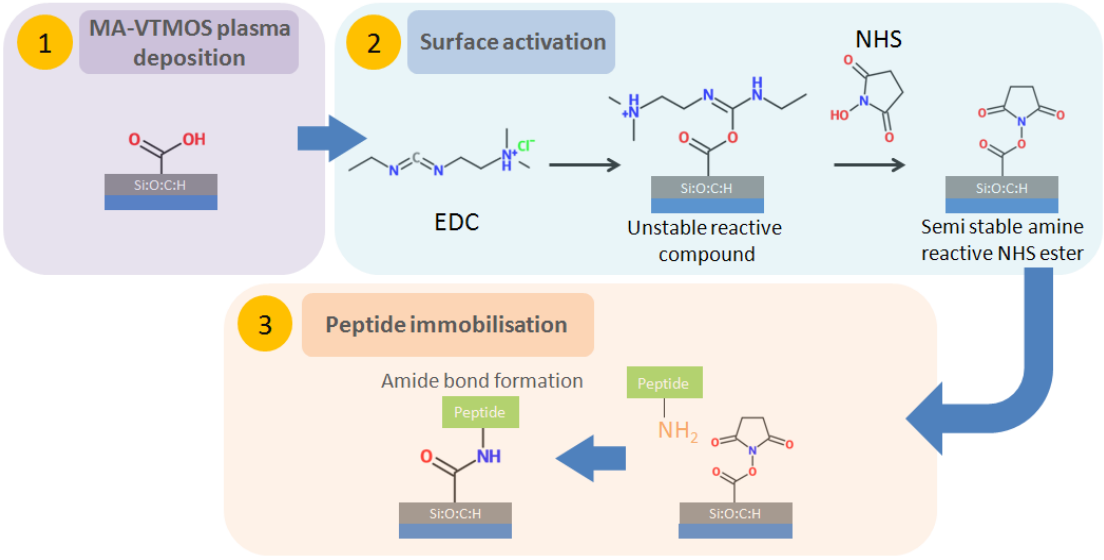

Figure 2: Scheme of the proposed three-step protocol for peptide immobilization.

3.1.1. Step 1. Plasma-enhanced CVD of COOH functionalised layer

The MA-VTMOS plasma deposition step, aiming at forming an interlayer with a strong adhesion to the metallic substrate and providing a functional carboxyl groups rich surface, has already been described elsewhere.[30,31,32] In the present study, both continuous and pulsed plasma conditions (**Table 1**) with average power density ranging from 0.11 to 1.60 W cm^{-2} have been investigated in order to optimize the surface functional groups concentration, highly related to the targeted antibacterial efficiency.[33]

Table 1. Roughness parameters and COOH surface quantification obtained from XPS C1s curve fitting analysis from MA-VTMOS layers deposited in continuous and pulsed mode.

	P_{peak} *W*	Pulse	$P_{average}$ *W* cm^{-2}	COOH *at%*	Ra *nm*	Rz *nm*	RSm *µm*	Rz/RSm x10^{-3}
a	10	10:40ms	0.11	13.5	1.1	4.5	1	4.5
b	20	10:40ms	0.21	13.5	2.8	10.5	1.1	9.9
c	60	10:40ms	0.64	5.6	2.1	8.6	2.6	3.3
d	5	CW	0.27	12.9	1.1	4.9	1	5
e	10	CW	0.53	9.8	3.2	15.2	1.3	11.5
f	20	CW	1.07	6.4	4.9	20.4	0.8	27.1
g	30	CW	1.60	5.5	7.7	33.2	0.6	58.6

FT-IR analysis of the layers shows that the increase of the plasma peak power, either in the continuous or pulsed mode, generally leads to a decrease of the maleic anhydride groups retention. Indeed, when compared to the intensity of the Si-O-Si bonds (around 1100–1200 cm^{-1}), the intensity of the peaks corresponding to the vibration of the C=O from the maleic anhydride groups (1780-1850 cm^{-1}) and to the formation of by-products such as carboxyl (C=O vibration at 1730 cm^{-1}) and hydroxyl groups (around 3000-3600 cm^{-1}) are shown to become smaller with increasing power (**Figure 3a**). The organic functional groups are likely to be degraded due to high energy and high concentration of active species leading to high fragmentation of maleic anhydride. Nevertheless, for a same plasma peak power, the thin films deposited from the plasma pulsed mode show higher maleic anhydride retention with smaller ratios between the peaks corresponding to vibrations of C=O from maleic anhydride/C=O from COOH and the Si-O-Si peak. This higher conservation of the monomer structure into the deposited film is inherent to the use of a plasma pulsed mode. In pulsed plasma, active species are generated during the t_{on} and the deposited layer is composed of cross-linked fragmented monomer, during t_{off} the injected monomers can adsorb on the

surface and perform a conventional polymerisation on the surface with available radicals thus leading to the conservation of the monomer structure.[34] As in the presence of residual humidity, single maleic anhydride group tends to convert into two carboxyl groups, anhydride rich layers should lead to films carrying high carboxyl groups content. To accurately control the carboxyl group formation while ensuring the Si-O network crosslinking, a step of annealing has been performed. The efficiency of this step has been confirmed by FT-IR analysis. Indeed, comparison of the layer chemistry prior and after annealing (**Figure 3b & c**), revealed that annealing induced a decrease of the anhydride groups peak (1780-1850 cm^{-1}) and the formation of carboxyl groups (1720-1730 cm^{-1}). A slight broadening of the Si-O-Si band (1100-1200 cm^{-1}) is also observed. Finally, by carrying out several FT-IR COOH mappings on the elaborated surfaces (as reported in **Figure 3.d**), it was possible to conclude that, whatever the deposition conditions, all the surfaces are homogeneously covered by COOH groups.

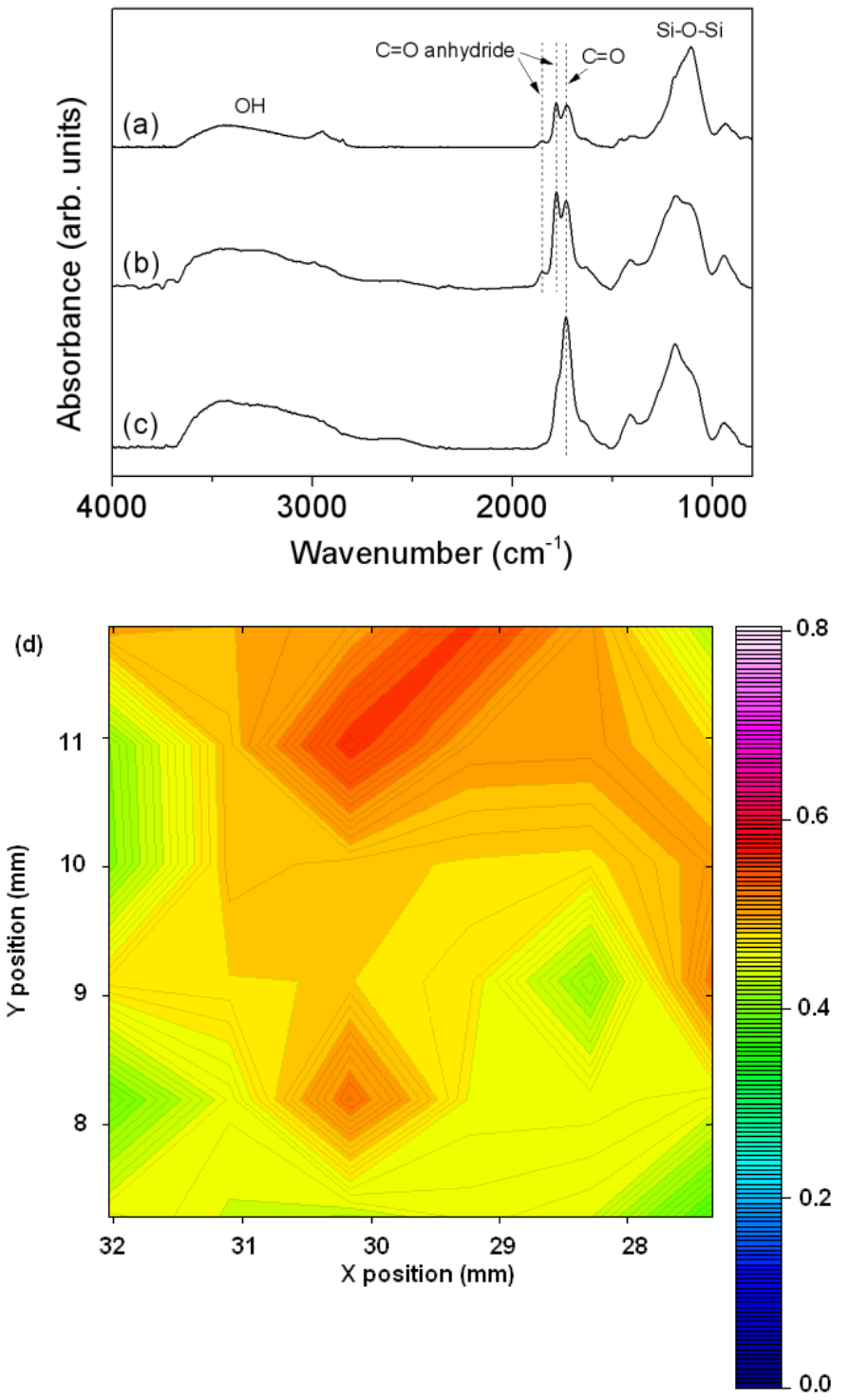

Figure 3: IR spectra of MA-VTMOS deposited at: (a) 1.6 W cm^{-2} in CW mode, (b) 0.11 W cm^{-2} in 10:40ms pulsed discharge and (c) of layer "b" after the annealing step. The FT-IR COOH mapping of layer "c" is shown in (d).

The COOH surface quantification was carried out by XPS C 1s curve fitting (**Table 1**). In both continuous and pulsed mode, the increase of the average power density leads to a decreasing amount of COOH on the surface. COOH surface concentrations ranging from

5.5% to 13.5% are obtained.

Tuning of plasma treatment parameters, which has been shown to influence the thin film chemistry, is also known to influence surface morphologies. Irrespective of the plasma deposition conditions studied in this chapter, SEM analysis (**Figure 4**) revealed that the thin films covered homogenously the surface and were pinhole free. Obvious roughness differences were noticed, with a tendency for rougher surfaces when using continuous mode conditions.

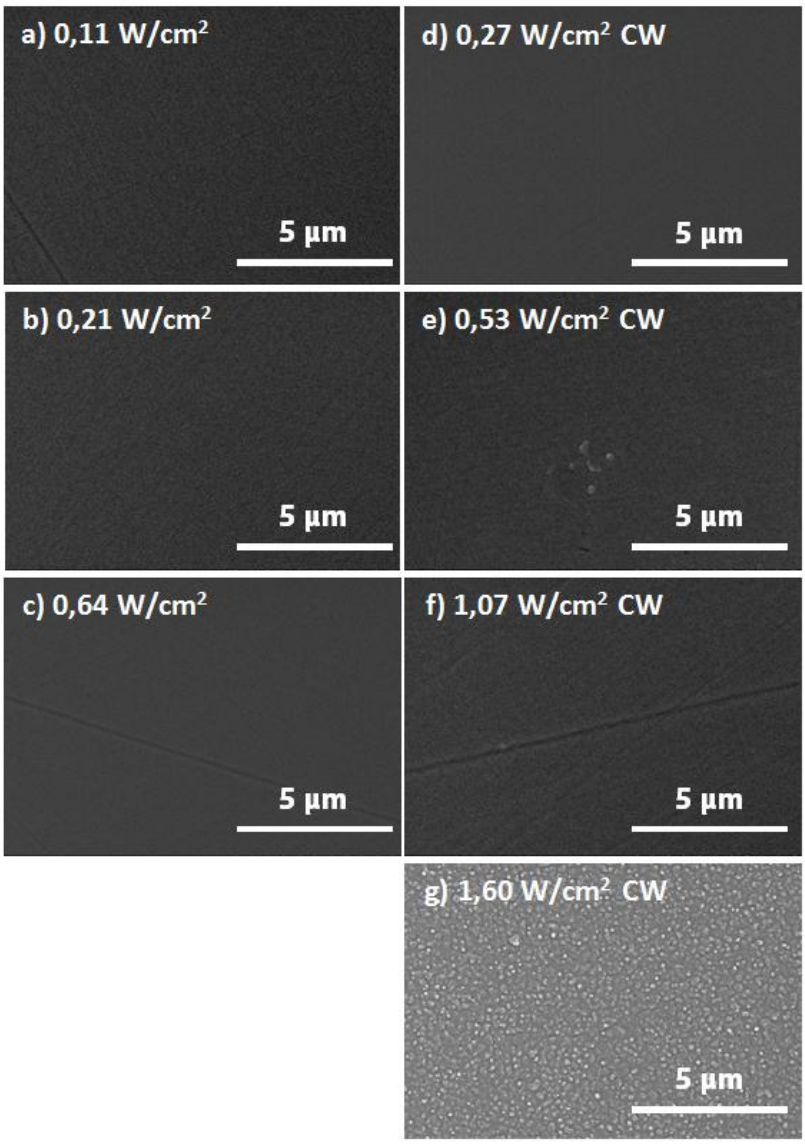

Figure 4: SEM pictures of the MA-VTMOS deposits “a” to “g” from Table 1.

AFM measurements were performed on all the thin films in order to quantify the observed morphology differences. As reported in **Table 1**, while working in continuous mode, increasing the average power density leads to an increase of both Ra and Rz

parameters and a decrease of the RSm parameter (**Figures 5d to 5g**). In this mode, the formation of a high streamer density would probably lead to a rough morphology, as a competition between etching and deposition occurs during the thin film polymerisation.[35,36] Pulsed deposition allowed us to be able to keep a smooth morphology on the surface; the increase of the power density has only a slight impact on the surface morphology (**Figure 5a & c**). Etching phenomenon might be reduced compared to the continuous mode because of chain growth polymerisation occurring during time off leading to the growth of the layer without the etching contribution of plasma thus leading to smooth morphology.

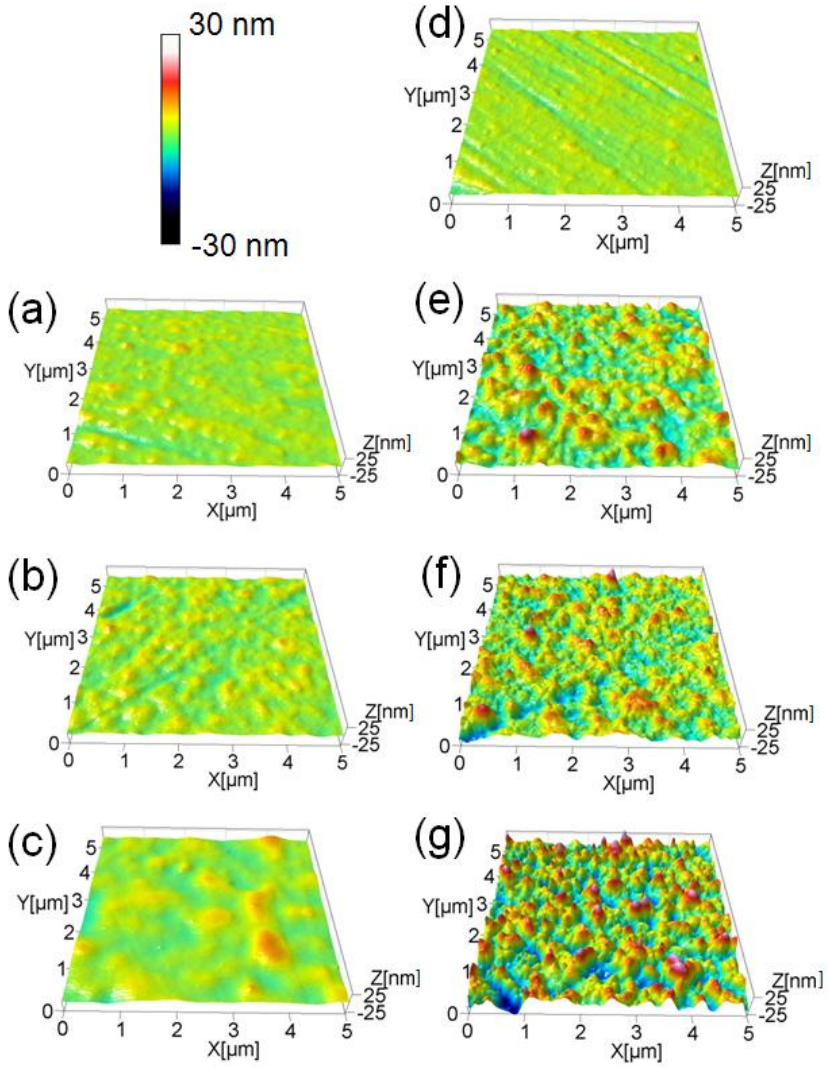

Figure 5: AFM images (5x5 µm) of MA-VTMOS deposits "a" to "g" from Table 1.

3.1.2. Step 2: EDC/NHS surface activation

The second step towards the immobilization of antibacterial nisin peptides involves the EDC/NHS activation of the available carboxyl groups. According to FT-IR analyses, it appears that the EDC/NHS surface activation was successfully performed on all the tested COOH functionalised layers. Indeed, as it is reported in **Figure 6** with a 0.11 W cm^{-2} 10:40 ms pulsed deposited, one can see the slight shift of the C=O peak from 1730 cm^{-1} to 1740 cm^{-1}, that is likely to be related to the conversion of C=O of the carboxylic acid groups available at the surface into the C=O bond of the NHS ester formed.[37] Additionally, contributions at 1780 cm^{-1} and 1805 cm^{-1} might also be assigned to the C=O bond of the NHS ester. Finally, the apparition of a peak around 1590 cm^{-1} can be related to an ionized carboxylate group resulting from the water molecule diffusion into the layer.[38]

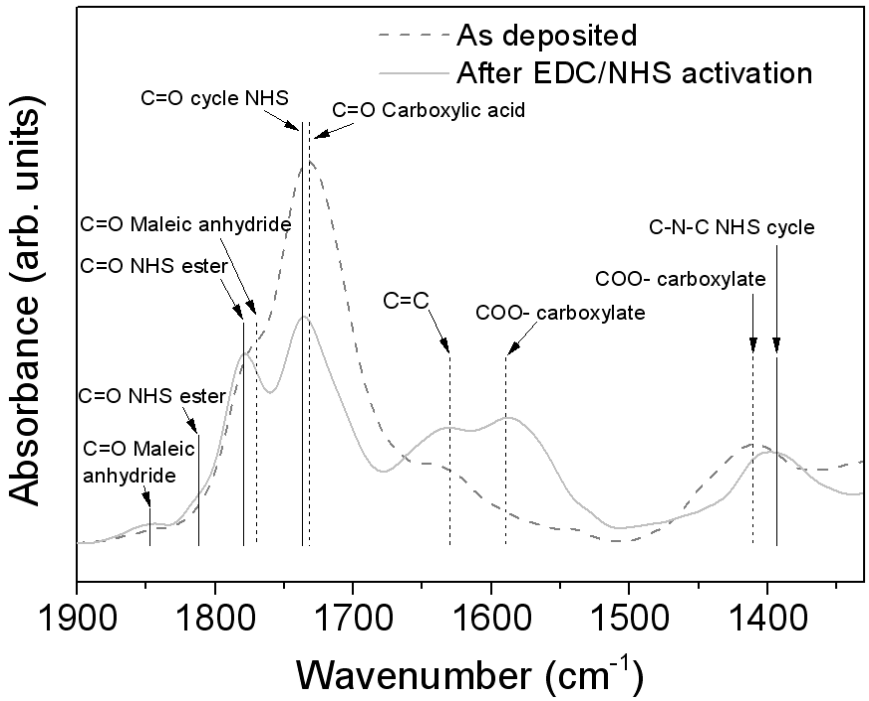

Figure 6: FT-IR spectra in the 1900-1350 cm^{-1} range of a 0.11 W cm^{-2} 10:40 ms pulsed discharge deposited layer before (dotted line) and after EDC/NHS activation (solid line).

3.1.3. Step 3: Nisine covalent immobilization

During the peptide immobilization step, it was observed that the solution remained clear and transparent over the 1 hour stirring. In contrast, a noticeable color change of the

substrate from dark (**Figure 7a**) to blue (**Figure 7b**) was observed after the rinsing of the surface with water.

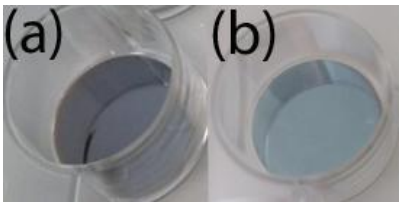

Figure 7: Pictures of an activated layer (0.11W cm^{-2} in pulsed mode) (a) and layer (a) after nisin-immobilization (b).

Prior to the FT-IR and XPS analysis of those layers, all the sample were meticulously rinsed with water. The effect of such washings for the removal of adsorbed peptide was first investigated by FT-IR analysis. However, as no particular chemical surface modification was noticed according to this technique, complementary ElectroSpray Ionization Mass Spectrometry (ESI-MS) analyses were carried out. For that, after each rinsing, the residue solutions were collected and analysed. It was shown that after three successive washings, no residual peptide was found in the solution (according to the sensitivity of the analyser in full-scan MS) while it was possible to still confirm the nisin presence on the surface according to FT-IR and XPS analysis.

The chemistry surface modification induced by the peptide immobilization step was investigated by FT-IR analyses. Comparison of the FT-IR spectra of activated layers (**Figure 8a**) and nisin-immobilized layer (**Figure 8b**) shows obvious chemical differences. After the immobilization step (**Figure 8b**), in spite of the presence of residual C=O peak around 1730 cm^{-1}, probably related to the carboxyl groups present in the bulk material, the layer contains the characteristic peptide amide peaks, *i.e.* NH stretching at 3200 cm^{-1}, C=O stretching around 1650 cm^{-1} (amide I) and NH bending at 1550 cm^{-1} (amide II). FT-IR mappings of the amide I peak on the surface (as reported in **Figure 8c**) allowed concluding that nisin was homogenously covering all the surfaces.

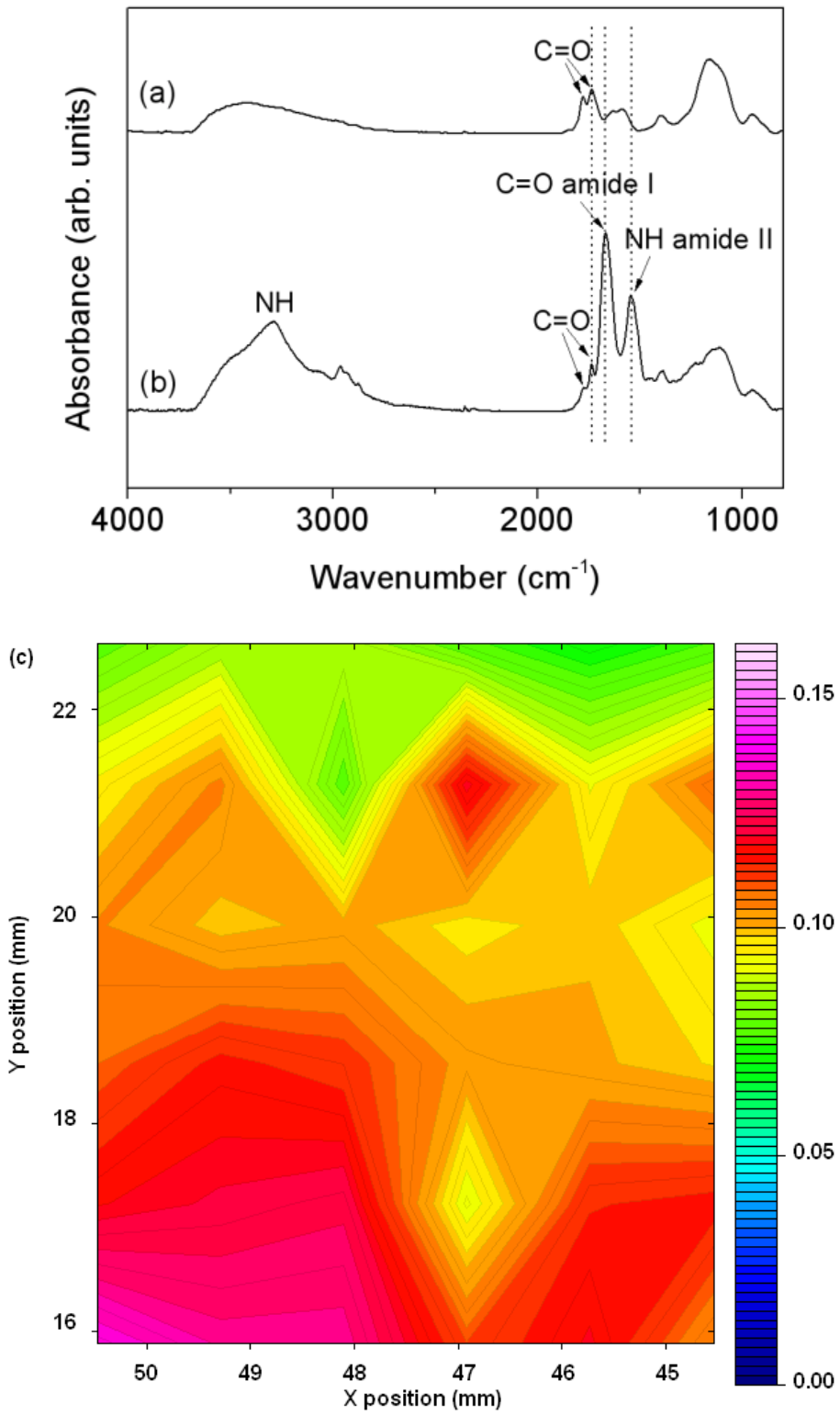

Figure 8: FT-IR spectra of an EDC/NHS activated COOH functionalised layer deposited at 0.11 W cm^{-2} in pulsed mode (a); layer (a) after nisin immobilization (b); and FT-IR amide I mapping of layer "b" (c)

To gain knowledge on the grafted nisin secondary structure, the IR amide I peak was curve-fitted as it is now well-established that its position is related to the particular peptide secondary structure.[39] Inspired by the work of El-Jastimi et al.[40] and Surewicz et al.[41], the peak reported in **Figure 9** was fitted with four different component bands: i) β-turns at 1680 cm^{-1}, ii) free amide and unordered conformation at 1660 cm^{-1}, iii) β-turns/ β-sheets at 1640 cm^{-1} and iv) side-chains vibration of histidine residues and antisymmetric mode of the terminal COOH group at 1620 cm^{-1} . By comparing with the amide I spectra of free nisin in solution reported in literature[40], it can be observed that binding of the peptide induced a change in its secondary structure. Indeed, while the free nisin structure is mainly disordered with the presence of a major wide and intense peak in the 1660 cm^{-1} region and β-turns, the developed immobilization route reported here tends to promote the formation of β-turns at the expense of the disordered component, which is in accordance with other surface-immobilized nisin reported in the literature.[40]

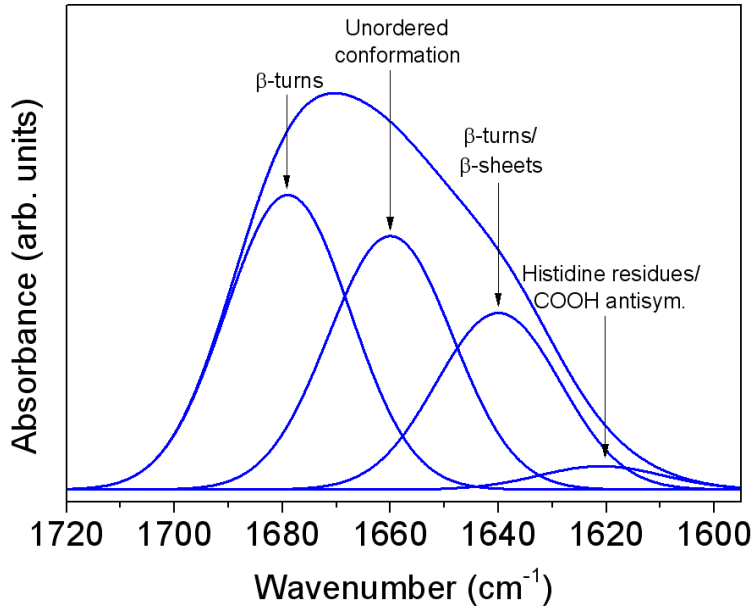

Figure 9: Deconvolved FT-IR spectra of the amide I band of nisin immobilized onto EDC/NHS activated MA-VTMOS surface.

According to XPS atomic percentages of the surfaces, the peptide immobilization can proceed on both smooth samples with high COOH surface concentration and on rough surfaces with low COOH surface content (**Table 2 samples b & d**). After the peptide immobilization step (**Table 2 samples c & e**), the layers present an increased amount of nitrogen and sulphur, two peptide characteristic trace elements, compared to their corresponding as-deposited COOH functionalised layers. Additionally, one can notice that

the nisin-immobilized layer elemental composition is getting close to the theoretical nisin composition. The detection of silicon element originating from the activated COOH functionalised layer correlated to the XPS analysis maximum depth (*ca.* 10 nm) and to the peptide size (*ca.* 2 nm x 5 nm[42]) indicates the immobilization of a thin peptide layer.

Table 2: XPS atomic percentages in different MAA-VTMOS layers before and after nisin immobilization. (a) Theoretical Nisin (b) 0.11 W cm^{-2} pulsed mode layer (c) layer 'b' after nisin immobilization (d) 1.60 W cm^{-2} continuous mode layer (e) layer 'd' after nisin immobilization

Sample	C [at. %]	O [at. %]	N [at. %]	Si [at. %]	S [at. %]
a	61.0	18.0	18.0	0.0	3.0
b	50.1	42.4	0.0	7.5	0.0
c	63.1	21.5	12.3	1.6	1.5
d	47.8	41.6	0.0	10.6	0.0
e	55.1	31.2	6.6	6.9	0.2

3.2 Correlations between layers chemistry, morphology and antibacterial properties

Nisin was successfully immobilized on the activated layer. In a second part of this work, the correlation between layer chemistry and morphology onto the antibacterial activity of the nisin-immobilized layer was investigated. In the COOH surface concentration range investigated, *i.e.* 5.5 to 13.5 at.%, the antibacterial properties did not seem to be related to the COOH content and both antibacterial and non-antibacterial deposits were obtained (**Figure 10)**. In contrast, the Ra roughness parameter was shown to influence the antibacterial properties of the final layer, which was only achieved for Ra values lower than 3.2 nm. In an attempt to elucidate the behavior beyond such observation, the surface roughness depth Rz and the mean width of the roughness profile elements RSm parameters were examined. It is interesting to note that the films leading antibacterial surfaces have shallower and wider surface asperities. The plot of the COOH concentration against the Rz/RSm ratio (**Figure 10**) allows highlighting the influence of the roughness on the antibacterial properties. Hence, irrespective of the COOH surface concentration, ranging from 5.5 to 13.5 at.%, smooth

deposits, with Rz/RSm varying from 3.3 10^{-3} to 11.5 10^{-3}, presented antibacterial properties. In contrast, no antibacterial properties were achieved for Rz/RSm greater than 27.1 10^{-3}. Finally, layers presenting a same COOH surface concentration, *e.g.* 5.5 %, but different surface morphologies (respectively Rz/RSm 3.3 10^{-3} and 58.6 10^{-3}) showed opposite antibacterial activities.

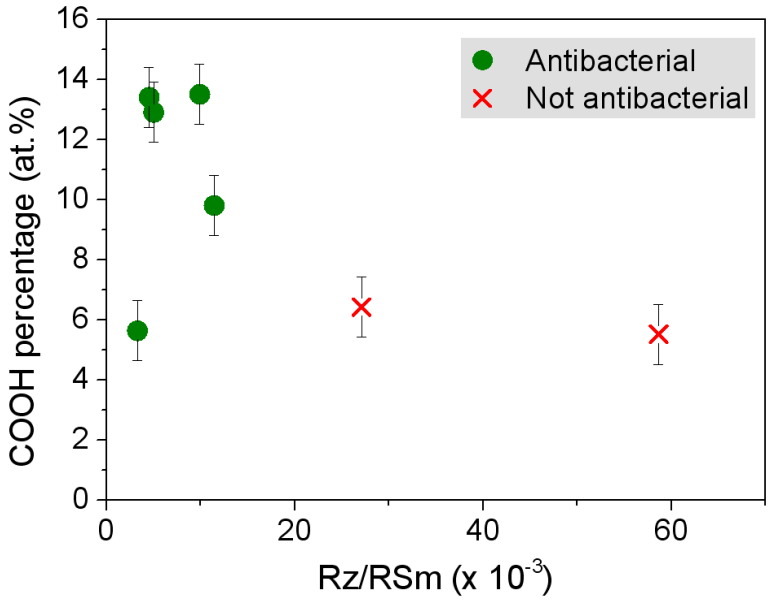

Figure 10: Plot of COOH surface concentration (at.%) against the Rz/RSm ratio. The antibacterial tests results were here represented simply as an "all-or-nothing" round and cross signs for respectively antibacterial and not antibacterial deposits. Herein, the positive antibacterial results obtained through the ISO 22196 test show a log reduction comprised between 3 and 8.3 with a median value of about 8.

This effect could come from the fact that the small size of nisin (2 nm x 5 nm) compared to the high roughness depth Rz allows it to be grafted in the valley floor of all the samples described in present work (**Figure 11**). In the case of a surface with narrow roughness elements, the length of the *bacillus subtilis* bacteria, *ca.* 2-6 µm,[43] largely superior to the RSm, does not permit to the nisin immobilized in the valleys to participate to the degradation of the bacteria membrane (**Figure 11**). In contrast, smoother surfaces (Rz < 16 nm) with a RSm in the same range of the bacteria size or greater *(i.e.* small Rz/RSm ratio), allow the bacteria to come in the large valleys and interact with nisin, as depicted in **Figure 11**.

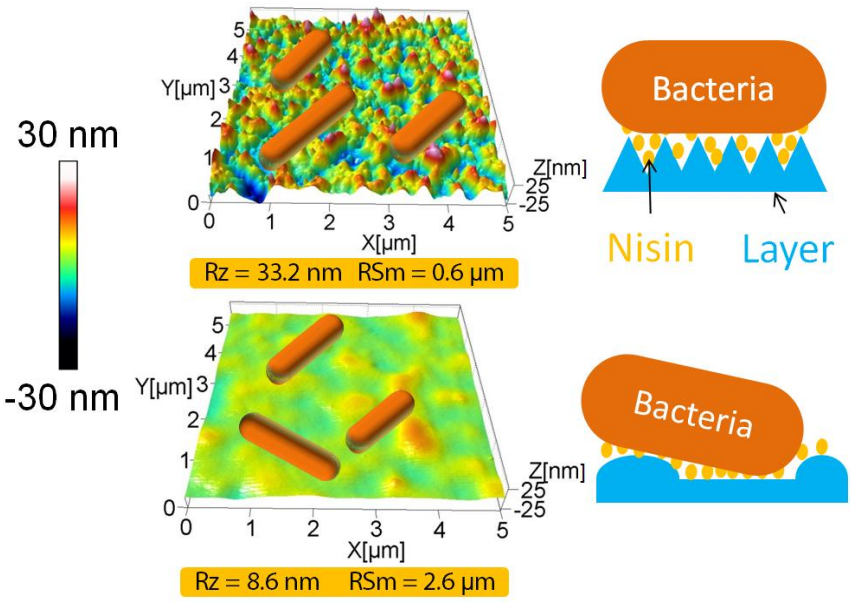

Figure 11: AFM 3D pictures of a rough (Rz = 33.2 nm, RSm = 0.6 µm) and smooth (Rz = 8.6 nm, RSm = 2.6 µm) surface carrying a similar 5.5 at.% COOH density with on the top a representation to scale of a bacteria.

3.3 Relevance of the activation step (Step 2) on the peptide immobilization (Step 3)

To deeper investigate the role of the EDC/NHS surface activation, the peptide immobilization was carried out directly on COOH functionalised layers without the use of coupling agents. In contrast with the procedure previously described and followed along Step 3, it was possible to observe the formation of insoluble peptide aggregates during the peptide immobilization step. After the immobilization step, the surface presented a blue color with a whitish film (**Figure 12b**) persistent even after several water rinsing of the surface.

Comparison of the FT-IR spectra of immobilized peptide layers achieved with (**Figure 8b**) and without surface activation (**Figure 12**), revealed a slight difference in the 1720-1600 cm^{-1} zone with the broadening and shift of the amide I peak toward the lower wavenumbers around 1650 cm^{-1} for the peptide immobilized layer achieved without surface activation (Step 2). The amide I peak shape observation (**Figure 13A**) as well as its deconvolution (F**igure 13B**) shows that the proportion of β-turn/β-sheets and histidine vibrations/terminal COOH is higher. As it has been reported the β-turn/β-sheets contribution around 1640 cm^{-1} might come from intermolecular interactions due to aggregation of peptide and leading to a new β structure, this result is perfectly corroborating with the observation of

solid aggregates on our films (*i.e.* whitish film).[44,45,46] It can then be concluded that the final peptide conformation is affected by the way the immobilization was performed. The activated layers allow the peptide to be immobilized without the formation of such aggregates.

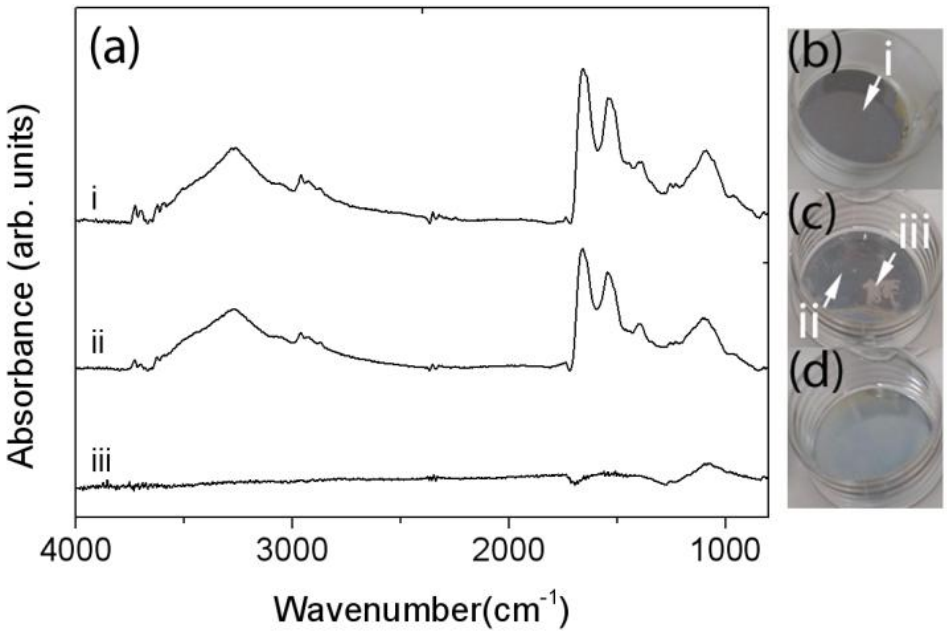

Figure 12: a) FT-IR spectra of a MA-VTMOS layer deposited at 0.11W cm^{-2} in pulsed conditions after nisin immobilization achieved without EDC/NHS activation (i), layer (i) after immersion 1h in PBS (ii) delaminated area of layer (i) (iii); Pictures of MA-VTMOS 0.11W cm^{-2} pulsed 10:40 ms layer recovered with nisin without EDC/NHS activation (b); layer (b) after immersion 1h in PBS (c); grafted nisin on activated MA-VTMOS 0.11W cm^{-2} pulsed 10:40 ms deposit after immersion 1h in PBS (d).

In order to assess the influence of the nisin immobilization route on the layer stability, the peptide immobilized layers, with and without the EDC/NHS activation Step 2, was immersed in a PBS solution during 1 h. Such immersion has been reported as an efficient way for both removing silanized coating[47] and detaching peptide immobilized through weak bonds (such as electrostatic or hydrophobic interactions). Activated layers with nisin immobilized on the surface did only undergo a slight color change after immersion (**Figure 12d**). No visually noticeable crack or delamination was observed on the surface. The characteristic peaks of the nisin peptide as well as peaks of the COOH functionalised layer were observed by FT-IR, confirming the presence of both. In contrast, the immersion of an activated layer without nisin immobilized on the surface led to the localized delamination and dissolution of this one. Hence, it can be concluded that the homogeneous repartition of the

peptide onto the surface acted as a protective layer for the silanized films and that the peptide immobilization is performed through a strong chemical covalent bond. The same stabilising effect was reported in a recent article where a thin layer of protein (IgG and Fg) on the surface prevented the dissolution of the plasma polymerized layer.[48] Interestingly, in the case of a non-activated COOH functionalised layer with nisin immobilized on the surface, the film behaviour was drastically different. Even if a small protecting effect was noticed, as it can be seen from the FT-IR spectra confirming the presence of both the layer and the peptide, the surface is not homogenous. Indeed, the partial delamination of the coating was observed (**Figure 12c**) and further confirmed by FT-IR measurements in different areas (**Figure 12a**). It is reasonable to assume that the peptide was mainly immobilized by electrostatic and adsorption route.

In the case of non-activated surface, the surface, recovered by carboxylic groups is mainly negatively charged when in immersion in buffer pH 6 for nisin grafting, due to the pKa of carboxylic deprotonated groups (pKa~4-5). As Nisin isoelectric point is about pH 8.5, it is mainly charged positively at pH 6. The peptide, present in high concentration (5 mg/mL), is then fastly attracted and adsorbed on the entire surface. When the deposit is immersed in PBS the weak electrostatic interaction are reduced and nisin can be desorbed from the surface. Hence, the naked part of plasma layer directly exposed to PBS, delaminated. However, as some other areas are not dissolved; one should also consider the presence of nisin immobilized through additional weak interactions or even, through covalent bonds issued from condensation reactions between the peptide amine and the plasma layer aldehydes groups (i.e, secondary chemical groups detected by XPS C1s deconvolution). The combination of these effects could then explain why when we are performing the grafting of the nisin, the entire delamination of the layer does not occur.

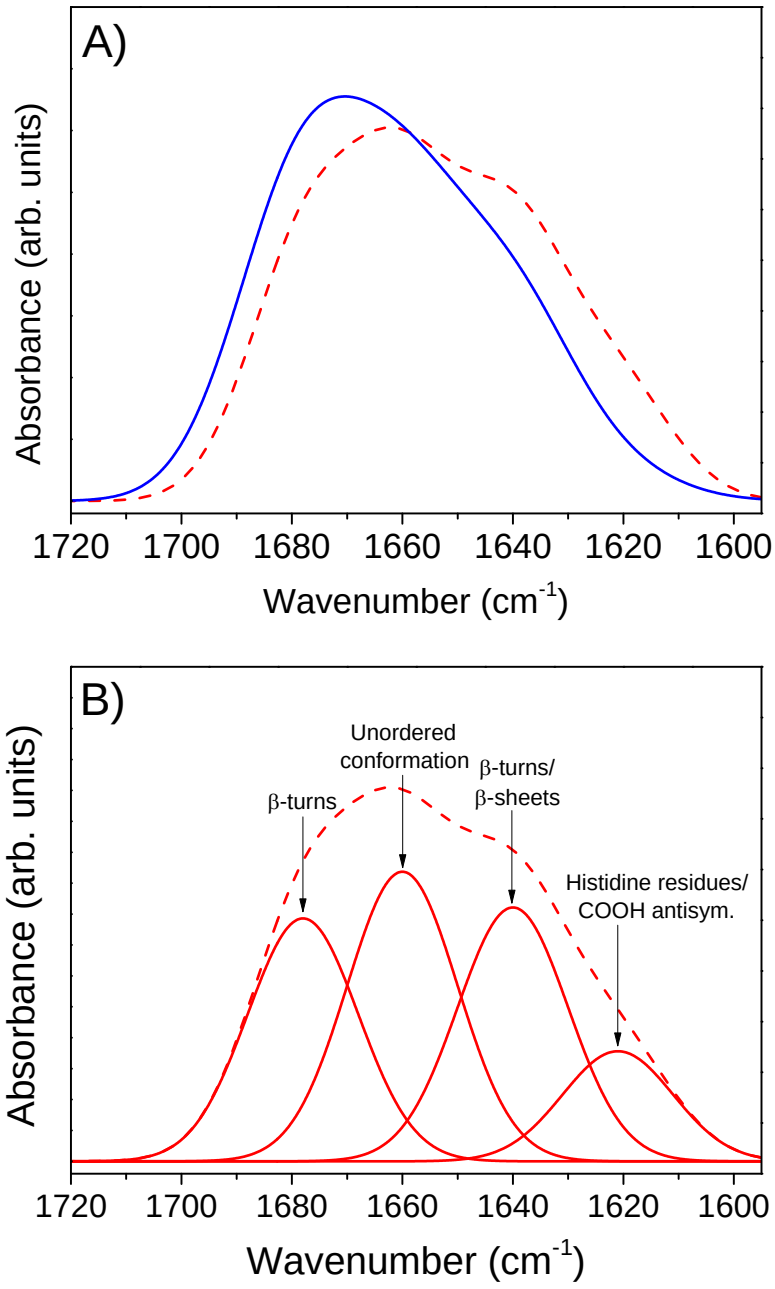

Figure 13: A) FT-IR spectra of amide I of nisin directly immobilized onto a COOH functionalised layer (red dashed line) or onto an activated layer (blue solid line). B) Deconvolution of nisin immobilized on a non-activated COOH functionalized surface.

Uncontrolled and non-covalently peptide immobilization is achieved on non-activated layers, thus resulting in unstable coatings when immersed in PBS solution. The successful grafting of nisin and the stability of the layer clearly show that the covalent immobilization lead to stable layer. All our layers, with different COOH content, lead to the same shape of FT-IR peak when using EDC/NHS. In conclusion, the relevance of the EDC/NHS surface

activation and covalent immobilization has been proved.

Among the numerous cited methods towards the deposition of functional coatings, AP-DBD is particularly suitable for industrial processes.[49] COOH functionalised layers are obtained in a few tens of seconds of treatment, due to high growth rates, compared to the already well documented wet methods involving several and/or long steps. In addition, tuning of the plasma deposition parameters allows simultaneously controlling both the chemistry and the morphology of the layer. A next step of this work will aim at up-scaling the developed method on an industrial roll-to-roll process prototype for the treatment of stainless steel coils. Although the current method involves 3 steps, including an additional activation of natives COOH groups towards peptides functional groups, some advantages exist. Indeed, due to their stability, COOH functionalised layers can be stored for days in a place prior to any peptide grafting. The activation step being performed right before the grafting of the peptide.

4. Conclusion

A three-step procedure has been developed to confer antibacterial properties to metallic substrates. MA-VTMOS plasma copolymerization was performed to deposit COOH containing layers, further activated by using EDC/NHS coupling reagents. Nisin was covalently grafted onto the functionalised stainless steel. FT-IR method is a fast and easy to set method for the analysis of each step of the surface functionalization. The activation of the carboxyl rich surface with EDC/NHS coupling reagent was successfully validated thanks to the appearance of characteristic peaks of NHS ester C=O bond by FT-IR. The apparition of amide bonds in FT-IR analysis as well as the increase of carbon, nitrogen and sulphur content observed by XPS, confirm the nisin immobilization on the layer. The deconvolved FT-IR amide I band post immobilization shows that EDC/NHS allows preventing the aggregation of peptides. The immobilization through covalent bond of nisin confers a protective effect to the final multilayer towards delamination and dissolution in solution such as PBS. Antibacterial tests show that the morphology of the layer is a key parameter to control the peptide efficiency; as the surface roughness depth Rz and the mean width of the roughness profile elements RSm parameters are likely to have an influence on the accessibility of the nisin to interact with bacteria. Finally, logarithmic reduction of the survival bacteria up to 8 were achieved for layers with a COOH surface density greater than 5.5 at.% and a Rz/RSm value lower than 27.1 10^{-3}.

References

[1] C.C. Shih, Y.Y. Su, L.C. Chen, C.M. Shih and S.J. Lin, *Acta Biomaterialia*. 2010, **6**, 2322-2328.

[2] C. Jullien, T. Benezech, C. Le Gentil, L. Boulange-Petermann, P.E. Dubois, J.P. Tissier, M. Traisnel and C. Faille, *Biofouling*. 2008, **24**, 3, 163-172.

[3] J. Królasik , Z. Zakowska, M. Krepska and L. Klimek, *Pol. J. Microbiol.* 2010, **59**, 281-287.

[4] I. B Beech and J. Sunner, *Curr. Opin. Biotech.* 2004, **15**, 181-186.

[5] L. Boulangé-Petermann, B. Baroux and M.N. Bellon-Fontaine, *Industries Alimentaires et Agricoles*, 1994, **111**, 671-675.

[6] L. Hall-Stoodley, J. William Costerton and P. Stoodley, *Nat. Rev. Microbiol.* 2004, **2**, 95-108.

[7] M. Jimenez, H. Hamze, A. Allion, G. Ronse, G. Delaplace and M. Traisnel, *Mater. Sci. Forum.* 2012, **706-709**, 2523-2528.

[8] G.J Chi, S.W Yao, J Fan, W.G Zhang and H.Z Wang, , *Surf. Coat. Technol.* 2002, **157**, 162-165.

[9] M.K. Rai, S.D. Deshmukh, A.P. Ingle and A.K. Gade, *J. Appl. Microbiol*. 2012, **112**, 5.

[10] K.H. Liao, K.L. Ou, H.C. Cheng, C.T. Lin and P.W. Peng, *Appl. Surf. Sci*. 2010, **256**, 3642-3646.

[11] P. Chairuangkitti, S. Lawanprasert, S. Roytrakul, S. Aueviriyavit, D. Phummiratch, K. Kulthong, P. Chanvorachote and R. Maniratanachote, *Toxicol. In Vitro.* 2013, **27**, 330-338.

[12] C. Angebault and A. Andremont, *Eur. J. Clin. Microbiol.* 2013, **32**, 581-595.

[13] S. Walia, S. W. Rana, D. Maue, J. Rana, A. Kumar and S. K. Walia, *Int. J. Environ. Heal. R.* 2013, **23**, 2.

[14] S. B. Levy, *J. Antimicrob. Chemoth*. 2002, **49**, 25-30.

[15] J. C. Cooper, , *Ecotox. Environ. Safe.* 1988, **16**, 65-71.

[16] K.V.R. Reddy , R.D. Yedery and C. Aranha, *Int. J. Antimicrob. Agents.* 2004, **24**, 536-547.

[17] R.D. Joerger, *Poult. Sci.* 2003, **82**, 640-647.

[18] S.A. Onaizi, S.S.J. Leong, *Biotechnol. Adv.* 2011, **29**, 67-74.

[19] D.C. Kim and D.J. Kang, *Sensors.* 2008, **8**, 6605-6641.

[20] E. Faure, P. Lecomte, S. Lenoir, C. Vreuls, C. Van De Weerdt, C. Archambeau, J. Martial, C. Jérôme, A.S. Duwez and C. Detrembleur, *J. Mater. Chem.* 2011, **21**, 7901-7904.

[21] M. Mohorčič, I. Jerman, M. Zorko, L. Butinar, L., R. Orel, R. Jerala and J. Friedrich, *J. Mater. Sci.: Mater. Med.* 2010, **21**, 2775-2782.

[22] A. Héquet, V. Humblot, J-M. Berjeaud and C-M. Pradier, Colloid. Surface. B. 2011, **84**, 301-309.

[23] K. Vasilev, S.S. Griesser and H. J. Griesser, *Plasma. Process. Polym.* 2011, **8**, 1010–1023.

[24] B. Thierry, M. Jasieniak, L.C.P.M. de Smet, K. Vasilev and H.J. Griesser, *Langmuir.* 2008, **24**, 10187-10195.

[25] C. Vreuls, G. Zocchi, B. Thierry, G. Garitte, S.S. Griesser, C. Archambeau, C. Van de Weerdt, J. Martial and H. Griesser, *J. Mater. Chem.*, 2010, **20**, 8092-8098.

[26] D. Duday, C. Vreuls, M. Moreno, G. Frache, N.D. Boscher, G. Zocchi, C. Archambeau, C. Van De Weerdt, J. Martial and P. Choquet, *Surf. Coat. Technol.* 2013, **218**, 152-161.

[27] G.T. Hermanson, *Bioconjugate Techniques 2nd Edition*, Elsevier, 2008.

[28] S. Sam, L. Touahir, J. Salvador Andresa, P. Allongue, J.-N. Chazalviel, A. C. Gouget-Laemmel, C. Henry de Villeneuve, A. Moraillon, F. Ozanam, N. Gabouze, and S. Djebbar, *Langmuir.* 2010, **26**, 809-814.

[29] X. Punet, R. Mauchauffé, M.I. Giannotti, J.C. Rodríguez-Cabello, F. Sanz, E. Engel, M.A. Mateos-Timoneda and J.A. Planell, *Biomacromolecules.* 2013, **14**, 2690-2702.

[30] A. Manakhov, M. Moreno-Couranjou, N.D. Boscher, V. Rogé, P. Choquet and J.J. Pireaux, *Plasma. Process. Polym.* 2012, **9**, 435 – 445.

[31] A. Manakhov, M. Moreno-Couranjou, P. Choquet, N. D. Boscher and J.J. Pireaux, *Surf. Coat. Technol.* 2011, **205**, 466-469.

[32] M. Moreno-Couranjou, A. Manakhov, N. D. Boscher, J. J. Pireaux and P. Choquet, *ACS Appl. Mater. Interfaces.* 2013, **5**, 8446-8456.

[33] L. Cao, *Carrier-bound Immobilised Enzymes*, Wiley-VCH, **2005**.

[34] J. Friedrich, *Plasma. Process. Polym.* 2011, **8**, 783 – 802.

[35] N.D. Boscher, P. Choquet, D. Duday and S. Verdier, *Plasma. Process. Polym.* 2010, **7**, 163 – 171.

[36] N.D. Boscher, D. Duday, S. Verdier and P. Choquet, *ACS Appl. Mater. and Interfaces.* 2013, **5**, 1053 – 1060.

[37] T. Böcking, K.A. Kilian, P.J. Reece, K. Gaus, M. Galb and J. J. Gooding , *Soft Matter.* 2012, **8**, 360-366.

[38] W.Jiang, A. Saxena, B. Song, B.B. Ward, T.J. Beveridge and S.C.B. Myneni, *Langmuir.* 2004, **20**, 11433–11442.

[39] M. Byler and H. Susi, *Biopolymers.* 1986, **25**, 469-487.

[40] R. El-Jastimi and M. Lafleur, *BBA-Biomembranes*. 1997, **1324**, 151-158.

[41] W.K. Surewicz and H.H. Mantsch, *Biochim. Biophys. Acta.* 1988, **952**, 115-30.

[42] C. K. Bower, M. A. Daeschel and J. McGuire, *J. Dairy. Sci.* 1998, **81**, 10, 2771-8.

[43] M.G. Sargent, *J. Bacteriol.* 1975, **123**, 7-19.

[44] K.E. Routledge, G.G. Tartaglia, G.W. Platt, M. Vendruscolo and S.E. Radford, *J. Mol. Biol.* 2009, **389**, 776-786.

[45] B. Shivu, S. Seshadri, J. Li, K.A. Oberg, V.N. Uversky and A.L. Fink, *Biochemistry.* 2013, **52**, 5176-5183.

[46] D.M. Byler, H. Susi, *Biopolymers.* 1986, **25**, 469 – 487.

[47] C.M. Dekeyser, C.C. Buron, S.R. Derclaye, A.M. Jonas, J. Marchand-Brynaert and P.G. Rouxhet, , *J. Colloid. Interf. Sci.* 2012, **378**, 77-82.

[48] M. Donegan and D.P. Dowling, *Plasma Process. Polym.* 2013, **10**, 526 – 534.

[49] F. Massines, C. Sarra-Bournet, F. Fanelli, N. Naude and N. Gherardi, *Plasma Process. Polym.* 2012, **9**, 1041-1073.

Chapter 3

Atmospheric-Pressure Plasma Deposited Epoxy-Rich Thin Films as Platforms for Biomolecule Immobilization - Application for Anti-Biofouling and Xenobiotic-Degrading Surfaces

Giuseppe Camporeale, Maryline Moreno-Couranjou, Sébastien Bonot, Rodolphe Mauchauffé, Nicolas D. Boscher, Carine Bebrone, Cécile Van De Weerdt, Henry-Michel Cauchie, Pietro Favia and Patrick Choquet, *Plasma Processes and Polymers*, **2015**, *12*, 1208.

1. Introduction

Materials scientists are still inspired by nature for manufacturing materials presenting advanced surface properties based on the immobilization of enzymes onto solid surfaces. Enzymes are polyfunctional charged macromolecules composed of amino acid chains linked with peptide bonds and a more or less rigid three-dimensional structure.[1] Nowadays, immobilized enzymes have various practical applications in catalysis, analytics, therapeutics and bio-separation, due to their several advantages. Among others, it can be reported an easy recovery of the product at the end of an enzymatically catalyzed reaction. Considering industrial applications, the possibility to reuse the immobilized enzymes leads to a significant cost saving. Finally, the surface immobilization might enhance the enzyme efficiency and stability compared to their free form in solution. [1,2] There are numerous approaches to irreversibly immobilize enzymes, including their inclusion/encapsulation into polymeric matrices, their crosslinking or their covalent binding onto carrier materials.[3] This latter method is the most widely used and it is generally achieved through a nucleophilic substitution reaction between a modified/activated support and the enzyme amino-acid residues.

As an environmentally friendly technique, low-pressure plasma deposition processes have been successfully exploited for the deposition of adherent thin films functionalized with groups such as halogenide [4], amino, carboxylic, hydroxyl or epoxy [4-13] groups for the covalent bonding of a wide variety of peptides/proteins with biological activity retention.[14] Considering industrial issues where each manufactured step must be connected to realize an efficient production line, the atmospheric-pressure (AP) plasma technology offers the possibility to be easily integrated into existing production systems, along with other advantages.[15] However, the exploitation of this technology remains scarcely reported in literature. Nisol *et al.* [16, 17] have reported the elaboration of non-fouling coatings AP-plasma deposited by using a RF plasma torch in two different modes. The tetraglyme precursor was injected in the post-discharge zone either as a liquid (i.e, spray-AP plasma liquid deposition) or as a vapor (i.e, AP plasma enhanced chemical vapor deposition). Recently, Da Ponte *et al.* [18] reported the successful deposition of non-fouling coatings using aerosol-assisted Atmospheric-Pressure Dielectric-Barrier-Discharges (AP-DBD) fed with helium. Concerning antibacterial surfaces, Chen *et al.* [19] used an atmospheric-pressure plasma jet fed with argon for polymerizing acrylic acid on silk fibers. The resulting carboxylic-functionalized surfaces

were then exposed to an antibacterial peptide after an activation step. The potential of AP-DBD has been also demonstrated for the elaboration of such surfaces via the deposition of carboxylic and N-containing plasma interlayers.[20, 21] However, despite promising results, these strategies present the drawback to rely on a multi-step procedure, justifying thus the necessity to develop a novel one-step immobilization method.

Recently, Klages *et al.* reported the deposition of plasma polymer layer carrying a high density of epoxy groups by using a glycidyl methacrylate (GMA) monomer in an AP-DBD process.[22] The current work has a two-fold objective: i) a deeper understanding of the influence of AP-DBD process parameters on the chemistry and morphology of deposited epoxy-containing layers from GMA, ii) the demonstration that these reactive interlayers can act as an efficient universal interlayer for one-step biomolecule immobilization. Hence, in the first part of the chapter, it will be shown how adjustments of the plasma process parameters can allow to tune the morphology, the deposition rate and the epoxy surface density of the deposited films. In a second part, as a proof of concept, epoxy rich layers will be exploited for the immobilization of two biomolecules. In particular, it will be reported and discussed how the pH of the solution used during the enzyme immobilization step can modify the coating biological performances.

2. Experimental Section

Materials

Plasma depositions were carried out on two kinds of substrates, namely: i) mirror polished stainless steel disks (304-8ND, AC&CS, 2 cm diameter, 1 mm thickness), used for Grazing Angle Fourier Transform - Infrared (FT-IR) measurements and biological tests and ii) two face-polished silicon (111) wafers (Siltronix) for FT-IR analysis in transmission mode and SEM analysis. Conventionally polymerized poly(GMA) powder (Sigma Aldrich, Mn ~20 000 g/mol) was also characterized for comparison.

Two enzymes with very different activities have been used in order to explore the possibilities of the epoxy-containing plasma functional layer as a platform for biomolecule immobilization. Enzymes immobilization on plasma treated samples was carried out in sterile polystyrene non adhesive not-treated 12 well plates (Costar®).

The first enzyme is dispersin B (DspB), a 42 kDa protein with anti-biofouling activity. It is active against both Gram negative and positive bacteria.[23] Its anti-biofouling activity was tested against the biofilm forming bacterial strain *Staphylococcus epidermidis* ATCC35984. DspB immobilization on plasma treated samples was carried out in sterile polystyrene 12 well plates (Thermo Scientific).

The medium used for the anti-biofouling tests are liquid Luria-Bertani (LB) medium, solid LB medium (LB agar) and liquid M63 medium. The composition of liquid LB medium for one liter is 10 g of bactotryptone (BD Biosciences), 5 g of yeast extract (BD Biosciences) and 10 g of NaCl (VWR). Solid LB medium has a similar composition supplemented with 15 g of agar (VWR). M63 medium is composed of 100 mM KH_2PO_4 (VWR), 15 mM $(NH_4)_2SO_4$ (VWR), 16 mM $MgSO_4$ (VWR), 0.004 mM $FeSO_4$ (VWR), 0.5 % casamino acids (VWR), 0.2 % glucose (VWR) and KOH (VWR) for setting pH.

The second biomolecule chosen is a laccase (from *Pleurotus ostreatus*, Sigma-Aldrich), a non-specific hydrolase known to degrade many families of xenobiotics, including antibiotics.[24, 25] Laccase degradation assays were carried out in sterile polystyrene non adhesive not-treated 12 well plate (Costar®). In the present study, the target xenobiotic is the sulfamethoxazole, an antibiotic used in human medicine and detected in residual waste water treatment plants. [26]

Film deposition

The AP-DBD plasma source, depicted in **Figure 1**, consists of two high-voltage electrodes covered by alumina and a moving table as ground electrode with a gap distance of about 1 mm. In order to avoid border effect, the stainless steel substrates (1 mm thickness) are placed into a stainless steel plate with drilled hole of 1mm deep. This latter is fixed on the table, which is moving at a 1 cm/s speed. The distance between the HV electrodes and the stainless steel plate of 1 mm is kept constant. A 15 standard litres per minute (slm) argon flow (99.999 %, Air Liquide), used as carrier gas, was bubbled through the reservoir of glycidyl methacrylate (GMA) (≥ 97 %, Sigma Aldrich, **Figure 2)**. Considering that GMA has a vapour pressure of 0.7 mbar at 20 °C [22] and assuming a complete saturation of the carrier gas stream with the GMA within the bubbler, the GMA flow rate was around 10.5 ml/min.

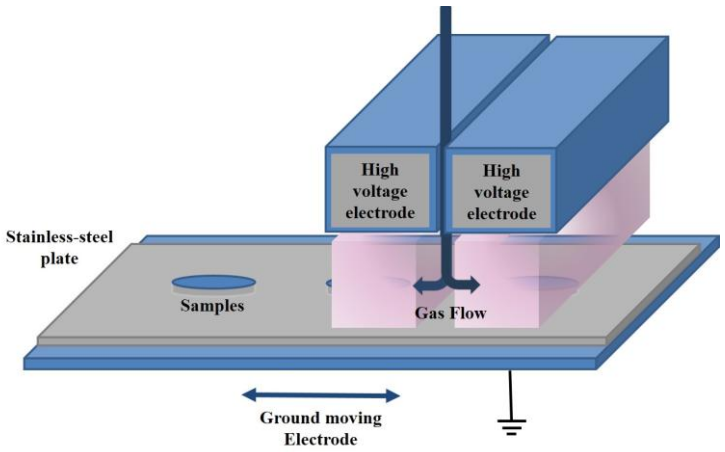

Figure 1: Schematic illustration of the AP-DBD source used for the layer deposition from GMA.

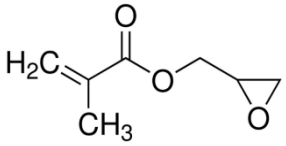

Figure 2. Chemical structure of glycidyl methacrylate (GMA).

The plasma was generated using a "corona generator" 7010R (SOFTAL electronic GmbH) delivering a continuous or pulsed sinusoidal voltage signal, whose frequency was fixed at 10 kHz. Different depositions were carried out by adjusting the discharge mode *i.e.* continuous, (CW) or pulsed (PW) discharges, and by using a 50 W dissipated power (P_{peak}). The plasma-on time (t_{on}) was fixed at 10 ms, the plasma-off time (t_{off}) was varied from 10 to 80 ms. Hereafter, a suitable notation giving the t_{on} and t_{off} duration will be used. For example, 10:80 ms means that a 10 ms t_{on} and a 80 ms t_{off} were used. Average power densities (P_{av}) ranging from 0.2 to 2.8 W/cm^2 were tested. P_{av} can be defined as follows:

$$P_{av} = P_{peak} [t_{on} / (t_{on} + t_{off})] / A$$

where P_{peak} is the power of each plasma pulse and A is the electrode surface area.

Prior deposition, substrates were first cleaned by successive ultrasonic washings in butanone (5 min), acetone (1 min) and absolute ethanol (1 min) and further dried under a nitrogen flux. Then, substrates were activated through an Ar: O_2 (19 slm/ 1slm) plasma

treatment in continuous mode at 1.6 W/cm^2 during 30 seconds. This Ar/O_2 plasma activation step aims to proceed to an ultimate cleaning of the surface of the substrate. [27, 28] It is also performed in order to grow an oxide layer subsequently exploited for the better adhesion stability of the functional layer.

Layer characterization

Scanning electron microscopy (SEM) images were obtained with a Leica Stereoscan 430i (LEO) microscope after sputtering a 5 nm Pt thin film on the top of the plasma coating. The thickness of the plasma-polymerized GMA (ppGMA) deposited on silicon wafers was determined by examination of their cross sections through SEM analysis. The plasma coated silicon wafers were broken along the cleavage plane by the help of a diamond tip cutter. It is a very conventional procedure to obtain cross-sections of coated silicon wafers for subsequent visualization. Before SEM investigation, however, the substrates were coated by a thin Pt layer in order to avoid charging effect. The film deposition rate was determined from the film thickness value and the total plasma deposition duration. The coating thickness measurements were carried out on at least three samples for each plasma deposition condition.

Atomic force microscopy (AFM) analysis was performed in ambient atmosphere using a PicoSPM LE instrument in intermittent-contact mode (Agilent Technologies). Topographic images were recorded at a 1 Hz scanning rate, 200-400 kHz resonance frequency and 25-75 N m^{-1} spring constants.

Fourier-transform infrared analysis was performed with a Bruker Hyperion 2000 spectrometer in transmission and in grazing angle modes (200 scans, 4000-500 cm^{-1} range, 4 cm^{-1} resolution). The epoxy content in the coatings was estimated by integration of the 922-892 cm^{-1} absorption band of normalized spectra according to the layer thickness and by using the OPUS software.

X-ray photoelectron spectroscopy (XPS) was carried out with a Kratos Axis Ultra DLD instrument (equipped with a monochromatic Al Kα X-ray source, hυ = 1486.6 eV working at 50W). The samples being insulating, a charge neutralizer producing low energy electrons of 3 eV was used. The energy calibration was done by fixing the main contribution (adventitious carbon and hydrocarbon) at 285.0 eV. The survey and narrow scans were acquired with 160 eV pass energy, 1 eV step size and 20 eV pass energy, 0.1 eV step size

respectively. The XPS spectra were fitted with the CasaXPS software after subtraction of a Shirley type background. The XPS C1s signal was fitted into six different carbon chemical components [29] , namely: i) C1: hydrocarbon (C_xH_y) at 285.0 eV,, ii) C2: secondary shifted carboxyl (C-CO-O) at 285.7 eV, iii) C3: ether (C-O) at 286.7 eV, iv) C4: epoxy at 287.0 eV, iv) C5: ketone, aldehyde (C=O) or O-C-O at 287.8eV and v) C6: ester (O-C=O) at 289.1 eV. For all components, the full width at half maximum (FWHM) was kept between 1.1 and 1.3 eV. The peak contributions for the C-CO (C2) and O-C=O (C6) chemical groups were kept equal. The experimental uncertainty related to the XPS surface elemental composition is around 2 at %. For each deposition condition, at least two replicates were done and one point per sample (localized in the middle of the coating) was analyzed.

Expression and purification of recombinant antibiofilm dispersin B (DspB)

A strain of *Escherichia coli* is transformed with the introduction of a pET-28a/*DspB* plasmid (Life Technologies, UK). This plasmid is an expression vector for the DspB production allowing the obtention of DspB with an hexa-histidine tag at the C-terminal extremity of its sequence. The transformed bacteria was grown overnight at 37 °C with shaking in 50 ml LB medium supplemented with 50 µg/ml kanamycin. The bacterial suspension was diluted 100-fold in a total of 2 liters of LB supplemented with kanamycin (50 µg/ml), and the expression of DspB was induced with isopropyl-β-D-thiogalactopyranoside (final concentration 0.5 mM). The induced culture was incubated for further 4 h (37 °C, shaking). DspB was purified by nickel affinity chromatography as previously described in the literature. [30] Fractions were analyzed by sodium dodecyl sulfate-polyacrylamide gel electrophoresis (SDS-PAGE) and by the ability to hydrolyze the chromogenic substrate 4-nitrophenyl-N-acetyl-β-D-galactosaminide (Sigma Aldrich). Those fractions containing DspB were pooled and dialyzed against a 10 mM phosphate buffer at pH 5.9 with 100 mM NaCl overnight at 4 °C. Proteins were quantified using the BCA kit (Pierce).

DspB immobilization on ppGMA layers

The ppGMA coated stainless-steel coupons were immersed in 1 mg/mL of DspB-containing 10 mM phosphate buffered solution with pH ranging from 7.0 to 8.5. The substrates were allowed to react for 1 hour (ambient temperature, gentle agitation).

Afterwards, the surfaces were rinsed with deionized water (4 times in 5 min, 250 rpm stirring) to remove unreacted proteins.

In-vitro antiadhesion tests

A preculture of biofilm forming *S. epidermidis* ATCC35984 was grown overnight at 37 °C in a 3 mL Luria-Bertani (LB) media under 150 rpm agitation and used the next morning to seed a fresh culture in LB (50 mL). The bacterial concentration of test inoculum was adjusted to about 10^7 cells/mL in M63 medium. Test inoculum (200 µL) was pipetted onto each substrate. After 24 h of incubation at 37 °C, the substrates were twice rinsed with 10 mL sterile deionized water to remove non-adherent bacteria and then, they were placed face downward in glass jars containing 500-fold-diluted LB (20 mL) and 4-mm glass beads. The jars were shaken and then, their contents were sonicated in a water bath (50-60 kHz) for 2 min. Adherent bacteria were counted by plating 10-fold dilution on LB agar. The plates were incubated at 37 °C overnight before the counting of the colony-forming units. The reported results in this chapter are the averages of at least 3 replicates.

Laccase immobilization on ppGMA layers

Laccase were immobilized on ppGMA coated stainless-steel coupons through immersion in 1 mL of a 10 mM PBS containing 1 mg/mL laccase at pH 7.0 or 8.5 (1 h, room temperature, 150 rpm stirring). The samples were then washed (5 times during 5 min, purified water, 250 rpm stirring).

Estimation of the immobilized laccase quantity on the coupons

The enzymatic concentrations in solution were determined with the RC DC™ Protein Assay (Bio-Rad). The amount of immobilized laccase on the functionalized surfaces was estimated from the difference of laccase concentrations in solution before and after the immobilization procedure.

Degradation Assays

For the immobilized enzymes, an enzymatic activity was estimated by monitoring the sulfamethoxazole degradation over time. Enzymes were incubated in a 2 mL degradation medium composed of sterile MilliQ water, HEPES (12.5 mM) and sulfamethoxazole (100 µg/mL). Each 24 h, the degraded sulfamethoxazole concentration was estimated by absorbance measurement at 260 nm with a Synergy 2 Multi-Mode Plate Reader (Biotek). The medium was removed every 24 h. Wells were washed 3 times with filtered tap water and further filled with a fresh degradation medium.

For the free enzymes in solution, in the wells used for the first measurements (t = 24 h), 8 µg of enzymes were directly dissolved in a 2 mL degradation medium containing sulfamethoxazole at a 100 µg/mL concentration.

For all other wells, at time t0, enzymes were dissolved in a 300 µL medium containing 20 µg/mL of sulfamethoxazole. All wells were supplemented with the same media every 24 h. Also, 24 h prior the enzymatic activity measurement, wells were amended with a 100 µg/mL antibiotic solution and supplemented to achieve a 2 mL final volume.

3. Results and Discussion

3.1. Influence of process deposition conditions on chemistry and morphology of ppGMA layers

The AP-DBDs fed with Ar and GMA and operating under continuous or pulsed discharges lead to the deposition of ppGMA films well adherent to the metallic substrates.

As shown in **Figure 3,** reporting the dependence of film deposition rate with t_{off}, one can notice that over the t_{off} range investigated, pulsed discharges lead to higher growth film rates than the CW one, suggesting the occurrence of different deposition mechanisms during t_{on} and t_{off}, which influence the chemistry and morphology of the deposited films.

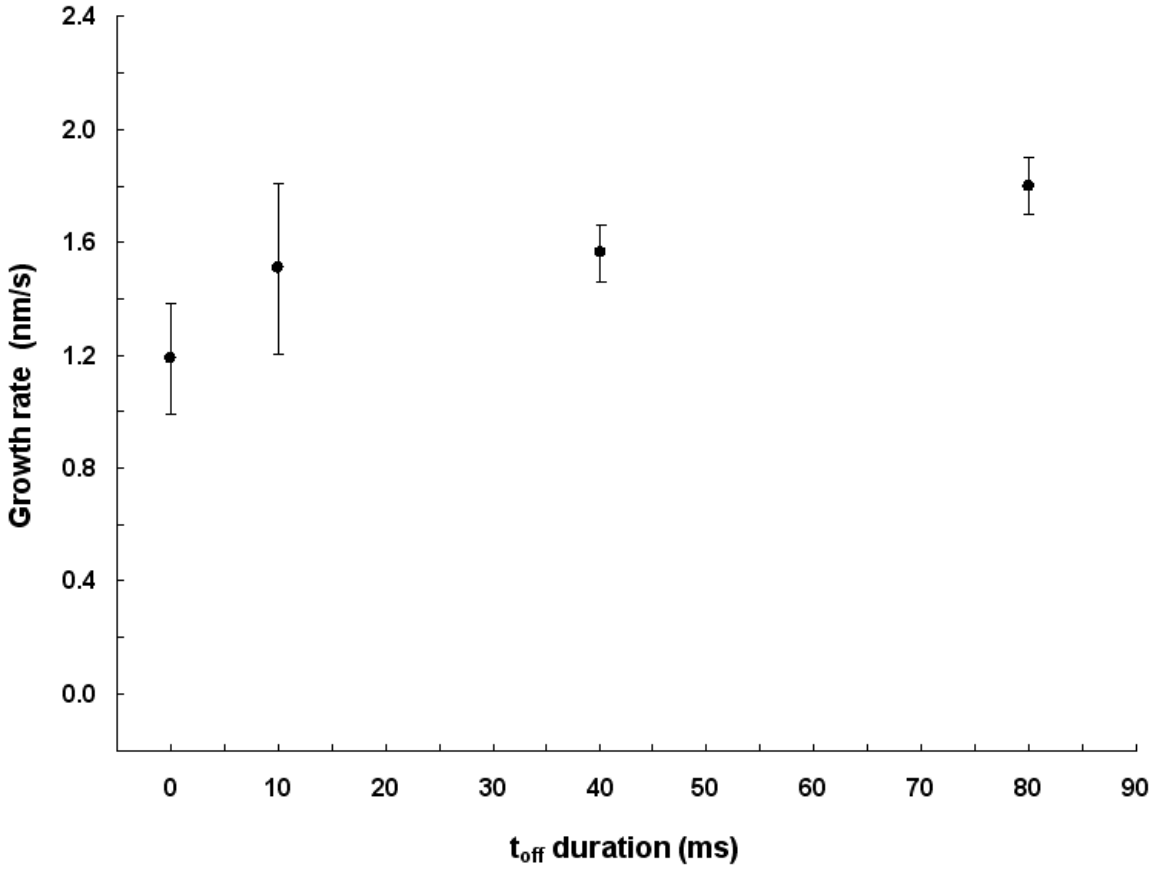

Figure 3: Evolution of the ppGMA film growth rate as a function of the plasma-off time (t_{off}), ranging from 0 (CW mode) to 80 ms. (t_{on} fixed at 10 ms; 50 W peak power).

SEM observations reported in **Figure 4** reveal that, whatever the deposition conditions, pinhole-free coatings covering homogeneously the entire substrate surface are achieved. Interestingly, one can notice that the electrical discharge parameters are likely to affect both layer deposition rate and morphology. In particular, working in CW mode lead to rough nanostructured surfaces with an averaged roughness value (Ra) around 148 nm (**Figure 4.a** and **Table 1**) and composed of an abundant amount of aggregates presenting an average size distribution of 94 ± 11 nm. This kind of topography is typical of coatings deposited through an atmospheric-pressure plasma-enhanced CVD process [31, 32] and is related to higher plasma energy density favoring gas phase reactions and surface etching. Pulsing the discharge leads to smoother layers with Ra value close to 24 nm at 10:80 ms conditions. Interestingly, compared to the layers deposited in CW, those deposited in 10:10 ms conditions have an intermediate roughness (Ra 43 nm *vs* 148nm), with a higher average feature size (168 ± 25 nm). Finally, layers deposited at 10:80 ms are almost aggregate-free,

which may indicate that the growth mechanism of these layers is largely controlled by predominant surface reaction.

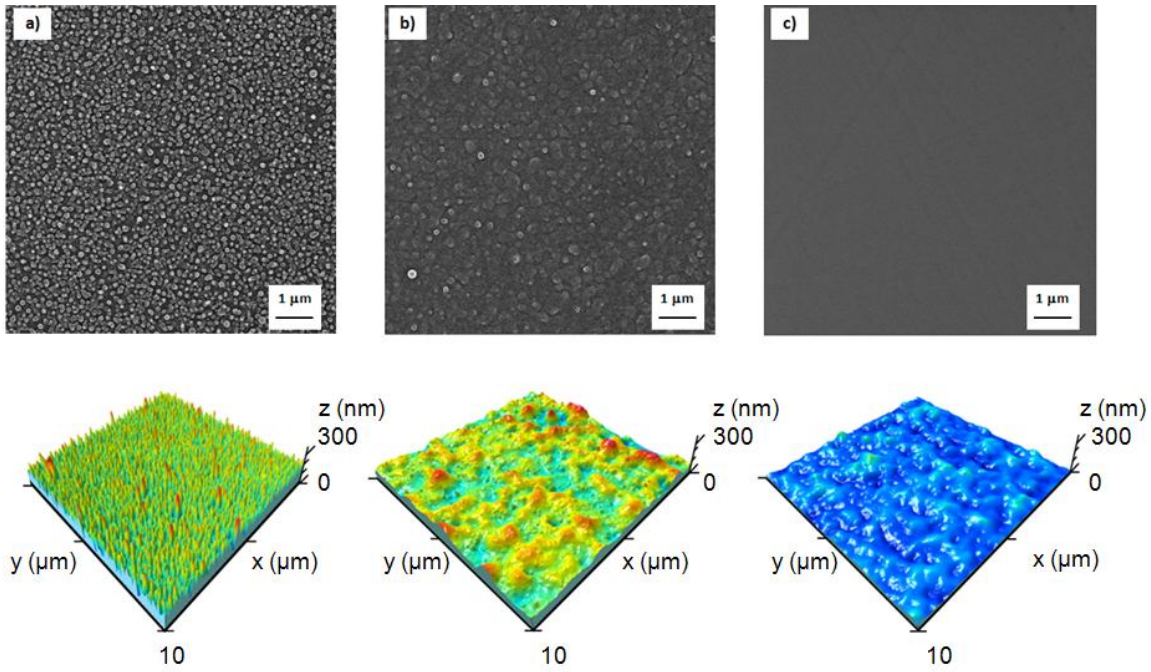

Figure 4: SEM (top) and AFM (bottom) pictures of ppGMA layers deposited at 50 W in CW mode (a) and 10:10 ms (b) and 10:80 ms PW modes (c).

Table 1. Roughness values of ppGMA layers estimated by AFM measurements.

Deposition conditions	Average Roughness (Ra, nm)	Increment of surface area (%)
50 W, CW	148 ± 13	66.00 ± 1.00
50 W, 10:10 ms	43 ± 8	0.20 ± 0.02
50 W, 10:80 ms	24 ± 11	0.10 ± 0.04

FT-IR analysis (**Figure 5**) was carried out in order to study the chemistry of the deposited film. Particular attention was paid to the detection of the four epoxide characteristic peaks, namely the epoxide ring C-H stretching at 3063 cm^{-1}, the ring breathing mode at 1258 cm^{-1}, the asymmetric and symmetric ring deformation bands at 910 cm^{-1} and 852 cm^{-1}, respectively.[33] For the ppGMA layers deposited at 50W in CW mode, all the above mentioned bands were barely detectable, suggesting that most epoxide rings were opened during the deposition. In contrast, epoxide bands were clearly noticeable for ppGMA

deposited in pulsed mode. This result suggests the existence of two distinct layer growth mechanisms when depositions are carried out in continuous or pulsed mode. In particular, one can notice that increasing t_{off} from 10 to 80 ms (*i.e.* decreasing the duty cycle) leads to increasing the epoxide bands intensity, indicating a higher content of epoxide groups in the films. These results are in agreement with Klages *et al.* [22], demonstrating that pulsed AP-DBD allows the formation of coatings with high monomer structure retention due to chemical reactions occurring during the t_{off} between intact monomer molecules and surface radical centers generated during the t_{on} period.

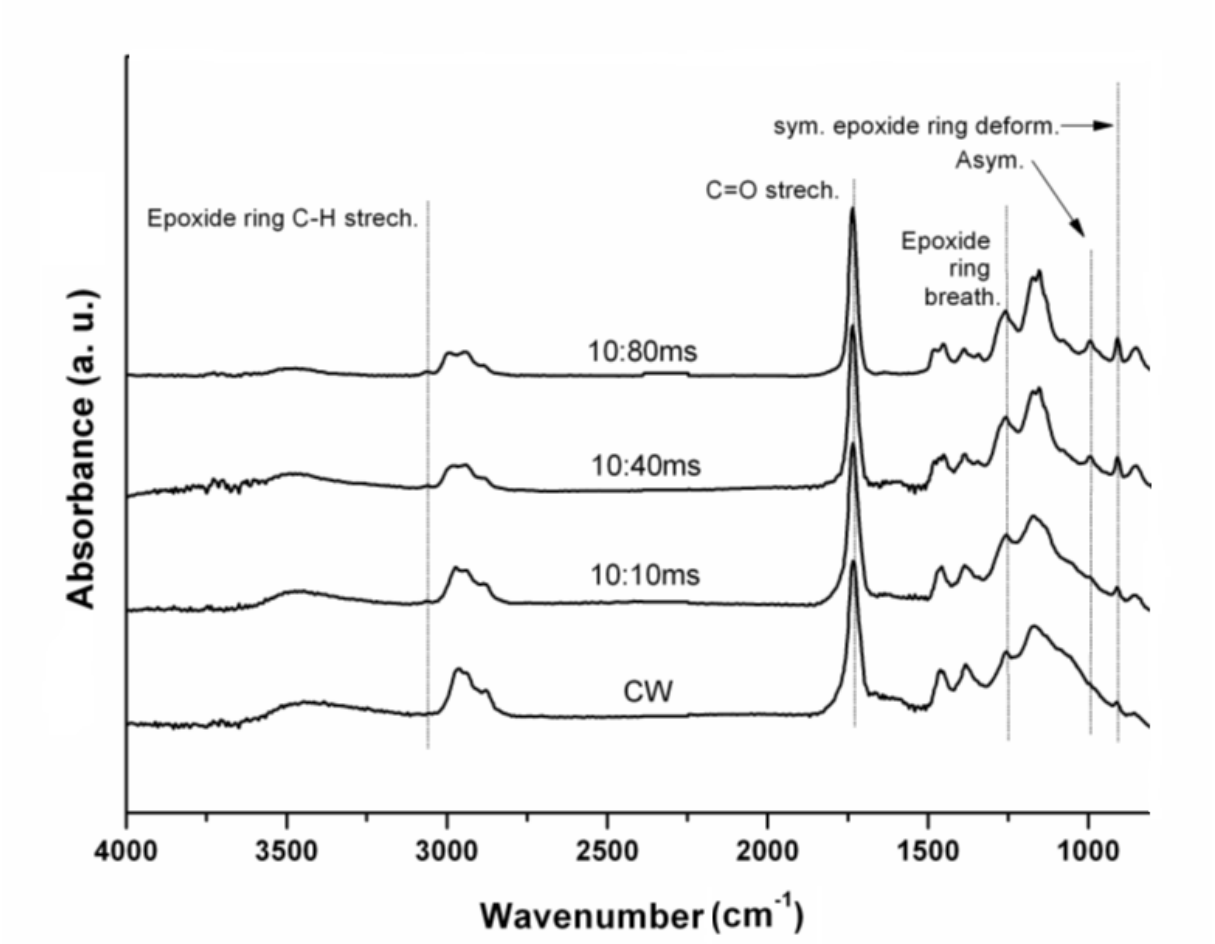

Figure 5: FT-IR spectra of ppGMA films deposited at 50 W with different duty cycles. All spectra were normalized to the maximum value of the C=O band (1735 cm^{-1}).

To estimate the epoxide content in the ppGMA layers, the area of FT-IR asymmetric epoxide stretching band was calculated. Hence, as shown in **Figure 6**, it is concluded that working in pulsed mode allows to drastically increase the epoxy content in the deposited film up to a factor of 4.

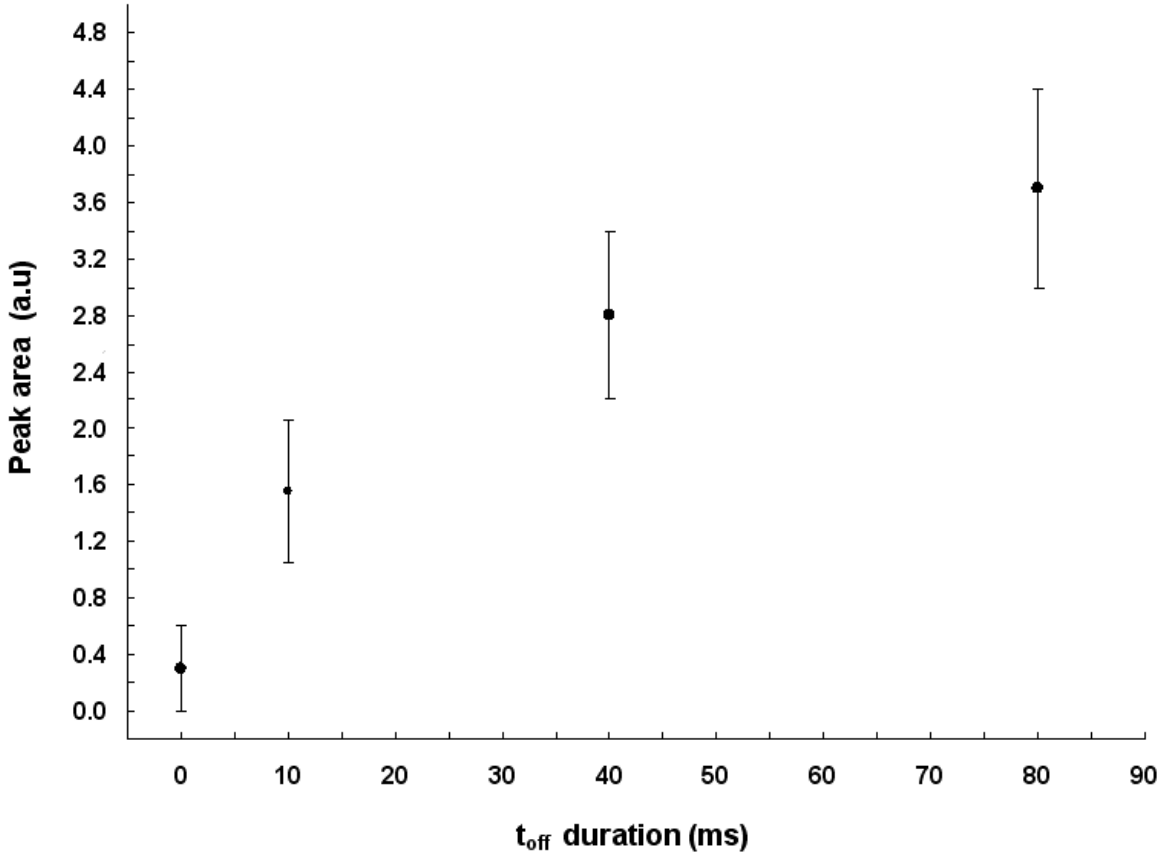

Figure 6: Area evolution of the FT-IR asymmetric epoxide ring deformation band as a function of the plasma-off time (t_{off}), ranging from 0 (CW mode) to 80 ms. (t_{on} fixed at 10 ms; 50 W peak power).

In the aim of later exploiting chemical interfacial reactions between atmospheric-pressure plasma functionalized solid surfaces and free biomolecules, XPS analysis was carried out to get some insights concerning the ppGMA uppermost surface composition. In particular, this analysis allows to estimate the reactive epoxy surface density, a parameter which is reported to be strongly related to the biological performance of the functionalized surfaces.

Considering ppGMA deposited in CW mode, the XPS atomic percentages of the surfaces for the C:O elements were found to be equal to 77:23 (**Table 2**). Compared to the commercial poly(GMA) stoichiometry of 73:27, a lesser amount of oxygen was detected in the CW ppGMA layers, which might be correlated to the significant loss of the epoxy ring (*i.e.* monomer structure degradation), already highlighted in IR analysis (Figure 5). In

contrast, it can be observed that PW deposited ppGMA layers and poly(GMA) present similar XPS compositions.

The influence of the discharge mode (CW vs PW) on the layer composition chemistry is particularly noticeable by overlapping their XPS C1s spectra (**Figure 7**). Indeed, one can clearly observe that a pulsed discharge allows a higher retention of the initial monomer ester group (C1s contribution at 289.1eV) accompanied by the retention of epoxy groups (C1s contribution at 287.0 eV). In particular, from the XPS C1s curve-fitting data shown in Table 2, it appears that increasing the t_{off} leads to an increase of the epoxy surface content with values ranging from 7 to 18 at. % for layers deposited at 10 and 80 ms t_{off} duration, respectively. Interestingly, despite using mild process conditions, the maximal 27% epoxy content estimated for poly(GMA) is never reached in ppGMA layers. An explanation is that, despite a short t_{on} duration, there is a non-negligible contribution of the film chemistry growth during this period associated to a high fragmentation of the monomer, and thus, a loss of the epoxy group. This theory is fully consistent with the results obtained in CW mode.

The ageing of the richest epoxy ppGMA layer (*i.e.* 50 W, in 10:80 ms mode) was investigated through a 50 days storage period at ambient temperature and humidity. According to XPS analysis (Table 2), these storage conditions seem to have no significant influence on the layer composition that remains comparable to the poly(GMA)'s one, with C and O content equal to 73 and 27 at.% respectively.

However, a careful C1s curve fitting allows highlighting a two folds decrease of the epoxy surface density down to 9 % content, suggesting the relative chemical instability of epoxy groups.

Table 2. XPS atomic percentages and C1s curve fitting data for ppGMA layers deposited in CW and PW modes. The results for a PW ppGMA layer after ageing 50 days at air, and for a commercial poly(GMA) polymer are also reported.

	Samples:	50 W, CW	50 W, 10:10 ms	50 W, 10:80 ms	50 W, 10:80ms after 50 days at air	Poly(GMA)
►**XPS surface composition (at. %):**						
	C	77	75	72	73	73
	O	23	25	28	27	27
►**XPS C1s peak fitting (%):**						
Contribution	**Binding energy (eV)**	**Functional group**				
C1	285.0	C-C	52	36	33	38	42
C2	285.7	C-CO-O	8	11	13	12	11
C3	286.7	C-O	25	25	22	25	8
C4	287.0	epoxy	0	7	18	9	27
C5	287.8	C=O/ C-O-C	5	10	2	4	-
C6	289.1	O-C=O	8	11	13	12	11

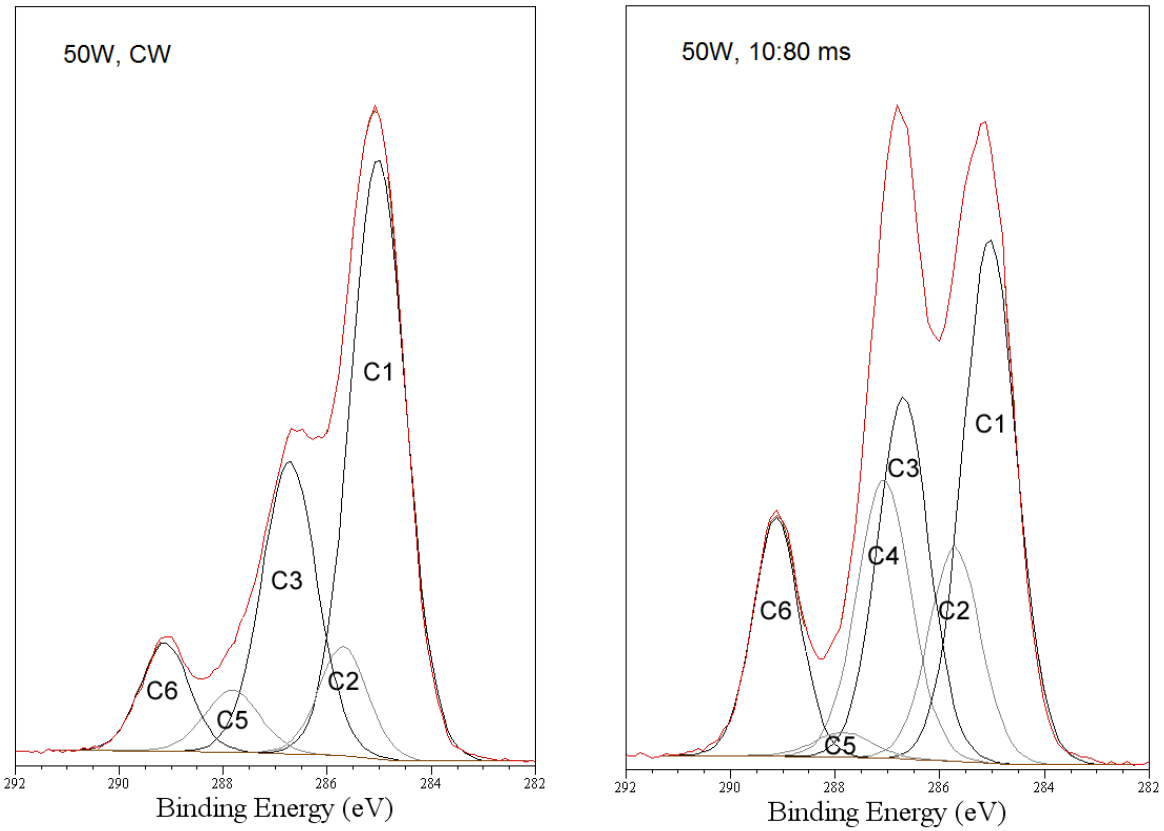

Figure 7: XPS C1s curve fittings for ppGMA layers deposited at 50W, CW mode (left) and 50 W, 10:80 ms mode (right).

In conclusion, it can be reported that, among the different plasma process conditions investigated, the pulsed atmospheric-pressure plasma polymerization of GMA carried out at 50 W in 10:80 ms allows for the fast deposition of adherent and smooth layers presenting the highest epoxy surface density, up to 18 % (XPS data). Such freshly deposited ppGMA layers were selected in order to maximize the efficiency of biomolecule immobilization. [34]

3.2. DspB immobilization and anti-biofouling assessment

To ascertain the immobilization of DspB enzyme on the ppGMA layers, FT-IR analysis was carried out. From the data reported in **Figure 8,** one can notice that, independently of the pH of the DspB solution used during the immobilization step (*i.e.* pH= 7.0 or 8.5), ppGMA layers allow to efficiently immobilize the enzyme, as it is suggested by the appearance of new peaks related to peptide bonds, namely secondary amide N-H stretching, amide C=O stretching and amide N-H bending bands located at 3281 cm^{-1}, 1645 cm^{-1} and 1539 cm^{-1}, respectively.[35] The peaks, characteristic of epoxide groups, at 1258, 910 and 852 cm^{-1} are probably linked to their presence into the plasma film bulk, highlighting that the mild basic immobilization condition used does not lead to the epoxy loss through the ester group hydrolysis.

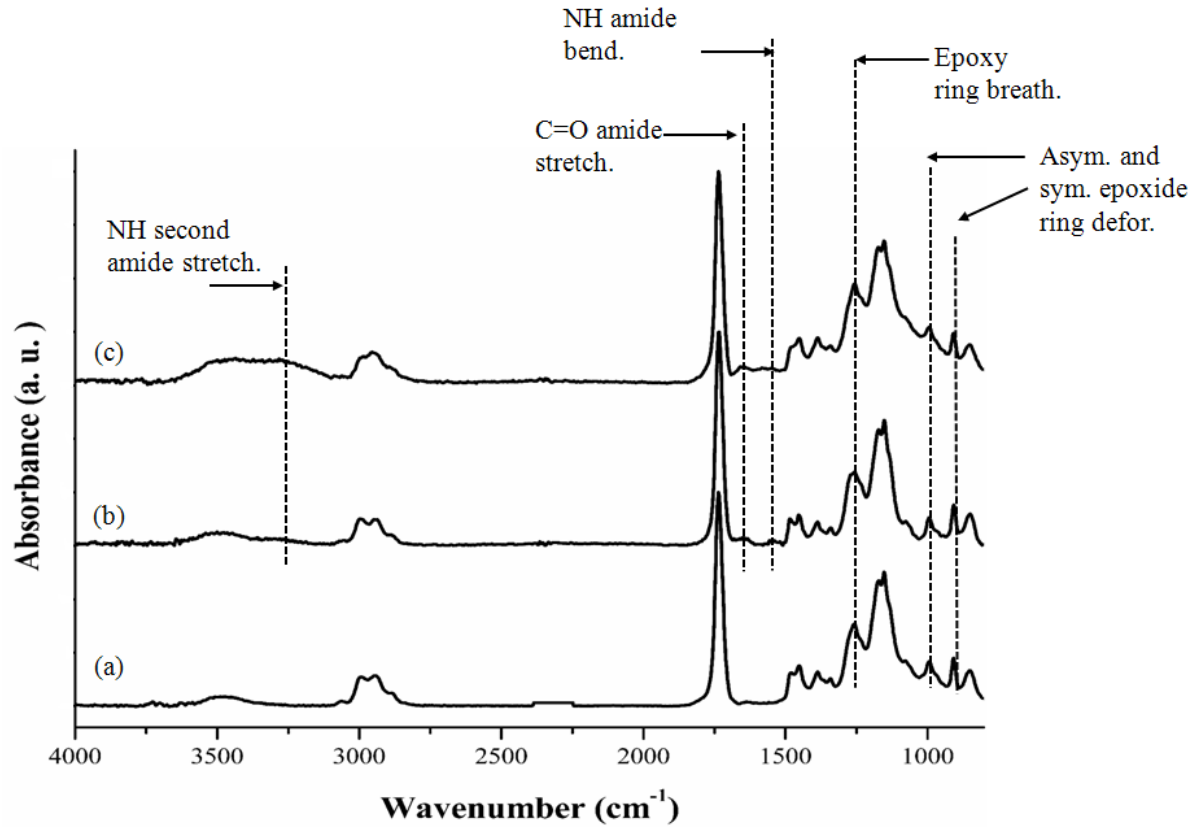

Figure 8: FT-IR spectra of freshly deposited ppGMA layers at 50 W in 10:80 ms (a), layer "a" after DspB immobilization at pH 7.0 (b) and pH 8.5 (c).

As reported in **Table 3**, independently of the pH of the DspB solution used during the immobilization steps, the DpsB-grafted coatings provide a comparable reduction of the number of viable adherent bacteria, up to 84 %, after only 1 day of contact. This result highlights that this enzyme has maintained its anti-biofouling property even after its covalent immobilization on the ppGMA layers. The fact that the immobilized enzyme has kept its activity can suggest that its biological reaction sites have not been affected during the reaction with the ppGMA layer. The pH change during the enzyme grafting step has no effect on the final measured enzymatic activity. This suggests that the active immobilized enzyme amount is similar in both cases.

By reference with other works reported in literature, the reason of this success can probably be associated to the presence of an hexahistidine tag (his-tag) added at the C-terminal extremity of the enzyme.[23] Kurzatkowska *et al.*[36] have already reported the exploitation of His-tag to ensure an enzyme immobilization in a proper orientation, or at least, to initiate an attachment which could then be supplemented by other interactions with the rest of the enzyme structure, and consequently, preventing or limiting the interaction and/or masking of the enzyme active site. Martin *et al.* [37] have also reported that his-tagged biomolecules can be covalently immobilized on supports through the nucleophilic reaction of the imidazole group (*i.e.* secondary amine) with the epoxy groups. In conclusion, if His-tag sequence has been initially introduced at the protein chain end to ensure its purification on a nickel affinity column during its production step, the present work highlights its usefulness for a covalent immobilization purpose.

Table 3. Anti-biofouling activity against *S. epidermidis* biofilm forming of modified stainless-steel surfaces compared to uncoated ones.

Samples	Reduction of adherent population (%)
Stainless-steel	0
ppGMA layers	0
Dsp B immobilized at pH 7.0	79 ± 16
Dsp B immobilized at pH 8.5	84 ± 11

3.3. Enzyme immobilization for xenobiotic degradation

Irrespective of the pH (*i.e.* pH= 7.0 or 8.5) used during the enzyme immobilization step, pp-GMA layers allow the grafting of laccases, which are later active for the degradation of sulfamethoxazole. In **Table 4**, the average enzyme activity duration and the total quantity of degraded sulfamethoxazole for free and immobilized laccase are reported after different periods of time and **Figure 9** shows their degradation kinetics.

All these results show clearly that the immobilization of the enzyme increases its efficiency and the duration of the enzymatic activity. By comparing the results between the test where the enzymes are in solution and the other one, where they are immobilized on a ppGMA surface at pH 7, it was observed that the total duration activity was multiplied by at least a factor of 4 (36 h vs 144 h for free and immobilized enzymes respectively). Two hypotheses can support this interesting result. The first one can be attributed to the advantage of carrying out a strong enzyme immobilization through a multipoint anchorage. Indeed, this situation is known to confer a rigidity to the three-dimensional structure of the enzyme thus, limiting breakdown and autolysis phenomena due to physico-chemical environmental factors. [38, 39] The second one can be associated to the combined effect of pH and stirring when the enzymes are in solution. Indeed, these two parameters have been reported to promote free-form protein aggregation in solution [40] and to partly inactivate or neutralize enzymes.[3] In particular, the study of Shleev *et al.*[41] reports that free-form laccase in phosphate buffer solution at pH 6.5, value closed of the experimental conditions, can be aggregated and/or inactivated.

In addition, the results show that during the enzyme immobilization, if the pH of the solution is lightly basic (pH = 8.5), the total amount of fixed enzyme is increased by a factor of 2. One hypothesis can be given to explain this result, it relies on the existence of different isoenzyme forms as it is known that pH can generate new rearrangement of the laccase periphery. Consequently, an improvement of the enzyme- plasma-treated surface interactions might be expected at pH 8.5.

Finally, it was also observed that bioactive layers generated at pH 8.5 present an increased xenobiotic degradation activity duration compared to the ones generated at pH 7.0 (240 h vs 144 h, respectively). More precisely, during the first 36 h of bioactivity, both surfaces presented a similar efficiency. However, after this time lapse, the laccase activity set at pH 7.0 sharply decreased while the enzymatic activity of active layer generated at pH 8.5

slowly decreases until to reach zero after 240 h. One explanation might come from the increased amount of fixed enzymes. Indeed, the density of immobilized proteins might have an influence on the three-dimensional structure of the protein due to the existence of numerous and deleterious protein-surface interactions. As reported by Tiller *et al.* [42], when the surface of a substrate is covered with a high density of immobilized proteins, there are few possible interactions between the protein and the substrate, thus ensuring probably the integrity of the 3D protein structure and the preservation of its enzymatic activity. In conclusion, these results highlight the importance of a well-adapted pH solution selection for the enzyme immobilization step.

Table 4. Summary of the averaged enzyme activity duration and the total quantity of degraded sulfamethoxazole for free and immobilized laccase. The quantity of immobilized enzymes on ppGMA layers is also reported.

Assays	**Averaged activity duration (h)**	**Quantity of immobilized enzyme (µg)**	**Quantity of degraded sulfamethoxazole for a 1 mL solution (µg)**
Free enzyme in solution	36	-	75 ± 5
Laccase immobilized at pH 7.0	144	5.5 ± 4.0	174 ± 15
Laccase immobilized at pH 8.5	240	12.0 ± 1.0	275 ± 14

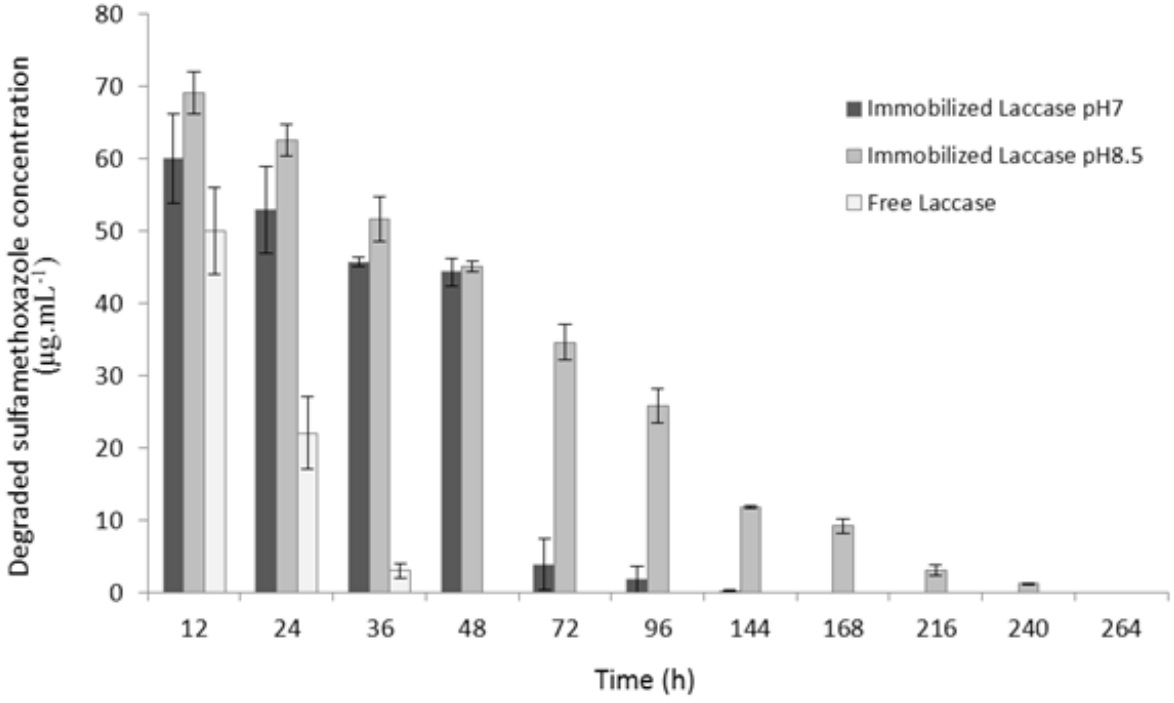

Figure 9: Activity of free and immobilized laccase.

4. Conclusion

A novel atmospheric-pressure method has been developed to efficiently immobilize enzymes onto solid surfaces, based on the AP-DBD deposition of an epoxy-rich layer and its subsequent interfacial one-step reaction with biomolecules in mild aqueous conditions. The method has highlighted that it is possible: i) to modify the coating morphology by the use of continuous or pulsed discharges, ii) to tune the epoxy surface density by adjusting the t_{on}/ t_{off} ratio and iii) to optimize the amount of grafted enzymes by selecting an appropriate pH during the immobilization step. Here, bioactive surfaces with anti-biofouling and xenobiotic degrading properties have been successfully elaborated. In particular, the immobilized laccase on ppGMA layers present an extended duration activity and efficiency around 4 and 7 times higher than for the free enzyme in solution, respectively. Importantly, these results tend to show the versatility of the method as these epoxy-rich layers might offer the possibility to immobilize different functional biomolecules paving the way to the elaboration of novel advanced bioactive materials.

References

[1] W. Tischer, F. Wedekind, *Top. Curr. Chem.*, vol.200, **1999**, p. 96

[2] S. Aggarwal, S. Sahni, *International Conference on Environmental, Biomedical and Biotechnology, 201, 18*

[3] B. M. Brena, F. Batista-Viera, *Methods in Biotechnology: Immobilization of enzymes and cells*, Second Edition, J. M. Guisan, Humana Press Inc., Totowa, NJ, **2006**

[4] J. D. McGettrick, T. Crackford, W.C.E Shofield, J.P.S Badyal, *Appl. Surf. Sci.* **2009**, *256S*, S30

[5] C. Vreuls, G. Zocchi, B. Thierry, G. Garitte, S. S. Griesser, C. Archambeau, C. Van de Weerdt, J. Martial, H. Griesser, *J. Mater. Chem.* **2010**, *20*, 8092

[6] B. Thierry, M. Jasieniak, L. C. P. M. de Smet, K. Vasilev, H. J. Griesser, *Langmuir* **2008**, *24*, 10187

[7] L. Chu, W. Knoll, R. Förch, *Biosens. Bioelectron.* **2008**, *24*, 118

[8] L. De Bartolo, S. Morelli, A. Piscioneri, L. C. Lopez, P. Favia, R. d'Agostino, E. Drioli, *Biomol. Eng.* **2007**, 24, 23

[9] L. C. Lopez, M. G. Buonomenna, E. Fontananova, G. Iacoviello, E. Drioli, R. d'Agostino, P. Favia, *Adv. Funct. Mater*. **2006**, *16*, 1417

[10] E. Sardella, L. Detomaso, R. Gristina, G. S. Senesi, H. Agheli, D. S. Sutherland, R. d'Agostino, P. Favia, Plasma Process. Polym. **2008**, *5*, 540

[11] L. De Bartolo, S. Morelli, L. C. Lopez, L. Giorno, C. Campana, S. Salerno, M. Rende, P. Favia, L. Detomaso, R. Gristina, R. d'Agostino, E. Drioli, *Biomaterials* **2005**, *26*, 4432

[12] M. Kastellorizios, G. P. K. Michanetzis, B. R. Pistillo, S. Mourtas, P. Klepetsanis, P. Favia, E. Sardella, R. d'Agostino, Y. F. Missirlis, S. G. Antimisiaris, *Int. J. Pharm.* **2012**, *432*, 91

[13] S. Pavlica, S. Schmitmeier, P. Gloeckner, A. Piscioneri, F. Peinemann, K. Krohn, M. Siegmund-Schulz, S. Laera, P. Favia, L.D. Bartolo, A. Bader, *J. Tissue Eng. Regen. Med.* **2012**, *6*, 486

[14] B. R. Coad, M. Jasieniak, S. S. Griesser, H. J. Griesser, *Surf. Coat. Technol.* **2013**, *233*, 169

[15] G. Da Ponte, E. Sardella, F. Fanelli, R. d'Agostino, P. Favia, *Eur. Phys. J. Appl. Phys*. **2011**, *56*, 24023

[16] B. Nisol, C. Poleunis, P. Bertrand, F. Reniers, *Plasma Process. Polym.* **2010**, *7*, 715

[17] B. Nisol, G. Oldenhove, N. Preyat, D. Monteyne, M. Moser, D. Perez-Morga, F. Reniers, *Surf. Coat. Technol.* **2014**, *252*, 126

[18] G. Da Ponte, E. Sardella, F. Fanelli, R. d'Agostino, R. Gristina, P. Favia, *Plasma Process. Polym.* **2012**, *9*, 1176

[19] G. Chen, M. Zhou, Z. Zhang, G. Lv, S. Massey, W. Smith, M. Tatoulian, *Plasma Process. Polym.* **2011**, *8*, 701

[20] R. Mauchauffé, M. Moreno-Couranjou, N.D. Boscher, C.Van De Weerdt, A-S. Duwez, P. Choquet, *J. Mater. Chem. B* **2014**, *2*, 5168

[21] D. Duday, C. Vreuls, M. Moreno, G. Frache, N. D. Boscher, G. Zocchi, C. Archambeau, C. Van De Weerdt, J. Martial, P. Choquet, *Surf. Coat. Technol.* **2013**, *218*, 152

[22] C. –P. Klages, K. Höpfner, N. Kläke, R. Thyen, *Plasmas Polym.* **2000**, *5*, 79

[23] J. B. Kaplan, C. Ragunath, N. Ramasubbu, D. H. Fine, *J. Bacteriol.* **2003**, *185*, 4693

[24] S. Rodríguez Couto, J. L. Toca Herrera, *Biotechnol. Adv.* **2006**, *24*, 500

[25] C. E. Rodríguez-Rodríguez, M. A. García-Galán, P. Blánquez, M. S. Díaz-Cruz, D. Barceló, G. Caminal, T. Vicent, *J Hazard Mater*. **2012**, *213-214*, 347

[26] A. Göbel, A. Thomsen, C. S: McArdell, A. Joss, W. Giger, *Environ. Sci. Technol.* **2005**, *39*, 3981

[27] G. Baravian, D. Chaleix, P. Choquet, P. L. Nauche, V. Puech, M. Rozoy, *Surf. Coat. Technol.* **1999**, *115*, 66

[28] J. M. Thiébaut, T. Belmonte, D. Chaleix, P. Choquet, G. Baravian, V. Puech, H. Michel, *Surf. Coat. Technol.* **2003**, *169–170*, 186

[29] G. Beamson, D. Briggs, High Resolution XPS of Organic Polymers The Scienta ESCA 300 Database, Wiley-VCH, New York, **1992**

[30] E. Faure, C. Falentin-Daudré, T. S. Lanero, C. Vreuls, G. Zocchi, C. Van De Weerdt, J. Martial, C. Jérôme, A.-S. Duwez, C. Detrembleur, *Adv. Funct. Mater.* **2012**, *22*, 5271

[31] A. Manakhov, , M. Moreno-Couranjou, N. D. Boscher, V. Rogé, P. Choquet, J.-J. Pireaux, *Plasma Process. Polym.* **2012**, *9*, 435

[32] H. Hody, P. Choquet, M. Moreno-Couranjou, R. Maurau, J.-J. Pireaux, *Plasma Process. Polym.* **2010**, *7*, 403

[33] C. Tarducci, E. J. Kinmond, J. P. S. Badyal, S. A. Brewer, C. Willis, *Chem. Mater.* **2000**, *12*, 1884

[34] L. Cao, *Carrier-bound immobilized Enzymes*, Wiley, Weinheim, Germany **2005**.

[35] B. Smith, *Infrared Spectral Interpretation. A Systematic approach*, Second Edition, CRC Press LLC, Bocar Raton, FL, **1999**

[36] K. Kurzątkowska, M. Mielecki, K. Grzelak, P. Verwilst, W. Dehaen, J. Radecki, H. Radecka, *Talanta* **2014**, *130*, 336

[37] M. T. Martin, F. J. Plou, M. Alcalde, A. Ballesteros, *J. Mol. Catal. B: Enzym*. **2003**, *21*, 299

[38] H. –C. Mahler, W. Friess, U. Grauschopf, S. Kiese, *J. Pharm. Sci*. **2009**, *98*, 2909

[39] C. Garcia-Galan, A. Berenguer-Murcia, R. Fernandez-Lafuente, R-C. Rodrigues, *Adv. Synth. Catal.* **2011**, *353*, 2885

[40] C. Mateo, V. Grazù, B. C. Pessela, T. Montes, J. M. Palomo, R. torres, F. López-Gallego, R. Fernández-Lafuente, J. M. Guisán, *Biochem. Soc. Trans*. **2007**, *35*, 1593

[41] S. Shleev, C. T. Reimann, V. Serezhenkov, D. Burbaev, A. I. Yaropolov, L. Gorton, T. Ruzgas, *Biochimie* **2006**, *88*, 1275

[42] J. C. Tiller, R. Rieseler, P. Berlin, D. Klemm, *Biomacromolecules* **2002**, *3*, 1021

Chapter 4

Self-defensive Coating for Antibiotics Degradation – Atmospheric Pressure Chemical Vapor Deposition of Functional and Conformal Coatings for the Immobilization of Enzymes

Sébastien Bonot, Rodolphe Mauchauffé, Nicolas D. Boscher, Maryline Moreno-Couranjou, Henry-Michel Cauchie and Patrick Choquet, *Advanced Materials Interfaces*, **2015**, *2*, 1500253.

1. Introduction

A wide variety of xenobiotics are released into wastewater, including antibiotics which are extensively used in human and veterinary medicine. They are found in the effluents of wastewater treatment plants but also in tap water itself and even in drinking water sources.[1] Present in sub-inhibitory concentrations, antibiotics can have many effects profoundly altering the physiology of the bacteria with various consequences such as the increase of virulence, the induction of biofilm formation, some changes in the balance of populations and finally the risk of the emergence of new resistant bacteria through the induction of gene transfers.[2,3,4,5,6] More precisely, in water treatment plants (WTP), a fraction of the xenobiotics is adsorbed to suspended solids and removed by settling, while another part is dissolved in the water and partially degraded through physico-chemical and biological reactions.[7] However, an important quantity still persists after these primary and secondary treatments. Therefore tertiary treatments, such as UV or ozonation, are investigated for the ultimate degradation of these molecules. Nevertheless, despite their efficiency, they are also known to generate undesirable and sometimes toxic secondary metabolites molecules, which are usually more pernicious than the parental antibiotics compounds.[8,9] The use of specific enzymes might provide a new alternative or a complement to existing treatments commonly used in WTP. Numerous enzymes which degrade and inactivate antibiotics are known and are encoded by the antibiotics resistance genes of bacteria.[10] However it has been shown that under certain conditions antibiotics inactivated by these enzymes could be reactivated by a reverse chemical or enzymatic reaction.[11,12] This is why it is necessary to degrade the target molecules into more ultimate products through the combination of several enzymes. In this case the use of less specific hydrolase such as laccases, which are known to degrade a wide variety of xenobiotics, is essential.[13]

Free enzymes can quickly lose their activity due to autolysis, physico-chemical and biological degradation in the medium and/or aggregation.[14,15] An efficient way to overcome these drawbacks is to immobilize the enzymes on a surface. As highlighted by a large number of studies, the immobilization of enzymes brings most of the time multiple benefits *e.g.* (1) limiting autolysis and ensuring protection against physico-chemical and biological degradation, (2) increasing the lifetime of the enzyme, (3) increasing the enzyme activity and

the degradation rate.[16] In addition, multi-anchoring may give more rigidity to the protein which increases its resistance. In the case of a surface immobilization via weak interactions the release of the enzyme can easily occur by simple parameter changes such as pH, temperature or surfactant presence, making the immobilized surfaces only usable in a limited range of conditions. In order to have long lasting properties under a wide range of conditions, a strong and irreversible immobilization is preferred. Among the various methods developed, the covalent binding of enzymes over a surface remains the most employed and studied method.[17] Surfaces with functional groups, *e.g.* amine, carboxylic, propargyl, aldehyde or epoxy groups, are able to form covalent bonds using a linker or through direct reaction, when possible, with the functional groups present in the enzymes, *i.e.* amine, carboxylic, thiol or imidazole groups, in aqueous buffer at room temperature.[18,19,20,21,22]

Surface functionalization can be achieved through many different methods. Among them, Chemical Vapor Deposition (CVD) processes, which are solvent-free environmentally friendly methods, provide several convenient routes for the conformal deposition of functional polymer thin films. Notably, initiated CVD (iCVD), which implies the use of a thermally labile initiator to form radicals that further initiate the free-radical polymerization reaction, has proven to be a suitable method for the conformal deposition of a large number of functional polymers.[23,24,25] If iCVD has already been successfully up-scaled for the coating of various materials, the required low-pressure is likely to induce some limitations (*e.g.* coating of very large sized objects). Recently, an atmospheric pressure CVD approach employing ultra-short plasma discharges was investigated for the deposition of polymer thin films. The method, called Plasma initiated CVD (PiCVD), combines the advantages of iCVD and atmospheric pressure Plasma Enhanced CVD (PECVD) while avoiding their respective drawbacks. Indeed, the ultra-short homogeneous discharge generated at atmospheric pressure thanks to a fast voltage rise (*i.e.* tens of nanoseconds), conveniently replaced the initiator and heating filaments used in iCVD by producing a range of reactive species with some of them that will efficiently initiate the free-radical polymerization reaction.[26] The well-reported negative impact of plasma on the monomer was minimized by pulsing the ultra-short plasma discharges (*ca.* t_{ON} = 100 ns) at very low frequencies (*ca.* 100 to 1000 Hz). As a consequence, plasma only affects the chemistry of the film for a very small portion of the time (*ca.* 0.003 %), whereas the free-radical polymerization pathway reaction occurs solely during most of

the plasma-off time (t_{OFF} = 33 ms) and polymer coatings with maximum functional groups retention are formed.[27]

In this work, epoxy functionalized coatings are synthesized by plasma polymerization of glycidyl methacrylate (GMA) via PiCVD at atmospheric pressure.[26] The coatings, deposited on various materials, are used for the grafting of two enzymes able to degrade antibiotics, *i.e.* Laccase and β-lactamase. The influence of their covalent immobilization on sulfamethoxazole and amoxicillin degradation performances is studied. The integrity of immobilized enzymes structure and the related enzymatic activity are studied under high velocity water flow inducing a mechanical shear stress in order to assess the potential applicability of covalently immobilized enzymes in real harsh conditions. In order to overcome the potential threat of microorganism adhesion, able to deteriorate immobilized enzymes and reduce degradation performances, self-defensive properties are developed. Surfaces are saturated with Tween 20, a non-toxic polysorbate surfactant commonly used to remove weakly bonded proteins, to saturate non-bonded sites for adhesion prevention and, in microbiology, to avoid microorganism aggregation and adsorption.[28] The overall efficiency of the newly developed advanced coatings is then herein investigated.

2. Experimental Section

Materials and Reagents

The glycidyl methacrylate (GMA, 97%) monomer was obtained from Sigma-Aldrich and used without further purification. Argon (99.999 %) and oxygen (99.999%) gases were obtained from Air Liquid. Laccase from Pleurotus ostreatus and β lactamase from Pseudomonas aeruginosa (Sigma-Aldrich) were resuspended (5 mg mL^{-1}) in phosphate buffered saline (PBS: 137 mM NaCl, 2.7 mM KCl, 1.5 mM KH_2PO_4, 8 mM Na_2HPO_4,$2H_2O$; pH=8). The mirror polished stainless steel 304 disks, with a total surface of 3.14 cm^2, were provided by the CRM group (Belgium) and the high-density polyethylene biochips (BiofilmChipTM M), with a total surface of 75 cm^2, were purchased from Anoxkaldnes (Lund, Sweden).

Plasma initiated Chemical Vapor Deposition:

The plasma-polymerized GMA thin films were deposited in an atmospheric pressure dielectric barrier discharge (AP-DBD) reactor, as previously described. [26] The plasma set-up is made of two high voltage electrodes (18.72 cm^2) and a stainless steel moving table as ground electrode. An ultra-short square pulse AP-DBD, generated using an AHTPB10F generator from EFFITECH (Gif-sur-Yvette, France), and was used to ignite the plasma discharge. One µs square peaks of 2 kV with a peak repetition frequency of 316 Hz were used (*i.e.* discharge time: 100 ns). Such conditions correspond to 0.003 % duty cycles (T_{OFF}: 33 ms). The deposition time was 25 s for all the experiments. Argon, used as a process and carrier gas, was flushed through the GMA bubbler at 15 L min^{-1}, *i.e.* leading to a monomer flow rate of about 61 mg min^{-1}. Overall argon flow through the reactor was maintained to 20 L min^{-1} for all experiments. The stainless steel disks and HDPE biochips were cleaned by a 30 s exposure to a 95:5 argon: oxygen AP-DBD plasma (1 W cm^{-2}). The discharge current and voltage signals were measured using a current probe (Lecroy, CP030) and a high voltage probe (Lecroy, PPE 20 kV). The traces were recorded using an oscilloscope (LeCroy, Wavesurfer 42XS, 400 MHz).

Grafting and estimation of immobilized protein quantity

Following the PiCVD step, the stainless steel disks and HDPE biochips were immerged in enzymatic solutions during 1 hour at room temperature with gentle agitation (160 rpm). The disks and biochips were then gently washed 5 times during 5 minutes with purified milliQ water and dried with a compressed air spray. The quantity of immobilized enzymes was estimated by measurement of proteic concentration in the enzymatic solution before and after sample immersion in the solution using the RC DC™ Protein Assay kit (Bio-rad). The difference between these two concentrations is considered as the immobilized enzyme quantity on the surfaces.

Saturation of bioactive surface with Tween 20

The bioactive material surfaces were saturated with Tween 20 by immersing in a Tween 20 solution (5% in PBS). Materials were incubated in 12-well plates or petri dishes for stainless steel disks and biochips respectively, for 1 hour at room temperature with an orbital agitation of 100 rpm. Surfaces were then washed 5 times with PBS solution and dried.

Cartography of immobilized enzyme repartition on functionalized surfaces

The bioactive disks and biochips were immersed in LavaPurple (Serva) diluted to a hundredth in acid solution (boric acid 31.5 g L^{-1}; NaOH 19.25 g L^{-1}) in 12-well plates or petri dishes for stainless steel disks and biochips respectively, under slow rocking motion (GFL Rocking Shaker model 3013) in the dark for 15 minutes. The disks and biochips were then washed 3 times with an acidic solution (citric acid 5%; 75% pure ethanol) to activate the fluorochrome and stored in the same solution. After drying, the surfaces were scanned with a FLA 9500 laser scanner typhoon (GE Healthcare Life Sciences) to the wavelength 450 nm. The images obtained were analyzed using the ImageJ software (http://imagej.nih.gov/ij/index.html). The image analysis was based on the processing of different grey levels indicating the presence of more or less important protein concentrations according to the grey intensity obtained. It is, in this case, a qualitative analysis to estimate the protein presence and distribution on the material surface. The significative difference between the samples is estimated by statistical non parametric Mann-Whitney tests comparing two by two the samples.

Surface Characterization

The SEM observations and film thickness measurements were performed on a Hitachi SU-70 FE-SEM. Prior to SEM observations, the non-conductive samples were sputter coated with 5 nm of platinum to prevent charging and distortion. FTIR analyses were performed on a Bruker Hyperion 2000 spectrometer equipped with an ATR objective.

Antibiotics Degradation Activity

Immobilized-enzymes: Enzymatic activity was estimated by the measurement of the amoxicillin (Sigma-Aldrich) and sulfamethoxazole (Sigma-Aldrich) degradation at different time. The immobilized enzymes were continuously incubated in successive baths containing a degradation medium composed of tap water filtered through a polyvinylidene syringe filter (0.22 µm), HEPES (12.5 mM) and antibiotic (100 µg mL^{-1}). The volumes used were 1 mL for stainless steel disks and 7 mL for the biochips. At an interval of 24h, the medium was renewed every 24 hours, wells were washed 3 times with filtered tap water and a new volume of the degradation medium was put in the wells. During weekends, the media was supplemented with a three-fold daily antibiotic concentration in order that the antibiotic

concentration was not limiting and the enzymes remain active throughout this period. At the different monitoring times the degraded antibiotic concentration was estimated by measuring appropriated absorbance (210 for amoxicillin or 260 nm for sulfamethoxazole) with a 2 Synergy microplate reader (Biotek).

Free-enzymes: In the wells used for the first measures (t = 24 h), enzymes were directly dissolved in a degradation medium (2 mL) containing 100 μg mL^{-1} of antibiotic. For all other wells, at time t_0, enzymes were dissolved in 500 μL of the degradation medium containing 50 μg mL^{-1} of antibiotic in order that the enzymes were active. All wells were fed by this same volume every 24 hours. 24 hours before measurement wells are amended with 100 μg mL^{-1} of antibiotic and supplemented to achieve a final volume of 2 mL.

Erosion flow tests

The resistance of functionalized surface / enzyme bonds was evaluated by erosion tests in the water flow. The samples were fixed to the rotor of a reactor of Biofilm Reactor Annular LJ 1320 (Biosurface Technologies Corporation). The disks were subjected to laminar water flows equivalent to a flow rate of 30 km h^{-1} over various times. At times of 48 hours and 6 days the enzymatic activity was measured as described in the "*Antibiotics Degradation Activity"* section and compared to disks used for degradation assays. The erosion of enzymes was estimated using LavaPurple. Bioactive materials were immersed in a solution of LavaPurple for 15 min, at 100 rpm. They were then rinsed 5 fold with an acid solution and then analyzed with a laser scanner as described in the "*Cartography of immobilized enzyme repartition on functionalized surfaces"* section.

Bacteria and Fungi Adhesion

A culture of *Pseudomonas aeruginosa* PAO1 grown on Luria Bertani media were concentrated by centrifugation at 5000 g for 3 min, and washed three times with PBS. The final bacterial concentration was 8 10^7 colony forming unit mL^{-1}. The spores of *Aspergillus nidulans* grown on potato dextrose agar media were dissolved in PBS to final concentrations of 2 10^5 spores mL^{-1}. The disks or biochips were immersed in these solutions for 4 days at room temperature with gentle agitation (100 rpm). The samples were then rinsed 5 times with MilliQ water and analyzed by SEM.

Storage of biochips

The biochips were dried and stored at 4 ° C in three different forms: (1) functionalized, (2) functionalized + enzymes and (3) functionalized + enzymes + Tween 20. At various times, 7, 15, 20, 30, 60, 90, 120 and 160 days, the biochips were used to estimate the integrity of their activity. For functionalized biochips, the enzyme immobilization and the surface saturation with Tween 20 were performed as described in the previous sections. The biochips were then immerged in the appropriate degradation media and degradation tests were performed as described in "*Antibiotics Degradation Activity*" section as the duration when the system keeps an activity above 90% of the activity of bioactive biochips prepared extemporaneously.

3. Results

3.1. Atmospheric Pressure Plasma Initiated Chemical Vapour Deposition of Epoxy-rich Coatings

Stainless steel disks and high-density polyethylene (HDPE) biochips are coated using an atmospheric pressure PiCVD method as described elsewhere (**Figure 1**).[26] Prior to the CVD step, samples are cleaned with solvents (butanone/acetone/ethanol) and just before deposition are exposed to a continuous 1 W cm^{-2} argon/oxygen plasma discharge (generated by a 10 kHz sinusoidal signal with a Softal generator) to remove remaining impurities and form surface hydroxyl, carbonyl and carboxylic acid groups.[29,30]

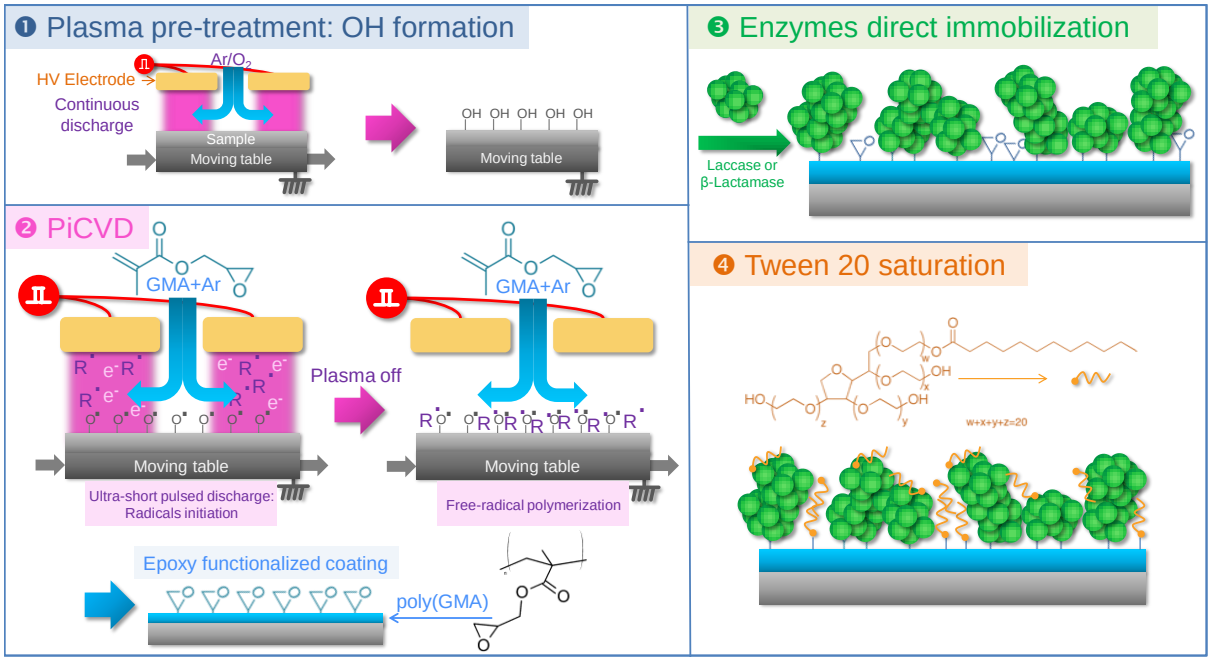

Figure 1: Schematic description of the method: 1) Surface Argon/Oxygen plasma pre-treatment generates hydroxyl groups which can provide radical surface groups during subsequent PiCVD, allowing good adhesion of the coating 2) PiCVD of a poly(glycidyl methacrylate) coating 3) Enzyme covalent immobilization 4) Tween 20 surface saturation.

Those groups provide during the subsequent deposition step reactive radicals groups to ensure the covalent anchoring of the formed polymer coating to the surface material. During the PiCVD step, thanks to periodic and well controlled ultra-short square pulses with

a fast voltage rise (30 ns) (**Figure 2**), plasma discharges with a large proportion of high energy electrons are generated.

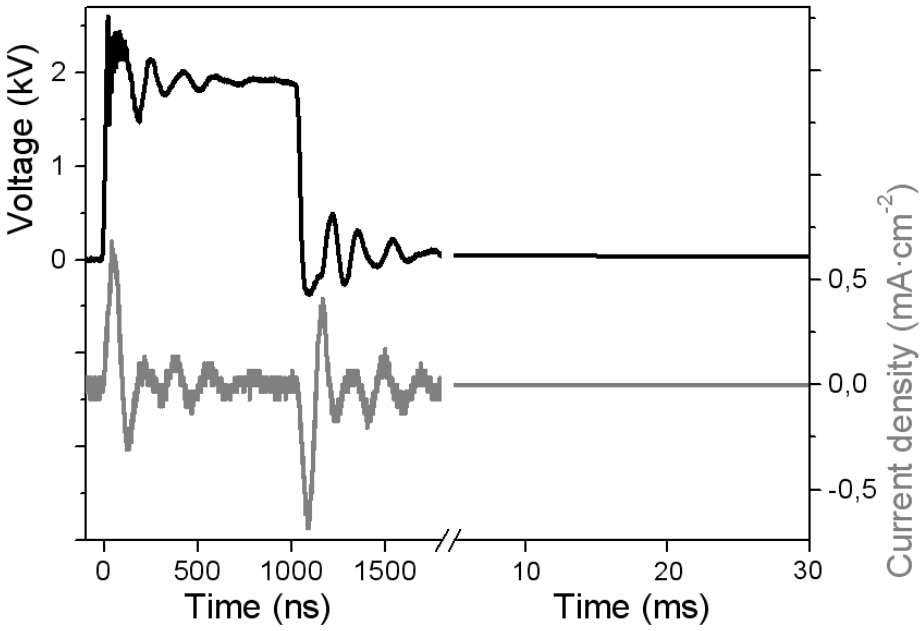

Figure 2: Measured gas applied external voltage and current density of the short square pulse plasma discharge.

Owing to the use of very short plasma discharges (*i.e.* t_{ON} = 100 ns per pulse) and several orders of magnitude longer plasma-off times (*i.e.* 33 ms), the negative impact of the energetic species created by plasma on the chemistry of the growing coating is minimized and the free-radical polymerization of GMA is greatly favored.[27] Irrespective of the substrate material, the PiCVD of poly(GMA) leads to the deposition of macroscopically smooth and adherent thin films over the entire surface of the samples. SEM observations confirmed that the formed coatings, covering the whole surface, are smooth and particle-free (**Figure 3**).

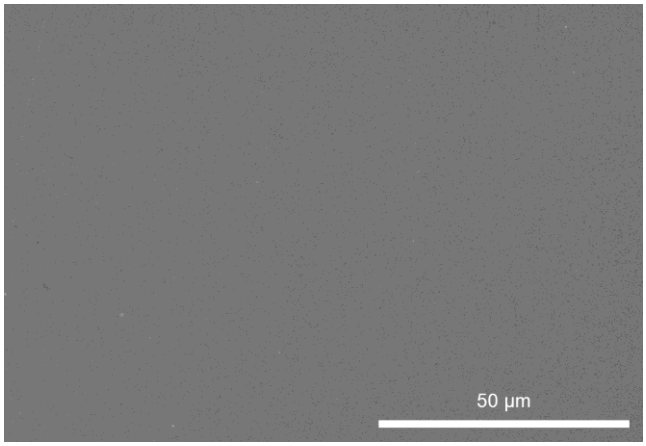

Figure 3: poly(GMA) coating on stainless steel disk observed by scanning electron microscopy.

The film thickness, measured from the SEM cross-section observation of PiCVD coated silicon wafer, is 65 nm for a 25 seconds deposition time. The conformal coverage of the HDPE biochip surface, for which the highest aspect ratio value is 2:1 (1 mm width and 2 mm depth), is likely to occur as suggested by the cross-section SEM observation of a covered 5 µm deep and 600 nm wide trench on a silicon wafer (**Figure 4**), with a higher aspect ratio value of 8:1, showing that conformal coverage is successfully achieved by PiCVD.

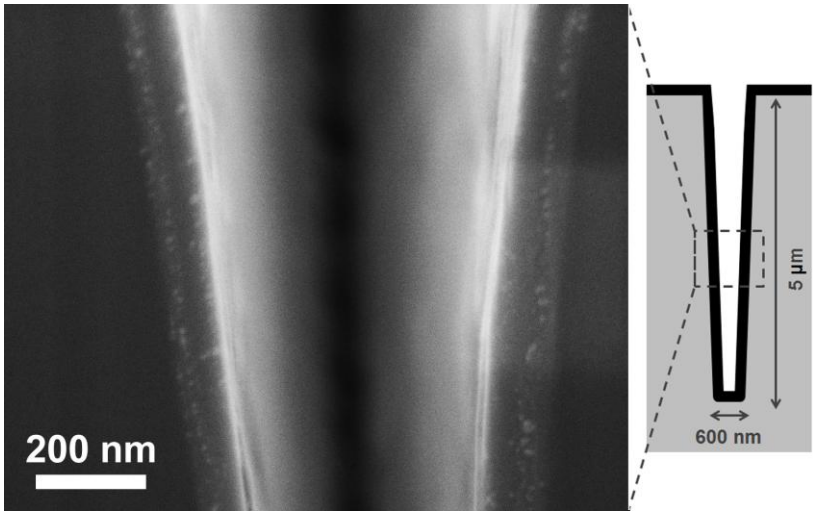

Figure 4: Cross sectional scanning electron microscopy (SEM) image of a 88 nm thick poly(GMA) coating conformally deposited on a 600 nm x 5 mm trench on an etched silicon wafer.

FTIR analysis of different zones of the samples, confirm the uniform coverage of the poly(GMA) coating, notably on the more complex geometry of the biochips. Irrespective of the material and surface morphology, the FTIR spectrum of the plasma-polymerized coating matches the spectrum obtained for conventionally polymerized poly(GMA) (**Figure 5**). Interestingly, an excellent retention of the pendant epoxy groups with the presence of well-defined FTIR absorption bands at 843 cm^{-1}, 905 cm^{-1}, 1253 cm^{-1} and 3063 cm^{-1} is observed.[31,32] It is also interesting to note that the C=C stretching band from the methacrylate group of the GMA monomer (1637 cm^{-1}), from which the polymerization is supposed to occur, is barely observed on the FTIR spectra of the deposited films.

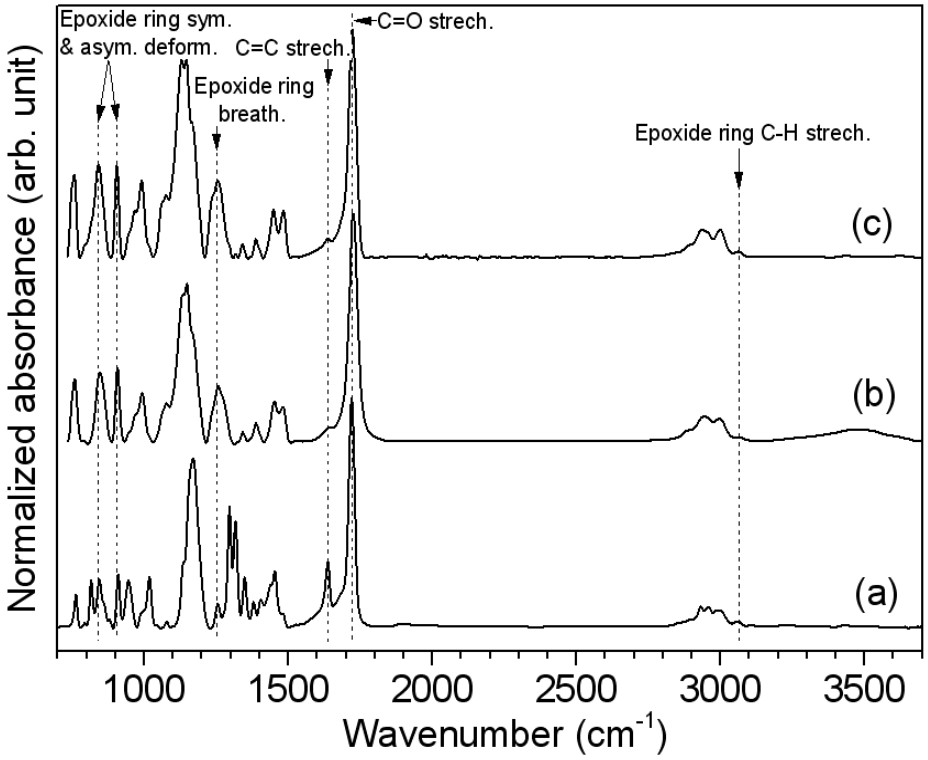

Figure 5: FTIR spectra of a) GMA monomer b) the poly(GMA) coating and c) conventionally polymerized poly(GMA) powder.

3.2. Enzymes Grafting for Water Treatment

The poly(GMA) coated samples are further investigated for the immobilization of β-lactamase and laccase enzymes such as described in the experimental section. The immobilized enzymes are labelled thanks to a fluorescent LavaPurple dye further observed by laser scanning analysis (**Figure 6**). The analysis of greyscale images, indicating the distribution and concentration of the immobilized enzymes, shows significant grey levels differences between the control disks and those immersed in the enzymatic solutions (Mann-Whitney test P = <0.001). This observation, made on both the poly(GMA)-coated stainless steel disk and the poly(GMA)-coated HDPE biochips, indicates that the enzyme immobilization is the result of an interaction with the functional coating on the surfaces. The immobilization of proteins by interactions with epoxy groups has already been demonstrated in numerous studies.[33] It results from multiple covalent bonds between the epoxy coating and unused peripheral reactive groups of enzymes.[34,35] However, denser areas are observed indicating that the covalently immobilized enzymes concentrations are higher in these areas and/or may correspond to protein/protein aggregation.

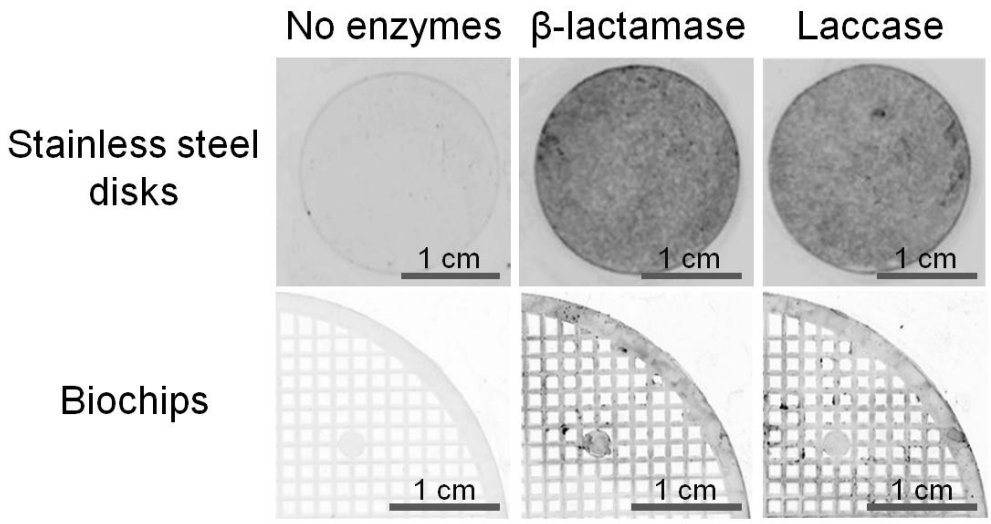

Figure 6: Surface enzyme distribution before and after grafting of Laccase and β-lactamase on functionalized stainless steel disks and HDPE biochips. Enzymes are labelled thanks to a fluorescent LavaPurple dye and observed by laser scanning analysis; their distribution is represented by grey levels according to local enzyme concentration where darker surfaces show higher enzyme concentrations.

The immobilized protein amounts depend on the materials (**Table 1**). The β-lactamase concentration on the stainless steel disks (76.4 ± 0.2 μg cm^{-2}) is 2.6 fold higher than the immobilized concentration on the surface of HDPE biochips (29.3 ± 0.6 μg cm^{-2}). Conversely, the immobilized laccase concentration on the biochips (77.3 ± 0.09 μg cm^{-2}) is 6.4 fold higher than the concentration on the stainless steel disks (12.4 ± 0.8 μg cm^{-2}). Such differences may be due to the combination of two factors: (1) the three-dimensional structuring of the material and (2) the enzyme's nature, which involves different enzyme global structures and different available amino acids that may interact differently with the poly(GMA) coating. Indeed, the three-dimensional protein conformations generate a steric hindrance that limits the proteins ability to be immobilized too close to each other.[36] The peripheral charges of enzymes also contribute according to their orientation to limit their close proximity. The probable enzyme immobilization through multiple anchors on the substrate material modifies the enzyme's three-dimensional structure which in the present case seems to limit the aggregation to only certain areas. The saturation with Tween 20 did not cause any variation in the amount of bound proteins (Mann-Whitney test P = <0.001) (**Table 1**). It is a non-ionic surfactant, used in our case as a surface saturator after the enzyme immobilization to prevent the microorganism adhesion on the bioactive surface.

Table 1. Quantity and distribution of enzymes on surface materials (mean ± standard deviation).

Enzyme	Material	Tween 20	Quantity of immobilized enzyme (μg per cm^2)
β-lactamase	Stainless steel disks	Without Tween 20	76.4 ± 0.2
		With Tween 20	78.3 ± 0.1
	HDPE Biochips	Without Tween 20	29.3 ± 0.6
		With Tween 20	28.6 ± 0.4
Laccase	Stainless steel disks	Without Tween 20	12.4 ± 0.8
		With Tween 20	12.1 ± 0.2
	HDPE Biochips	Without Tween 20	77.3 ± 0.9
		With Tween 20	74.6 ± 0.9

Surface of the stainless steel disks: 3.14 cm^2; Specific surface of the HDPE biochips : 75 cm^2

3.3. Antibiotic Degradation Activities

3.3.1. Laccase grafted poly(GMA) coatings performances

To evaluate the antibiotic degradation potential of the prepared surfaces, tests were conducted using sulfamethoxazole and amoxicillin as target molecules. The activity of the immobilized enzymes, measured by following the antibiotic disappearance in solution over time by UV spectrometry, is compared to the free enzyme activity (**Table 2**).

Table 2. Performances of immobilized enzymatic systems

	Enzyme free form		**Immobilized enzyme**			
	Average duration of activity (h)	Total degraded antibiotic quantity (µg)	Material	Tween 20	Average duration of activity (h)	Total degraded antibiotic quantity (µg)
β- Lactamase	48	50 ± 9	Stainless steel disks	Without Tween 20	288	72 ± 9
				With Tween 20	384	117 ± 2
		79 ± 2	HDPE Biochips	Without Tween 20	264	955 ± 63
				With Tween 20	576	1240 ± 50
Laccase	48	120 ± 5	Stainless steel disks	Without Tween 20	288	244 ± 18
				With Tween 20	648	761 ± 88
		183 ± 10	HDPE Biochips	Without Tween 20	240	2376 ± 100
				With Tween 20	648	6562 ± 363

When free laccases are immediately dissolved in media containing sulfamethoxazole, there is a degradation rate of 21 µg mL^{-1} h^{-1} of the antibiotic after just one hour of incubation. When the antibiotic is added in the solution where the enzymes have been stirred for 1 hour, only 12 µg mL^{-1} d^{-1} of sulfamethoxazole are degraded after 24 hours. The degradation rate continues to decrease until it drops to zero after 48 hours. This rapid loss of enzyme activity can be explained by the combination of different factors which are (1) the aggregation of these enzymes in solution favored by the combined effect of the pH and stirring, (2) the enzymes autolysis at room temperature and (3) the possible inhibitory effect of the secondary metabolites produced by the degradation.[37] To the best of our knowledge no study has shown the possible inhibitory effect of the sulfamethoxazole by-products on laccases.

For the immobilized laccases on HDPE biochips, the degraded sulfamethoxazole amount is equal to 79 µg mL^{-1} h^{-1}. This concentration is 3.8 times higher than the sulfamethoxazole concentration degraded by a similar concentration of free enzymes during the first hour. After 24h and 48h (2 cycles of regeneration medium) the activity remains important, and moderately decreases at 96 h to finally drop to zero after 240 h (**Figure 7a)**.

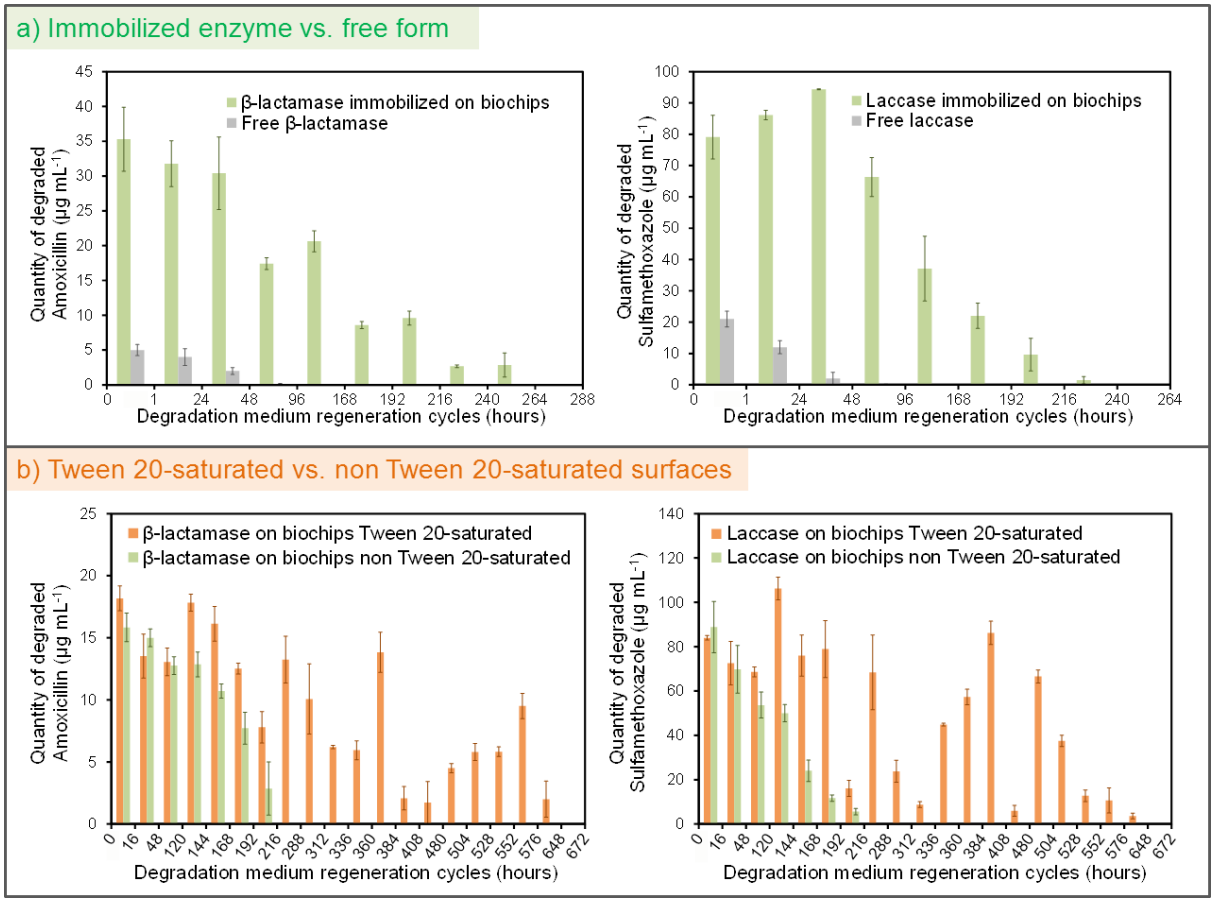

Figure 7: a) Effect of immobilization on the degradation performances of laccase and β-lactamase on HDPE biochips. The values of histograms correspond to the average value of three independent assays each composed of triplicates. b) Effect of Tween-20 saturation on HDPE biochips where β-lactamase and laccase are immobilized. The values of histograms correspond to the average value of two independent assays each composed of triplicates.

The maximum degraded sulfamethoxazole quantity represents 95 % of the initial antibiotic amount in the system after 24 h. The incomplete antibiotic degradation can mean that this residual concentration is the limiting target molecule concentration in the medium for the available enzyme amount and/or the generated secondary metabolites are inhibitors of the activity. When antibiotic is added in the degradation medium without renewing the media

and wherein the by-products accumulate, no inhibition effect is observed on the enzymatic activity (**Figure 8**).

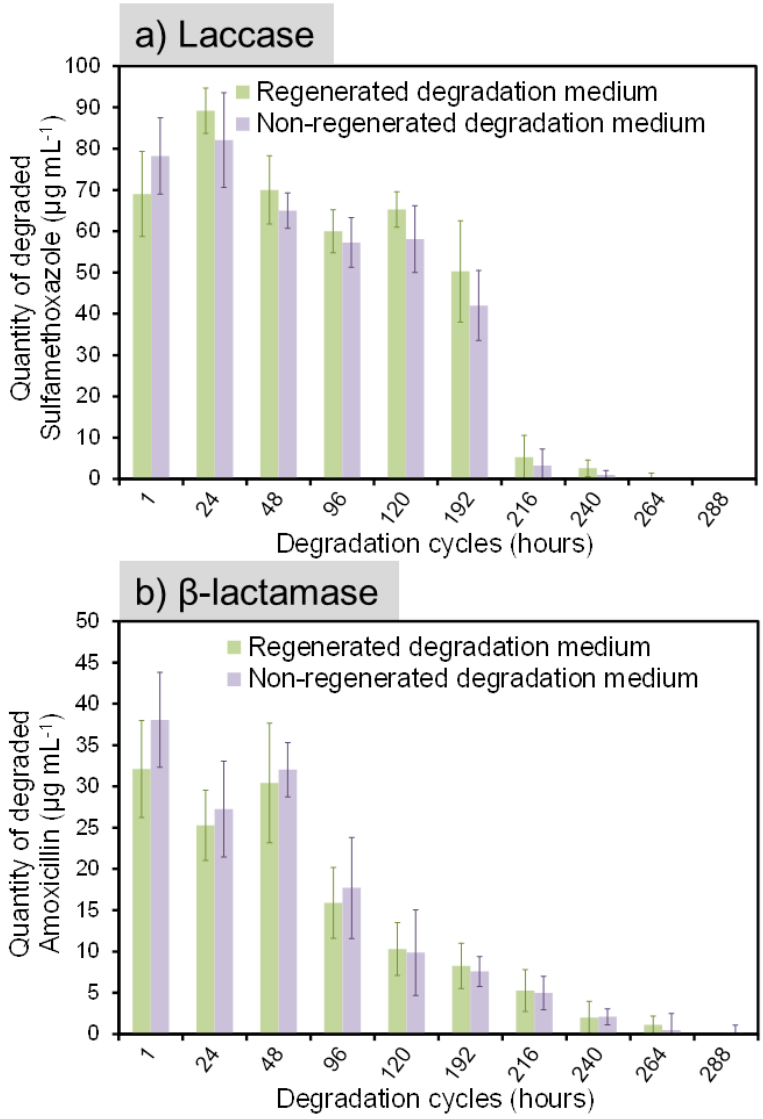

Figure 8: a) Effect of the accumulation of the sulfamethoxazole degradation products in the medium on the performance of the laccase immobilized on the HDPE biochips and b) effect of the accumulation of the amoxicillin degradation products in the medium on the performance of the β-lactamase immobilized on HDPE biochips. The values of histograms correspond to the average value of triplicates.

So this is the enzyme/target molecule ratio which is limiting. The enzyme immobilization allows increasing by 5 fold the enzyme activity over time and finally the degraded sulfamethoxazole quantity is 13 times higher than the degraded quantity by free form laccase (**Figure 7a** and **Table 2**). The assays performed with stainless steel disks show

both an increase of the enzyme activity in the system compared to the free-enzymes with an enzymatic activity that increases from 48 hours to 288 hours. The degraded sulfamethoxazole quantity is multiplied 2 fold for an equivalent enzyme concentration (**Table 2**). These results are important data for the perspective of using this kind of system in water treatment. Indeed, the water residence time in a tertiary treatment of WTP do not exceed a few hours in general. Here we show that most of the degradation can occur in the first hour. Finally, the high antibiotic concentrations that immobilized enzymes may degrade are also interesting data. The sulfamethoxazole concentrations in WTP basins and in its effluent range from 0.3 to 2 $\mu g\ L^{-1}$ which is $3\ 10^3$ to $4.7\ 10^4$ times lower than what can be degraded per hour by our system.[38,39]

3.3.2. β-lactamase grafted poly(GMA) coatings performances

Similarly to the observations made from laccases, the amoxicillin degradation rate by the free form β-lactamase during the first hour is equal to 5 $\mu g\ mL^{-1}\ h^{-1}$. The degradation rate decreases and drops to zero after 96 hours, indicating a full loss of activity of free enzymes. For the immobilized β-lactamase on HDPE biochips, an activity is observed until 264 hours. The amoxicillin degradation rate varies between 2.7 and 35 $\mu g\ mL^{-1}$ per 24 hours (**Figure 7**). Here again, the immobilization is beneficial for the enzyme. The enzymes are active on both functionalized materials and the total activity time is multiplied by 6 to 5.5 times with an amoxicillin degradation rate 1.44 to 12 times higher for HDPE biochips and stainless steel disks respectively than for free form enzymes.

3.3.3. Effect of Tween 20 on the β-lactamase and laccase grafted poly(GMA) coatings performances

In order to provide the developed surfaces with a self-defensive behavior, which would be of great interest for potential use in water treatments, the surfaces were saturated with Tween 20 to prevent microorganism adhesion. The activity of those new surfaces was investigated as the polysorbates may alter the degradation performances of bioactive surfaces.

For both functionalized laccase and β-lactamases biochips and irrespective of the used material, the Tween 20 saturation has a positive effect on the activity duration (**Figure 7b**). Indeed, comparing bioactive surfaces Tween 20-saturated or not, the enzymatic activity duration is multiplied by 2.7 in the case of the laccases and by 2 for the β-lactamases grafted ones. Compared to free-enzyme, the immobilization and Tween 20-saturation surface allows in both cases a multiplication of about 13.5 fold of the activity duration. Concerning the quantities of degraded antibiotics, both saturated and non-saturated present similar efficiency for a duration below 120 h, but along with the time while non-saturated surfaces are clearly losing activity, in the case of saturated surfaces, the degraded quantities follow a "wave phenomena" with important resurgences of enzymatic activity as shown in **Figure 7b**. Interestingly, as shown in **Figure 9**, the presence of enzymes in the liquid degradation media is detected just before activity resurgence is observed, concentrating the solution by 200-fold during the first step of the RC DC™ Protein Assay (a total precipitated volume of 5 mL instead of recommended volume of 25 µL).

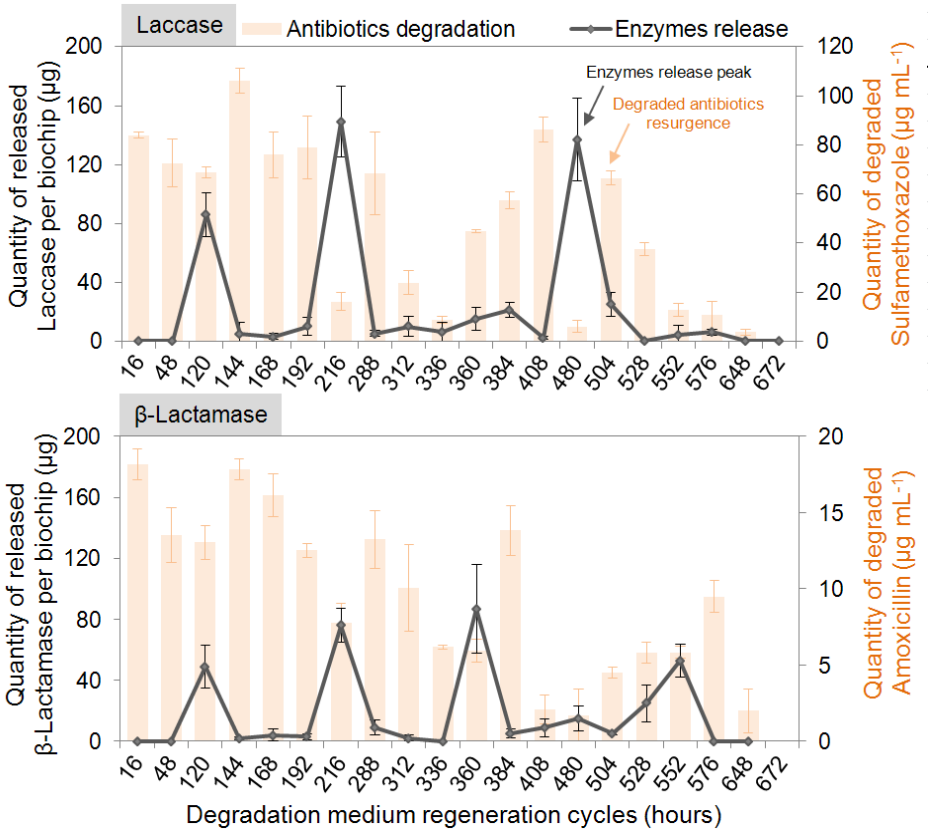

Figure 9: Quantification of released β-lactamase and laccase in the liquid media along degradation assays.

The majority of the time, a low release of enzymes is observed in the liquid medium and this release becomes from time to time more important with peaks ranging from 87 to 149 µg for the laccase and from 49 to 87 µg for the β-lactamase before an observed resurgence of antibiotic-degradation activity. The observed enzyme release from the active layer over time suggests that this "wave phenomenon" mechanism may occur as depicted in **Figure 10**.

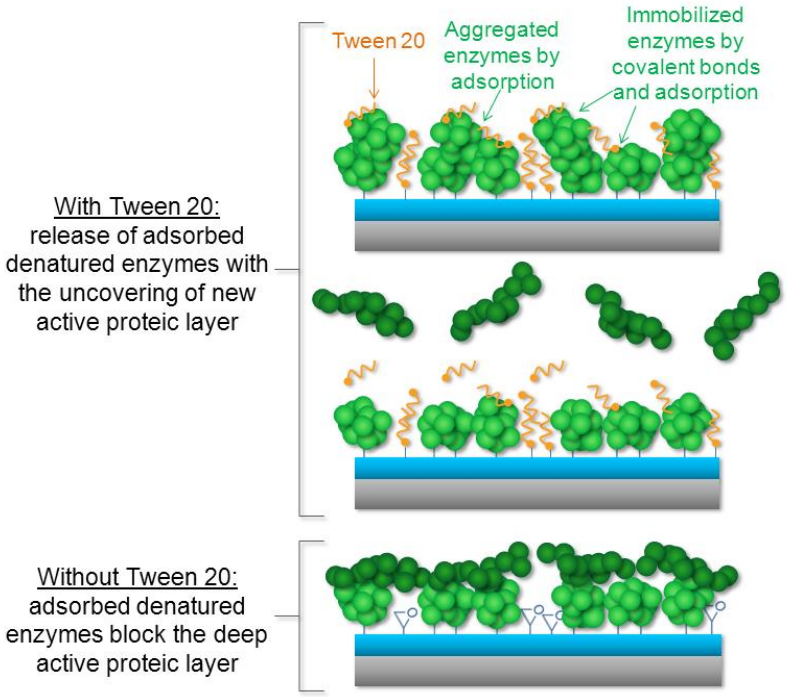

Figure 10: Effect of Tween 20 on the desorption of adsorbed laccases and β-lactamases.

Over time the adsorbed proteins by weak and few bonds on the other proteins may lose their three-dimensional structure. The Tween 20 used for saturation helps to detach adsorbed proteins and bare new enzymes located in the layer below, that are both structurally intact and active, to become accessible to degrade antibiotics. Indeed, the Tween 20 allows the total or partial release of proteins that are adsorbed to other enzymes or to a support as it was found in the works of Feng *et al.* and Seo *et al.*.[40,41] Then there is an activity resurgence of the bioactive surface and the phenomenon is repeated. Hence Tween 20 saturation clearly shows a duration increase and the observed wave phenomenon allows maintaining a

relatively regular high activity, compared to non-saturated surfaces, leading to higher amounts of total degraded antibiotics (**Table 2**).

3.4. Surface Performance Durability

3.4.1. Erosion test

In order to highlight the durability of the enzyme-functionalized surfaces, the prepared samples were tested under several conditions that can be met in WTP. The enzymes are immobilized at least partly by covalent bonds. The resistance of bioactive surfaces over time is dependent in part on (1) the coating adhesion to the material and its integrity (2) the surface/enzymes bonds resistance to shear stresses (3) and the conservation of the enzyme three-dimensional structure integrity to ensure an activity. The annular reactor assays mimicking the mechanical stresses generated by a water flow rate of 30 km h^{-1} show that thanks to enhanced surface adhesion brought by the plasma treatment, functionalized coating are not delaminated and the enzymes remain anchored to the support. For the sake of comparison it is worth adding that the flow velocities in water networks (distribution and wastewater) vary from 10^{-3} to 15 km h^{-1}.[42] LavaPurple analyzes show that the enzyme repartition on the surfaces before and after the tests remains unchanged. Enzymes are partially immobilized to the support by covalent bonds and it is precisely this multi-anchor that provides good resistance enzymes to erosion. The measured enzymatic activity does not show a significant difference before and after the disks were subjected to erosion testing (**Table 3**). The enzyme multi-anchorage seems therefore to increase the rigidity of the enzyme structure allowing the enzyme conformation conservation and consequently the active site spatial conformation guaranteeing the enzymatic activity.[15]

Table 3. Compared performance of immobilized β-lactamase and laccase on stainless steel disks and HDPE biochips submitted or not to erosion.

Enzyme	Material	Without erosion		After erosion	
		Average duration of activity (h)	Total degraded antibiotics quantity (µg)	Average duration of activity (h)	Total degraded antibiotics quantity (µg)
β- Lactamase	Stainless steel disks Tween20	384	117 ± 2	368 ± 14	100 ± 20
	HDPE biochips Tween 20	576	1240 ± 50	552 ± 24	1180 ± 32
Laccase	Stainless steel Disks Tween20	648	761 ± 88	616 ± 24	624 ± 127
	HDPE biochips Tween 20	648	6562 ± 363	632 ± 14	6289 ± 450

3.4.2. Bacteria and Fungi Adhesion

In addition to the water flow, the bacteria and fungi encountered in WTP may also hinder the degradation potential of the prepared coatings. Adhesion tests were performed using *Pseudomonas aeruginosa* and *Aspergillus nidulans*, which are known to have a large ability to adhere on supports. Based on SEM observations, *Pseudomonas aeruginosa* does not adhere to the bioactive surfaces without Tween 20 saturation after 72 hours of contact. No similar results were reported in the literature concerning potential inhibitor effects of laccase and β- Lactamase on bacteria adhesion but some work has reported this kind of effect on different proteins without precise explanations of the mechanisms.[43,44,45,46] In contrast, *Aspergillus nidulans* spores are present in large numbers on the surfaces and successive surface washings do not allow to eliminate the spores (**Figure 11a-b**). This interaction can be explained by the specific adhesive spore surface properties.[47] If these spores adhere it will cause the neutralization of the enzyme layer that will be covered by the fungus and or metabolized by the developing fungi as a carbon source. The saturation with Tween 20 of bioactive surfaces completely prevents fungal spores' adhesion (**Figure 11c-d**) on the surface even in the presence of high concentrations of spores and under conditions favoring adhesion (not stirred medium to allow spores and bacteria sedimentation on treated surfaces) after a long contact time of 168 hours. The polysorbates antifouling properties are well known and

Tween 20 is commonly used in the fungal spores resuspension to avoid their aggregation and adsorption on the surfaces.[28]

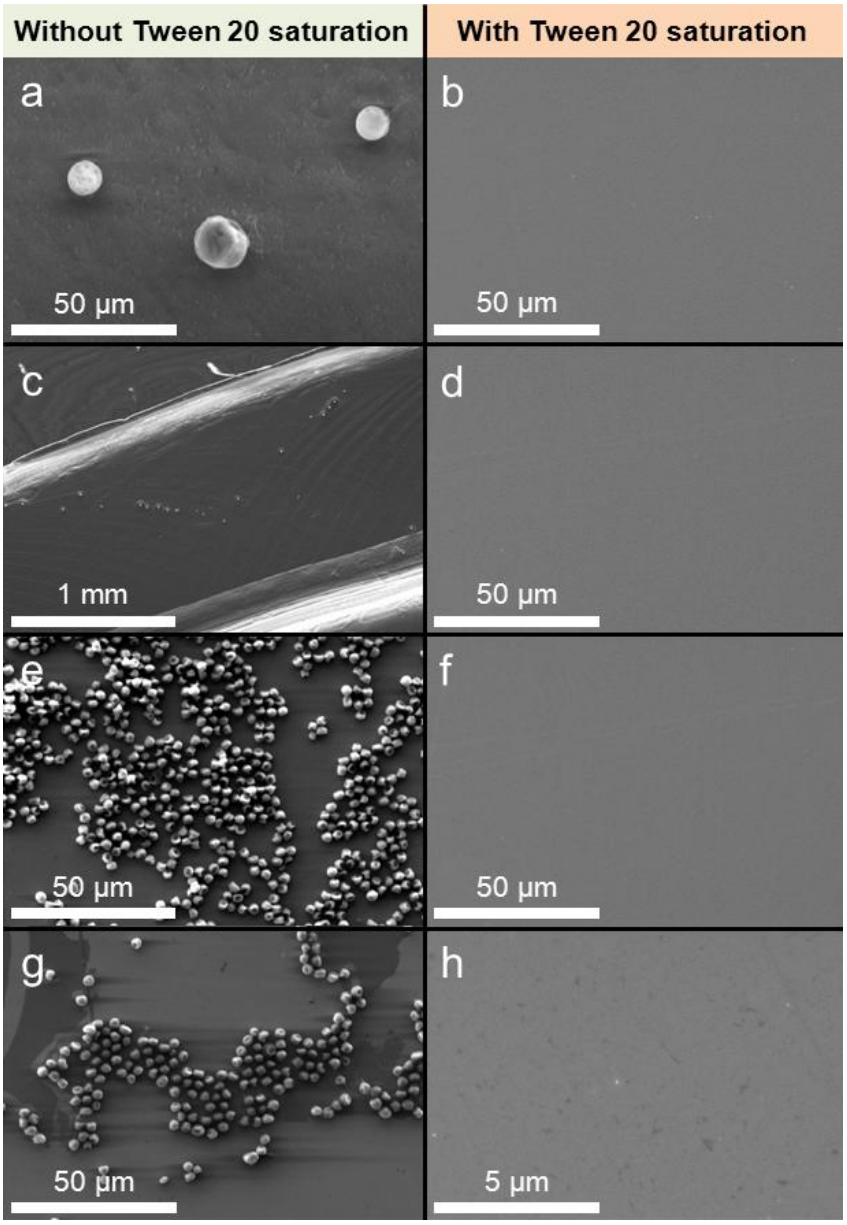

Figure 11: Scanning electron micrographs showing adhesion of *Aspergillus nidulans* after 168 h of contact on poly(GMA)-functionalized HDPE biochips with (a) immobilized β-lactamases without Tween-20 saturation; (b) with immobilized β-lactamases and Tween-20 saturation; (c) with immobilized laccases without Tween-20 saturation; (d) with immobilized laccases with Tween-20 saturation; and Adhesion of *Aspergillus nidulans* after 168 h of contact on poly(GMA)-functionalized stainless steel disks with (e) immobilized β-lactamases without Tween-20 saturation; (f) with immobilized β-lactamases with Tween-20 saturation; (g) with immobilized laccases and without Tween-20 saturation; (h) with immobilized laccases with Tween-20 saturation.

3.4.3. Long-term storage of bioactive surfaces

The use of bioactive biochips in industrial processes requires that they can be stored for a long time, at least between their production and delivery to treatment plants where they will be used. The storage of different conditionings has been tested: functionalized biochips, functionalized biochips + enzymes and functionalized biochips + enzymes saturated with Tween 20 (**Figure 12**).

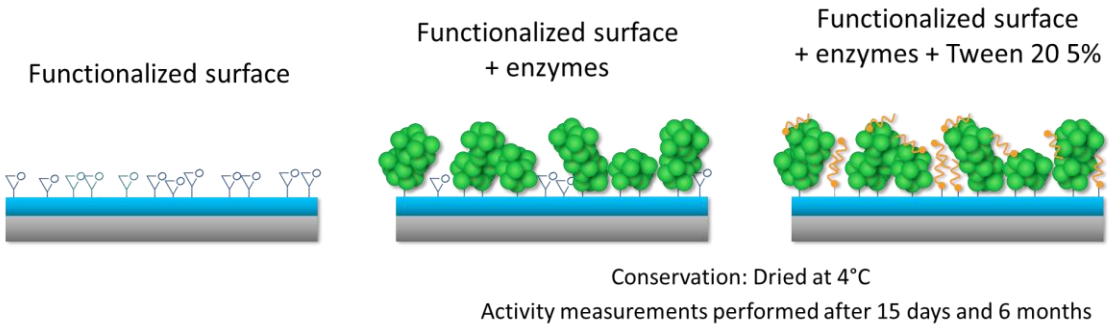

Figure 12: Different conditionings tested for long term biochips storage

We defined the maximal storage duration as the duration when the system keeps an activity above 90 % of the activity of bioactive biochips prepared extemporaneously. These tests (**Table 4**) show that after 30 days of storage, the functionalized biochips show an activity decrease when the enzymes are immobilized extemporaneously.

Table 4. Maximum storage durations for which biochips maintain their degradation activity.

	Functionalized biochips	**Functionalized biochips + enzymes**	**Functionalized biochips + enzymes + Tween20**
β-lactamase	30 days	90 days	15 days
Laccase	30 days	120 days	30 days

This means that the coating has aged and a lower enzyme concentration is immobilized on the surface and/or the surface coating oxidation generate new enzyme orientation when they are immobilized on surfaces which impedes the accessibility of the

active site. Whatever the conservation mode, when enzymes are immobilized before storage, there is a better activity retention of laccases compared to the β-lactamases. The explanation probably lies in the number of interactions between functional coating and enzyme ensuring better temporal stability of laccases. As mentioned earlier it also may be that there are enzymes adsorbed on top of the others. Denaturation of β-lactamases adsorbed could be faster than that of laccases. Surprisingly, when biochips are saturated with Tween 20, overall activity declines to 15 and 30 days for the β-lactamase and laccase respectively. This deleterious effect on the activity retention could be caused by the Tween 20 oxidation. The generated by products from polysorbates oxidation have also been characterized (formic acids resulting from the cleavage of long carbon chains, resulting linoleic acids oxidation of these chains and autoxidation generating hydroperoxides) and their negative oxidative effect on the stability of proteins (structure and activity) has also been demonstrated.[48,49] From a general point of view, it is the oxidation that contributes to the protein denaturation. Storage at 4 °C slows down this phenomenon. The storage duration could probably be increased by limiting the presence of oxygen by a partial vacuum or saturation of the environment with nitrogen.

The long term durability and activity of the developed surfaces, even when exposed to significant water flow rates and high bacteria or fungi concentrations, associated to the combination of easily up-scalable steps makes the approach described herein particularly suitable for industrial use, and in this case suitable for water treatment. Indeed, the proposed approach can be easily up-scaled for the functionalization of various materials and notably HDPE biochips that are already widely used in water treatment processes as moving beds biofilm reactors in which water has a residence time ranging from a minimum of 1 h to 5 days. Indeed, tests carried out with one liter tap water reactors containing each 50 biochips allow to confirm the degradation performances of the systems for larger volumes in batch reactors, with results similar to those observed in smaller volumes after one hour of contact (**Figure 13**).

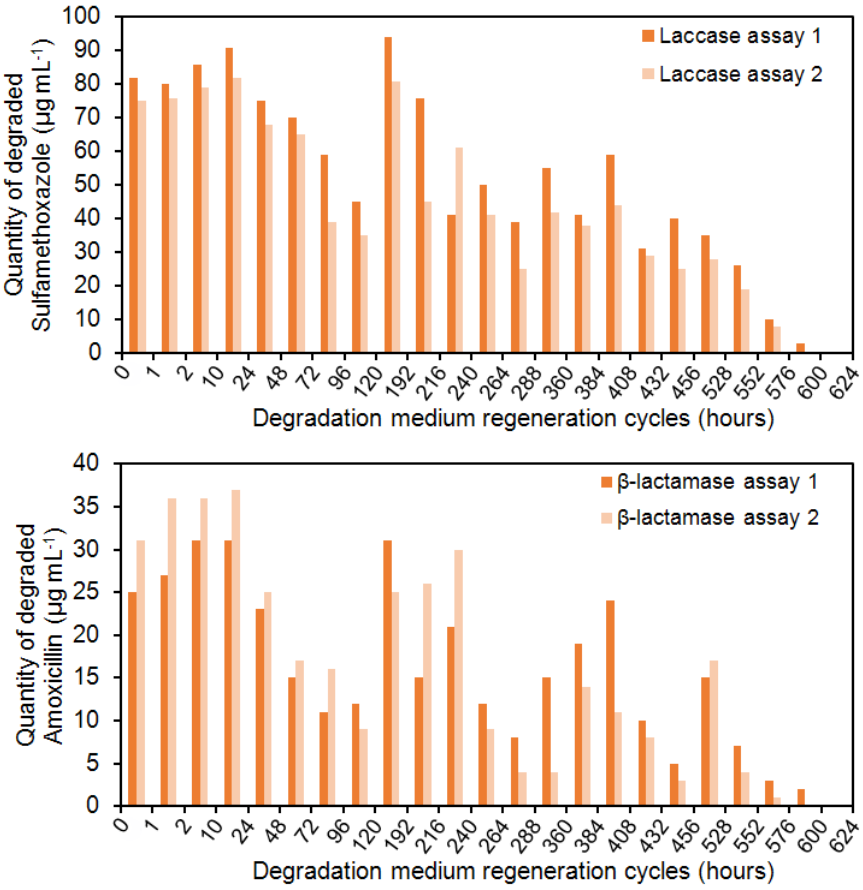

Figure 13: Degradation performances, in one liter tap water, of laccase and β-lactamase immobilized on HDPE biochips and saturated with Tween-20. Each batch contains 50 grafted biochips in one liter of filtered tap water supplemented with 100 µg mL^{-1} of either sulfamethoxazole or amoxicillin. The values of histograms correspond to two independent assays.

It is worth mentioning that the PiCVD technique, in addition to leading to conformal coatings and to be independent of the material nature and shape as shown by Boscher *et al.* and Hilt *et al.*, it may be used to functionalize surfaces with a large variety of functional groups just by tuning the precursors used. Indeed, the PiCVD polymerization of any precursor presenting polymerizable bonds, *e.g.* vinyl or allyl bonds, may be performed to form functional coatings. Among the numerous different functional groups, amine or carboxylic groups containing coatings could be synthesized using, for example, respectively allylamine and acrylic acid. [50,51] The developed coatings may be grafted with numerous types of proteins and are not specific to the immobilization of laccases and β-lactamases. The transposition for the grafting of other enzymes can lead to new durable surface functionalities, including antibacterial or antibiofilm for example through the grafting of antimicrobial peptides and proteins. The saturation step of the surface by tween 20 described

herein and leading to an outstanding increase of enzymatic efficiency might be potentially used to enhance surface properties of grafted enzymes on any type of functionalized coating.

4. Conclusion

A conformal and adherent poly(GMA) coating with high epoxy group retention is prepared from an up-scalable atmospheric pressure plasma initiated chemical vapor deposition method. The developed coating is a solid platform for immobilizing enzymes to obtain a powerful bioactive material for antibiotic degradation in water. The amounts of immobilized enzymes are very high and explain the high degradation performance observed. Moreover, the robustness of multiple enzymes/material interactions allow that enzymes remain fixed on the surface and the generated rigidity in the protein structure allows a resistance to mechanical stress under water flow such that the enzymes remain active with an unchanged degradation yield. This is a first argument to show the possible use of this process in water treatment. No studies before this one had considered the possible alteration of immobilized enzymes by microorganism's adhesion which would degrade these enzymes. The surface saturation with Tween 20 prevents the microorganism's adhesion and improves the duration and intensity of the degradation potential of the active surfaces. This method is then promising for the development of alternative water treatment processes.

References

[1] C. J. Houtman, J. Kroesbergen, K. Lekkerkerker-Teunissen, J. P. van der Hoek, *Sci. Total. Environ*. **2014**, *496*, 54.

[2] S. Herold, J. Siebert, A. Huber, H. Schmidt, *Antimicrob. Agents. Ch.* **2005**, *49*, 931.

[3] Y. Morita, J. Tomida, Y. Kawamura, *Front. Microbiol.* **2014**, *4*, 422.

[4] D. Chang, H. Jianzhong He, *Appl. Microbiol. Biotechnol.* **2010**, *87*, 925.

[5] A. Rodríguez-Rojas, J. Rodríguez-Beltrán, A. Couce, J. Blázquez, *Int. J. Med. Microbiol*. **2013**, *303*, 293.

[6] M. Prudhomme, L. Attaiech, G. Sanchez, B. Martin, J. P. Claverys, *Science* **2006**,*313*, 89.

[7] A. Joss, E. Keller, A.C. Alder, A. Göbel, C.S. McArdell, T. Ternes, H. Siegrist, *Water Res.* **2005**, *39*, 3139.

[8] V. Homem, L. Santos, *J. Environ. Manage.* **2011**, *92*, 2304.

[9] Mdel M. Gómez-Ramos, M. Mezcua, A. Agüera, A. R. Fernández-Alba, S. Gonzalo, A. Rodríguez, R. Rosal, *J. Hazard Mater.* **2011**, *192*, 18.

[10] G. D. Wright, *Adv. Drug. Deliv. Rev.* **2005**, *57*, 1451.

[11] J. Jeong, W. Song, W. J. Cooper, J. Jung, J. Greaves, *Chemosphere* **2010**, 78, 533.

[12] F. Kudo, T. Kawashima, K. Yokoyama, T. Eguchi, *J. Antibiot.* **2009**, *62*, 643.

[13] B. Viswanath, B. Rajesh, A. Janardhan, A. P. Kumar, G. Narasimha, *Enzyme Res.* **2014**, 163242. DOI:10.1155/2014/163242

[14] A. A. Khan, S. Akhtar, Q. Husain, *J. Mol. Catal. B-Enzym.* **2006**, *40*, 58.

[15] R. C. Rodrigues, C. Ortiz, A. Berenguer-Murcia, R. Torres, R. Fernández-Lafuente, *Chem. Soc. Rev.* **2013**, *42*, 6290.

[16] R. K. Singh, M. K. Tiwari, R. Singh, J. K. Lee, *Int. J. Mol. Sci.* **2013**, *14*, 1232.

[17] S. Datta, L. R. Christena, Y. R. S. Rajaram, *Biotech.* **2012**, *3*, 1.

[18] R. Mauchauffé, M. Moreno-Couranjou, N. D. Boscher, C. Van De Weerdt, A. S. Duwez, P. Choquet, *J. Mater. Chem. B* **2014**, *2*, 5168.

[19] A. Manakhov, P. Skládal, D. Nečas, J. Čechal, J. Polčák, M. Eliáš, L. Zajíčková, *Phys. Status Solidi A* **2014**, *211*, 2801.

[20] S. G. Im, K. W. Bong, B. S. Kim, S. H. Baxamusa, P. T. Hammond, P. S. Doyle, K. K. Gleason, *J. Am. Chem. Soc.* **2008**, *130*, 14424.

[21] B. Brena, P. González-Pombo, F. Batista-Viera, *Methods Mol. Biol.* **2013**, *1051*, 15.

[22] G. Camporeale, M. Moreno-Couranjou, S. Bonot, R. Mauchauffé, N. D. Boscher, C. Bebrone, C. Van de Weerdt, H.-M. Cauchie, P. Favia, P. Choquet, *Plasma Process. Polym.* **2015**, DOI: 10.1002/ppap.201400206.

[23] S. G. Im, K. W. Bong, C. H. Lee, P. S. Doyle, K. K. Gleason, *Lab Chip*. **2009**, *9*, 411.

[24] J. L. Yagüe, A. M. Coclite, C. Petruczok, K. K. Gleason, *Macromol. Chem. Physic.* **2013**, *214*, 302.

[25] W. E. Tenhaeff, K. K. Gleason, *Adv. Funct. Mater.* **2008**, *18*, 979.

[26] N. D. Boscher, F. Hilt, D. Duday, G. Frache, T. Fouquet, P. Choquet, *Plasma Process. Polym.* **2015**, *12*, 66.

[27] F. Hilt, N. D. Boscher, D. Duday, N. Desbenoit, J. Levalois-Grützmacher, P. Choquet, *ACS Appl. Mater. Interfaces* **2014**, *6*, 18418.

[28] J. F. Leslie, B. A. Summerell, S. Bullock, *The Fusarium Laboratory Manual*, Wiley-Blackwell, Hoboken, NJ, **2006**.

[29] K. S. Siow, L. Britcher, S. Kumar, H. J. Griesser, *Plasma Process. Polym.* **2006**, *3*, 392.

[30] N. Inagaki, *Plasma Surface Modification and Plasma Polymerization*, Technomic, Lancaster, Basel **1996**.

[31] C. Tarducci, E. J. Kinmond, J. P. S. Badyal, S. A. Brewer, C. Willis, *Chem. Mater.* **2000**, *12*, 1884.

[32] C. P. Klages, K. Höpfner, N. Kläke, R. Thyen, *Plasmas Polym.* **2000**, *5*, 79.

[33] C. Mateo, J. M. Palomo, G. Fernandez-Lorente, J. M. Guisan, R. Fernandez-Lafuente, *Enzyme Microb. Tech.* **2007**, *40*, 1451.

[34] V. M. Balcão, M. M. D. C. Vila, *Adv. Drug Deliv. Rev*. **2014,** DOI: 10.1016/j.addr.2014.10.005.

[35] O. Barbosa, R. Torres, C. Ortiz, A. Berenguer-Murcia, R. C. Rodrigues, R. Fernandez-Lafuente, *Biomacromolecules* **2013**, *14*, 2433.

[36] D. Kim, A. E. Herr, *Biomicrofluidics* **2013**, *7*, 041501.

[37] H. C. Mahler, W. Friess, U. Grauschopf, S. Kiese, *J. Pharm. Sci*. **2009**, *98*, 2909.

[38] R. Hirsch, T. Ternes, K. Haberer, K. L. Kratz, *Sci. Total Environ.* **1999**, 225, 109.

[39] A. Göbel, A. Thomsen, C. McArdell, A. C. Alder, W. Giger, N. Theib, D. Löffler, T. A. Ternes, *J. Chromatogr. A* **2005**, *1085*, 179.

[40] M. Feng, A. Berdugo Morales, A. Poot, T. Beugeling, A. Bantjes, *J. Biomat. Sci-Polym. E.* **1995**, *7*,415.

[41] D. J. Seo, H. Fujita, A. Sakoda, *Adsorption*, **2011**, *17*, 813.

[42] A. Hogetsu, Y. Ogino, T. Takemika, *Technology Transfer Manual of Industrial Wastewater Treatment*, Ministry of Environment, Government of Japan, Tokyo, **2002**.

[43] R. B. Dickinson, J. A. Nagel, R. A. Proctor, S. L. Cooper, *J Biomed. Mater. Res.* **1997,** *36,* 152.

[44] M. Fletcher, K. C. Marshall, *Appl. Environ. Microbiol.* **1982,** *44*, 184.

[45] I. K. Kang, B. K. Kwon, J. H. Lee, H. B. Lee, *Biomaterials.* **1993,** *14*, 787.

[46] Y. H. An, R. J. Friedman, R. A. Draughn, E. A. Smith, J. H. Nicholson, J. F. John, *J. Microbiol. Methods.* **1995,** *24*, 29.

[47] R. J. Howard, N. A. R. Gow, *The Mycota: A comprehensive treatise on fungi as experimental systems for basic and applied research. VIII Biology of the Fungal Cell*, Springer-Verlag, Berlin and Heidelberg, **2001**.

[48] V. M. Knepp, J. L. Whatley, A. Muchnik, T. S. Calderwood, *J. Pharm. Sci. Technol.* **1996**, *50*,163.

[49] B. A. Kerwin, *J. Pharm. Sci.* **2008**, *97*, 2924.

[50] Z. Zhang, S. Liu, Y. Shi, Y. Zhang, D. Peacock, F. Yan, P. Wang, L. He, X. Feng, S. Fang, *J. Mater. Chem. B* **2014**, *2*, 1530.

[51] S. Mourtas, M. Kastellorizios, P. Klepetsanis, E. Farsari, E. Amanatides, D. Mataras, B. R. Pistillo, P. Favia, E. Sardella, R. d'Agostino, S. G. Antimisiaris, *Colloids Surf. B. Biointerfaces* **2011**, *84*, 214.

Chapter 5

Fast Atmospheric Plasma Deposition of Bio-Inspired Catechol/Quinone-Rich Nanolayers to immobilize NDM-1 Enzymes for Water Treatment

Rodolphe Mauchauffé, Sébastien Bonot, Maryline Moreno-Couranjou, Christophe Detrembleur, Nicolas D. Boscher, Cécile Van De Weerdt, Anne-Sophie Duwez and Patrick Choquet, *Advanced Materials Interfaces*, **2016**, DOI: 10.1002/admi.201500520

The widespread use of antibiotics in urban and hospital medicine is inducing their important releases in wastewaters. In spite of the existing water treatment processes, antibiotics can still be found in the effluents of wastewater treatment plants.[1] In addition to their relative inefficiency, advanced oxidation processes (*i.e.* UV or ozonation) currently in use can also lead to the generation of secondary metabolites which are even more toxic than their parental compounds.[2,3] As a consequence, antibiotic levels detected in environmental water are becoming of greater concern. As an example, amoxicillin, one of the most widely used antibiotic and considered as a priority micropollutant, was detected at concentrations ranging from 10 to 200 ng L^{-1} in environmental waters.[4,5] This subinhibitory concentrations can promote various disturbances such as antibiotic resistance gene transfer and the emergence of new antibiotic-resistant bacteria.[6,7] A recent example was the discovery in 2009 of the gene encoding the New Delhi Metallo-β-lactamase-1 (NDM-1) enzyme, which possesses the ability to inactivate β-lactams.[8] Since, bacteria carrying the gene encoding NDM-1 have spread globally and pose a significant public health threat due to their very high resistance to these antibiotics. Mimicking those multi-drug resistant bacteria, enzymes encoded by their antibiotic resistance genes can be produced and used for the elaboration of an effective method for the degradation of antibiotics, limiting considerably the generation of potential toxic metabolites.[9]

Taking inspiration from Nature, the development of new surface properties through enzyme immobilization currently attracts strong interest.[10] Appropriate enzyme immobilization most often enhances their activity, stability and lifetime compared to their free form in solution.[11,12] Numerous types of functional coatings bearing amine, carboxylic or epoxy groups, obtained through various deposition routes have been investigated for the covalent tethering of proteins.[12,13,14,15] Inspired by the remarkable adhesion properties of mussel under tough conditions, a new kind of functional coatings have been recently reported based on the reactivity of catechol and quinone groups.[16] The presence of catechol groups, responsible for the mussel feet surface adhesion, ensures a strong anchoring onto virtually any kind of substrate, while the quinone groups (*i.e.* catechol oxidized form) responsible for the mussel feet cohesion, allows the formation of strong covalent bonds with proteins via reaction with thiol, amine or imidazole groups.[17] Currently, catechol/quinone containing layers are exclusively issued from wet chemistry and among the various strategies reported, two main routes emerged.[17] The first one relies on the auto-polymerization of dopamine in alkaline solution, while the second consists in the deposition of polymers bearing

catechol/quinone from aqueous or organic solutions.[16,18,19] Despite promising applications in the fields of biotechnology and biomedicine, these wet chemical methods present several limitations, such as slow deposition rates often associated to the generation of huge amount of waste (*e.g.* polydopamine technique) or a multi-step procedure when considering the upstream catechol/quinone-bearing polymer preparation before their deposition.[20]

A promising arising technology for the fast deposition of functional coatings is the up-scalable atmospheric pressure plasma-enhanced chemical vapor deposition (AP-PECVD) method.[15,21] In addition, when assisted by an aerosol, such approach can even allow the use of non-volatile monomers.[22] Therefore, we pioneered the preparation of a hybrid catechol/quinone-bearing coating from a dopamine-based monomer. The resulting novel coating is further employed to covalently graft for the first time the NDM-1 enzyme to efficiently degrade amoxicillin from polluted water.

The proposed strategy relies on the AP-PECVD copolymerization of a catechol-containing monomer (*i.e.* dopamine acrylamide, DOA) and an organosiloxane monomer (*i.e.* vinyltrimethoxysilane, VTMOS), both bearing a vinyl bond. Such as depicted in **Scheme 1**, a solution of DOA in VTMOS (0.5 mg mL^{-1}) is first sprayed onto the surface of mirror polished stainless steel substrate by means of an ultrasonic nebulizer. The thin liquid layer formed is then promptly exposed (*ca.* 1 second) to a pulsed argon plasma ignited in a dielectric barrier discharge configuration (**Scheme 1.a** and complete description in Experimental Section).[23] The reactive species (*i.e.* metastable and radicals species) provided by the argon plasma interact with the VTMOS molecules present in the gas phase, due to its high vapor pressure, and with the surface of the thin liquid layer deposited to induce a range of reactions. Among these reactions, including fragmentation, dissociation and crosslinking, a conventional free-radical polymerization pathway is also initiated, ensuring the efficient curing of the co-monomers.

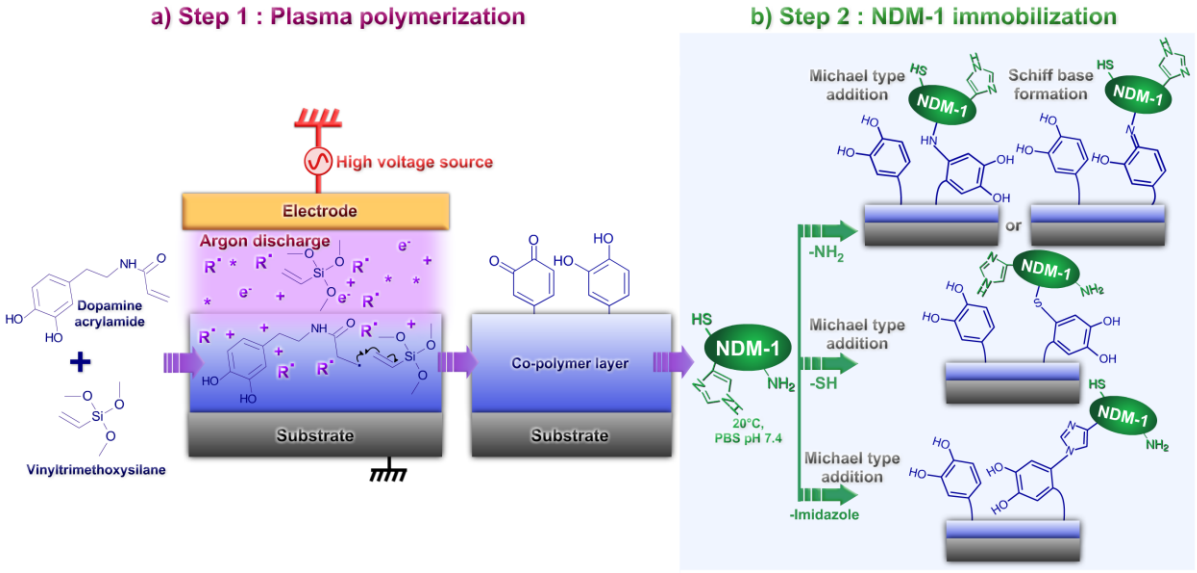

Scheme 1: Schematic description of the innovative two-steps deposition method for the fast preparation of bio-active surfaces. a) Step 1: aerosol liquid-assisted atmospheric-pressure plasma deposition of a catechol-quinone-containing layer from a dopamine acrylamide/vinyltrimethoxysilane solution b) Step 2: covalent bonding of NDM-1 onto the coated surface through different pathways.

The formed coating, macroscopically smooth and adherent across the whole length of the substrate, is shown to be non-soluble in common organic solvent such as dimethylsulfoxide, ethanol or acetone and in aqueous solutions in mild conditions (*i.e.* pH comprised between 5 to 8). Scanning Electron Microscopy (SEM) confirmed that the deposited layer is smooth, powder-free and covers homogeneously the whole surface of the substrate (**Figure 1**). Estimated from contact profilometry measurement and deposition duration, the deposition rate is 10 nm s^{-1}, which is three orders of magnitude higher than the one observed for current wet methods.[18] In addition, the deposition process being performed in a dynamic mode, the thickness of the deposited layer can easily be tuned from several nanometers to hundreds of nanometers by varying the number of passages in the deposition zone (*i.e.* spray and plasma).

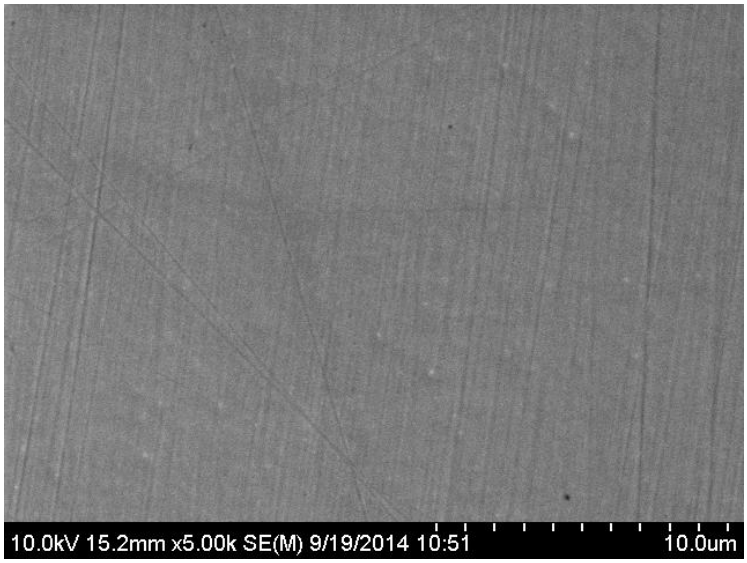

Figure 1: Scanning Electron Microscope micrograph of a DOA-VTMOS plasma deposited coating on stainless-steel substrates.

Fourier Transform InfraRed spectroscopy (FTIR) analyses (**Figure 2A**) confirms that the structure of the hybrid coating is composed of a silica-based network with organic functional groups. The different modes of vibration of the organosilicon network are present, Si-O-Si stretching (~1200 cm^{-1}, 1160 cm^{-1}, 1100 cm^{-1}), Si-O-CH_3 (~1100 cm^{-1}) and Si-OH (~940 cm^{-1}).[24,25] In addition, some characteristic bonds of DOA monomer are observed such as C=O bending (~1650 cm^{-1}) of amide I bond and quinone groups, NH bending from amide II band (~1550 cm^{-1}), aromatic ring vibration (~1520 cm^{-1}) and CN/NH vibrations from amide III (~1260 cm^{-1}).[26,27,28] The strong C=C peak at 1600 cm^{-1}, characteristic of the monomer vinyl bond, is not observed in the deposited layer spectra (**Figure 2.A.b and c),** corroborating their consumption during the polymerization process. The UV absorption spectra of a DOA-VTMOS plasma deposited layer (**Figure 2.B.b**), shows the presence of a peak, centered at about 280 nm attributed to catechol groups and also observed in the monomer mixture (**Figure 2.B.a**).[29] The presence of a large peak at higher wavenumber and centered at about 425 nm suggests the formation of polymerization derivatives and quinone groups formed upon exposure to plasma generated oxidant species.[30,31]

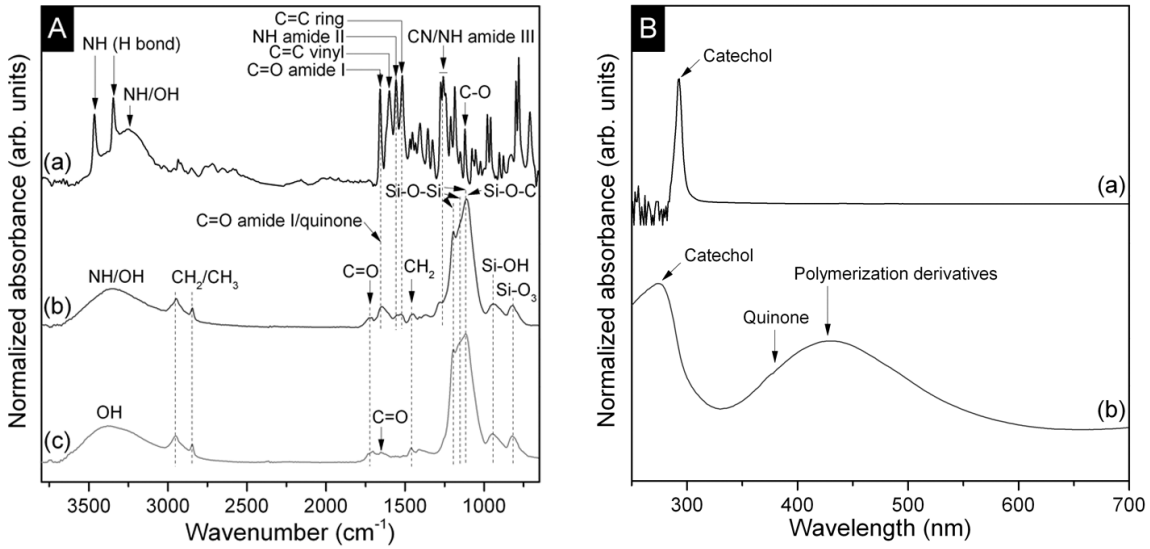

C

XPS chemical composition (at. %)	C	N	O	Si
DOA (theory)	73	7	20	0
DOA-VTMOS coating	44	2	42	12
VTMOS coating	38	0	45	17

Figure 2: A) FTIR spectra of: a) DOA monomer in powder form b) plasma deposited hybrid coating from a sprayed DOA-VTMOS solution c) plasma deposited coating from a sprayed pure VTMOS solution B) UV-Visible spectra of a) a 0.5 mg mL^{-1} solution containing DOA in VTMOS b) plasma deposited coating from solution "a" C) XPS chemical surface quantification of VTMOS and DOA-VTMOS coatings and theoretical composition of DOA.

To investigate the upmost surface chemical composition of plasma deposited layers X-ray Photoelectron Spectroscopy (XPS) analyses were carried out on the DOA-VTMOS layer and a pure VTMOS layer (**Figure 2.C**). Non-surprisingly, the DOA-VTMOS hybrid layer did contain nitrogen and silicon, originating from the DOA and VTMOS monomers, respectively. It should be noted that nitrogen is not detected in the pure VTMOS layer, highlighting the possibility to operate under atmospheric conditions without introducing a significant amount of atmospheric contaminants. The N1s spectra curve fitting, composed of a main component at 400.1 eV (**Figure 3**), indicates that the nitrogen atoms are mainly engaged in amide bonds (*ca.* 90 %).[32]

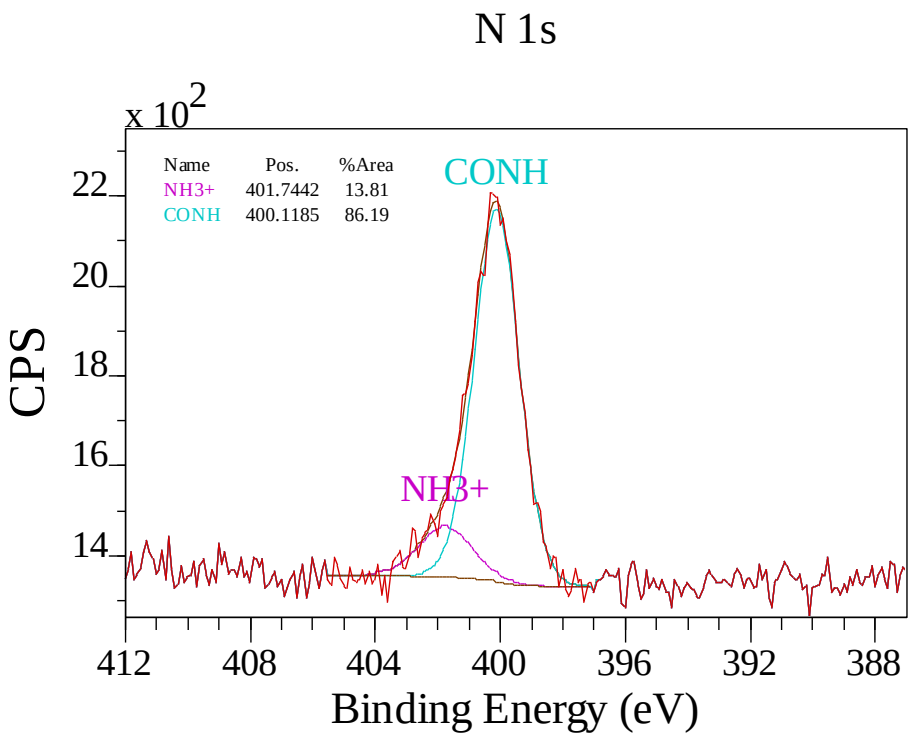

Figure 3: XPS N1s core-level deconvolution of a DOA-VTMOS layer.

This result, together with the previously shown FTIR and UV analyses, suggests that the DOA monomer structure is preserved through the plasma process while the polymerization of the monomers vinyl bonds is initiated. The nitrogen content detected in the hybrid film, 2 at.%, suggests a relatively high loading of the DOA, which roughly represent 30 mol.% of the hybrid layer. Such concentration, significantly higher than the starting DOA-VTMOS solution where the nitrogen content is only 0.002 at.%, is related to the high vapor pressure of VTMOS, which evaporates along the deposition process, leading to hybrid films with a high DOA content. In order to undoubtedly confirm the availability of functional catechol group at the surface of the hybrid coating, their redox property is then exploited to form and immobilize silver nanoparticles. In that sense, the hybrid-coated substrate is dipped in a silver nitrate aqueous solution. Catechols can reduce Ag^{+} into Ag^{0} while the subsequently formed quinone groups are expected to stabilize the metallic nanoparticles.[19,33] SEM analyses (**Figure 4.A**) show the presence of nanoparticles onto the surface while Energy-Dispersive X-ray spectroscopy (EDX) analyses (**Figure 4.B**) confirmed their composition with the Ag^{0} characteristic peaks detection at about 3 and 3.2 keV. This

experiment clearly demonstrates that catechol groups from DOA are preserved during the plasma deposition.

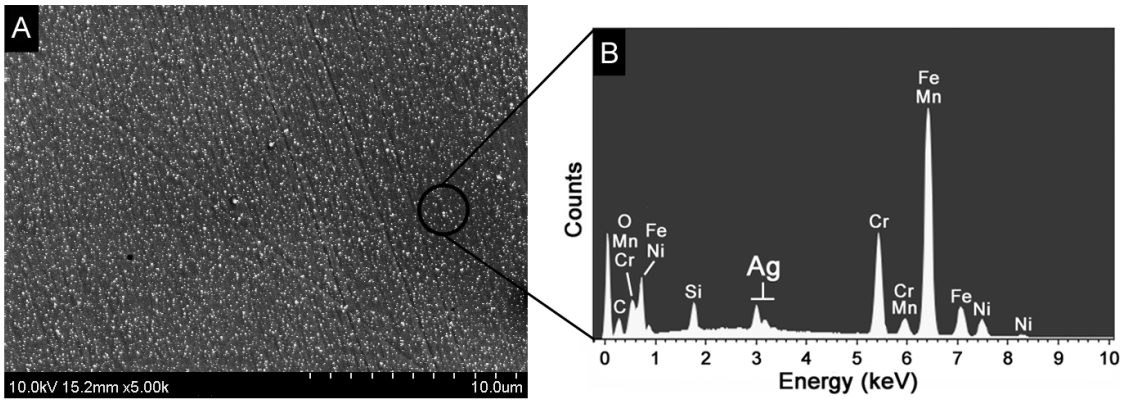

Figure 4: A) SEM micrograph of a DOA-VTMOS plasma coated surface after immersion 24h in $AgNO_3$ solution (1g L^{-1}) and rinsed with H_2O B) EDX analysis of the coating with immobilized nanoparticles.

In the second step of the method, the deposited hybrid layer is exploited for the covalent immobilization of NDM-1 (**Scheme 1.b**). Finally, the efficiency of the developed surfaces for the degradation of amoxicillin is reported. Quinone groups, formed during the deposition process under the oxidative plasma atmosphere can react with the amine, thiol and/or imidazole groups of the NDM-1 enzyme through Michael type addition or with a Schiff base formation (for amine groups) in mild pH condition. [17] Interestingly, the NDM-1 enzyme also presents a hexahistidine tag (his-tag) added at the N-terminal extremity. Initially exploited in the enzyme purification step, the his-tag also provides a supplementary reactive site (see Experimental Section). Moreover, this tag is expected to promote the appropriate enzyme orientation during binding and lead to a better conservation of the enzymatic activity keeping an easy access to the active site of the biomolecule.[34] The NDM-1 immobilization is performed at room temperature, in a PBS solution (pH 7.4) where enzyme is diluted (1 mg mL^{-1}), during 1 hour under gentle stirring. Samples are then washed with PBS to remove unbound enzymes. The surface density of immobilized NDM-1 is estimated to 1.1 ± 0.2 µg cm^{-2}, corresponding to approximately 2.4 10^{13} proteins cm^{-2}, using a colorimetric protein assay (see Experimental Section) to determine the enzyme concentration in the grafting solutions, hence also giving an indirect approximate underestimated value of the surface groups density. The performances of the biofunctional surfaces for antibiotic degradation are

then assessed against amoxicillin. The activity of the immobilized enzymes (*ca.* 3 µg per disk) is compared to the one of free enzymes in solution (3 µg mL^{-1}) (**Figure 5.A & B**). As a consequence, the same amount of free form enzymes and immobilized enzymes are introduced in the degradation assays, *i.e.* 3 µg (see Experimental Section). Both series are incubated in degradation medium (HEPES 12.5 mM, BSA 10 µg mL^{-1}, amoxicillin 100 µg mL^{-1} in filtered tap water (0.22 µm) with final volume of 1 mL). Enzymatic activity is estimated by the amoxicillin degradation monitoring over time by measuring absorbance at 210 nm (complete protocol in Experimental Section). Immobilized NDM-1 shows an activity until 320 hours, slowly decreasing from 25 µg mL^{-1} of degraded amoxicillin during the first 24 hours to about 10 µg mL^{-1} after 320 hours. No significant activity is observed later on.

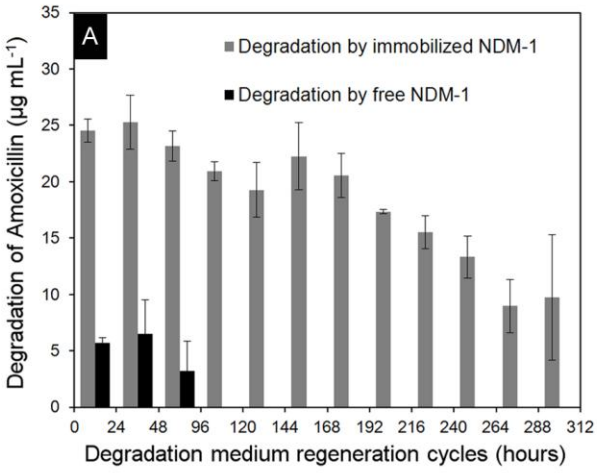

B

	Amount of immobilized NDM-1 (µg cm^{-2})	Average activity duration (h)	Total degraded amoxicillin amount (µg)
Free NDM-1 in solution (3±0.1µg mL^{-1})	-	96	22 ± 9
Immobilized NDM-1 surfaces	1.1 ± 0.2	312	175 ± 27
Immobilized NDM-1 surfaces after flow test	1.1 ± 0.2	298	146 ± 9

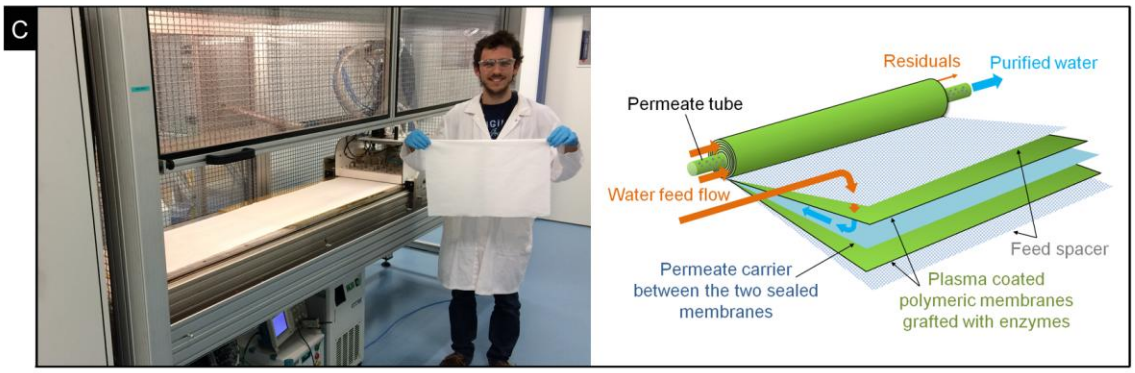

Figure 5: A) Degradation assay of amoxicillin by free and immobilized NDM-1 onto coated stainless steel B) Average duration of NDM-1 activity under different forms and degraded amoxicillin quantity obtained for coated stainless steel substrate for 3 independent series and after flow test. C) Industrial scale PE-CVD setup for the coating of polyamide membranes commonly employed in spiral membrane filters used for water purification.

The reproducibility of these results were assessed for 3 different batches of NDM-1 grafted on 3 independent deposited series, each composed of 4 samples. Importantly, free NDM-1 remains only active during 96 hours, degrading 1 to 10 μg mL^{-1} of amoxicillin each 24h. After this period of time, no activity is observed, clearly highlighting the beneficial effect of the enzyme grafting to the plasma coated substrate. It is worth noting that the test is performed using a large excess of amoxicillin compared to waste water concentrations of about 0.001-0.2 μg L^{-1}.[4,5] The immobilized enzyme is therefore able to degrade in a short period of time a high content of antibiotics that is present in high concentrations. These results are in agreement with previous works reporting that immobilizing enzymes enables to increase both their activity lifetime and performance due to the reduction of enzymes aggregation, autolysis and denaturation occurring for free form enzymes in presence of chemical and biological compounds.[12,15,35]

In a water treatment process, water flows over the bioactive surfaces and generates strong shear stresses that may affect the activity of the purification system. The developed functional hybrid coating is therefore tested under extreme flow conditions, by immersing the substrate in an annular reactor under a high laminar water flow (30 km h^{-1}) during 144 hours. In comparison, the flow velocities in distribution and wastewater networks vary from 10^{-3} to 15 km h^{-1}.[36] The measured activities remain the same than those observed for references that are not exposed to this extreme flow (**Figure 5.B**). It reflects a strong anchoring of enzymes to the surface and an enhanced rigidity through multipoint anchoring on different reactive areas of the NDM-1 conferring integrity to the three-dimensional enzyme conformation necessary for its activity.[35] Moreover no delamination of the functional coating is noted under these extreme conditions, highlighting its strong adhesion to stainless steel. To demonstrate the up-scalability of the proposed approach this coating was also performed on polyamide fabric commonly involved in the fabrication of spiral membrane filter for water purification used in water treatment plant and showed successful immobilization of NDM-1 and degradation properties up to 240 h. The mussel-inspired method could then be easily up scaled to large industrial-scale PE-CVD setups to develop spiral membrane filters (**Figure 5.C**).

In summary, catechol and quinone functionalized hybrid layers are readily deposited onto stainless steel by atmospheric-pressure plasma-assisted polymerization of a mixture of dopamine acrylamide and vinyltrimethoxysilane. In particular, the quinone groups at the surface of the coating are exploited for the grafting of an enzyme (NDM-1) that is able to degrade a commonly used antibiotic, amoxicillin. The performance of this biofunctional substrate for the depollution of water contaminated by this antibiotic is assessed. Thanks to the successful immobilization of the enzyme, the antibiotics degradation activity remains high during a long period of time, and largely surpasses that of the free enzyme. The system is highly active, even under extreme flow conditions and no coating delamination is observed. The grafting of virtually any biomolecules can be considered, diversifying the range of applications for this adherent catechol and quinone-bearing hybrid coating. Moreover, the environmentally friendly plasma process described in this chapter is easy to implement under atmospheric pressure with no need for waste treatment, and provides high deposition rates on any type of substrate, comprising heat sensitive materials. An industrial up-scaling is possible with roll-to-roll technology for the treatment of plastic and metallic foils and it is also expected to extend this process to manufactured products with complex geometries thanks to a plasma torch configuration. The ability to deposit these materials as robust thin films with a well-controlled thickness could have significant impact in the field of photocatalysis, self-healing materials and energy storage.[37,38]

Experimental Section

Synthesis of N-(3,4-Dihydroxyphenethyl)acrylamide (DOA)

A two-neck round-bottom flask was charged with 12.1 g (31.6 mmol) of $Na_2B_4O_7.10H_2O$ and 5.0 g of Na_2CO_3, and 475 mL of milli-Q water (18.2 MΩ.cm, Millipore). This basic aqueous solution was degassed in sonicator bath (Branson 2510, 100 W, 42 KHz) for 1 h, applying light vacuum followed by, bubbling with argon for another 2 h. 3 g (15.8 mmol) of Dopamine hydrochloride (Sigma-Aldrich) was added under argon atmosphere and continued stirring for 30 minutes. The flask was then cooled at 0°C before drop-wise addition of 5.1 mL (63.2 mmol) of acryloyl chloride with stirring. Another 9.0 g Na_2CO_3 was added to maintain the pH of the solution above 9 during the reaction. After

stirring for 12 h at room temperature, the solution was acidified to pH 1–2 with 6N HCl and continued stirring for 1 h. The mixture was extracted five times with ethyl acetate, washed with 0.1 M HCl and dried over $MgSO_4$. The solvent was removed in vacuum to yield crude greyish paste, which was further purified by flash silica gel column chromatography eluting with dichloromethane/methanol (9:1) mixture (80% yield).

Atmospheric-pressure plasma-assisted polymerization

A solution of DOA in vinyltrimethoxysilane (VTMOS) (0.5 mg mL^{-1}) was sprayed by a 48 kHz ultrasonic atomising nozzle (Sono-Tek Corporation). The created mist was composed of droplets of median diameter of 40 microns and the range of size was 5 to 200 microns. 0.5 mL min^{-1} of solution was injected in the nozzle by using a syringe driver. The Sonotek generator was set up to 2W to generate the mist, while at the output of the nozzle, a nitrogen flow was used in order to shape the mist, and entrain it on the substrate. Plasma polymerization in argon was then performed with a dielectric barrier discharge reactor composed of two flat alumina covered electrodes connected to high voltage and ensuring an efficient plasma surface zone of 18.72 cm^2. The samples were placed on the moving table (*i.e.* grounded electrode) ensuring a dynamic deposition mode. The table speed and the gap between the electrodes were fixed at 100 mm s^{-1} and 1 mm, respectively. The plasma discharge was ignited with a sinusoidal signal at 10 kHz chopped by a 1667 Hz rectangular signal. The power density was set up to 1.6 W cm^{-2}.

Silver nanoparticles formation protocol

Inspired by the protocol of Faure *et al.* [19], plasma coated samples were immersed in the dark in an $AgNO_3$ aqueous solution (1g L^{-1}) under stirring (300 rpm) at ambient temperature during 24h and then subsequently rinsed 5 times during 5 minutes each in distilled H_2O under stirring (500 rpm) and then dried under nitrogen flux.

NDM-1 production

The poPINF plasmid containing the synthetic gene encoding *K. pneumoniae* was provided by R.Owens from the Oxford Protein Production Facility UK. The protein production and purification were performed according to the Green *et al*. protocol (2011) with an additional freezing step carried out before cell lysis with french press. The NDM-1 (28 kDa) isolation and purification were solely performed with a HisTrap FF column (GE

Healthcare). Excess of imidazole was removed via three washes in Amicon ® Ultra-4 Centrifugal Filter Units 3,000 NMWL (1000 x g for 15 min). Enzymes were then resuspended in a phosphate buffered saline (PBS) solution.

Enzymes immobilization

The enzyme immobilization was performed in PBS solution at pH 7.4 at a final concentration of 1 mg mL^{-1} during 1h at room temperature under gentle agitation (100 rpm). Samples were then washed 5 times during 5 minutes with PBS under 500 rpm stirring to remove unbound enzymes. Enzyme concentrations were doubly measured by 2D Quant Kit (GE Healthcare) and RC DC protein assay (Bio rad). The measured immobilized NDM-1 concentration on the steel discs was equal to 1.1 ± 0.2µg cm^{-2}.

Antibiotics degradation assays

Enzymatic activity was estimated by the amoxicillin degradation monitoring over time. Samples with immobilized enzymes were incubated in a degradation medium at ambient temperature (4-(2-hydroxyethyl)-1-piperazineethanesulfonic acid (HEPES) 12.5 mM, Bovine Serum Albumin (BSA) 10 µg mL^{-1}, amoxicillin 100 µg mL^{-1} in filtered tap water (0.22 µm) with final volume of 1 mL). Each 24h, the degraded amoxicillin concentration is estimated by measuring absorbance at 210 nm with 2 Synergy microplate reader (Biotek). The medium was removed every 24 hours, wells were washed 3 times with filtered tap water and a new volume of the degradation medium was added in wells. The procedure was slightly different for the free enzymes in solution. In order to compare the activities of the free form and the immobilized enzymes, the same amounts of enzymes are introduced in the 1 mL degradation medium. The measured immobilized amount of NDM-1 on the surface was found to be about 1.1 µg cm^{-2}, *i.e.* about 3 µg of enzymes are present on the surface for the 3 cm^2 samples. Hence, the free form NDM-1 concentration was set to 3 µg mL^{-1} to maintain the same amount of enzymes in the degradation assay. In the wells used for the first measurement (t= 24h), enzymes were directly dissolved in a volume of 1 mL of the degradation medium containing 100 µg mL^{-1} of amoxicillin. For all other wells, at time t_0, enzymes were dissolved in a volume of 300 µL containing 20 µg mL^{-1} of amoxicillin in order that the enzymes are in activity. All wells were fed by this same volume every 24 hours. When wells were used to measure, 24 hours before they are amended with 100 µg mL^{-1} of antibiotic and supplemented to achieve a final volume of 1 ml.

Flow test - Resistance to shear stress

Immobilized enzymes onto plasma functionalized samples were fixed to the rotor of an annular reactor (Biofilm Reactor Annular LJ 1320 reactor, Biosurface Technologies Corporation). The samples were then subjected to laminar water flows equivalent to a 30 $km.h^{-1}$ flow rate. After 144 hours the enzymatic activity was measured and compared to the disks used for degradation assays.

References

[1] A. Gobel, A. Thomsen, C. McArdell, A. Joss, W. Giger, *Environ. Sci. Technol.* **2005**, *39*, 3981.

[2] J.Q. Chen, R.X. Guo, *J. Hazard. Mater.* **2012**, *209-210*, 520.

[3] O.S. Keen, K.G. Linden, Environ. *Sci. Technol.* **2013**, *47*, 13020.

[4] A. Lamm, I. Gozlan, A. Rotstein, D. Avisar, *J. Environ. Sci. Heal. A.* **2009**, *44*, 1512.

[5] J. Rossmann, S. Schubert, R. Gurke, R. Oertel, W. Kirch, *J. Chromatogr. B.* **2014**, *969*, 162.

[6] J. Davies, *J. Ind. Microbiol. Biotechnol.* **2006**, *33*, 496.

[7] C. Merlin, S. Bonot, S. Courtois, J-C. Block, *Water Res.* **2011**, *45*, 2897.

[8] D. Yong, M. A. Toleman, C. G. Giske, H. S. Cho, K. Sundman, K. Lee, T. R. Walsh, *Antimicrob. Agents Chemother.* **2009**, *53*, 5046.

[9] M. Llorca, S. Rodríguez-Mozaz, O. Couillerot, K. Panigoni, J. de Gunzburg, S. Bayer, R. Czaja, D. Barceló, *Chemosphere* **2015**, *119*, 90.

[10] Z. Zhou, R. N. Klupp Taylor, S. Kullmann, H. Bao, M. Hartmann, *Adv. Mater.* **2011**, *23*, 2627.

[11] C. Mateo, J. M. Palomo, G. Fernandez-Lorente, J. M. Guisan, R. Fernandez-Lafuente, *Enzyme Microb. Technol.* **2007**, *40*, 1451.

[12] G. Camporeale, M. Moreno-Couranjou, S. Bonot, R. Mauchauffé, N. D. Boscher, C. Bebrone, C. Van de Weerdt, H.-M. Cauchie, P. Favia, P. Choquet, *Plasma Process. Polym.* **2015**, DOI: 10.1002/ppap.201400206.

[13] D. Duday, C. Vreuls, M. Moreno, G. Frache, N.D. Boscher, G. Zocchi, C. Archambeau, C. Van De Weerdt, J. Martial, P. Choquet, *Surf. Coat. Technol.* **2013**, *218*, 152.

[14] R. Mauchauffé, M. Moreno-Couranjou, N.D. Boscher, C. Van De Weerdt, A-S. Duwez, P. Choquet, *J. Mater. Chem. B* **2014**, *2*, 5168.

[15] S. Bonot, R. Mauchauffé, N. D. Boscher, M. Moreno-Couranjou, H.-M. Cauchie, P. Choquet, *Adv. Mater. Interfaces* **2015**, DOI: 10.1002/admi.201500253.

[16] H. Lee, S. M. Dellatore, W. M. Miller, Phillip B. Messersmith, *Science* **2007**, *318*, 426.

[17] E. Faure, C. Falentin-Daudré, C. Jérôme, J. Lyskawa, D. Fournier, P. Woisel, C. Detrembleur, *Prog. Pol. Sci.* **2013**, *38*, 236.

[18] Q. Wei, F. Zhang, J. Li, B. Li, C. Zhao, *Polym. Chem.* **2010**, *1*, 1430.

[19] E. Faure, C. Falentin-Daudré, T. Svaldo Lanero, C. Vreuls, G. Zocchi, C. Van De Weerdt, J. Martial, C. Jérôme, A-S. Duwez, C. Detrembleur, *Adv. Funct. Mater.* **2012**, *22*, 5271.

[20] J. Sedó, J. Saiz-Poseu, F. Busqué, D. Ruiz-Molina, *Adv. Mater.* **2013**, *25*, 653.

[21] D. Merche, N. Vandencasteele, F. Reniers, *Thin Solid Films* **2012**, *520*, 4219.

[22] P. Heier, N. D. Boscher, T. Bohn, K. Heinze, P. Choquet, *J. Mater. Chem. A* **2014**, *2*, 1560.

[23] N. D. Boscher, P. Choquet, D. Duday, N. Kerbellec, J. C. Lambrechts, R. Maurau, *J. Mater. Chem.* **2011**, *21*, 18959.

[24] I. Montero, L. Galán, O. Najmi, J. M. Albella, *Phys. Rev. B* **1994**, *50*, 4881.

[25] Y-S. Li, P.B. Wright, R. Puritt, T. Tran, *Spectrochim. Acta A.* **2004**, *60*, 2759.

[26] J. Breton, C. Boullais, J.R. Burie, E. Nabedryk, C. Mioskowski, *Biochem.* **1994**, *33*, 14378.

[27] G. Socrates, *Infrared and Raman Characteristic Group Frequencies: Tables and Charts, 3rd Edition*, Wiley, Hoboken, NJ, USA **2004**.

[28] K. Kaiden, T. Matsui, and S. Tanaka, *Appl. Spectrosc.* **1987**, *41*, 180.

[29] M.-H. Ryou, J. Kim, I. Lee, S. Kim, Y. K. Jeong, S. Hong, J. H. Ryu, T.-S. Kim, J.-K. Park, H. Lee, J. W. Choi, *Adv. Mater.* **2013**, *25*, 1571.

[30] A. Rompel, H. Fischer, D. Meiwes, K. Büldt-Karentzopoulos, A. Magrini, C. Eicken, C. Gerdemann, B. Krebs, *FEBS Letters* **1999**, *445*, 103.

[31] B.P. Lee, J.L. Dalsin, P.B. Messersmith, *Biomacromolecules* **2002**, *3*, 1038.

[32] J. S. Stevens, S. J. Byard, C. C. Seaton, G. Sadiq, R.J. Davey, S. L. M. Schroeder, *Phys. Chem. Chem. Phys.* **2014**, *16*, 1150.

[33] H. Lee, Y. Lee, A. R. Statz, J. Rho, T. G. Park, P. B. Messersmith, *Adv. Mater.* **2008**, *20*, 1619.

[34] H. Lee, J. Rho, P. B. Messersmith, *Adv. Mater.* **2009**, *21*, 431.

[35] C. Garcia-Galan, A. Berenguer-Murcia, R. Fernandez-Lafuente, R.C. Rodrigues, *Adv. Synth. Catal.* **2011**, *353*, 2885.

[36] A. Hogetsu, Y. Ogino, T. Takemika, *Technology Transfer Manual of Industrial Wastewater Treatment*, Ministry of Environment, Government of Japan, Tokyo, **2002**.

[37] M. Lee, J. U. Kim, J. S. Lee, B. Il Lee, J. Shin, C. B. Park, *Adv. Mater.* **2014**, *26*, 4463.

[38] M.-H. Ryou, Y. M. Lee, J.-K. Park, J. W. Choi, *Adv. Mater.* **2011**, *23*, 3066.

Chapter 6

Liquid-Assisted Plasma-Enhanced Chemical Vapor Deposition of Catechol and Quinone Functionalized Coatings: Insights into the Surface Chemistry and Morphology

Rodolphe Mauchauffé, Maryline Moreno-Couranjou, Nicolas D. Boscher, Anne-Sophie Duwez and Patrick Choquet, *In preparation*.

1. Introduction

Atmospheric-pressure (AP) cold plasma processes are drawing an ever growing interest for the deposition of nanofilms.[1,2] This one-step deposition approach, easily integrable into production lines, is recognized for its fast deposition rates and its green and up-scalable characters (*i.e.* ability to treat large planar surfaces of few meter width thanks to plane to plane configuration equipment). In addition, it can enable localized deposition, below 100 microns width or deposition on complex shape substrates using plasma "pen"/torch configuration. Originally involving monomer gas phase injection into the discharge via the use of vaporizing systems, the numbers of coatings and applications that can be reached by AP-Plasma Enhanced Chemical Vapor Deposition (PECVD) have evolved quite spectacularly over the past twenty years, notably thanks to the exploitation of liquid injection systems.[3,4,5] These feeding systems allow of the use of precursors with high boiling point, including solid compounds dissolved or dispersed in a liquid medium.[3] In addition, the simultaneous feeding of two phases (*i.e.* liquid precursor containing suspended molecules/nanoparticles) offers new perspectives for the elaboration of functional nanocomposite coatings at a high deposition rate. Recently, some works have shown that thanks to the careful adjustment of the plasma parameters, the deposition of coatings containing sensible chemical compounds such as porphyrins or proteins can be achieved with a high retention of their chemical structure.[3,6,7] The liquid injection of precursor is most commonly achieved using an atomizer. The formed aerosol is subsequently directly injected into the plasma discharge,[8,9] such as in Aerosol Assisted-Dielectric Barrier Discharge (AA-DBD).[5,6] An alternative approach relies on the deposition of a fine liquid layer over a surface just before its exposure to plasma. This approach, related to an Atmospheric-Pressure Plasma Liquid Deposition process (AP-PLD), [10,11,12,13,14] can be considered as a Liquid-Assisted Plasma Enhanced Chemical Vapor Deposition (LA-PECVD).

AP-PECVD provides a convenient route towards the preparation of reactive functionalized surfaces, including carboxylic acid,[15] epoxy[16,17] and amine functionalized surfaces.[18] Recently, the range of functionalized surfaces available from an atmospheric plasma deposition process was extended to catechol and quinone functionalized layers thanks

to the use of a solid dopamine derivative compound in a LA-PECVD approach (*cf.* Chapter 5).[19] Catechol and quinone groups, *i.e.* oxidized catechol, are providing new adhesive and molecules grafting options inspired by the mussels' feet, which have the ability to strongly adhere to surfaces in harsh conditions.[20] More particularly, catechols are responsible for the adherence of mussels on surfaces such as metals thanks to the formation of coordination bonds, while quinones confer cohesion to the feet due to its ability to form covalent bonds through Michael addition and/or Schiff-base formation with functional groups present in proteins constituting the feet. [21,22] Until recently, catechol and quinone containing layers were only deposited by wet chemical techniques. Those well-documented techniques, considered as batch processes, often involve numerous steps, present a low deposition rate and generally lead to the production of wastes.[23] Considering quinone functionalized layers deposited by the layer by layer technique (LbL), Faure *et al.* succeeded in considerably improving the deposition time (*i.e.* 1 nm/min compared to about 0.04 nm/min for the dopamine autopolymerization technique).[21,24,25] However, numerous and complex process steps are required. Alternative wet chemical methods were investigated, such as UV curing photo polymerization ones. However, they required the use of photo-initiators and mainly lead to the formation of gels.[26] In addition, the nature of the starting precursor (*i.e.* catechol or quinone-bearing monomers/polymers) governs the chemistry of the deposited layers, thus leading to catechol or quinone functionalized layers. Moreover, it is worth noting that only the dopamine autopolymerization technique enables depositing catechol and quinone functionalized layers. The LA-PECVD of dopamine acrylamide (DOA) provides a dry, versatile and up-scalable alternative towards the deposition of catechol and quinone groups-containing layers. This method enables the deposition, at high deposition rate (10 nm s^{-1}), *i.e.* three orders of magnitude higher than the one observed for current wet methods, of coatings, enabling the grafting of biomolecules. The elaborated biofunctional surfaces are able to sustain extreme laminar water flow (30 km h^{-1}) for at least 6 days while maintaining high biological activity as reported in Chapter 5.[19]

Herein, we report on the growth mechanisms of catechol and quinone groups-containing layers formed thanks to the copolymerization of DOA and vinyltrimethoxysilane (VTMOS) in a LA-PECVD process involving an Atmospheric-Pressure Dielectric Barrier Discharge (AP-DBD). In a first part of the present work, the influence of the precursor delivery rate on the chemistry, growth rate and ageing of the deposited layer is studied. The

influence of the applied power on the chemical composition of the formed cross-linked network and on the DOA monomer functional group retention is also reported. The growth rate and ageing of the layer are investigated thanks to mass measurements and FTIR analyses. The layer chemistry is studied thanks to bulk chemistry analysis such as FTIR and UV-Vis spectroscopy while surface chemistry is followed by X-Ray photoelectron spectroscopy (XPS). In a second part of this work, a deeper investigation of the growth mechanism based on surface morphology observations is carried out in order to understand the plasma-surface interactions in LA-PECVD and its influence on the surface chemistry. To this end, the surface topography is analyzed by optical microscopy and contact profilometry, while the surface chemistry is investigated by ToF-SIMS. The surface distributions of catechol and quinone groups are indirectly estimated from the formation and immobilization of silver nanoparticles and the grafting of a model protein, respectively.

2. Experimental Section

2.1 Materials

A home synthesized N-(3,4-dihydroxyphenethyl)acrylamide, called dopamine acrylamide (DOA), was produced through a modified procedure inspired by the work of Lee *et al.*[26] A two-neck round-bottom flask was charged with 12.1 g (31.6 mmol) of $Na_2B_4O_7.10H_2O$ and 5.0 g of Na_2CO_3, and 475 mL of milli-Q water (18.2 MΩ.cm, Millipore). This basic aqueous solution was degassed in sonicator bath (Branson 2510, 100 W, 42 KHz) for 1 h, applying light vacuum followed by, bubbling with argon for another 2 h. 3 g (15.8 mmol) of dopamine hydrochloride (Sigma-Aldrich) was added under argon atmosphere and continued stirring for 30 minutes. The flask was then cooled at 0°C before drop-wise addition of 5.1 mL (63.2 mmol) of acryloyl chloride with stirring. Another 9.0 g Na_2CO_3 was added to maintain the pH of the solution above 9 during the reaction. After stirring for 12 h at room temperature, the solution was acidified to pH 1–2 with 6 N HCl and continued stirring for 1 h. The mixture was extracted five times with ethyl acetate, washed with 0.1 M HCl and dried over $MgSO_4$. The solvent was removed in vacuum to yield crude greyish paste, which was further purified by flash silica gel column chromatography eluting with dichloromethane/methanol (9:1) mixture (80% yield). The DOA monomer was then dissolved at a final 0.5 mg mL^{-1} concentration in vinyltrimethoxysilane (VTMOS, 98%,

Sigma-Aldrich) during 10 hours to obtain the precursor solution. β-lactamase from *Pseudomonas Aeruginosa*, an enzyme able to degrade amoxicillin antibiotic, was provided by Sigma-Aldrich. Mirror polished stainless steel (SS) disks 304-8ND (2 cm diameter and 1 mm thickness) were used as substrates. They were cleaned by successive ultrasonic washings in butanone (5 min), acetone (1 min) and absolute ethanol (1 min) and further dried under a nitrogen flux. Prior to the plasma deposition experiments, the disk surfaces were cleaned and activated thanks to a 30 s $Ar–O_2$ plasma treatment (19 L min^{-1}/1 L min^{-1}) ignited by a 10 kHz sinusoidal electrical excitation (SOFTAL generator) and operated at 1.6 W cm^{-2}.

2.2 Liquid-Assisted Plasma-Enhanced Chemical Vapor Deposition

The DOA-VTMOS solution was sprayed onto the SS substrates, directly in the plasma deposition chamber, using a 48 kHz ultrasonic atomizing nozzle (Sono-Tek Corporation). The created mist was composed of droplets with size ranging from 5 to 200 µm. Median diameter being 40 µm and 90 % of the droplet sizes (measured for water with a viscosity of 0.9 cST at 25°C, sensibly equal to VTMOS with a 0.6 cST viscosity at 25°C) are inferior to 100 µm. A variable precursor solution delivery rate, ranging from 0.25 mL min^{-1} to 1.5 mL min^{-1}, was carried to the atomizing nozzle using a syringe driver (**Figure 1a**). The Sono-Tek generator was set up to 2 W to form the mist, while at the output of the atomizing nozzle, a 10 L min^{-1} nitrogen flow was used to shape the mist and direct it on the SS disks. As consequence, a thin liquid layer composed of DOA and VTMOS was formed at the surface of the substrate (**Figure 1b**). Immediately (~1 s) after the thin liquid layer deposition, plasma polymerization was performed via an AP-DBD fed with a 20 L min^{-1} constant flow of argon (99.999%) and ignited by a 10 kHz sinusoidal signal (**Figure 1c**). The power density was tuned from 0.3 to 2.7 W cm^{-2}. The AP-DBD reactor was composed of two flat high voltage electrodes covered with alumina, creating a plasma discharge zone of 18.72 cm^2. The SS samples, located on a moving table (*i.e.* grounded electrode) ensuring a dynamic deposition mode (100 mm s^{-1}), were placed into a 1 mm thick pierced SS mask in order to ensure an uniform electrode gap distance (1 mm) and prevent undesirable border effects. The number of LA-PECVD cycles (*i.e.* in the aerosol zone and plasma discharge) was varied between 17 and 100, according to the precursor delivery rate, in order to keep a constant amount of injected

precursor per deposition experiment (*i.e.* 5 mL). For the layer morphology study, the number of cycles was tuned from 1 to 50 (using a 0.5 mL min^{-1} precursor delivery rate). **Table 1** summarizes the different parameters investigated in this study.

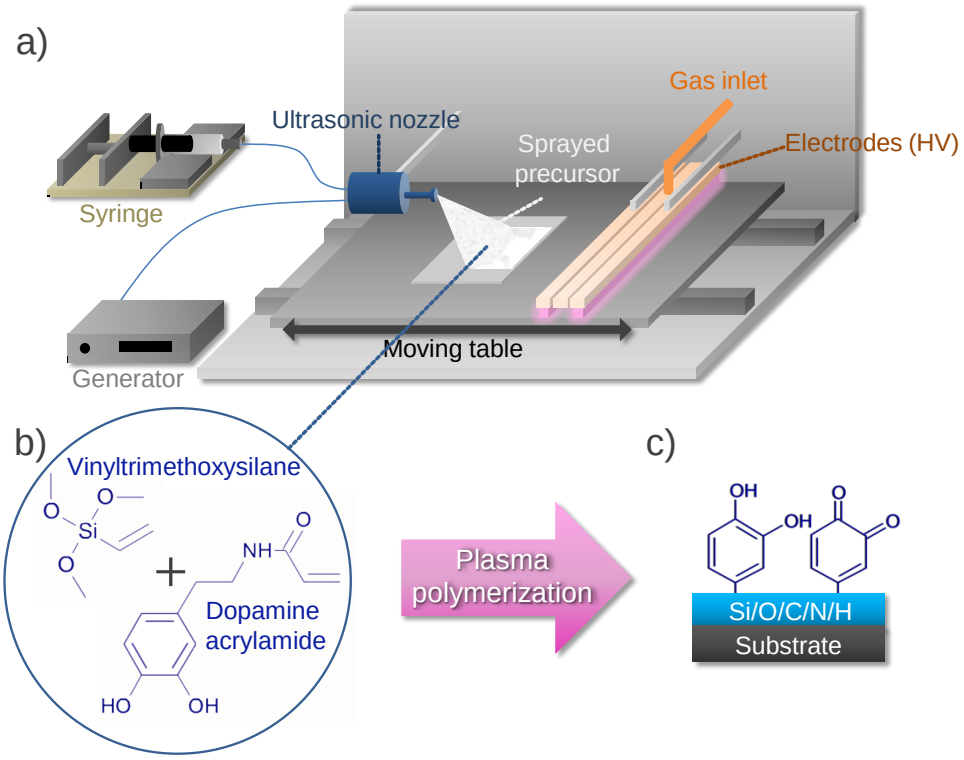

Figure 1: Schematic of the DOA-VTMOS copolymer deposition method through ultrasonic spray deposition (a) of a precursor liquid layer (b) and AP-DBD plasma polymerization (c).

Table 1. Experimental liquid-assisted plasma deposition conditions of catechol/quinone functionalized films.

Fixed parameters	
Precursor solution	DOA in VTMOS, 0.5 mg mL^{-1}
Injected precursor amount	5 mL
Plasma gas	Argon
Electrical discharge mode	Continuous mode (CW)
Variable parameters	
Precursor delivery rate (φ)	0.25 mL min^{-1}-1.5 mL min^{-1}
Plasma power density	0-2.7 W cm^{-2}

2.3 Sample characterization

Mass measurements of deposited coatings were performed in triplicate on at least 3 independent disks using a Sartorius ME36-S scale. Optical microscopy observations were carried out using an Olympus BX51 microscope. A KLA Tencor P-17 apparatus was used for contact profilometer measurements and 3D mapping of 225x250 µm surfaces. FT-IR analyses of coated surfaces were carried out on a Brüker Hyperion 2000 microscope equipped with a grazing angle objective. Liquid VTMOS and solid DOA samples were analyzed using an IR Bruker Vertex 70 apparatus operating in the attenuated total reflectance (ATR) mode equipped with a diamond crystal. All IR spectra were recorded using 200 scans in the 4000-400 cm^{-1} range (4 cm^{-1} resolution). X-ray photon spectroscopy (XPS) analyses were carried out on samples using a Kratos Axis-Ultra DLD instrument having a monochromatic Al Kα X-ray source (1486.6 eV) at a 20 eV pass energy. CasaXPS software was used to process the XPS spectra. The Si 2p core level was fitted with 2 main components noted: i) T: Si^{3+} (SiO_3C, 102.8 ± 0.1 eV), corresponding to a similar silicon atom environment than in VTMOS; ii) Q: Si^{4+} (SiO_2, 103.6 ± 0.1 eV), attributed to a Si atom bonded to 4 oxygen atoms through Si-O-Si bridging bonds or Si-OH bonds. [27] For clarity, single components, comprising both Si $2p_{3/2}$ and $2p_{1/2}$ peaks, were reported. The N 1s core level was fitted with 2 components at 400.1 ± 0.1 eV and 401.8 eV, corresponding to an amide (CONH) and a protonated amine NH_3^+, respectively.[28] The full width at half maximum (fwhm) was fixed at 1.5 ± 0.1 eV. The Gaussian/Lorentzian ratio was fixed at 30 %. PerkinElmer Lambda 950 UV–vis-NIR (InGaAs) spectrophotometer equipped with an integrating sphere was used for UV-visible absorption spectroscopy. Raman spectra were

recorded between 1800 and 400 cm^{-1} on a Renishaw spectrometer, using a 633 nm excitation radiation from a HeNe laser at 4.7 mW of power with a 100 x magnification objective.

A Zeiss LSM 510 confocal laser scanning microscope using a laser excitation at a wavelength of 405 nm allowed observing the distribution of catechol and quinone groups coming from DOA in the layer thanks to their fluorescence properties. ToF-SIMS analysis was carried out in triplicate using a TOF-SIMS V time-of-flight mass spectrometer (ION-TOF GmbH). Relative abundance images of Si^+ (m/z = 27.97638 u), CH_4N^+ (m/z = 30.03383 u), $C_4H_{10}N^+$ (m/z = 72.08078 u) and $C_5H_{10}N^+$ (m/z = 84.08078 u) fragments were calculated over 500x500 µm surfaces using the SurfaceLab 6.3 software (ION-TOF GmbH).[29]

Catechol surface distribution was estimated via the immobilization of silver nanoparticles formed thanks to the catechol reduction properties according to the procedure reported in [24]. Briefly, coated samples were immersed in the dark in an $AgNO_3$ aqueous solution (1 g L^{-1}) under stirring (300 rpm) at ambient temperature during 24 h and then subsequently rinsed 5 times during 5 minutes each in distilled H_2O under stirring (500 rpm) and then dried under nitrogen flux. The surface distribution of quinone groups was estimated from a chemical derivatization reaction coupled with a ToF-SIMS analysis using a β-lactamase protein as chemical reagent. The protein was immobilized onto coated samples in a Phosphate Buffered Saline (PBS) solution containing 1 mg mL^{-1} of β-lactamase during 1 h under stirring (200 RPM). Surfaces were then rinsed 5 times 5 minutes with PBS and 2 times 5 minutes with distilled H_2O to efficiently remove unreacted enzymes, and dried under nitrogen flux. Enzymatic activity of the grafted surfaces was estimated by monitoring the amoxicillin (Sigma-Aldrich) degradation. To this end, the coated surface was immersed in a 1 mL filtered degradation medium composed of filtered (0.22 µm) tap water, 4-(2-hydroxyethyl)-1-piperazineethanesulfonic acid (HEPES, 12.5 mM), Bovine Serum Albumin (BSA, 10 µg mL^{-1}) and amoxicillin (100 µg mL^{-1}). The concentration of degraded antibiotic was estimated by absorbance measurements at 210 nm using a 2 Synergy microplate reader (Biotek). In order to investigate the surface activity over time, wells were washed 3 times with filtered tap water and filled with fresh degradation medium.

3. Results and Discussion

3.1 Influence of LA-PECVD parameters

3.1.1 Influence of precursor delivery rate in LA-PECVD

The first part of the present work focuses on the influence of the precursor delivery rate onto the mass deposition rate and chemical composition of the LA-PECVD thin films. From **Figure 2a**, which reports on the mass deposition rate of the as-deposited coatings (mass per surface area and plasma exposure time) for different precursor delivery rates (φ) and plasma power densities, two different growth kinetic behaviors are readily noticeable. For $\varphi \leq 0.5$ mL min^{-1}, the mass deposition rate is solely dependent on the precursor delivery rate and the values obtained for each of the investigated plasma power densities are all superimposable. On the other hand, for $\varphi > 0.5$ mL min^{-1}, the deposition rate is also driven by the plasma power density. After one week of ageing at air, films deposited at $\varphi \leq 0.5$ mL min^{-1} present no mass loss (mass loss per surface area and plasma exposure time) (**Figure 2b**). In contrast, significant mass losses are observed for all the films prepared from higher monomers delivery rates (*i.e.* $\varphi > 0.5$ mL min^{-1}). These different ageing behaviors suggest different growth mechanism along with various layer chemistry depending on the precursor delivery rate and plasma power density used during the LA-PECVD process.

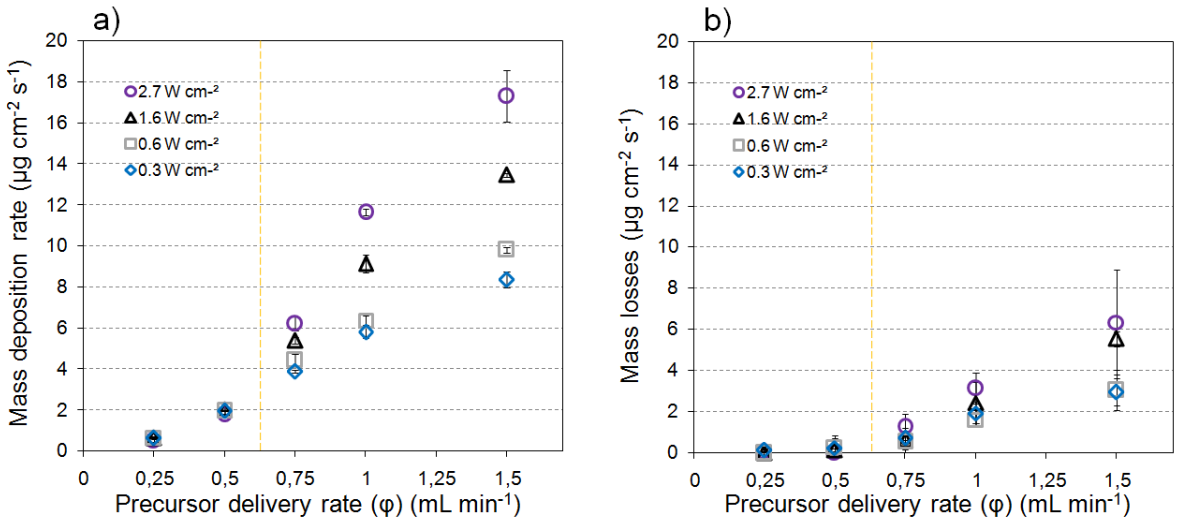

Figure 2: a) Influence of the precursor delivery rate and of the plasma power density onto the mass deposition rate for as-deposited coatings b) Layers mass losses after one week of ageing at air.

According to **Figure 3**, one can notice that the FTIR spectra of the liquid VTMOS (**Figure 3b**) and the layer deposited at 1.6 W cm^{-2} using φ = 1 mL min^{-1} (**Figure 3d**) reveal strong similarities, notably with the presence of the peak at 1075 cm^{-1} attributed to the Si-O-C bond vibration. [30] Some differences are also observed such as an intensity decrease of the C=C vinyl bond peaks at 1600, 1410, 1010 and 968 cm^{-1} that might be correlated to the polymerization of the VTMOS monomer. [31] After ageing, the shape of the layer spectrum changes in the 1200-1000 cm^{-1} range, suggesting that post-deposition reactions are occurring (**Figure 3e**). Firstly, it can be assumed that unreacted VTMOS is likely to evaporate from the layer, as suggested by the significant layer mass-losses measured (**Figure 2b**). In parallel, the relative increase of Si-O-Si peaks at 1150-1200 cm^{-1} related to the inorganic network formation suggests the hydrolysis of Si-O-CH_3 into Si-OH, in presence of the ambient humidity, and its subsequent condensation into Si-O-Si bonds.

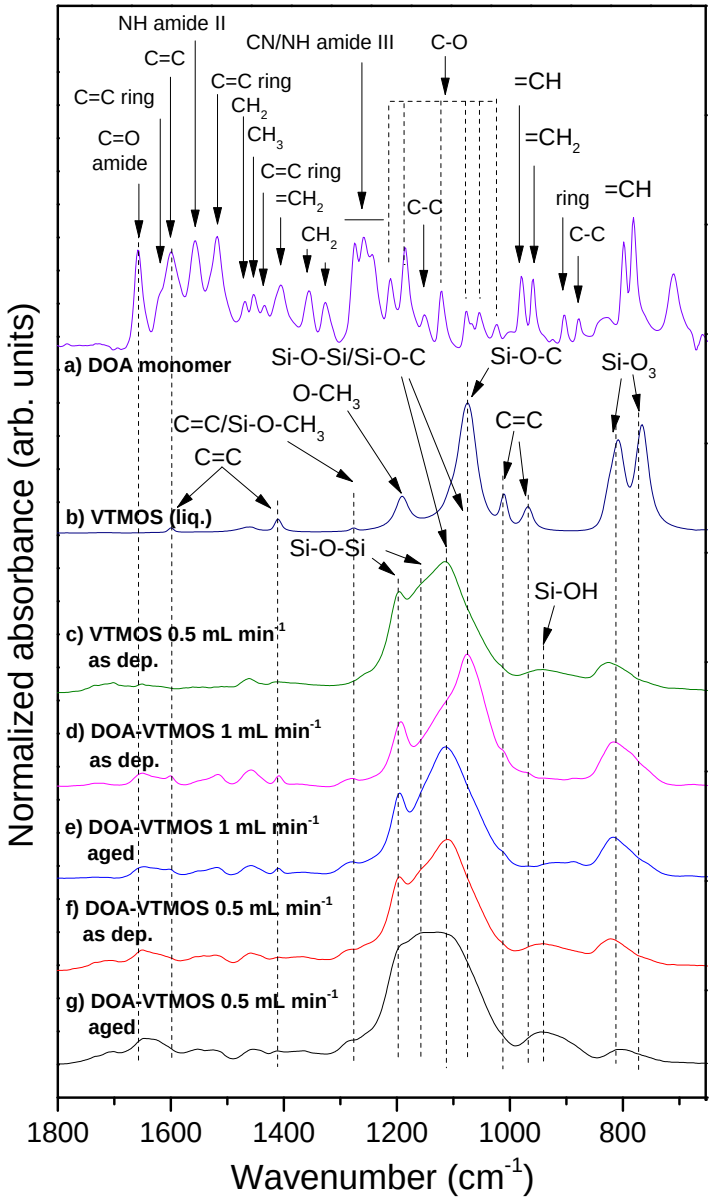

Figure 3: FT-IR spectra in the 1800-650 cm^{-1} range of a) DOA monomer, b) liquid VTMOS, c) as deposited VTMOS coating obtained at 1.6 W cm^{-2} (0.5 mL min^{-1}), DOA-VTMOS as-deposited and after ageing coatings obtained at (d & e respectively) 1 mL min^{-1} and (f & g respectively) 0.5 mL min^{-1} precursor delivery rate at 1.6 W cm^{-2}.

Complementary Raman analyses were carried out for a better monitoring of the carbon-carbon double-bonds. For φ = 1 mL min^{-1}, the as-deposited DOA-VTMOS layer Raman spectrum (**Figure 4b**), shows the presence of the VTMOS monomer vinyl bond (**Figure 4a**) with peaks at 640 cm^{-1} (vinyl CH bend), 1270 cm^{-1} (vinyl CH in plane bend),

1404 cm^{-1} (CH_2 deformation), indicating its incomplete polymerization in the deposited layers **(Figure 4a&b)**. [32,33,34] The presence of all above-mentioned vinyl bonds peaks in the aged coatings exhibiting high mass losses (*i.e.* for $\varphi \geq 0.75$ mL min^{-1}) tends to confirm that high precursor delivery rates lead to incomplete radical polymerization reactions. In spite of their expected fast evaporation, the persistence of unreacted monomer units in the aged thin films suggests the entrapment of liquid VTMOS into the layer network during the LA-PECVD process and/or during post polymerization reactions.[30,35]

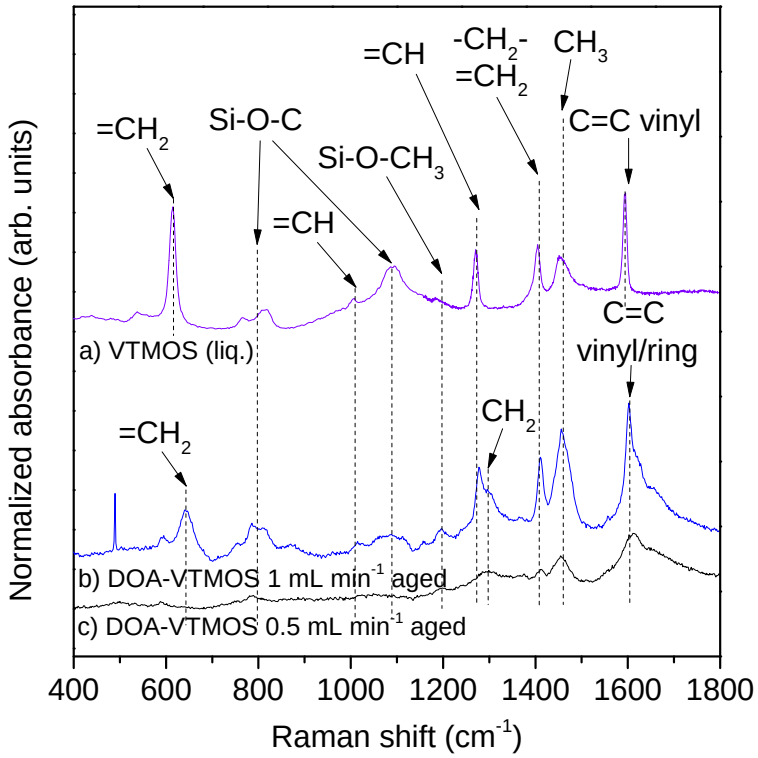

Figure 4: Raman spectra of DOA-VTMOS layers deposited at 1 mL min^{-1} and 0.5 mL min^{-1} precursor delivery rate and 1.6 W cm^{-2}.

In contrast to the layers deposited from high precursor delivery rates, the FTIR spectra of as-deposited coatings grown at $\varphi \leq 0.5$ mL min^{-1} suggest that they are more polymerized and cross-linked. The resulting DOA-VTMOS coatings (**Figure 3f**) are notably composed of a strong inorganic part attributed to a cross-linked Si-O network from VTMOS. The broad peak in the 1200-1000 cm^{-1} region, also observed on a pure VTMOS coating spectrum (**Figure 3c)**, is mainly assigned to the Si-O-Si and Si-O-C bonds. [31] Si-O-C bond is giving

rise to a band around 1110 cm^{-1}, while the Si-O-Si bonds due to the different modes of the Si-O-Si asymmetric vibrations occurring in grazing angle mode, involving transversal and longitudinal modes, give rise to several peaks at 1200 cm^{-1}, 1160 cm^{-1} and 1110 cm^{-1}. [36] It is worth noting that the C-C and C-O contributions from DOA monomer (**Figure 3a**) also present in this area cannot be clearly evidenced due to overlaps with the strong absorption bands of the organosiloxane network. After ageing, those coatings, which exhibited no mass loss, only show a small decrease of the Si-O-Si/Si-O-C peak intensity at 1100 cm^{-1}, suggesting the hydrolysis of Si-O-C bonds to Si-OH (950 cm^{-1}), commonly occurring in organosilicon-based polymer followed by a condensation reaction to form a Si-O-Si cross-linked network. Lower delivery rates (**Figure 5**), leading to a higher energy/amount of precursor ratio, *i.e.* higher energy/molecule ratio, results in a higher Si-O-C bond fragmentation and to the formation of thin films with even less intensity ratio changes after ageing between the Si-O-Si peak at 1200 cm^{-1} and the Si-O-C peak present at 1100 cm^{-1}. Considering the DOA-VTMOS Raman spectra (**Figure 4c**), the absence of the characteristic vinyl bond peaks at 640 cm^{-1} (vinyl C-H bend) and 1270 cm^{-1} (vinyl CH in-plane bend) suggests their major consumption in polymerization reaction occurring for low precursor delivery rate injection. Here, for clarity, only the 1.6 W cm^{-2} condition is reported in **Figure 4** but it is worth noting that, irrespective of the investigated powers, coatings deposited at low delivery rates (*i.e.* $\varphi \leq 0.5$ mL min^{-1}) do not present vinyl bond peaks in their Raman spectra.

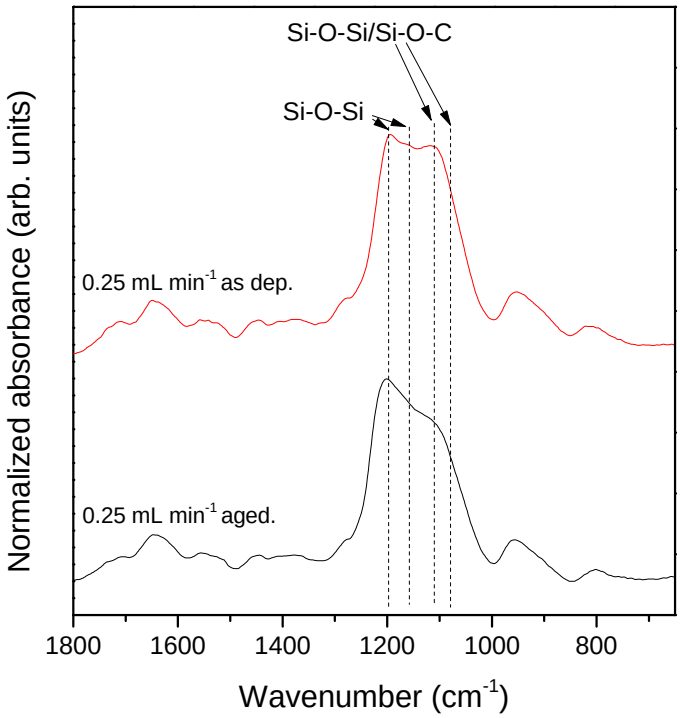

Figure 5: FT-IR spectra in the 1800-650 cm^{-1} range of as-deposited and aged DOA-VTMOS coatings obtained at 0.25 mL min^{-1} at 1.6 W cm^{-2}.

3.1.2 Influence of plasma power density in LA-PECVD

Irrespective of the plasma power density used, high precursor delivery rate (*i.e.* $\varphi >$ 0.5 mL min^{-1}) did result in insufficiently polymerized layers. Therefore, in the present section, the influence of the plasma power density on layers deposited at $\varphi \leq 0.5$ mL min^{-1} will be investigated. Firstly, the influence of power on the silicon-based network is studied by FTIR. For precursor delivery rate of 0.25 or 0.5 mL min^{-1}, an increase of the power from 0.3 W cm^{-2} to 2.7 W cm^{-2} is leading to more inorganic and cross-linked networks with a decrease of the Si-O-C/Si-O-Si peak at 1110 cm^{-1} and an increase of the peaks assigned to Si-O-Si network formation (**Figure 6**). Among the Si-O-Si contributions, the 1200 cm^{-1} one, at grazing incidence angle, is sometimes observed in highly cross-linked samples containing silica network.[36] The lower frequencies vibrations at 1160 cm^{-1} and 1110 cm^{-1}, can be attributed to a coupling of the Si-O-Si vibrations mode, as well as linear Si-O-Si or less cross-linked network vibrations.[37,38,39] Therefore, high plasma power densities are unsurprisingly

more prone to lead to the Si-O-C bond breaking and to the formation of a Si-O-Si cross-linked network.

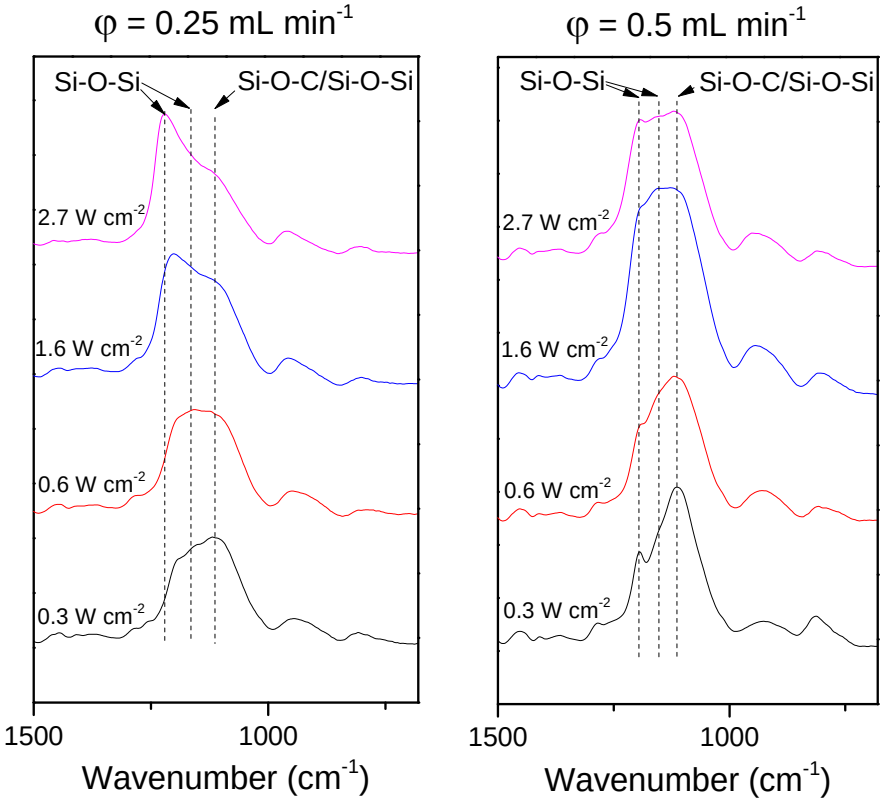

Figure 6: FT-IR spectra in the 680-1500 cm^{-1} region for DOA-VTMOS coatings deposited at 0.25 and 0.5 mL min^{-1} and power densities ranging from 0.3 W cm^{-2} to 2.7 W cm^{-2}.

According to the XPS chemical composition of the layers reported in **Table 2**, it is shown that increasing the plasma power leads to a decrease of the carbon concentration coupled to an increase of the oxygen content while silicon and nitrogen concentrations remain constant. Based on the Si 2p core level fitting, the oxidation state and chemical environment of the silicon (**Figure 7**) can be investigated. It appeared that increasing the applied power leads to an increase of the "Q" contribution, which is in agreement with the oxygen uptake observed in the XPS layer composition and with the FT-IR analyses. [27] This result might be explained by the high energetic species in the plasma able to easily break Si-C bonds (3.3 eV), thus leading to the Q oxidation state. Interestingly, it is worth noting that by adjusting the power and the precursor delivery rate used, it is possible to form coatings

presenting similar chemical compositions, and more specifically similar silicon-network, as it is shown by the similarities of the IR shape spectra (**Figure 6**), XPS elementary quantification (**Table 2**) and Si 2p core level spectra (**Figure 7**) of layers deposited at 1.6 W cm^{-2} and 0.5 mL min^{-1} precursor delivery rate and at 0.6 W cm^{-2} using a 0.25 mL min^{-1} precursor delivery rate.

Table 2. XPS chemical composition for VTMOS monomer (theory) and coatings deposited at 0.25 ml min^{-1} and 0.5 mL min^{-1} for applied powers ranging from 0.3 W cm^{-2} to 2.7 W cm^{-2}.

		XPS chemical composition (at. %)			
Samples	**Power (W cm^{-2})**	**C**	**O**	**N**	**Si**
VTMOS (theory)	-	56	33	0	11
VTMOS coating φ = 0.5 mL min^{-1}	1.6	40	44	0	16
DOA-VTMOS coating φ = 0,25 mL min^{-1}	0.3	45	40	2	13
	0.6	41	44	2	13
	1.6	36	46	3	15
	2.7	33	48	3	16
DOA-VTMOS coating φ = 0,5 mL min^{-1}	0.3	49	37	1	13
	0.6	47	39	1	13
	1.6	41	43	2	14
	2.7	39	44	2	15

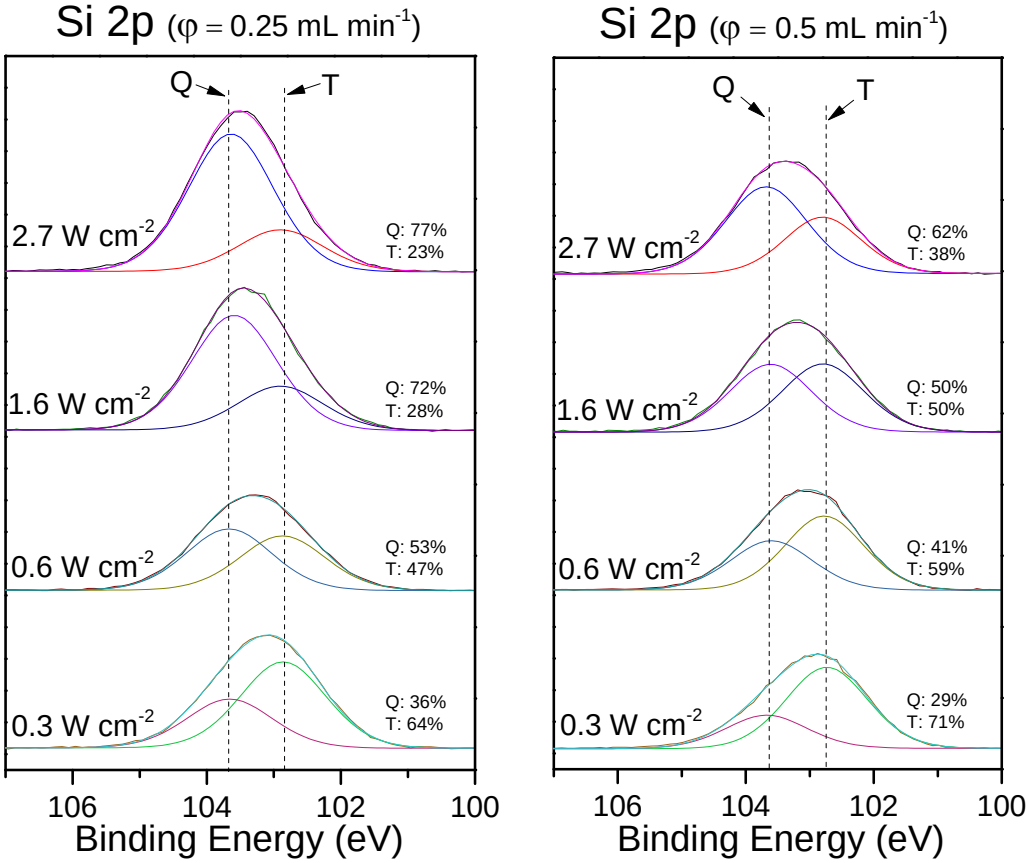

Figure 7: XPS core level fitting of the Si 2p peak between 100-107 eV for layers deposited at power ranging from 0.3 W cm^{-2} to 2.7 W cm^{-2} for a 0.25 and 0.5 mL min^{-1} precursor delivery rate.

In this second part, the influence of the power on the organic moieties of the films is investigated. Irrespective of the applied power, XPS analyses (**Table 2**) show that the amount of nitrogen remains constant, *i.e.* about 2-3 at.%. As no nitrogen is detected in a pure VTMOS coating prepared in the same atmospheric pressure PECVD reactor, it could be assumed that nitrogen contained in the DOA-VTMOS coatings is mainly originating from the DOA monomer. The XPS curve-fitting of N 1s core level was carried out to elucidate the nitrogen environment. Irrespective of the applied power and precursor delivery rate used, the XPS N1s signal fitting revealed the presence of amide bonds with a contribution up to 80%, suggesting a rather good retention of the DOA chemical structure in the deposited films (**Table 3**). Interestingly, the nitrogen content in the DOA-VTMOS coatings, around 2-3 at.% (**Table 2**), is higher than the theoretical one in the starting DOA-VTMOS solution (*i.e.* 0.002 at.%). This suggests a rather high evaporation rate of the VTMOS monomer during the spray

deposition, leading to an increased DOA concentration in the deposited liquid film prior the plasma polymerization step.

Table 3. XPS N1s curve fitting of DOA-VTMOS coatings obtained for power ranging from 0.3 W cm^{-2} to 2.7 W cm^{-2} and using a 0.25 and 0.5 mL min^{-1} flow rate.

	P (W)	NH_3^+ (%)	CONH (%)
0,5 mL/min	6	26	74
	12	30	70
	30	19	82
	50	28	72
0,25 mL/min	6	30	70
	12	29	71
	30	24	76
	50	24	76

Additional investigations on the FTIR analyses are completed in order to study the influence of the plasma power density on the organic moieties of the DOA-VTMOS films. Whatever the applied power and considering the 1480-1800 cm^{-1} region (**Figure 8**), similar FTIR spectra are obtained with the presence of DOA related peaks, namely C=O (amide) at 1650 cm^{-1}, NH (amide) at 1554 cm^{-1}, C=C (ring) at 1620 and 1527 cm^{-1}.[40] It is however worth noticing a small shoulder for a 0.3 W cm^{-2} deposit at 0.5 mL min^{-1}, at about 1600-1620 cm^{-1} and also at 1525 cm^{-1}, possibly coming from higher C=C ring contribution in this area.[34]

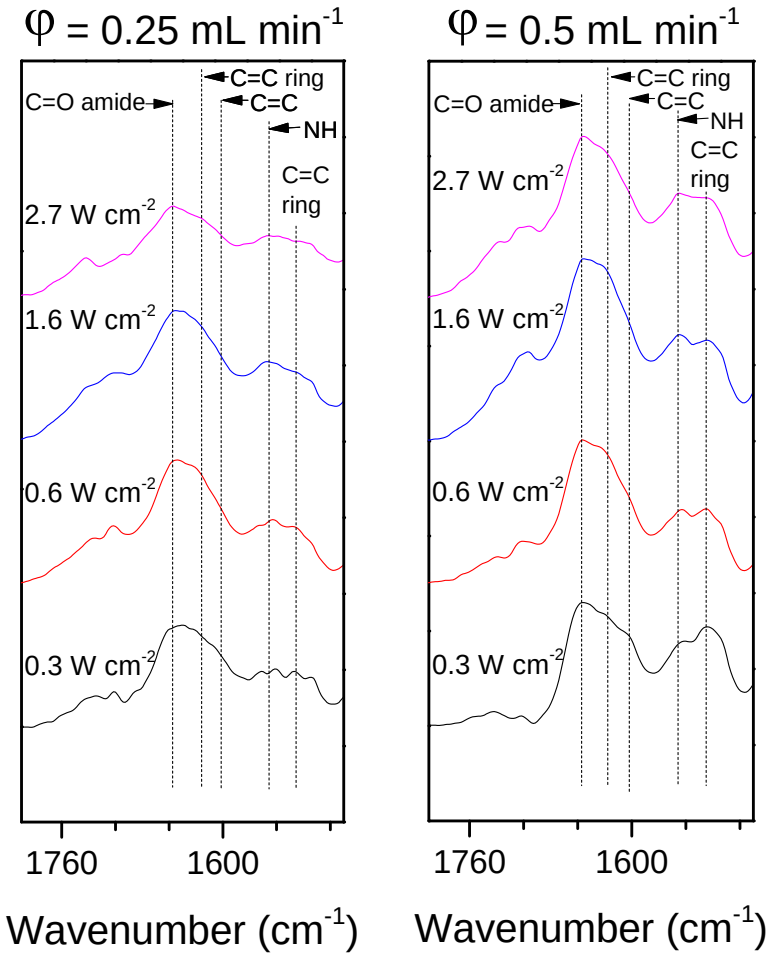

Figure 8: FT-IR spectra in the range of 1800-1480 cm^{-1} of DOA-VTMOS coatings obtained at 0.3 W cm^{-2} to 2.7 W cm^{-2} at precursor delivery rates of 0.25 and 0.5 mL min^{-1}.

From the UV-vis spectra reported in **Figure 9a**, the presence of catechol chromophore groups in the DOA-VTMOS deposited layers was assessed thanks to the presence of its characteristic peak at 280 nm.[41] This result is fully consistent with the XPS and IR analyses highlighting the retention of the DOA structure. In addition, confocal microscopy observations (**Figure 9b**), based on the fluorescence properties of catechol and its oxidized form under an excitation wavelength of 405 nm, suggest the presence of catechol groups all over the length of the DOA-VTMOS coatings.[42] The liquid-assisted approach seems to have a protective effect on the DOA chemical structure, with the retention of aromatic and hydrocarbon rings despite exposure to highly energetic plasma species. This hypothesis is in agreement with previous observations reported in the work of Heyse *et al.* and more recently

of Palumbo *et al.*, with the successful elaboration of bioactive biocomposite based on proteins entrapped in a plasma polymerized matrix.[6,7]

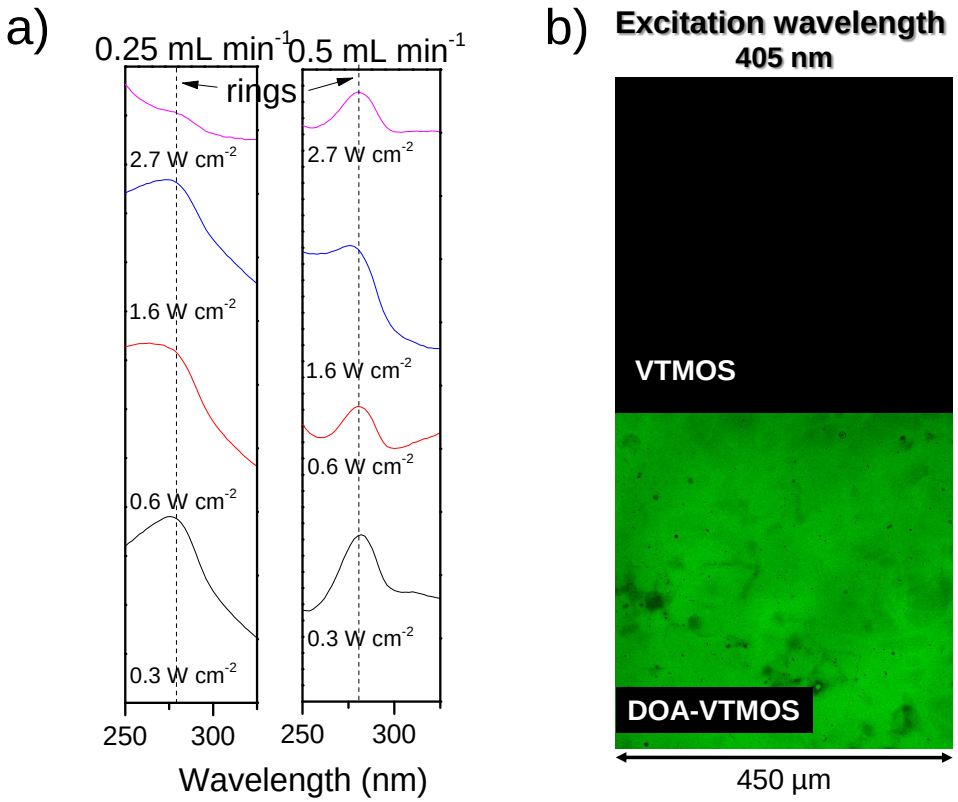

Figure 9: a) UV-Vis spectra in the range of 250-325 nm of DOA-VTMOS coatings obtained varying the power at precursor delivery rates of 0.25 and 0.5 mL min^{-1}. b) Confocal microscope images (excitation wavelength of 405 nm) of VTMOS and DOA-VTMOS coatings deposited at 1.6 W cm^{-2} and 0.5 mL min^{-1} flow rate.

3.2 Surface characterization

In this section, the surface morphology as well as the catechol and quinone surface distributions of the liquid-assisted plasma-polymerized layers deposited at 0.5 mL min^{-1} are reported in detail.

3.2.1 Surface morphology

Firstly, according to the Scanning Electron Microscopy (SEM) observations (**Figure 10**), the deposited layers are smooth, powder-free and cover homogeneously the whole surface of the substrate.

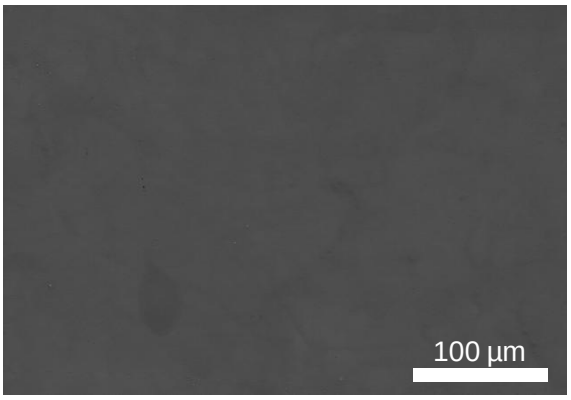

Figure 10: Scanning electron micrograph of DOA-VTMOS 1.6 W cm^{-2} at 0.5 mL min^{-1}.

High magnification optical microscopy (**Figure 11a**) shows that the reflected light passing by the sample is slightly dispersed, revealing some heterogeneities in the deposited films. In particular, the presence of rings, with a diameter ranging from 100 to 300 µm, is visible. The 3D mapping of the surface enables to attribute this ring observation to the existence of ridges with a 100 nm height at the surface of the films (**Figure 11b)**. A first hypothesis of this ring formation could be the well-known coffee ring effect where a solute is likely to migrate and aggregate at the edge of an evaporating droplet due to the formation of a preferential flow toward this area where the liquid evaporates faster. [43,44] However, as the optical microscopy picture of a pure VTMOS deposited layer (**Figure 11c)** also revealed this droplet-like morphology, it can be concluded that the coffee ring effect is probably not the main phenomenon leading to the rings formation.

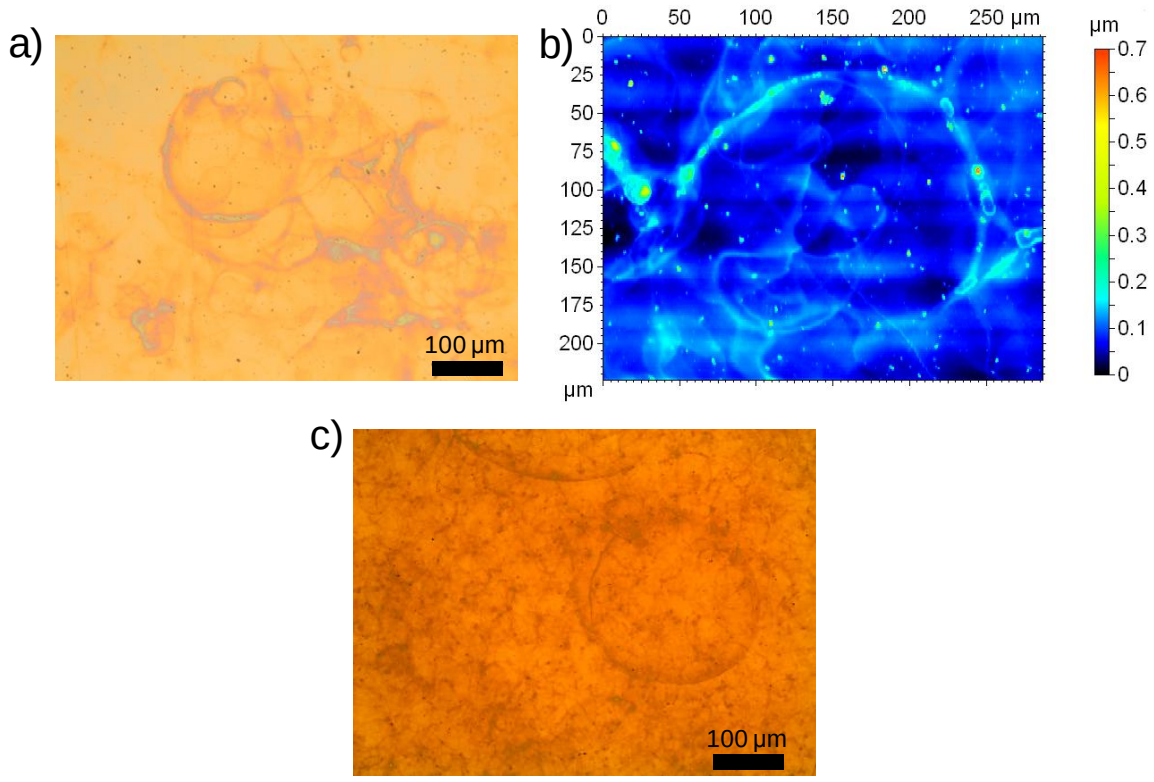

Figure 11: a) Optical micrograph and b) 3D contact profilometer mapping picture of a DOA-VTMOS deposited layer at 1.6 W cm^{-2} and 0.5 mL min^{-1}. c) Optical micrograph of a VTMOS polymerized layer at 1.6 W cm^{-2} at 0.5 mL min^{-1}.

3.2.2 Surface chemistry study

To get insights into the layer growth mechanisms, the distribution of chemical species was investigated through various characterization approaches. ToF-SIMS analyses were notably carried out in order to investigate the surface chemical distribution of nitrogen (CH_4N^+) and silicon-containing fragments (Si^+), which are fingerprints of the DOA and VTMOS monomers, respectively. From **Figure 12a**, it can be noticed that after a single cycle of the plasma deposition process (1.6 W cm^{-2} at 0.5 mL min^{-1} condition), *i.e.* two passes in the discharge zone, the surface is partially covered by isolated droplets or few stacked droplets. CH_4N^+ fragments were mainly found in the center of the droplets while Si-rich compounds are preferentially present on the edges of the droplets, forming rings (**Figure 12a**). Additional ToF-SIMS investigations carried out after 2, 5, 15 and 50 cycles (**Figure**

12), show that above 15 cycles, the whole surface is covered and the resulting coatings appear as a pileup of polymerized droplets with Si-rich outer edges (**Figure 12d & e**).

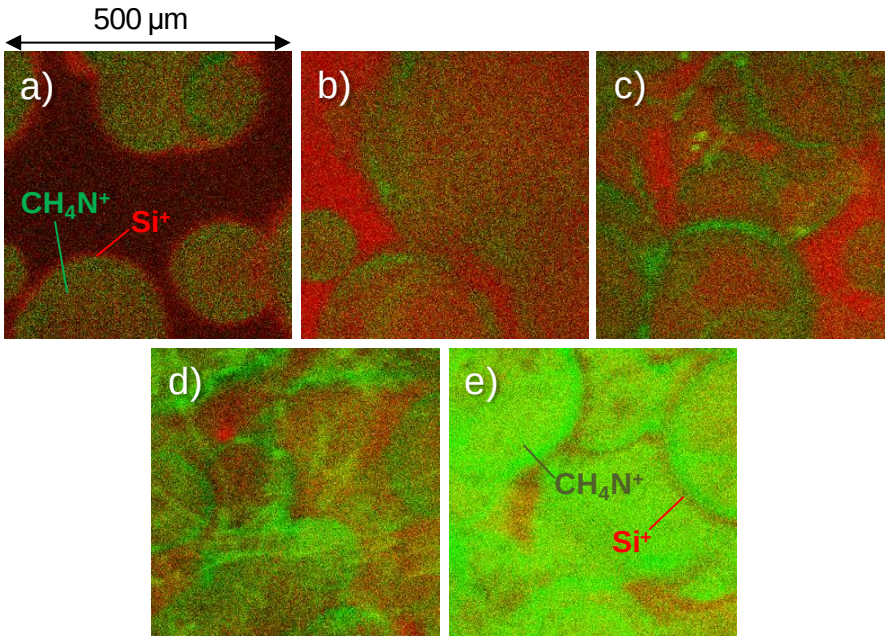

Figure 12. ToF-SIMS images issued from the superimposition of Si^+ (red) and CH_4N^+ (green) fragments distributions images for a DOA-VTMOS layer deposited at 1.6 W cm^{-2} using a 0.5 mL min^{-1} precursor delivery rate after a) 1 b) 2 c) 5 d) 15 and e) 50 deposition cycles.

To investigate the presence of catechol groups at the layer topmost surface, coatings were immersed in a silver nitrate ($AgNO_3$) solution. The formation of silver nanoparticles (NPs), resulting from the following oxydo-reduction reaction: catechol + 2 Ag^+ = quinone + Ag^0 + $2H^+$, was then investigated via SEM and EDX analyses. SEM analyses (**Figure 13 c & d**) revealed the presence of numerous NPs, which silver nature was confirmed through EDX analysis showing peaks at 3 and 3.2 keV. The formed NPs were then immobilized onto the surfaces through stabilizing bonds involving both catechol and quinone functional groups. [24] As a reference test, no NP was observed for VTMOS coating (**Figure 13 a & b**). SEM images allowed also observing the surface distribution of the immobilized NPs, indirectly providing information on the catechol groups distribution (**Figure 13**). Lower density of silver NPs were observed on the edges of the droplets, suggesting a lower concentration of groups in these regions corroborating the Tof-SIMS analyses.

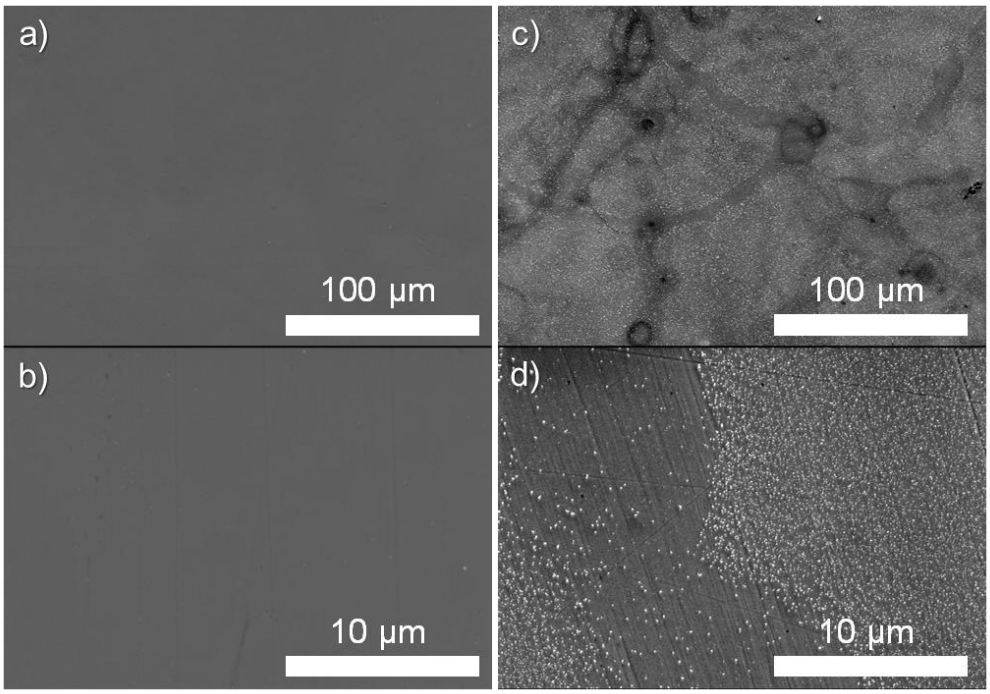

Figure 13: SEM images after overnight immersion in a $AgNO_3$ solution of: a pure VTMOS reference layer (a,b) and a DOA-VTMOS coating (c,d).

The Si^+ (**Figure 12**) and nanoparticles distribution studies (**Figure 13**), combined with the strong silicon-based network changes observed by FTIR and XPS analyses, clearly suggests that the chemical distribution is mainly related to the VTMOS monomer properties. Tynan *et al.* observed similar ring-like morphology in their work and related it to a high surface tension of the precursor without further analyses.[12] Indeed, in our case, the surface tension of the VTMOS is high enough to not totally wet the surface. As reported in literature, a droplet evaporates faster at its edge due to thinner periphery, hence forming a flux from the center of the droplet to the edge.[45] The volatile VTMOS is likely to locally evaporate faster at the thin droplets edges leading to a "pure" VTMOS plasma polymerization near the edges compared to the center where VTMOS evaporation rate is slower and DOA molecules are still entrapped by VTMOS monomer (*cf.* scheme **Figure 14**). While exposed to plasma, a polymerized ring mainly composed of VTMOS may form, explaining the observed morphology both for pure VTMOS and DOA-VTMOS coatings.

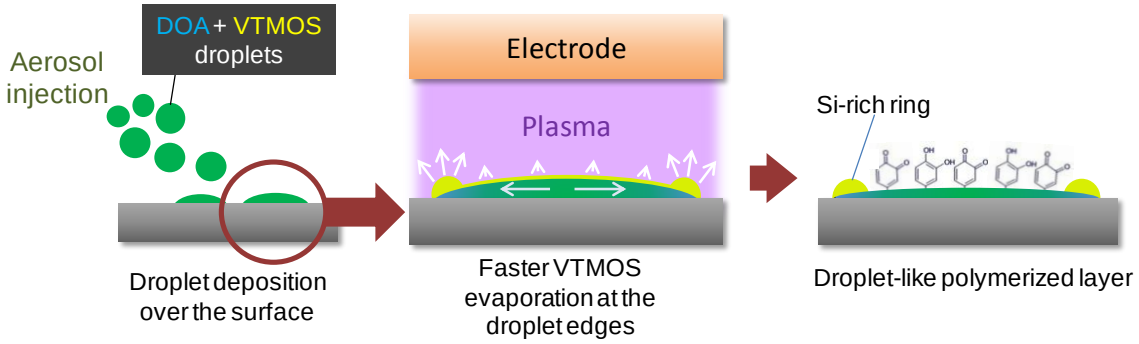

Figure 14: Ring-like morphology formation mechanism proposition for a single deposition cycle of the process, in the case of an aerosol injection system, leading to a polymerized droplets pileup.

To investigate the presence and distribution of quinone groups on the DOA-VTMOS layer topmost surfaces after deposition, a β-lactamase enzyme was exploited as a derivatization agent. Indeed, quinone groups are potentially able to react with enzymes functional groups (*i.e.* thiol, amine and imidazole groups) to form covalent bonds through Michael addition and Schiff base formation.[23] Here, the presence of Valine (Val, $C_4H_{10}N^+$) and Lysine (Lys, $C_5H_{10}N^+$) fragments, detected by ToF-SIMS (**Figure 15**) analyses, on the derivatized DOA-VTMOS surfaces confirmed the successful β-lactamase immobilization. For both amino-acids, the fragments were relatively homogeneously distributed over the surface, although droplets edges are slightly observed, suggesting a fewer amount of immobilized proteins on those areas, as previously shown. Hence, it can be concluded that part of the catechol groups from the DOA monomer are likely to be oxidized to quinone groups because of the formation of oxidant species generated from the fragmentation of the oxygen containing monomers or because of the bombardment of the growing layer with highly energetic species, possibly breaking the OH bonds, leading to H abstraction.

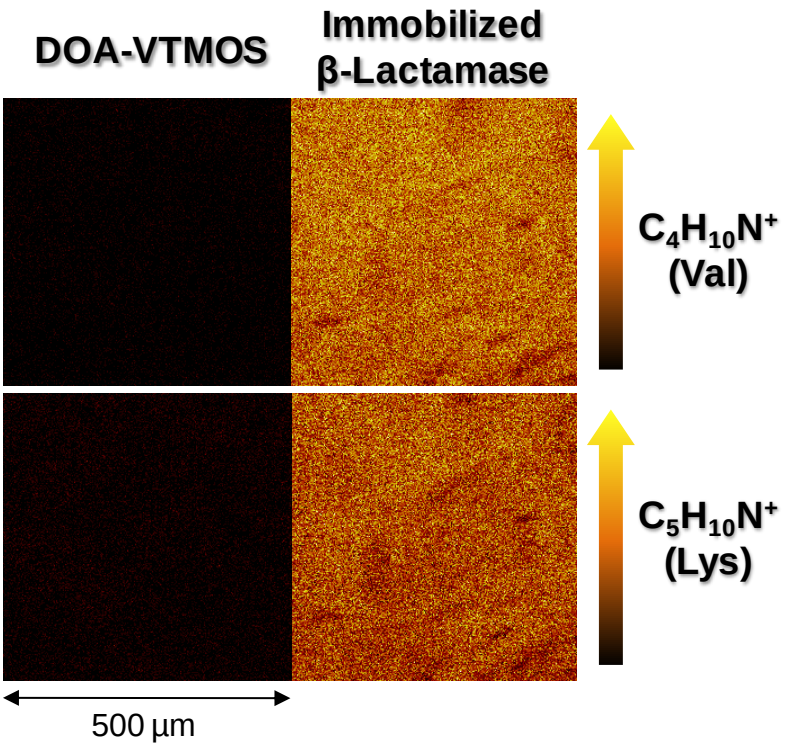

Figure 15: ToF-SIMS images of the distribution of Valine ($C_4H_{10}N^+$) and Lysine ($C_5H_{10}N^+$) fragments on a DOA-VTMOS coating and a DOA-VTMOS coating after immersion in a β-lactamase solution.

Further amoxicillin degradation tests highlighted the bioactivity of the immobilized β-lactamase surfaces (**Figure 16**). The protein conformation was retained after the immobilization step and the resistance of the formed covalent bond at the interface was also assessed as the surfaces are still actives after one week in solution under 300 RPM stirring. The latter results highlight the potential of such DOA-VTMOS deposited layers for the elaboration of bioactive functional surfaces through the immobilization of biomolecule of interests.

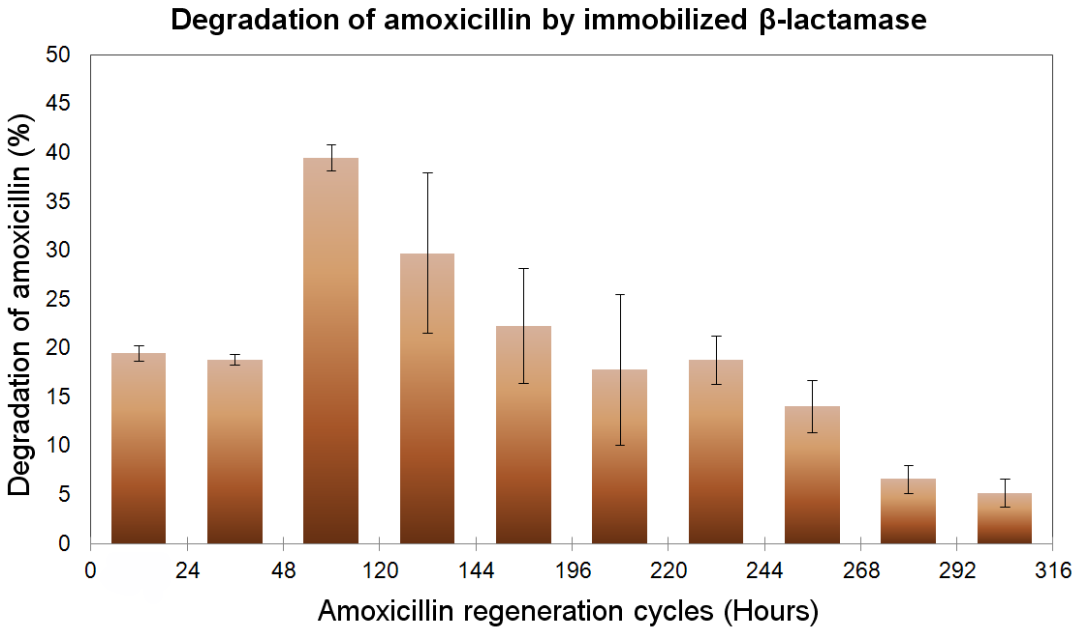

Figure 16: Degradation assay of amoxicillin by immobilized β-lactamase on a DOA-VTMOS coating obtained at 1.6 W cm^{-2} at a flow rate of 0.5 mL min^{-1}.

3.3 Growth mechanism of the catechol/quinone functionalized layer deposited by LA-PECVD

LA-PECVD provides a convenient and substrate independent method toward the one-step and fast deposition of catechol and quinone-functionalized layers from a non volatile monomer (*i.e.* DOA). The LA-PECVD approach present several significant assets in the preparation of such surfaces, being notably 1000 times faster than current fastest wet chemical deposition methods, *i.e.* the oxidant-induced dopamine polymerization.[46] Moreover, the LA-PECVD approach is not specific to the preparation of catechol and quinone-rich coatings as it was previously successfully investigated for the preparation of nanocomposite coatings grown from luminescent NPs or sensing layers composed of heterocyclic macrocycles.[4,47] To prepare such coatings, a low vapor pressure monomer (*e.g.* DOA) or NPs were solubilized or dispersed in a volatile matrix forming monomer (*e.g.* VTMOS), which was further deposited as a very thin liquid layer (deposited from a mist in the present work, but possibly deposited through any other suitable mean, *e.g.* roll coating, dipping…) and subsequently exposed to a plasma discharge to promote the formation of a plasma-polymerized layer enclosing the low vapor pressure molecules or particles.

In the present example, the volatile compound of the liquid deposited layer (*i.e.* VTMOS) is evaporating during the deposition process (**Figure 17a & b**). This statement is, in that case, corroborated by XPS analyses showing a high nitrogen content (*i.e.* 2-3 %), originating from the non-volatile moieties (*i.e.* DOA), in comparison to the original solution concentration (*i.e.* 0.002 at.%). Due to this evaporation process, VTMOS is likely to be present both under vapor and liquid form while interacting with the plasma (**Figure 17c**). Under plasma exposition, the layer growth mechanism is governed both by plasma interactions with the gas and liquid phase. In **Figure 2**, using low precursor delivery rates, mass deposition rate estimations show that the deposition is likely to be independent of the power used and solely governed by the precursor delivery rate. In contrast, using higher precursor delivery rate values, the mass deposition rate seems dependent both of the plasma power used and the precursor delivery rate. Indeed, at these high precursor delivery rates, an ageing phenomenon is highlighted; layer mass losses after an ageing step at air suggest the presence of liquid VTMOS in the layer (assessed by FTIR analyses) and its subsequent evaporation. The saturation of the gas phase by the evaporating VTMOS is then believed to be reached during plasma deposition, thus promoting mainly gas phase reactions during layer growth and leading to a strong influence of the used plasma power density. This then suggests that even though at low precursor delivery rates this effect is not clearly evidenced, part of the deposition mechanism might also be driven by gas phase reactions.

As depicted in **Figure 17c**, evaporated VTMOS is fragmented and forms excited species in the gas phase while the possibly remaining liquid fraction is participating to the partial protection of the DOA monomer from direct exposure to the energetic plasma species. The DOA monomer copolymerization is then expected to occur thanks to the generated VTMOS species formed, propagating radical polymerization reactions through the vinyl bonds (vinyl bond peaks disappearance in FTIR and Raman spectra). Thanks to this reaction mechanism, it can be proposed that the conservation of the functional groups is then achieved (**Figure 17d**). Indeed, catechol groups presence is undoubtedly assessed on the deposited layers through formation of silver nanoparticles thanks to their reductive properties. Quinone groups are also shown to be present thanks to successful immobilization of biomolecules, possibly formed due to oxidative species generation during deposition or hydrogen abstraction. The presence in the deposited layer of fragile chemical structures such as the aromatic catechol group and the quinone hydrocarbon ring can be explained by the high

plasma polymer layer deposition rate and the protective effect of the VTMOS molecules surrounding the DOA monomer compound. Despite a slightly different setup, an analogy can be drawn with the works of Boscher *et al.* where they were able to incorporate active porphyrins even though they were exposed to the plasma.[47] While protecting the DOA monomer, a compromise between power and precursor delivery rate has to be found in order to obtain well cross-linked silica based network, as shown in figure 2, 3 and 4. Tuning the power is shown to greatly influence the organic/inorganic ratio in the Si/O/C based network and could be potentially exploited in order to tune the chemical and mechanical stability of the layers according to the targeted application environment. This deposition method also offers the possibility, in addition to simply vary the initial concentration of the DOA-VTMOS solution, to tune the DOA/VTMOS ratio, and hence the functional group density coming from DOA, through the evaporation control of VTMOS, influenced by the delay between liquid deposition and plasma exposure or by the adjustment of the substrate temperature.

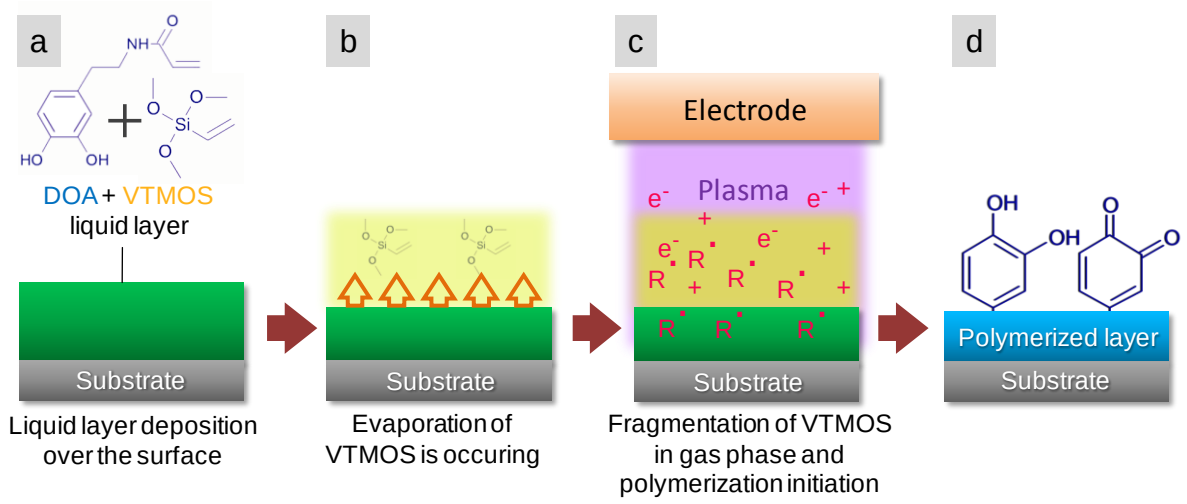

Figure 17: a to d) Scheme of the proposed growth mechanism for layers deposited using Liquid-Assisted PECVD and based on a low vapor pressure monomer solubilized in a high vapor pressure solvent.

The growth mechanism of the coating is then essentially based on VTMOS and DOA copolymerization reactions initiated via radical species formation. Consequently, through the tuning of the monomer delivery rate and the plasma power density, it is possible to modify

the inorganic-organic character of the film and, depending on the substrate temperature and delay between the liquid deposition and the plasma exposure, it would be possible to tune the density of the catechol/quinone functional groups.

4. Conclusion

A plasma copolymer coating functionalized with catechol and quinone groups has been formed from dopamine acrylamide (DOA) and vinyltrimethoxysilane (VTMOS) by using an atmospheric-pressure liquid-assisted plasma polymerization method. The precursor delivery rate was shown to be a key parameter for the formation of the coatings. Indeed, for a critical delivery rate value ($\varphi > 0.5$ mL min^{-1}) and irrespective of the applied power, the plasma process was not able to form cross-linked coatings. An ageing mechanism has also been observed and characterized by a mass loss of the coating with time. However, precursor delivery rate and plasma power conditions (*i.e.* $\varphi \leq 0.5$ mL min^{-1} for power ranging from 0.3 to 2.7 W cm^{-2}) were found to enable the high deposition rate of cross-linked coatings. The tuning of the applied power was shown to have an influence on the SiO_x matrix formed by VTMOS, as high power apparently led to the fragmentation of the Si-O-C bond, forming silica like cross-linked networks. Interestingly, the integration and conservation of the catechol functional group from the DOA monomer, whatever the conditions used in this study, was highlighted. According to FTIR, XPS and UV analyses, a protective effect of VTMOS upon DOA is expected and the plasma copolymerization of the two monomers offers the possibility to have catechol but also quinone functionalized surfaces. The observations by optical microscope and contact profilometer showed that the surface present droplet ring morphology. A ToF-SIMS study showed that the coatings are formed by a pile-up of polymerized droplets with high amount of fragments corresponding to a fingerprint of DOA mainly distributed in the center of the droplets while the border were likely to be composed of SiO containing species from the matrix forming VTMOS. The SEM observation of these LA-PECVD layers after reduction reaction of a silver nitrate solution by catechol groups and subsequent coordination of formed silver nanoparticles on those groups enabled to confirm the presence of catechol groups and their surface distribution. Quinone groups are however likely to be formed during the plasma treatment, either due to a possible direct plasma interaction with some catechol groups and due to the presence of oxidant generated

species. The successful direct grafting of β-lactamase enzymes on these plasma layers enabled to indirectly confirm the presence of the quinone groups and to study their distribution on the surface thanks to ToF-SIMS analyses. The conservation of both functional groups on the surface makes this type of layer promising for numerous applications. Quinone groups provide a real platform for the immobilization of biomolecules with various properties, *e.g.* antibiotics degradation, antibacterial, while the catechol groups are interesting for trapping radicals or metal ions for water treatment applications.

The LA-PECVD deposition method used in the present work appears as a simple and efficient route towards the one-step deposition of a wide range of functional coatings.[3,4,19,47] The developed approach is not specific to the planar DBD configuration and could be implemented with other plasma configurations, including DBD plasma torches, to coat complex 3D pieces. In addition, the thin liquid layer deposition step, achieved prior to the plasma exposure, could be performed using a range of suitable methods, including the mist injection approach described in this work and the roll-coating method widely used in industry to provide homogeneously distributed liquid layers. As a consequence, the LA-PECVD technique, easily up-scalable and operating at room temperature and atmospheric pressure, provides an interesting route toward the easy and fast deposition of innovative multifunctional coatings. Beyond the use of dopamine-based chemicals employed to form adhesive layers, a plethora of low vapor pressure or solid smart compounds, such as enzymes, cage compounds and metallic nanoparticles, could be exploited, together with the wide choice of available matrix-forming precursors, to reach a diverse range of applications, *e.g.* sensing, anti-corrosion, photocatalysis, drug delivery, antibacterial surfaces.

.

References

[1] B. R. Coad, M. Jasieniak, S. S. Griesser, H. J. Griesser, *Surf. Coatings Technol.* **2013**, *233*, 169.

[2] F. Massines, C. Sarra-Bournet, F. Fanelli, N. Naudé, N. Gherardi, *Plasma Process. Polym.* **2012**, *9*, 1041.

[3] P. Heier, N. D. Boscher, T. Bohn, K. Heinze, P. Choquet, *J. Mater. Chem. A* **2014**, *2*, 1560.

[4] N. D. Boscher, P. Choquet, D. Duday, N. Kerbellec, J.-C. Lambrechts, R. R. Maurau, *J. Mater. Chem.* **2011**, *21*, 18959

[5] Y. W. Yang, G. Camporeale, E. Sardella, G. Dilecce, J. S. Wu, F. Palumbo, P. Favia, *Plasma Process. Polym.* **2014**, *11*, 1102.

[6] F. Palumbo, G. Camporeale, Y.-W. Yang, J.-S. Wu, E. Sardella, G. Dilecce, C. D. Calvano, L. Quintieri, L. Caputo, F. Baruzzi, P. Favia, *Plasma Process. Polym.* **2015**, *12*, 1302.

[7] P. Heyse, A. Van Hoeck, M. B. J. Roeffaers, J. -P. Raffin, A. Steinbüchel, T. Stöveken, J. Lammertyn, P. Verboven, P. a. Jacobs, J. Hofkens, S. Paulussen, B. F. Sels, *Plasma Process. Polym.* **2011**, *8*, 965.

[8] G. Da Ponte, E. Sardella, F. Fanelli, R. D'Agostino, R. Gristina, P. Favia, *Plasma Process. Polym.* **2012**, *9*, 1176.

[9] F. Fanelli, A. M. Mastrangelo, F. Fracassi, *Langmuir* **2014**, *30*, 857.

[10] B. Nisol, C. Poleunis, P. Bertrand, F. Reniers, *Plasma Process. Polym.* **2010**, *7*, 715.

[11] B. Twomey, M. Rahman, G. Byrne, A. Hynes, L. A. O'Hare, L. O'Neill, D. Dowling, *Plasma Process. Polym.* **2008**, *5*, 737.

[12] J. Tynan, P. Ward, G. Byrne, D.P. Dowling, *Plasma Process.Polym.* **2009**, *6*, S51.

[13] B. Nisol, G. Oldenhove, N. Preyat, D. Monteyne, M. Moser, D. Perez-Morga, F. Reniers, *Surf. Coatings Technol.* **2014**, *252*, 126.

[14] L.-A. O'Hare, L. O'Neill, A. J. Goodwin, *Surf. Interface Anal.* **2006**, *38*, 1519.

[15] R. Mauchauffé, M. Moreno-Couranjou, N. D. Boscher, C. Van De Weerdt, A.-S. Duwez, P. Choquet, *J. Mater. Chem. B* **2014**, *2*, 5168.

[16] G. Camporeale, M. Moreno-Couranjou, S. Bonot, R. Mauchauffé, N. D. Boscher, C. Bebrone, C. Van De Weerdt, H.-M. Cauchie, P. Favia, P. Choquet, *Plasma Process. Polym.* **2015**, *12*, 1208.

[17] S. Bonot, R. Mauchauffé, N. D. Boscher, M. Moreno-Couranjou, H.-M. Cauchie, P. Choquet, *Adv. Mater. Interfaces* **2015**, *2*, 1500253.

[18] A. Manakhov, P. Skládal, D. Nečas, J. Čechal, J. Polčák, M. Eliáš, L. Zajíčková, *Phys. Status Solidi* **2014**, *211*, 2801.

[19] R. Mauchauffé, S. Bonot, M. Moreno-Couranjou, C. Detrembleur, N.D. Boscher, C. Van De Weerdt, A.S. Duwez, P. Choquet, *Submitted* **2016**.

[20] J. –H. Waite, *Nat. Mater.* **2008**, *7*, 8.

[21] H. Lee, S. M. Dellatore, W. M. Miller, Phillip B. Messersmith, *Science.* **2007**, *318*, 426–430.

[22] H. Lee, J. Rho, P. B. Messersmith, *Adv. Mater.* **2009**, *21*, 431-434.

[23] E. Faure, C. Falentin-Daudré, C. Jérôme, J. Lyskawa, D. Fournier, P. Woisel, C. Detrembleur, *Prog. Polym. Sci.* **2013**, *38*, 236.

[24] E. Faure, C. Falentin-Daudré, T. S. Lanero, C. Vreuls, G. Zocchi, C. Van De Weerdt, J. Martial, C. Jérôme, A.-S. Duwez, C. Detrembleur, *Adv. Funct. Mater.* **2012**, *22*, 5271.

[25] E. Faure, P. Lecomte, S. Lenoir, C. Vreuls, C. Van De Weerdt, C. Archambeau, J. Martial, C. Jérôme, A.-S. Duwez, C. Detrembleur, *J. Mater. Chem.* **2011**, *21*, 7901.

[26] B. P. Lee, K. Huang, F. N. Nunalee, K. R. Shull, P. B. Messersmith, J. Biomater. Sci. Polym. Ed. **2004**, *15*, 449.

[27] J. Heo, H. J. Kim, J. Han, J.-W.Shon, *Thin Solid Films* **2007**, *515*, 5035.

[28] X. Luo, C. L. Weaver, S. Tan, X. T. Cui, J. Mater. Chem. B **2013**, *1*, 1340.

[29] E. Kaivosoja, S. Virtanen, R. Rautemaa, R. Lappalainen, Y.T. Konttinen, *Eur. Cell Mater.* **2012**, *24*, 60.

[30] C. O. Ruud, J. F. Bussière, R. E. Green, *Nondestructive Characterization of Materials IV, Volume 4,* Springer Science and Business Media, **1991**.

[31] Y.-S. Li, P. B. Wright, R. Puritt, T. Tran, *Spectrochim.Acta. A. Mol. Biomol. Spectrosc.* **2004**, *60*, 2759.

[32] Y.-S. Li, T. Tran, Y. Xu, N. E. Vecchio, *Spectrochim.Acta. A. Mol. Biomol. Spectrosc.***2006**, *65*, 779.

[33] L.-H. Lee, *Characterization of Metal and Polymer Surfaces V2: Polymer Surfaces*, Elsevier, **2012**.

[34] N. Colthup, L. Daly, S. Wiberley, *Introduction to Infrared and Raman Spectroscopy*, Elsevier, **1990.**

[35] Y. Abe, K. Tuchida, Y. Nagao, *J. Non-Cryst. Solids* **1992**, *148*, 47.

[36] J. Wang, B. Zou, M. A. El-Sayed, *J. Mol. Struct.* **1999**, *508*, 87.

[37] R. M. Almeida, C. G. Pantano, *J. Appl. Phys.* **1990**, *68*, 4225.

[38] P. Lange, *J. Appl. Phys.* **1989**, *66*, 201.

[39] R. Lenza, W. Vasconcelos, *Mater. Res.* **2001**, *4*, 175.

[40] G. Socrates, *Infrared and Raman Characteristic Group Frequencies: Tables and Charts, 3rd Edition*, Wiley, Hoboken, NJ, USA **2004**.

[41] M.-H. Ryou, J. Kim, I. Lee, S. Kim, Y. K. Jeong, S. Hong, J. H. Ryu, T.-S. Kim, J.-K. Park, H. Lee, J. W. Choi, *Adv. Mater.* **2013**, *25*, 1571.

[42] X. Zhang, S. Wang, L. Xu, L. Feng, Y. Ji, L. Tao, S. Li, Y. Wei, *Nanoscale* **2012**, *4*, 5581.

[43] R. Deegan, O. Bakajin, T. Dupont, G. Huber, *Nature* **1997**, 827.

[44] K. L. Maki, S. Kumar, *Langmuir* **2011**, *27*, 11347.

[45] T. Ondarçuhu, J. P. Aimé, *Nanoscale Liquid Interfaces: Wetting, Patterning and Force Microscopy at the Molecular Scale*, CRC Press, **2013**.

[46] Q. Wei, F. Zhang, J. Li, B. Li, C. Zhao, *Polym. Chem.* **2010**, *1*, 1430.

[47] N. D. Boscher, D. Duday, P. Heier, K. Heinze, F. Hilt, P. Choquet, *Surf. Coatings Technol.* **2013**, *234*, 48.

General conclusions

Nowadays, willing to impart new properties to non-reactive materials surfaces, the surface modification for the immobilization of active compounds became a topic of main interest. Several routes were investigated to allow the immobilization of those active molecules. The emergence of dry processes few decades ago for the treatment of material surfaces has provided a real environmentally friendly alternative to waste-generating wet chemical methods. Among the dry processes used for surface modification, plasma assisted methods offer a high versatility. Indeed, thanks to this method, it is possible, at low temperature, with a low consumption of chemicals and generating few wastes, to modify any type of surfaces. Roughness and surface energy tuning as well as functional groups introduction can be achieved through mere plasma treatment, while plasma polymerized thin films deposition, using a wide range of available precursors, may provide a large variety of functional groups and the ability to form composites coatings. Till now the processes used for surface modification are mainly ran at low pressure. Atmospheric pressure processes, of main interest for industrial production up scaling, due to their easy implementation, are still not very widespread as reported in chapter 1.

It is worth noticing that sustainable and green approaches are more and more being favored. The discovery in Nature of biomolecules with marvelous properties provides an interesting renewable resource to provide various new surface properties through their surface immobilization.

This work aimed, through the 5 last chapters, at highlighting the versatility and the potential of atmospheric pressure plasma polymer deposition combined to the immobilization of various peptides and enzymes in order to successfully impart properties such as antibacterial, antibiofouling or antibiotics degradation properties to originally non-reactive surfaces, *e.g.* stainless steel.

Atmospheric Pressure Plasma Enhanced Chemical Vapor Deposition (AP-PECVD) was performed here thanks to a Dielectric Barrier Discharge plasma reactor and allowed obtaining carboxyl, epoxy and quinone groups. The precise tuning of the surface properties such as functional groups density, roughness and cross-linking of the coating was controlled through the modification of the plasma deposition parameters.

The first part of this work, presented in the second chapter, highlighted the potential of this method to impart antibacterial properties to stainless steel. Indeed, high antibacterial

efficiency was reached thanks to a 3 steps procedure based on the covalent immobilization of Nisin, an antimicrobial peptide, on a carboxylic functionalized maleic anhydride – vinyltrimethoxysilane (MA-VTMOS) plasma copolymer layer thanks to the well-known and largely investigated EDC/NHS coupling reagents. Plasma parameters such as power and pulse of the discharge were tuned to modify both surface chemistry and morphology. A correlation between the carboxylic group surface concentration and the surface roughness onto the antibacterial properties of the layers was evidenced. Antibacterial tests showed that the morphology of the layer is a key parameter to control the surface efficiency. Smooth layers allowed obtaining good antibacterial surface properties, due to possible interactions between bacteria membrane and the easily accessible immobilized peptides. Highly rough surfaces, however, reduced the accessibility of the small peptide and then the interactions possibilities between immobilized Nisin with the bacteria. Interestingly, covalent immobilization of the peptide showed protective effect towards delamination/dissolution of coatings in solution. Finally, in this chapter, FT-IR analyses appeared as a fast, simple and powerful analytical tool allowing us to validate the different steps of the method, comprising the chemical surface modifications, activation step and grafting of the peptide for which secondary structure investigation was also possible.

As a numerous steps method is often synonymous with time taking and fastidious process, we were then concerned in chapter 3 to reduce the number of steps. In order to do so, plasma polymerization of glycidyl methacrylate (GMA) was performed to obtain reactive epoxy groups functionalized surfaces to immobilize biomolecules in mild conditions without requiring prior surface activation. As studied in the second chapter, it has been shown that tuning the pulsing of the discharge has a strong influence during GMA plasma polymerization either on the roughness of the deposited layer and on the epoxy group density. Indeed, reducing the duty cycle D.C. from 100% (continuous mode) to about 11% led to smooth layers containing on the surface up to 18 at.% epoxy groups. Although the poly(GMA) reference epoxy groups content, *i.e.* 27 at.%, was not reached, these results showed that atmospheric pressure plasma deposition is a promising method to allow the soft polymerization of monomer retaining their functional groups through simple tuning of the process parameters, being an asset for biomolecule immobilization. Two enzymes with drastically different biological properties, namely dispersin B and a laccase, with respectively anti-biofouling and xenobitics degrading properties were immobilized onto functionalized

metallic surfaces. The pH of immobilization was studied and appeared to be a key parameter to control the amount of immobilized enzyme leading to bioactive surfaces with improved stability and activity. The grafted layers, notably in the case of Laccase, showed an extended duration activity and higher efficiency, around four and seven times higher respectively, than for the free enzyme in solution.

An innovative approach was reported in the fourth chapter to form epoxy functionalized surfaces using a newly developed process at atmospheric pressure, *i.e.* Plasma initiated Chemical Vapor Deposition (PiCVD). As discharge pulsing was shown in the previous chapters to lead to high functional groups retention, ultra-short pulses were here exploited. Indeed, using this new method, as the plasma discharge was "on" only 0.003% of the time (Time on: 100 ns; Time off: 33ms), the effect of plasma on the growing layer was very limited. The generated species during the short time on greatly favor a free radical polymerization of the monomer during the long time off. PolyGMA coatings with high epoxy group retention were formed, offering surfaces similar to pure polyGMA polymer. This substrate independent process allowed the deposition of coatings both over stainless steel and polyethylene biochips, the latter one commonly used in water treatment and offering a high specific surface for enzyme/antibiotics interactions. On the basis of the good antibiotics degradation efficiency obtained in chapter 3, two antibiotics degrading enzymes, laccase and beta-lactamase were immobilized on these newly developed surfaces. The enhancement of the enzymes activity duration and intensity were observed as noticed in Chapter 3 on plasma polymerized GMA. The enzymes structure rigidification and stabilization upon immobilization was further studied here and was shown to allow them to endure mechanical stresses generated by a laminar water flow of 30 km h^{-1} and this with no reduction of their enzymatic activity. In order to upscale this method to water treatment where numerous microorganisms can adhere to the active surfaces and possibly alter the enzymes, self-defensive surface properties were investigated. Tween 20 was used to saturate the surfaces to prevent microorganisms adhesion and enzyme alteration in order to improve the degradation performances. Interestingly, particularly long lasting efficient degradation properties were observed after surface saturation. This epoxy based method remains interesting to provide a strong platform for the anchoring of various biomolecules.

However, as research groups and industries are more and more involved in sustainable development and green methods; we then focused our work on synthesizing bio-

inspired coatings. The last decade the emergence of mussel-inspired wet-chemical methods to coat surfaces, based on the polymerization of dopamine and its derivatives, attracted a large interest from the scientific community. Indeed, these coatings show really good adhesion properties thanks to catechol and quinone functional groups. In this chapter, mussel-inspired coatings were deposited for the first time with a dry process. Catechol and quinone functionalized reactive hybrid layers, about a hundred nanometers thick, were deposited in only few seconds onto stainless steel by atmospheric pressure liquid-assisted plasma polymerization of an aerosol mixture of dopamine acrylamide (DOA) and vinyltrimethoxysilane (VTMOS). This process was shown to be 1000 times faster than current wet chemistry methods. The New Delhi Metallo-β-Lactamase-1, NDM-1, an enzyme discovered in 2009 and responsible of outstanding bacteria resistance against β-lactam antibiotics, was exploited and immobilized for the first time in our work to degrade antibiotics in water. An efficient synergy resulted from the combination of those two nature-inspired discoveries. Indeed, the grafted coatings led to high and durable enzymatic activities and also sustained extremely high water flow, assessing the strong anchoring of the NDM-1, the robustness of the formed layer and then the overall robustness of the nature-inspired strategy.

A parametric study was performed in chapter 6 in order to investigate the influence of parameters such as precursor flow rate and plasma power on the DOA-VTMOS coating formation. It was shown that these parameters mainly influence the chemical composition of the silicon-based network and are likely to have a poor impact on the functional groups nature and density. Low precursor flow rate was shown to be a key parameter for the formation of cross-linked coatings and the tuning of the plasma power was likely to influence the chemistry of the SiOx formed matrix, *i.e.* high power leading to high fragmentation of the Si-O-C bonds, forming silica-like cross-linked networks. Interestingly, the functional groups were integrated in the layer and conserved whatever the conditions used in the study suggesting a protective effect of VTMOS upon DOA. The presence of catechol and quinone groups on the layer top surface was highlighted respectively through the successful formation of silver nanoparticles through reduction of silver nitrate solution and through biomolecule immobilization. Particular attention was paid to the special surface ring-like patterns observed after deposition likely to be due to the aerosol droplets during polymerization. The surface chemical distribution study, led thanks to ToF-SIMS analysis, showed that the surface

was composed of a pile-up of polymerized droplets with higher amount of nitrogen containing fragments distributed in the center of the rings, assigned to a fingerprint of DOA while the border of these rings were likely to be mainly composed of Si containing species from the matrix forming VTMOS. Further SEM observations of immobilized silver nanoparticles on plasma coated surfaces and ToF-SIMS analyses of biomolecules immobilized surfaces confirmed the functional groups distribution. The resulting droplets morphology and chemical distribution are then suggested to be due to a faster evaporation of VTMOS at the edges of the evaporating droplets and to its subsequent polymerization during plasma exposure. The layer growth mechanism was then believed to happen both in liquid and gas phase and shown to consist in a pileup of polymerized droplets. In spite of the slight surface functional group heterogeneities observations, enzymes are easily immobilized and antibiotics degrading surfaces were successfully obtained through the immobilization of beta-lactamase.

Atmospheric pressure plasma processes, through this work, clearly shows a strong potential for the production of functional bioactive surfaces. These processes appear as methods of choice for industrial up-scaling notably thanks to their easy implementation in existing production lines and their fast deposition rate. Indeed, they could be simply implemented in roll-to-roll processes commonly employed for the treatment of plastic and metallic foils or, thanks to plasma torch/pen configuration, implemented to treat manufactured products with complex 3D geometries. The fine tuning of the plasma parameters such as pulse duration or power enable the formation of layers with a wide range of properties to fulfill the specifications of the desired targeted application. Among those properties, mechanical stability and morphology, *i.e.* roughness, as well as chemical properties such as chemical stability, surface energy and the surface reactive group density could be tuned. The versatility of the obtainable surfaces properties hence opens great perspectives for production of robust reactive layers for biomolecule immobilization. Indeed, taking into account that biomolecules have structures and then reactivities differing from one another, atmospheric plasma techniques appear as a good way to adapt the surface properties to optimize the interactions favoring the immobilization of biomolecules, according to the targeted application. However, although the pioneering works completed over the past few years in this work and by the scientific community show promising applicative results, the development of bioactive surfaces, combining atmospheric plasma coatings and biomolecule

immobilization, fulfilling the industrial specifications, still requires further investigation and optimization from plasma surface treatment research groups in close cooperation with proteomic research groups. Indeed, the ongoing discovery of new biomolecules, with appealing properties, keeps widening the possibilities of use of such molecules as alternatives to existing industrial solutions. The determination of their range of use, *e.g.* working temperature, pH, storage stability; as well as the development and optimization of production protocols are mandatory to estimate their viability for further industrial exploitation. Concerning the layer deposition, the synthesis of viable interlayers fulfilling the applications specifications needs a complete study of the influence of the plasma deposition parameters on the properties of the synthesized layers and the optimization of these properties. Indeed, highly reactive surfaces can be obtained through quantification and optimization of the reactive surface groups density. The layers stability, for its part, can be improved through ageing study in various media, *e.g.* water and air, providing reactive robust layers for biomolecules immobilization. Atmospheric pressure plasma processes are environmentally friendly techniques producing few wastes, however their sustainable aspect could be reinforced notably i) through the use of natural precursors to form green applicative polymers, limiting the use of synthetic precursors made from non-renewable resources and ii) through the use of non-toxic precursors to facilitate their handling, hence totally avoiding toxic fumes and providing an healthy and safe work environment. To do so, a plethora of natural non-toxic precursors still remains to be explored by plasma deposition. Beyond the field of plasma layers deposition for biomolecule immobilization, promising results were obtained in literature in various other domains, *e.g.* anti-corrosion, superhydrophobic, anti-fouling, biocompatible coatings formation, thanks to the wide range of available precursors and to the possibility to finely tune the surface roughness. It is worth noting that the steady progresses in the atmospheric pressure plasma deposition field could bring major advances in current industrial hot topics such as photocatalysis or energy production and storage. Indeed, the development of new atmospheric pressure plasma reactors and precursors injection systems as well as the better control of the deposition parameters and the understanding of the plasma layer growth mechanisms through optimized analysis techniques are currently ongoing and offer promising new perspectives.